AD-A050 908 MASSACHUSETTS INST OF TECH CAMBRIDGE DEPT OF OCEAN E--ETC F/G 13/5
DEVELOPMENT OF ANALYTICAL AND EMPIRICAL SYSTEMS FOR PARAMETRIC --ETC(U)
NOV 77 V J PAPAZOGLOU, K MASUBUCHI N00014-75-C-0469

UNCLASSIFIED NL

1 OF 3
AD A050908


OF
3
0908

(12)
5C

Final Report

DEVELOPMENT OF ANALYTICAL AND EMPIRICAL SYSTEMS FOR PARAMETRIC STUDIES OF DESIGN AND FABRICATION OF WELDED STRUCTURES

by

Vassilios J. Papazoglou
Koichi Masubuchi

November 30, 1977

Massachusetts Institute of Technology
Cambridge, Massachusetts

Office of Naval Research
Contract N00014-75-C-0469 NR 031-773
(M.I.T. OSP 82558)

MASSACHUSETTS INSTITUTE OF TECHNOLOGY
DEPARTMENT OF OCEAN ENGINEERING
CAMBRIDGE, MASS. 02139

Final Report

Prepared Under

Contract No. N00014-75-C-0469, NR 031-773
(M.I.T. OSP #82558)

DEVELOPMENT OF ANALYTICAL AND EMPIRICAL SYSTEMS FOR PARAMETRIC STUDIES OF DESIGN AND FABRICATION OF WELDED STRUCTURES

to

Office of Naval Research

November 30, 1977

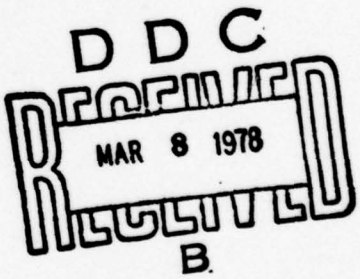

by

Vassilios J. Papazoglou

Koichi Masubuchi

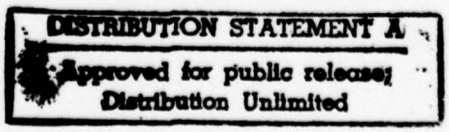

SECURITY CLASSIFICATION OF THIS PAGE (When Data Entered)

REPORT DOCUMENTATION PAGE

READ INSTRUCTIONS BEFORE COMPLETING FORM

1. REPORT NUMBER: Final Report
2. GOVT ACCESSION NO.
3. RECIPIENT'S CATALOG NUMBER

4. TITLE (and Subtitle): DEVELOPMENT OF ANALYTICAL AND EMPIRICAL SYSTEMS FOR PARAMETRIC STUDIES OF DESIGN AND FABRICATION OF WELDED STRUCTURES.

5. TYPE OF REPORT & PERIOD COVERED: Final Report 1 Dec 74 - 30 Nov 77

6. PERFORMING ORG. REPORT NUMBER

7. AUTHOR(s): Vassilios J. Papazoglou, Koichi Masubuchi

8. CONTRACT OR GRANT NUMBER(s): N00014-75-C-0469, NR 031-773

9. PERFORMING ORGANIZATION NAME AND ADDRESS: Department of Ocean Engineering, Massachusetts Institute of Technology, Cambridge, Massachusetts 02139

10. PROGRAM ELEMENT, PROJECT, TASK AREA & WORK UNIT NUMBERS

11. CONTROLLING OFFICE NAME AND ADDRESS

12. REPORT DATE: 30 Nov 77

13. NUMBER OF PAGES: ~~205~~ 215 pp.

14. MONITORING AGENCY NAME & ADDRESS (if different from Controlling Office)

15. SECURITY CLASS. (of this report): unclassified

15a. DECLASSIFICATION/DOWNGRADING SCHEDULE

16. DISTRIBUTION STATEMENT (of this Report)

This document has been approved for public release and sale; its distribution is unlimited. Reproduction in whole or in part is permitted by the U.S. Government.

17. DISTRIBUTION STATEMENT (of the abstract entered in Block 20, if different from Report)

18. SUPPLEMENTARY NOTES

19. KEY WORDS (Continue on reverse side if necessary and identify by block number)

Welding
Fabrication
Distortion
Residual Stress

20. ABSTRACT (Continue on reverse side if necessary and identify by block number)

Part I of the report covers the development of a monograph entitled "Analysis of Design and Fabrication of Welded Structures." The monograph deals with the prediction of stresses, strains and other effects produced by welding. Part II covers the development of analytical means for predicting and controlling weld distortion in welded aluminum structures. Distortion in welded structures is caused by three fundamental dimensional changes, namely transverse shrinkage, longitudinal shrinkage and angular change.

DD FORM 1 JAN 73 1473 EDITION OF 1 NOV 65 IS OBSOLETE
S/N 0102-014-6601

Unclassified
SECURITY CLASSIFICATION OF THIS PAGE (When Data Entered)

406 856

20. ABSTRACT (cont'd)

During the fabrication of actual structures, such as ships, airplanes and buildings which have various types of joints, these dimensional changes are conbined. Therefore, shrinkage distortion that occurs in structures can be extremely complex.

After a brief introduction, Section 2.2 discusses thermal stresses during welding, residual stresses and distortion in a general manner. The subsequent sections up to Section 2.6 discuss the analytical and experimental investigations carried out at M.I.T. on the prediction of various fundamental types of distortion. Finally, Section 2.7 deals with methods of distortion reduction, as they were tested by various investigators at M.I.T.

ACKNOWLEDGMENT

This is the final report of the Contract No. N00014-75-C-0469, NR 031-773.

We greatly appreciate the guidance and encouragement given by many people in the U.S. Navy, especially Dr. B. A. MacDonald and Dr. F. S. Gardner of the Office of Naval Research.

We would also like to thank Mr. F. R. Miller of the U.S. Air Force, Materials Laboratory for donating laser welded specimens for determining residual stresses.

ABSTRACT

This report is divided into two parts in accordance to the two tasks of the three-year research contract.

Part I covers the development of a monograph entitled "Analysis of Design and Fabrication of Welded Structures." The monograph deals with the prediction of stresses, strains and other effects produced by welding. A summary of the sixteen chapters, which consist the major portion of the work, is presented. Then, the computer programs contained in the six manuals of Section IV of the monograph are outlined.

Part II covers the development of analytical means for predicting and controlling weld distortion in welded aluminum structures. Basic background information is first presented and then the present state-of-the-art is summarized.

Distortion in welded structures is caused by three fundamental dimensional changes, namely transverse shrinkage, longitudinal shrinkage and angular change. During the fabrication of actual structures, such as ships, airplanes and buildings which have various types of joints, these dimensional changes are combined. Therefore, shrinkage distortion that occurs in structures can be extremely complex.

After a brief introduction, Section 2.2 discusses thermal stresses during welding, residual stresses and distortion in a general manner. The subsequent sections up to Section 2.6 disucss the analytical and experimental investigations carried out at M.I.T. on the prediction of various fundamental types of distortion. Finally, Section 2.7 deals with methods of distortion reduction, as they were tested by various investigators at M.I.T.

An Appendix presents results on residual-stress measurements of laser-welded joints.

TABLE OF CONTENTS

CONVERSION TABLE

To convert from	to	multiply by
inch (in.)	meter (m)	2.54×10^{-2}
inch	mm	2.54
foot (ft.)	meter	3.048×10^{-1}
$lbm/foot^3$	$kilogram/meter^3$	1.601×10
BTU	joule (J)	1.055×10^{3}
calorie	joule	4.19
lbf (pound force)	newton (N)	4.448
kilogram force (kgf)	newton	9.806
pound mass (lbm)	kilogram (kg)	4.535×10^{-1}
$lbf/inch^2$ (psi)	$newton/meter^2$ (N/m^2)	6.894×10^{3}
ksi	MN/m^2*	6.894
$kgf/meter^2$	$newton/meter^2$	9.806
Fahrenheit (t_F)	Celcius (t_c)	$t_c = (5/9)(t_F - 32)$

*MN (mega-newton) = 10^6 N (newton)

0.1 INTRODUCTION - OBJECTIVES AND TASKS

The objective of this three-year research contract is to develop analytical and empirical systems to assist designers, metallurgists and welding engineers in selecting optimum parameters in the design and fabrication of welded structures.

The program includes the following two tasks:

Task 1: Development of a monograph for predicting stresses, strains, and other effects produced by welding.

Task 2: Prediction and control of distortion in welded aluminum structures.

The first subject is of a general nature to assist designers and welding engineers so that they can utilize latest and most advanced information in design and fabrication of various types of welded structures. Computers have been used extensively to carry out computations required for various parametric studies.

The second subject, on the other hand, is aimed at developing information focused to a specific application. This subject has been selected because (1) the Navy is concerned about distortion problems which may occur during the fabrication of aluminum hulls of surface effect ships, and (2) information on distortion of aluminum structures is scarce.

The program started on December 1, 1974 and was completed on November 30, 1977.

0.2 PERSONNEL INVOLVED

The program was carried out under the supervision of Professor Koichi Masubuchi. He was assisted by a group of researchers whose names are given below. Professor Masubuchi was also assisted by several people including Mr. A. J. Zona (Instructor of the Welding Laboratory), Mr. F. Merlis (Specialist on stress measurement), and Mrs. June McLean (Secretary).

Those who made significant contributions to this research program include:

Professor Celio Taniguchi

Dr. Katsuhide Kitamura

Dr. Kouyu Itoga

Mr. Frank M. Pattee

Mr. Michael D. Serotta

Mr. Michio Nishida

Mr. David Beauchamp

Lt. Victor M. Brito

Mr. Vassilios J. Papazoglou

Lt. Guillermo E. Briceno

Mr. Chao Hsiung Lin

Mr. Edison Goncalves

Services by Professor Taniguchi, Dr. Kitamura, Dr. Itoga, Lt. Brito, Lt. Briceno, and Mr. Goncalves were available at no cost to this contract.

In addition, Dr. Toyohiko Muraki of the Atomic Energy of Canada, Ltd. has contributed in preparing manuals of computer programs.

0.3 REPORTS AND THESES

0.3.1 Reports

The following reports have been prepared:

1. The first status report issued on May 1, 1975.
2. The first special report on "Out-of-Plane Distortion of Welded Panel Structures" issued on July 3, 1975.
3. The first end-of-the-year report prepared in December, 1975.
4. A progress report issued on June 7, 1976.
5. The technical report entitled "Integration of M.I.T. Studies on Prediction and Control of Distortion in Welded Aluminum Structures" issued on September 20, 1976.
6. The second end-of-the-year report prepared in December, 1976.
7. The final report.

Copies of the technical report issued in September, 1976 were sent to all the people on the official distribution list as the first official technical report of this research contract.

In addition to these reports, drafts of Sections II and IV of the monograph were sent to the Navy reviewers.

0.3.2 Theses

The following theses were wholly or partially supported by this contract:

1. Frank M. Pattee, "Buckling Distortion of Thin Aluminum Plates During Welding," M.S. Thesis, August, 1975.
2. Michael D. Serotta, "Reduction of Distortion in Weldments," Ocean Engineer Thesis, August, 1975.

3. Michio Nishida, "Analytical Prediction of Distortion in Welded Structures," M.S. Thesis, March, 1976.

4. Victor M. B. Brito, "Reduction of Distortion in Welded Aluminum Frame Structures," Ocean Engineer Thesis, May, 1976.

5. David G. Beauchamp, "Distortion in Simpe, Welded Aluminum Structures," M.S. Thesis, May, 1976.

6. Chao Hsiung Lin, "Reduction of Distortion in Welded Aluminum Structures by Differential Heating," M.S. Thesis, February, 1977.

7. Guillermo E. Briceno, "The Distortion of Welded Thin Aluminum Stiffened Panels," Ocean Engineer Thesis, May, 1977.

8. Vassilios J. Papazoglou, "Analysis and Control of Distortion in Welded Aluminum Structures with Emphasis on Buckling Distortion," M.S. Thesis, to be submitted in January, 1978.

PART I DEVELOPMENT OF A MONOGRAPH FOR PREDICTING STRESSES, STRAINS, AND OTHER EFFECTS PRODUCED BY WELDING

1.1 PROGRESS OF TASK 1

The objective of Task 1 is to develop a monograph, which is now entitled "Analysis of Design and Fabrication of Welded Structures." In the early stages of the program it was thought that the monograph would consist of the following sections:

Section I: For practical users

Section II: Text

Section III: Additional tables and figures

Section IV: Computer programs

Section V: Material properties

Section VI: Annotated bibliography

Section II: Text is the main part of the monograph and provides detailed information for engineers who are interested in design and fabrication of welded structures. Section IV contains manuals of computer programs for analyzing heat flow, transient thermal stresses, residual stresses and distortion in weldments. Other sections provide supplementary information. Since Sections II and IV have become very extensive, it was decided toward the end of the program to reduce other sections to a minimum. The final composition of the monograph is as follows:

Section I: Summary of text

Section II: Text "Analysis of Design and Fabrication of Welded Structures"

Section III: Additional Tables and Figures, and Material Properties

Section IV: Computer Programs

This final report contains Section I: Summary of Text so that

people who read the final report will have some idea about the text which will be printed separately as a book. Another reason for not writing a section entitled "For Practical Users" is that Chapter I "Introduction" and Chapter 16 "Further Discussion on Some Selected Subjects" contains enough information which should help practical users of the monograph.

Section II will be published as a book. Arrangements for publication are being made with the Pergamon Press. The book will contain Section III, although its size will be kept to a minimum.

The distribution of Section IV: Computer programs has been limited to reviewers designated by the Office of Naval Research, primarily due to its volumenous size.

Section VI: Annotated bibliograph has been eliminated, because each chapter of Section II: Text contains an extensive list of references.

1.2 SUMMARY OF TEXT ENTITLED "ANALYSIS OF DESIGN AND FABRICATION OF WELDED STRUCTURES"

Table 1.1 shows the contents of the text. It is composed of 16 chapters and is about 1,300 pages long. The text is authored by Professor K. Masubuchi.

1.2.1 Major Objective of This Textbook

Figure 1-1 shows the importance of residual stresses and distortion in the design and fabrication of welded structures.

When a practicing engineer is concerned with residual stresses and distortion, he is also likely to be concerned with their adverse effects on the service performance of the structure which he is designing or fabricating. High tensile residual stresses in regions near the weld may promote brittle fracture, fatigue, or stress corrosion cracking. Compressive residual stresses and initial distortion may reduce buckling strength. What complicates the matter is that the extent of the effects of residual stresses is not only governed by residual stresses but also brittleness of the material. When the material is brittle, residual stresses may reduce the fracture strength of the weldment significantly. When the material is ductile, on the other hand, the effects of residual stresses are practically zero.

In fact what the practicing engineer wishes to do is to change design and fabrication parameters, such as plate thickness, joint design, welding conditions, welding sequence, etc., so that the adverse effects of residual stresses and distoriton can be reduced to acceptable levels. It is much better to achieve this goal during an early stage of design and fabrication rather than confronting the problem at later stages of fabrication.

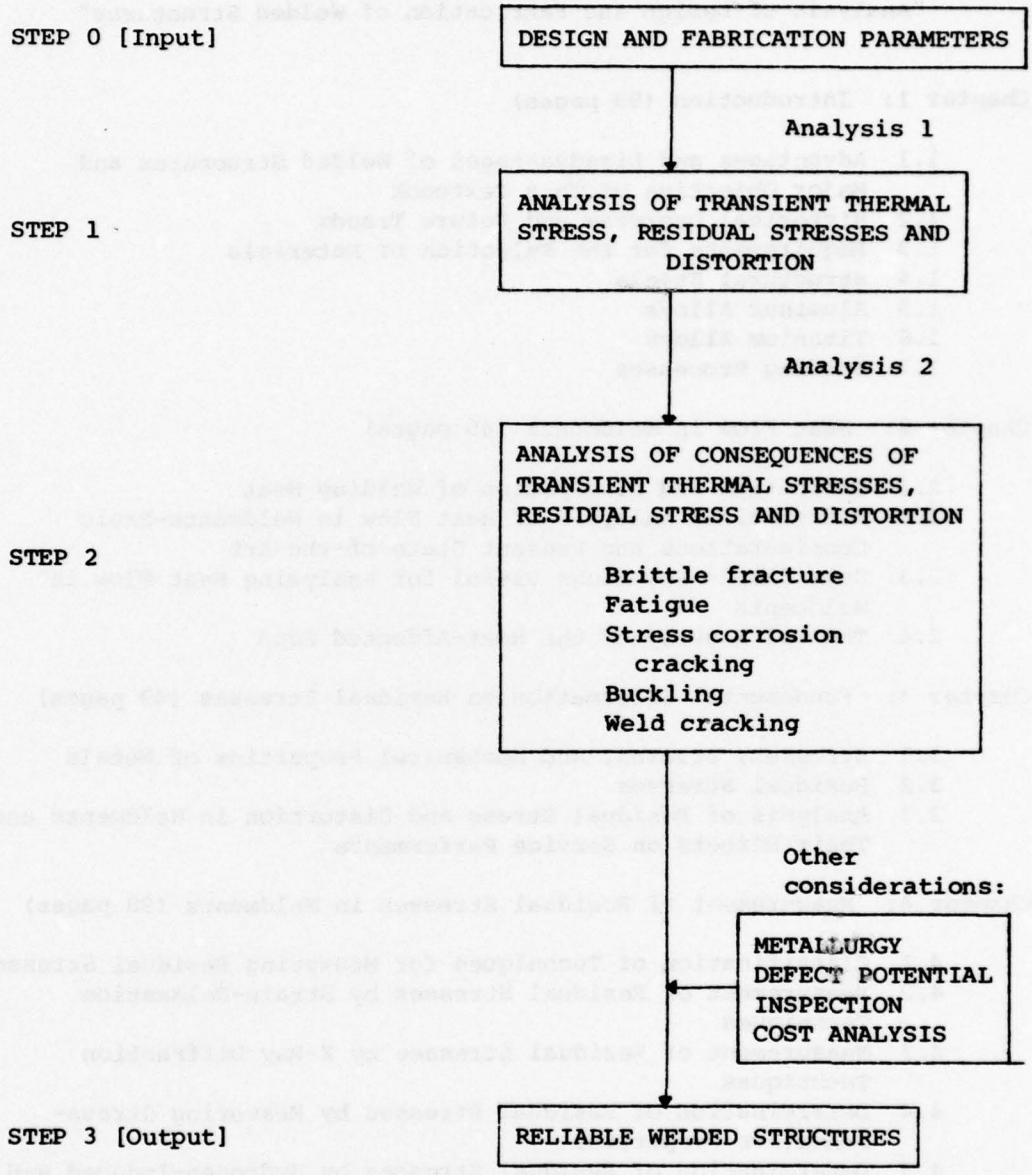

Figure 1-1 Importance of Residual Stresses and Distortion in the Design and Fabrication of Welded Structures

Table 1.1 Contents of the Text
"Analysis of Design and Fabrication of Welded Structures"

(Cont'd)

(Cont'd)

(Cont'd)

Chapter 13: Effects of Distortion and Residual Stresses on Buckling Strength of Welded Structures (52 pages)

- 13.1 Columns Under Compressive Loading
- 13.2 Plates and Plate Structures Under Compressive Loading
- 13.3 Corrugation Damage of Welded Ships and Allowable Distortion of Ship Bottom Plating
- 13.4 Spherical and Cylindrical Shells Subjected to External Pressure

Chapter 14: Weld Cracking and Joint Restraint (114 pages)

- 14.1 Classification of Weld Cracks
- 14.2 Hot Cracking
- 14.3 Cold Cracking
- 14.4 Weld Cracking Tests
- 14.5 Analytical and Experimental Determination of the Degree of Restraint of Weld Cracking Specimens and Joints in Actual Structures
- 14.6 Further Advancement of Mechanical Analysis of Cracking Especially by Use of Fracture Mechanics Theories

Chapter 15: Weld Defects and How They Affect Service Behavior (67 pages)

- 15.1 Weld Defects
- 15.2 Stress Concentrations Caused by Weld Defects
- 15.3 Effects of Defects on Ductile Fracture
- 15.4 Effects of Defects on Brittle Fracture
- 15.5 Effects of Defects on Fatigue Fracture
- 15.6 Nondestructive Inspection of Welds
- 15.7 Inspection of Welded Structures

Chapter 16: Further Discussions on Some Selected Subjects (46 pages)

- 16.1 Welding Design
- 16.2 Welding Fabrication

Total number of pages 1,297

In order to accomplish this task, the engineer needs at least two kinds of analyses:

1. An analysis of transient thermal stresses, residual stresses and distortion (Analysis 1 between Steps 0 and 1 in Figure 1-1).
2. An analysis of the effects of thermal stresses, residual stresses and distortion on the service behavior of welded structures (Analysis 2 between Steps 1 and 2).

The major objective of this textbook is to cover the present knowledge of these two analyses. Chapters 2 through 7 cover Analysis 1, while Chapters 8 through 14 cover Analysis 2.

The engineer also must consider many subjects other than residual stresses and distortion, and their consequences. These subjects include metallurgy, weld defect potential, inspection, fabrication cost, etc. The welding conditions that would give the minimum amount of distortion may not be useable because of the poor metallurgical properties or excessively high fabrication cost, for example. Therefore, what the enigneer really needs is an integrated system which can analyze all the relevant subjects required. However, such an integrated system, yet to be developed, would be too extensive to be covered in a single textbook.

This textbook primarily covers subjects related to residual stresses and distortion, and their consequences. Attempts have been made to minimize duplications with other existing textbooks. For example, a number of books have been written on brittle fracture, fatigue, stress corrosion cracking, buckling, etc. Discussions in this textbook

emphasize these subjects characteristic of welded structures, especially those related to residual stresses and distortion.

In preparing this textbook, discussions on welding processes, materials, and welding metallurgy have been kept to a minimum. The author plans to cover these subjects in subsequent textbooks with the desire that the entire system will one day be fully integrated.*

1.2.2 Chapter 1: Introduction

This chapter provides the necessary background information on structural materials and welding processes to enable those readers whose knowledge in these areas is limited to understand the remainder of this textbook.

Since this textbook discusses at length the problems associated with the design and fabrication of welded structures, it risks creating the impression that welded structures are impractical due to their many special problems and their tendency to fracture. On the contrary, welded structures are superior in many respects to riveted structures, castings and forgings. The first portion of Chapter 1 discusses briefly advantages and disadvantages of welded structures and the major objective of this textbook.

Chapter 1.2 presents a historical overview of materials and joining technologies used for building large structures including ships, bridges, pressure vessels, etc. It also discusses future trends.

Chapter 1.3 discusses requirements for selection of materials. The subjects covered include (1) fracture toughness, (2) fatigue strength,

*The following three textbooks are under preparation: (1) Welding Engineering, (2) Fracture of Welded Structures, (3) Materials for Ocean Engineering (revision of the first edition published in 1970).

(3) resistance against corrosion and stress corrosion cracking, and

(4) other properties.

Chapter 1.4 provides information on structural steels, including carbon steels, low-alloy high-strength steels, quenched-and-tempered steels, and maraging steels.

Chapter 1.5 discusses aluminum alloys, while Chapter 1.6 discusses titanium alloys.

Chapter 1.7 provides information on various welding processes, including shielded metal-arc, submerged arc, gas tungsten-arc, gas metal-arc, electroslag, and electrogas processes.

1.2.3 Chapter 2: Heat Flow in Weldments

The heat supplied by a welding arc produces complex thermal cycles in the weldment and these in turn cause changes to take place in the microstructure of the heat-affected zone, cause transient thermal stress and metal movement, and result in the creation of residual stress and distortion in the finished product. In order to analyze these problems, we must first analyze heat flow during welding.

Chapter 2.1 discusses generation and dissipation of welding heat.

Chapter 2.2 discusses mathematical analysis of heat flow in weldments. First a brief discussion is given on basic considerations on heat flow during welding. Then a discussion is made of the present state-of-art.

Chapter 2.3 presents some simple solutions useful for analyzing heat flow in weldments. Discussions cover temperature distributions in the quasi-stationary state as well as the non-stationary state.

Chapter 2.4 discusses the thermal history of the heat affected zone, while Chapter 2.5 discusses heat flow problems of the electrode and the

weld metal.

1.2.4. Chapter 3: Fundamental Information on Residual Stresses

This chapter presents introductory information on residual stresses.

First, a brief discussion is given on stresses, strains, and mechanical properties of metals.

Chapter 3.2 discusses fundamentals of residual stresses. A discussion is given on similarities among the analysis of residual stresses, the vortex theory in hydrodynamics and the fracture mechanics theory. Then a discussion is given on the development of methodologies for analyzing residual stresses and distortion in weldments and for determining their effect on service performance.

1.2.5 Chapter 4: Measurement of Residual Stresses in Weldments

First, a brief discussion is made of classification of techniques for measuring residual stresses. Chapter 4.2 discusses measurement of residual stresses by stress-relaxation techniques. It provides a review of different techniques, including the sectioning technique using electrical-resistance strain gages, the Gunnert technique, the Mathar-Soete drilling technique, the Stäblein successive milling technique, the Rosenthal-Norton sectioning technique, etc. Chapter 4.3 covers measurement of residual stresses by X-ray diffraction.

Chapter 4.4 discusses determination of residual stresses by measuring stress-sensitive properties. Techniques discussed include ultrasonic techniques and hardness measuring techniques. Chapter 4.5 discusses determination of residual stresses by hydrogen-induced and stress-corrosion cracking techniques.

Chapter 4.6 discusses selection and use of appropriate measurement techniques and evaluation of results. Chapter 4.7 discusses strain

measurement of transient strains during welding, and chapter 4.8 discusses use of mathematical analysis in the experimental study of residual stresses and distortion.

1.2.6 Chapter 5: Transient Thermal Stresses and Metal Movement During Welding

Because a weldment is heated locally by the welding heat source, the temperature distribution in the weldment is not uniform and changes as the welding progresses. During the welding cycle, complex strains occur in the weld metal and the base metal regions near the weld.

With the advancement of computer technology and new analytical techniques such as the finite-element method, it has become possible to analyze transient thermal stresses and metal movement without spending a prohibitive amount of time and money. These transient stresses can even be computer-simulated.

Chapter 5.1 discusses briefly how thermal stresses are produced during welding. Chapter 5.2 discusses historical developmentof studies of thermal stresses and metal movement during welding.

Chapter 5.3 discusses one-dimensional analyses which consider only the stress component parallel to the welding direction. Chapter 5.4 discusses two-dimensional analyses using finite-element methods. Chapter 5.5 discusses analyses of stresses in some three-dimensional cases including cylindrical shells and heavy weldments.

Chapter 5.6 discusses experimental studies on thermal stresses and metal movement. In a series of experiments conducted at M.I.T. on weldments made in various materials and thicknesses, thermocouples were used to measure temperature changes and electrical resistance strain gages were used to measure strain changes. The experiments were conducted

under different conditions as follows:

1. Materials: Low-carbon steel, high-strength steels, stainless steel, aluminum alloys, titanium alloys, columbium and tantalum.
2. Plate Thickness: 0.3 to 25 mm
3. Joint Types and Processes: Bead-on-Plate and butt welds in single and multipasses (up to 20 passes); gas metal-arc and gas tungsten-arc as well as flame heating of plates.

Chapter 5.6 presents some of the experimental results compared with analytical predictions.

Chapter 5.7 discusses experimental results on thermal stresses in weldments in high-strength steels. Chapter 5.8 discusses experimental results on thermal stresses and metal movement during welding along the longitudinal edge of a strip.

Chapter 5.9 discusses computer simulation. Once it is proved that the analytical models are reasonably accurate it is possible to simulate thermal stresses and metal movement by computer. Since the one-dimensional program is relatively inexpensive, it can be used in various ways. Chapter 5.9 discusses two sets of analyses as follows:

1. The effects of welding parameters on thermal stresses and the resulting residual stresses in aluminum welds.
2. The effects of welding parameters on the longitudinal distortion that takes place due to the edge welding of a strip.

1.2.7 Chapter 6: The Magnitude and Distribution of Residual Stresses in Weldments

Chapter 6 presents some fundamental information on residual stresses: How to understand their mechanisms and how to analyze the

effects of various factors on their magnitude and distribution.

Chapter 6.1 discusses development of techniques for analyzing residual stresses in weldments. Chapter 6.2 discusses residual welding stresses and reaction stresses. Chapter 6.3 discusses analysis of residual stresses in restrained butt welds.

Chapter 6.4 discusses the distribution of residual stresses in some typical joints, including plug weld, circular patch weld, welded shapes and columns, and welded pipes.

Chapter 6.5 discusses residual stresses in weldments in various materials, including low-carbon steel, low-alloy high-strength steels, stainless steel, aluminum, and titanium alloys.

Chapter 6.6 discusses the effect of specimen size on residual stresses. Chapter 6.7 discusses residual stresses in heavy weldments. Chapter 6.8 discusses effects of welding sequence on residual stresses.

1.2.8 Chapter 7: Distortion in Weldments

Residual stresses, discussed in Chapter 6, and distortion, discussed in this chapter, are closely related phenomena. During heating and cooling in the welding cycle, thermal strains occur in the weld metal and base-metal regions near the weld. The strains produced during heating are accompanied by plastic upsetting. The stresses resulting from these strains combine and react to produce internal forces that cause bending, buckling, and rotation. It is these displacements that are called distortion.

Chapter 7 presents the present state of knowledge of weld distortion analysis. Chapter 7.1 discusses fundamental types of distortion as

follows:*

1. Transverse shrinkage perpendicular to the weld line.

2. Longitudinal shrinkage parallel to the weld line.

3. Angular distortion (rotation around the weld line).

Chapter 7.2 presents general introduction to weld distortion. It first discusses different approaches to solving distortion problems. It then discusses books and reviews already available. A discussion is made on methodologies for analyzing weldment distortion.

Chapter 7.3 discusses existing allowable-distortion standards.

Chapter 7.4 discusses transverse shrinkage of butt welds. It presents formulas for estimating transverse shrinkage and then presents analytical and experimental results on transverse shrinkage.

Chapter 7.5 discusses transverse shrinkage in fillet welds, while chapter 7.6 discusses angular changes of butt welds.

Chapter 7.7 discusses angular changes of fillet welds and the resulting out-of-plane distortion. It presents experimental data and analytical predictions.

Chapter 7.8 discusses how various design and welding parameters affect the angular distortion of fillet welds. It also discusses various methods of reducing distortion.

Chapter 7.9 discusses longitudinal shrinkage of butt welds, while Chapter 7.10 discusses longitudinal shrinkage of fillet welds.

Chapter 7.11 discusses longitudinal bending distortion. When the weld line does not coincide with the neutral axis of a weld structure,

---

*For further definitions of various types of distortion see Figure 2-2 in Part II of this final report.

the longitudinal shrinkage of the weld metal induces bending moments, resulting in longitudinal distortion of the structure. This type of distortion is of special importance when fabricating T-bars and I-beams. Chapter 7.12 discusses buckling distortion. When thin plates are welded, residual compressive stresses occur in areas away from the weld and cause buckling. Buckling distortion occurs when the specimen length exceeds the critical length for a given thickness in a given size specimen. This chapter presents analytical predictions and experimental data.

Chapter 7.13 discusses the distortion-analysis of complex welded structures.

Chapter 7.14 discusses methods of reducing distortion in weldments. The following subjects are discussed:

1. A review of commonly-used distortion-reduction methods.
2. How external restraints affect residual stress and distortion.
3. Distortion-reduction through thermal-pattern control.
4. The reduction of out-of-plane distortion through stretching and heating.
5. The reduction of the longitudinal distortion of built-up beams through differential heating.

1.2.9 Chapter 8: The Strength of Welded Structures: Fundamentals

This short chapter is an introduction to the later chapters of this monograph which discuss various subjects related to the strength of welded structures. Chapter 8 covers the following subjects:

1. Strength of "idealistic" and "realistic" structures.
2. Changes in residual stresses in weldments subjected to tensile loading.

3. Local stress concentration caused by out-of-plane distortion.

4. Instability of columns under compressive loading.

1.2.10 Chapter 9: Fracture Toughness

Chapter 9.1 discusses elementary concepts of fracture. Chapter 9.2 discusses brittle fractures of welded structures.

To avoid brittle fractures in a welded structure, the material used must have adequate notch toughness. Chapter 9.3 discusses how to evaluate notch toughness. Chapter 9.4 discusses various tests for evaluating notch toughness.

Chapter 9.5 discusses low applied-stress fracture of welded structures. It has been found that:

1. Brittle fractures in welded structures often originate from small defects; the overall stress is often very low (only 70 MN/m^2 or so which is only about 1/3 the yield strength of the material used).

2. Based upon the fracture mechanics theory, which will be discussed in Chapter 10, unstable fractures occur when stresses are applied to a structure containing a crack longer than a given value. However, the critical crack of low-carbon steel at the yield stress is several inches long.

Then why does a welded structure fail at a stress level of only 1/3 the yield strength and from a very small crack? This subject is discussed in Chapter 9.5.

Chapter 9.6 discusses effects of chemical composition and manufacturing processes on notch toughness.

Chapter 9.7 discusses notch toughness requirements and fracture

control. Chapter 9.8 discusses notch toughness of weld metals.

1.2.11 Chapter 10: Theoretical and Experimental Studies of the Brittle Fracture of Welded Structures

Chapter 10.1 discusses theories of brittle fracture. Chapter 10.2 presents the fracture mechanics theory.

Chapter 10.3 discusses values of fracture toughness and critical crack length of various materials. The length of the critical crack generally decreases as the strength level of a material increases.

Chapter 10.4 discusses applications of fracture mechanics approach to fracture control in structural steel.

Chapter 10.5 discusses catastrophic failures of welded structures from subcritical cracks. There is evidence that fractures have occurred in actual structures from flaws smaller than critical size. Chapter 10.6 discusses how catastrophic failures can occur from cracks smaller than the critical size. Both experimental results and analytical predictions are presented.

1.2.12 Chapter 11: The Fatigue Fracture of Weldments as it Relates to Residual Stresses

This chapter discusses the fatigue fracture of weldments as it relates to residual stress. Although the question of how residual stresses affect the fatigue strength of a welded structure is even now, after many years of research, not fully understood, and although the experts on this subjects still disagree, conclusions can nevertheless be drawn.

Some experts blame residual stresses whenever the cause of a failure in a welded structure cannot be explained in some other way. Others believe residual stress effects are wiped out after the structure is subjected to repeated loading and therefore do not affect the fatigue

strength. It is the author's opinion that under certain conditions the residual stresses do affect the fatigue strength of a welded structure, though in many other cases the residual stresses present have only negligible effects on the fatigue strength.

In this chapter attempt was made to emphasize the practical rather than the theoretical approach, and such topics as how residual stresses may actually be used to increase the fatigue strength of a structure were examined.

Discussions in this chapter are presented in the following way:

1. Introduction to fatigue fracture
2. High-cycle fatigue
3. Low-cycle fatigue
4. Fatigue failures of structures
5. Some methods of improving the fatigue strength of weldments, including prior overloading, peening, local compression and spot heating.

1.2.13 Chapter 12: The Role of Residual Stress in Stress Corrosion Cracking and Hydrogen Embrittlement

This chapter discusses how various aspects of the environment affect the fracture characteristics of weldments. To avoid a lengthy discussion, it is assumed that the reader already has a basic knowledge of stress corrosion cracking and hydrogen embrittlement.

Chapter 12.1 discusses corrosion control problems in marine structures. Chapter 12.2 presents a brief discussion on stress corrosion cracking, while Chapter 12.3 discusses briefly hydrogen embrittlement.

Chapter 12.4 discusses the role of residual stresses in the stress

corrosion cracking and hydrogen-induced cracking of weldments.

Chapter 12.5 discusses a mathematical analysis based upon the fracture mechanics theory to determine the relationship between the residual stress distribution and the crack pattern.

1.2.14 Chapter 13: Effects of Distortion and Residual Stresses on Buckling Strength of Welded Structures

Failures due to instability, or buckling, sometimes occur in metal structures composed of slender bars and/or thin plates when they are subjected to compressive axial loading, bending, and/or torsional loading. It is known that residual compressive stresses decrease the buckling strength of a metal structure. Initial distortions caused by residual stresses also decrease the buckling strength. Presented in Chapter 8.4 are preliminary discussions on effects of initial distortion and residual stresses on buckling. Chapter 13 discusses the following subjects:

1. Columns under compressive loading.
2. Plates and plate structures under compressive loading.
3. Corrugation damage of welded ships and allowable distortion of ship bottom plating.
4. Spherical and cylindrical shells subjected to external pressure.

Numerous studies have been made on the general subject of effects of initial distortion and residual stresses on buckling; however, only a small portion of these studies concerned specifically with the effects of distortion and residual stresses on the buckling strength of welded structures.

This chapter discusses effects of distortion and residual stresses on buckling strengths of welded structures. We face a problem, however. The

analysis of buckling strength of a structure, especially beyond yielding, is very complex by itself. The inclusion of effects of initial distortion and residual stresses on plastic buckling of a welded structure requires very extensive mathematical analyses. To avoid too lengthy analyses, this chapter provides a summary of pertient experimental and analytical studies with limited analytical derivations.

1.2.15 Chapter 14: Weld Crackling and Joint Restraint

A large amount of research, primarily experimental and metallurgical, has been conducted to investigate cracks in weldments. Weld cracking occurs for one or both of the following reasons:

1. The material is brittle.

2. High tensile stresses (transient or permanent) are present.

Metallurgical studies tend to concentrate on material brittleness caused by welding, while mechanical studies tend to concentrate on the stresses produced during welding. There have been several books and reviews on metallurgical aspects of weld cracking. However, only a few books have discussed extensively the mechanical aspects of welding cracking. An obvious reason is the difficulty in analytically determining stresses in a weldment, especially in the weld metal and the heat-affected zone. This chapter discusses primarily mechanical aspects of weld cracking.

Discussions in this chapter are concerned primarily with cracks in weldments in steel, especially high-strength steels. Some of the fundamental aspects should also be applicable to weld cracks in other materials.

Chapter 14.1 discusses classification of weld cracks. Chapter 14.2 discusses hot cracking, while Chapter 14.3 discusses cold cracking.

Chapter 14.4 discusses weld cracking tests including:

1. Lehigh restraint test
2. Houldcroft fishbone test
3. Circular patch and U.S. Navy circular patch tests
4. Controlled thermal severity (CTS) test
5. Cruciform test
6. Longitudinal-weld underbead-cracking test
7. Varestraint test
8. Rigid restraint cracking (RRC) test and tensile restraint cracking (TRC) test
9. Implant test

Chapter 14.5 discusses analytical and experimental determination of the degree of restraint of weld cracking test-specimens and joints in actual structures.

Chapter 14.6 discusses further advancement of mechanical analysis of cracking especially by use of fracture mechanics theories.

1.2.16 Chapter 15: Weld Defects and How They Affect Service Behavior

The subject of weld defects and how they affect the service performance of welded structures is too complex to be thoroughly covered in just one chapter. Although this monograph covers subjects related to residual stress, a discussion of weld defects and their effects are presented here because residual stresses and weld defects are closely related:

1. Weld defects most frequently occur in regions near the weld where high residual stresses exist; how much weld defects affect the service behavior of a welded structure is affected in turn by the nature and the magnitude of these residual stresses.
2. Residual stresses and distortion can be classified as imperfec-

tions, or as deviations from an ideal structure (see Chapter 8).

This chapter will concentrate on how residual stress and distortion affect the extent to which weld defects will affect the service behavior of a welded structure.

This chapter covers the following subjects:

15.1 Weld defects

15.2 Stress concentrations caused by weld defects

15.3 Effects of defects on ductile fracture

15.4 Effects of defects on brittle fracture

15.5 Effects of defects on fatigue fracture

15.6 Nondestructive inspection of welds

15.7 Inspection of welded structures

1.2.17 Chapter 16: Further Discussions on Some Selected Subjects

In the preceding chapters, the emphasis of discussion was placed on scientific information on subjects covered by presenting experimental data and analytical results. Many figures, tables, and formulas were included to present quantitative rather than qualitative discussions. Although they contain useful information, the author feels that an additional chapter is needed to assist practicing engineers to fully utilize the information presented in the previous chapters.

For example, if one is interested in using peening for reducing distortion, one should also consider possible adverse effects of peening on brittle fracture. The use of intermittent welding is an efficient way of reducing distortion, especially longitudinal distortion; however, it may result in a reduction in fatigue strength. Although information pertinent to these subjects is given in various parts of this textbook,

this chapter attempts to draw these important considerations together for the convenience of the reader.

Thus, the major objective of this chapter is to discuss various subjects of design and fabrication considerations which practicing engineers are likely to face. However, this chapter is by no means intended to cover all important subjects related to design and fabrication; rather, it is limited to some selected subjects related to residual stresses, distortion and their consequences, which have been examined in previous chapters.

As shown in Figure 1-1, problems which practicing engineers face are related not only to residual stresses and distortion but also to various other subjects including welding metallurgy, nondestructive testing, etc. These problems are dealt with in this chapter.

Chapter 16.1 discusses welding design. The following subjects are discussed:

1. Basic principles for preventing brittle fractures.
2. Basic principles for preventing fatigue fractures.
3. Effects of structural discontinuities.
4. Butt joints vs. lap joints.
5. Intermittent vs. continuous fillet welds.
6. Scallops and small radius cuts.
7. Plug welds or slot welds.
8. Control of distortion in the design stage.

Chapter 16.2 discusses welding fabrication. The following subjects are discussed:

1. Welding heat input limitation.

2. Effects of welding parameters on shrinkage and cracking potential.
3. Preheat and interpass temperature.
4. Influence of joint restraint on residual stresses and distortion.
5. Postweld thermal treatments.
6. Vibratory stress relieving.
7. Peening.
8. Mechanical stress relieving and prooftesting.
9. Residual stresses and distortion in weldments in various materials.

1.3 SECTION IV: COMPUTER PROGRAM

Section IV contains manuals of computers programs for analyzing heat flow, transient thermal stresses, residual stresses and distortion in weldments. Six manuals were prepared and they were sent to reviewers designated by the Office of Naval Research. A brief description of these programs is given in the following pages.

Manual #1 contains several computer programs useful for the analysis of heat flow in weldments. It covers one-dimensional, two-dimensional as well as three-dimensional analyses. Some programs use analytical solutions while others use finite-element methods.

Manual #2 contains computer programs for one-dimensional analysis of thermal stresses during welding. The programs analyze only the stress component parallel to the weld line.

Manual #3 includes computer programs capable of analyzing stresses and strains in a two-dimensional stress field either in the plane stress or in the plane strain condition.

A typical case of the 2D plane stress condition is the stress field that is set up during the welding of plates, as shown in Figure 1-2. The program can analyze the transient stresses in any location on the plate, including the regions near the edges at the plate. However, it is assumed that stresses are uniform in the thickness direction.

A typical case of the 2D plane strain condition is the stress field in a cross section in the central portion of a long weldment, as shown in Figure 1-3. The weld line is in the z-direction. The stresses in cross section z at time t are assumed to be the same as the stresses in cross section $z + \Delta z$, provided that:

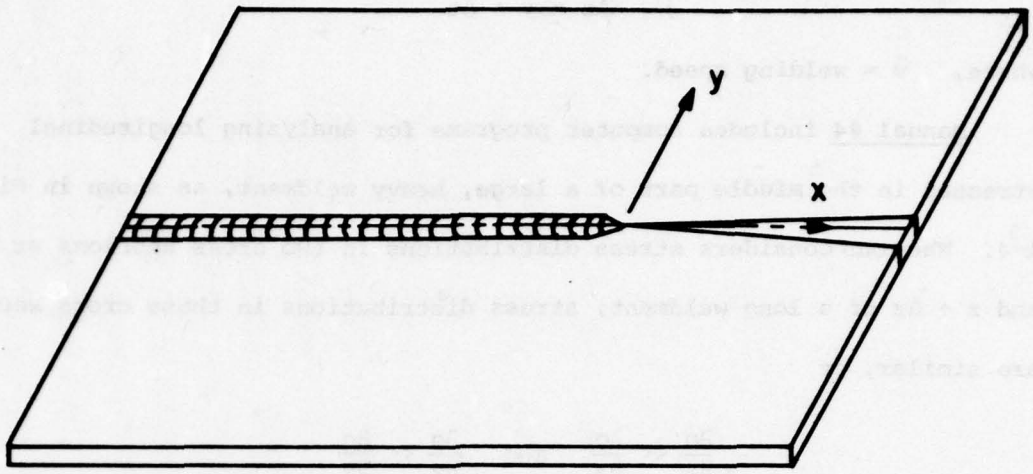

Fig. I-2 Typical 2D Plane Stress Field -- Welding Plates

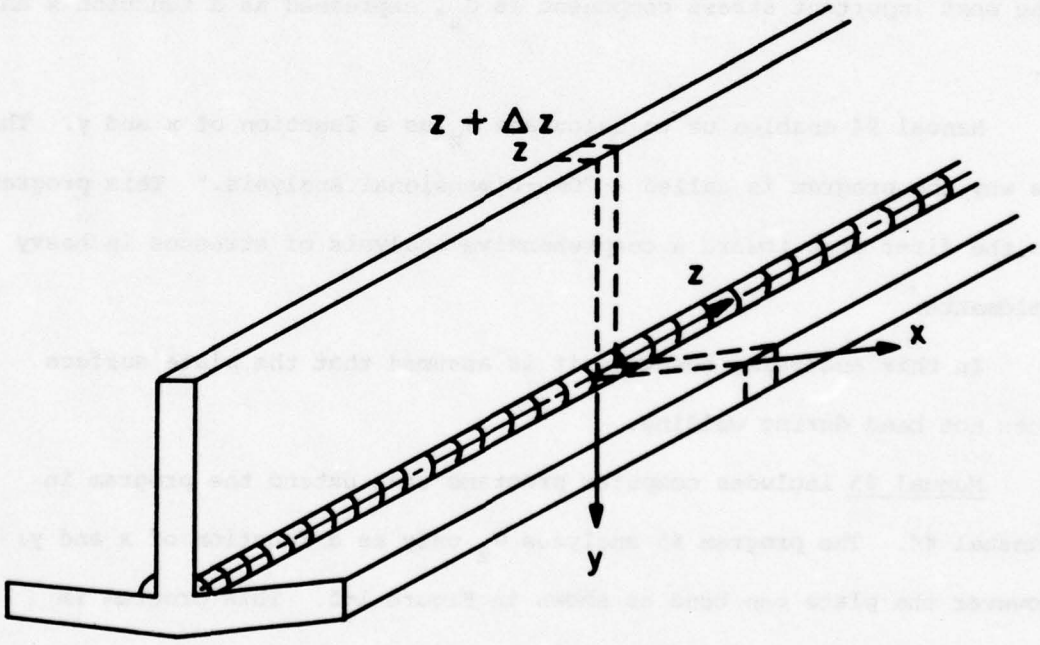

Fig. I-3 Typical 2D Plane Strain Field -- Angular Distortion of a Built-Up Beam

$$\Delta z = v \cdot \Delta t$$

where, v = welding speed.

Manual #4 includes computer programs for analyzing longitudinal stresses in the middle part of a large, heavy weldment, as shown in Figure 1-4. When one considers stress distributions in two cross sections at z, and $z + \Delta z$ of a long weldment, stress distributions in these cross sections are similar, or

$$\frac{\partial \sigma}{\partial z} << \frac{\partial \sigma}{\partial x} \quad \text{and} \quad \frac{\partial \sigma}{\partial z} << \frac{\partial \sigma}{\partial y}$$

In other words, stress changes in the z-direction are much smaller than those in the x-direction and the y-direction. Under such a condition, the most important stress component is σ_z, expressed as a function x and y.

Manual #4 enables us to calculate σ_z as a function of x and y. This is why the program is called a "One-Dimensional Analysis." This program is the first step toward a comprehensive analysis of stresses in heavy weldments.

In this analysis, however, it is assumed that the plate surface does not bend during welding.

Manual #5 includes computer programs that extend the program in Manaual #4. The program #5 analyzes σ_z only as a function of x and y; however the plate can bend as shown in Figure 1-5. This program is suitable for analyzing longitudinal bending distortion.

Manual #6 presents the one-dimensional program for analyzing thermal stresses and metal movement during welding fabrication of a built-up beam, as shown in Figure 4-8.

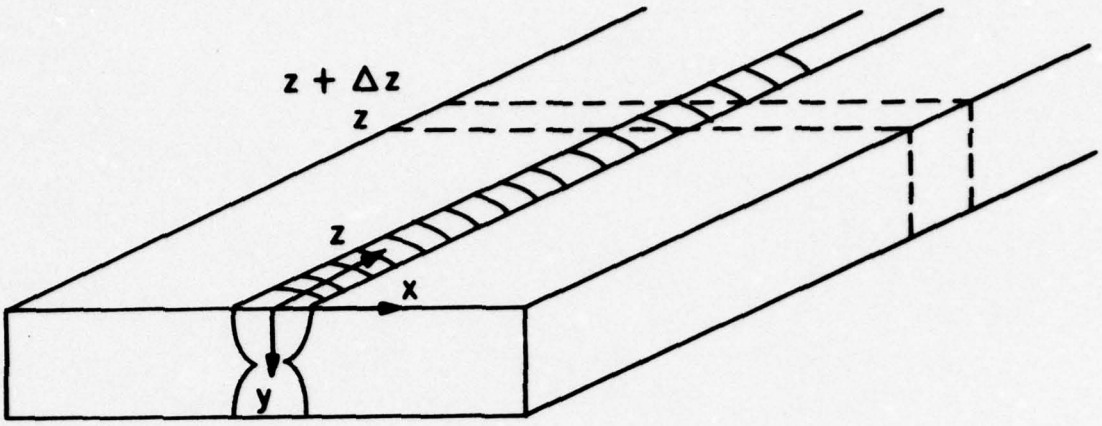

Fig. I-4 Typical Case for ID Analysis in Manual #4 - Heavy Weldment

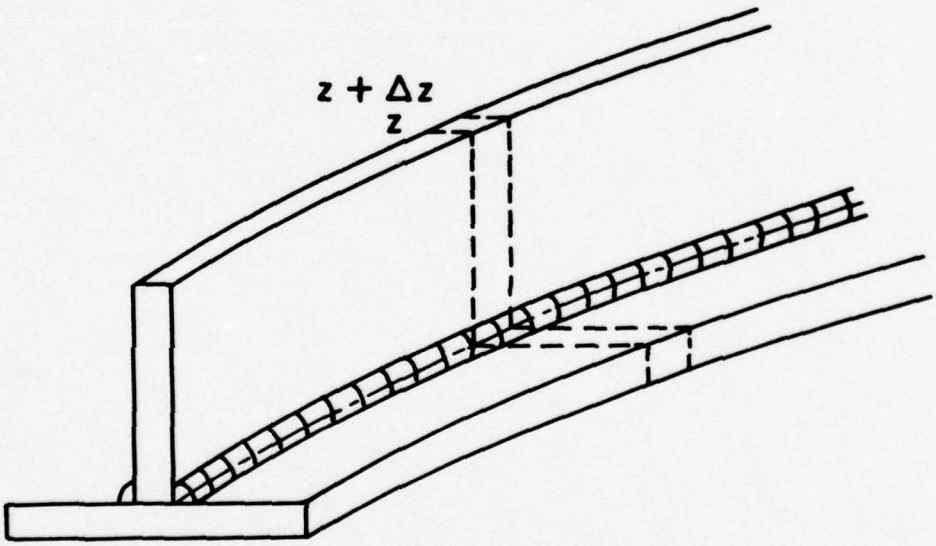

Fig. I-5 Typical Case for ID Analysis Including -- Longitudinal Bending Distortion of a Build-Up Beam

PART II PREDICTION AND CONTROL OF DISTORTION IN WELDED ALUMINUM STRUCTURES

2.1 PROGRESS OF TASK 2

The objectives of Task 2 are as follows:

1. Identify potential areas where distortion can cause problems during welding fabrication of aluminum structures, especially surface effect ships. And analyze, as much as possible, the extent of the problems.
2. Conduct parametric studies of some of the problems and suggest possible remedies which include changes of design and welding procedures.
3. Conduct research on methods for reducing and controlling distortion of several structural members of surface effect ships.

2.1.1 Accomplishment During the First Year Through November 30, 1975

Fairness Tolerance. First, an analysis was made of out-of-plane distortion of welded panel structures. Computer programs were developed by Kitamura and Taniguchi to do the following:

1. Determine allowable unfairness as a function of service conditions (compressive stresses and water pressure) and structural parameters (plate thickness, floor spacing, etc.)
2. Then determine the maximum weld size to produce the allowable unfairness.

Calculations were made of steel and aluminum strucutures. Analytical results were compared with unfairness values allowed by Navy Specifications. Results of the analysis were described in the Special Report dated July 3, 1975.

Buckling Distortion. Buckling distortion may become a serious problem in welding fabrication of structures in thin plates, say 6 mm or

less. When the plate is thin, it may buckle due to residual stresses only. A particular nature of buckling distortion is that the amount of distortion is much greater than that caused by angular distortion. Consequently, buckling distortion can be avoided by (1) avoiding the use of plates that are too thin and (2) reducing the spacing between the stiffeners.

As the first step, Pattee studied buckling distortion of butt welds in aluminum. The objectives of his study included the following:

1. To experimentally determine the buckling behavior (during and after welding) of aluminum plates of various dimensions using a number of different boundary conditions. The experiments were made using 18 butt welds 1.5 to 4.5 mm thick, 9.3 to 1.2 m wide, and 1.8 m long.
2. To analyze these transient temperature and strain changes by utilizing one-dimensional and two-dimensional computer programs developed at M.I.T. comparing the analytical results with the experimental data.
3. To determine the critical panel size under which buckling distortion would not occur.

As a result of this study, a computer-aided system was developed for the prediction and control of buckling distortion. Since the study by Pattee was well under way when this research contract started, only a small portion of his work was supported by the funds from ONR.

The best way to control buckling distortion is to prevent its happening by properly selecting design parameters and welding

procedures.* Currently there are no Navy specifications that deal with buckling.

2.1.2 Accomplishment During the Second Year Through November 30, 1976

Out-of-Plane Distortion. The results obtained in the analysis conducted during the first year indicated that serious distortion problems can occur during welding fabrication of aluminum structures using plates thinner than 12 mm or 9.5 mm. However, little data have been published on the two-dimensional distribution of distortion in panel structures of aluminum, i.e. a structure in which longitudinal and transverse stiffeners are fillet welded to a plate. Brito conducted a study with the following objectives:

1. To determine experimentally the out-of-plane distortion in welded panel structures, and compare the data with the Navy specification.
2. To develop an analytical procedure for predicting out-of-plane distortion caused by angular changes along the fillet welds.
3. To study experimentally how distortion can be reduced by altering the thermal pattern during welding a panel structure.

Beauchamp also studied ways of reducing out-of-plane distortion in panel structures. He studied the effects of both buckling distortion due

*The following is a typical example of buckling distortion that occurred in a manufacturing plant. Workers experienced a sudden increase of distortion after some changes of welding procedures of stiffened panel structures. Stiffeners were spot welded to a thin plate. Spacings between spot welds were decreased to increase the fatigue strength of the structure, and the sudden increase of distortion followed.

Answer: Buckling distortion occurred because the amount of welding exceeded the critical value. Therefore, the problem can be solved by (1) increasing plate thickness, (2) reducing stiffener spacing, or (3) reducing the amount of welding, or using some combination of the above three methods.

to butt welds and angular distortion due to fillet welds. He also studied how distortion can be reduced by clamping.

Buckling Distortion. Although Pattee's study provides basic data on butt welds, it is very important to extend the study to cover stiffened panel structures, beacuse in most practical applications the thin plate structures have stiffness. Beauchamp developed data on thermal strains and residual stresses in welded thin panel structures.

Longitudinal Distortion of Built-Up Beams. During the last few years a series of research programs were carried out at M.I.T. on the longitudianl distortion produced during the welding fabrication of T-beams.

Nishida carried out a study program having the following objectives:

1. To develop a computer program for the analyzing of thermal structures and metal movement during the welding fabrication of a built-up beam.
2. To analyze the effects of the use of clamping and the effects of the thermal pattern on weld distortion.

As a part of the thesis study, Nishida developed a computer program for analyzing the deflection that occurs during welding fabrication of a T-shaped beam by fillet welding a flange plate to a web plate. The program is capable of studying the effects of clamping and differential heating.*

*In this technique a web or a flange is heated to a certain temperature before welding to compensate for the welding distortion. Distortion can be reduced significantly by selecting a proper temperature differential.

Nishida analyzed experimental data obtained by Serotta on differential heating. The computer programs developed by Nishida can be used to determine optimum welding and preheating conditions for joining T-beams of various sizes.

Residual Stresses in Laser-Welded Joints. Laser welding, although not fully developed, seems to offer attractive possibilities. We have been fortunate to receive two laser welded specimens (in carbon steel and titanium) through the courtesies of Air Force Materials Laboratory, Sciaky Brothers, Inc., and Avco Everett Research Laboratories, Inc.

A study was made by Papazoglou to determine the residaul stresses in these plates. The results are given in the Appendix of the progress report dated June 7, 1976. It was found that residual stresses in the titanium welds are as we expected: High tensile residual stresses exist in the longitudinal direction in areas near the weld, but the width of the tension zone is very narrow. However, the results obtained on the carbon-steel welds were inconclusive.

Fortunately, arrangements were made to receive more laser-welded specimens for further investigation of residual stresses and distortion.

Results of the experiment are given in the APPENDIX A.

Preparation of the Integrated Report. The technical report entitled "Integration of M.I.T. Studies on Prediction and Control of Distortion in Welded Aluminum Structures" was prepared as a part of Task 2. The work was done primarily by Papazoglou. This report provides the present state-of-the-art on prediction and control of distortion in welded aluminum structures by integrating results obtained recently at M.I.T. The integration effort was continued during the third year.

2.1.3 Accomplishment During the Third Year Through November 30, 1977

Efforts during the third year covered the following:

1. Further study on weld distortion in aluminum structures
2. Further study on buckling distortion
3. Further studies on laser-welded specimens
4. Integration of research results obtained at M.I.T. and elsewhere

Study on Aluminum Welds. The efforts were carried out primarily by two graduate students, Lin and Briceno.

Lin, who received an M.S. degree in February 1977, conducted a thesis study on reduction of distortion by differential heating. As stated earlier, it has been found that distortion can be reduced significantly by intentionally altering the thermal pattern of a weldment. Nishida has analyzed using computer programs experimental data obtained by Serotta during joining T-beams.

Obviously distortion can be reduced significantly by properly altering the thermal pattern during welding fabrication.* However, the results also indicate that the reduction may be minimal or distortion may even increase if the thermal pattern is altered improperly. The question is "how to establish the most adequate thermal pattern?" The most adequate thermal pattern may be established experimentally for each structural model. However, it is much better if we could establish the optimum thermal pattern analytically. The effort by Lin was aimed at answering these questions.

*Kawasaki Heavy Industries has been using the differential heating technique successfully in reducing weld distortion of thin steel structures for railroad cars. Some of the results are given in Chapter 7 of the monograph prepared under Task 1.

Briceno, who received an Ocean Engineer degree in June, 1977, conducted a thesis study with the following objective:

"To integrate results obtained in earlier studies by Pattee, Beauchamp, Lin, and others, and develop most appropriate ways for reducing distortion of structural models representative of surface effect ships."

His study was both experimental and analytical.

Further Study on Buckling Distortion. Earlier, Pattee and Beauchamp studied buckling distortion. However, during the course of the integration effort conducted in the fall of 1976 Papazoglou felt a need for conducting a thorough analysis of buckling distortion of a welded plate. He conducted an extensive analytical investigation of buckling of rectangular plates using elasticity theory as well as plasticity theories (deformation theory and incremental theory). He also conducted limited experiments of buckling of aluminum structures. The results are included in an M.S. thesis by Papazoglou to be completed in January 1978.

Study on Laser Weldments. This study was conducted by Papazoglou and Gonçalves.

In the earlier study conducted during the second year, residual stresses were measured on two specimens, one in titanium and the other in low-carbon steel. During the third year, experiments were made on two more specimens, one in Inconel 718 and the other in high-strength steel AISI 4130.

The results are presented in APPENDIX A.

Integration Effort. During the three-year period a number of research efforts were made primarily by graduate students. Detailed results of individual studies were already reported in theses and previous reports.

Instead of presenting summaries of these studies in this final report we felt that it is most beneficial to readers of this final report to integrate all the important information generated in these studies in an orderly fashion. Consequently, the remainder of this report provides the state-of-the-art on prediction and control of distortion in welded aluminum structures. The report obviously draws much information from studies conducted under this contract, but it also covers information obtained in other studies conducted at M.I.T. and elsewhere. To avoid excessively lengthy discussion, it is assumed that potential readers of this report have already read or have access to the following two Welding Research Council Bulletins:

1. WRC No. 149, "Control of Distortion and Shrinkage in Welding," by K. Masubuchi, April 1970.
2. WRC No. 174, "Residual Stresses and Distortion in Welded Aluminum Structures and Their Effects on Service Performance," by K. Masubuchi.

2.2 THERMAL STRESSES DURING WELDING, RESIDUAL STRESSES AND DISTORTION

This chapter serves as an introduction to the following ones. After a brief outline of the state of the art of temperature distribution prediction during welding, an effort is made towards an understanding of the mechanism of residual stress formation. This is followed by a brief introduction to the various kinds of distortion, as established by Masubuchi [4, 5].

2.2.1 Temperature Distribution During Welding

Deformations during welding are caused by a plastic flow, due to the non-uniform heating of the material being welded. This fact leads to the conclusion that an accurate knowledge of the temperature distribution during welding is the first major step towards the determination of the magnitude of the various kinds of distortion. This is the reason for which so much effort was devoted during the last years at M.I.T. and elsewhere in heat flow analysis.

The governing equation of heat transfer during welding is:

$$\frac{\partial}{\partial x}(k\frac{\partial T}{\partial x}) + \frac{\partial}{\partial y}(k\frac{\partial T}{\partial y}) + \frac{\partial}{\partial z}(k\frac{\partial T}{\partial z}) + W_i = \rho c\frac{\partial T}{\partial t} \qquad (2.1)$$

where

(x, y, z) = Cartesian coordinates

T = temperature

k = thermal conductivity

ρ = material density

c = specific heat

W_i = heat source

Rosenthal [6,7,8] was the first to approach the problem analytically some fourty years ago. He solved the governing equation using a moving heat source, under the following basic assumptions:

(1) The physical characteristics of the metal are independent of temperature and uniform in space.

(2) The speed υ of the moving source and the rate of heat input are constant.

The solution to the above equation for the 2D case is:

$$T = T_o + \frac{q}{2\pi k} e^{-\frac{\upsilon}{2\lambda}\xi} K_o\left(\frac{\upsilon}{2\lambda} r\right) \qquad (2.2)$$

where

$q = \frac{1}{h} \eta_a (0.24\ VI)$

$\xi = x - \upsilon t$

$r = \sqrt{\xi^2 + y^2}$

K_o = modified Bessel function of second kind and zero order

T_o = initial temperature

V = voltage

I = current (amps)

η_a = arc efficiency

q = intensity of heat source

h = plate thickness (mm)

y = welding coordinate perpendicular to weld path (x)

λ = thermal diffusivity (= $\frac{k}{\rho c}$)

Some refinements to the above solution taking into account effects of heat loss from the surface, finite breadth of plates and variable properties (adopting an iterative procedure) are summarized by Nishida [9]. Computer programs, taking into account these modifications, were devised and are available [9,10].

Comparison of experimental results and predictions made using the above analytical procedure show that quite accurate results are found in the following cases:

1. Welding of workpieces having regular shape and small thickness,
2. welding of sufficiently long rectangular bars,
3. electron beam and laser welding.

In usual practice, however, some kind of welding groove is made and multipass techniques are used, which make the heat flow and heat dissipation near the weld extremely complex and difficult to predict from the point of view of welding distortion. To overcome these computational difficulties one has to rely on numerical methods using the high-speed computers which are available today.

The numerical methods mentioned comprise the finite difference and the finite element methods. Both of them are reviewed by Nishida [9], where the pros and cons of each one are investigated.

A computer program was also developed by Muraki [11], which can calculate the three dimensional temperature distribution during welding using the finite element method. However, it should be pointed out that due to its inefficiency (high cost) the program has not yet been tested extensively.

The latest effort at M.I.T. consists of a finite difference 3D computer program developed by Tsai [12], which is capable of calculating the temperature distribution very near the weld by using a distributed heat source, instead of the conventional point source used to the present.

For a more detailed discussion on the subject of heat flow during welding one is referred to the latest book by Masubuchi [13].

2.2.2 Thermal Stresses During Welding-Residual Stresses

Due to local heating by the welding arc, complex thermal stresses are produced in regions near the welding arc. Figure 2-1 shows schematically changes of temperature and stresses during welding. A butt joint is being welded along the x-axis. The welding arc, which is moving at speed V is presently located at the origin 0, as shown in Figure 2-1a.

Figure 2-1b shows the temperature distribution along several cross sections. Along section A-A, which is ahead of the welding arc, the temperature change due to welding, ΔT, is almost zero (see Fig. 2-1b-1). Along section B-B, which crosses the welding arc, the temperature distribution is very steep (Fig. 2-1b-2). Along section C-C, which is some distance behind the welding arc, the temperature change due to welding again diminishes (Fig. 2-1b-4).

Figure 2-1c shows the distribution of stresses in the x-direction, σ_x, across the sections. Stresses in the y-direction, σ_y, and shearing stresses, τ_{xy}, also exist in a 2D field.

Along section A-A thermal stresses due to welding are almost zero (Fig. 2-1c-1). The stress distribution along section B-B is shown in Figure 2-1c-2. Stresses in regions somewhat away from the arc are compressive. The expansion of these areas is restrained by the

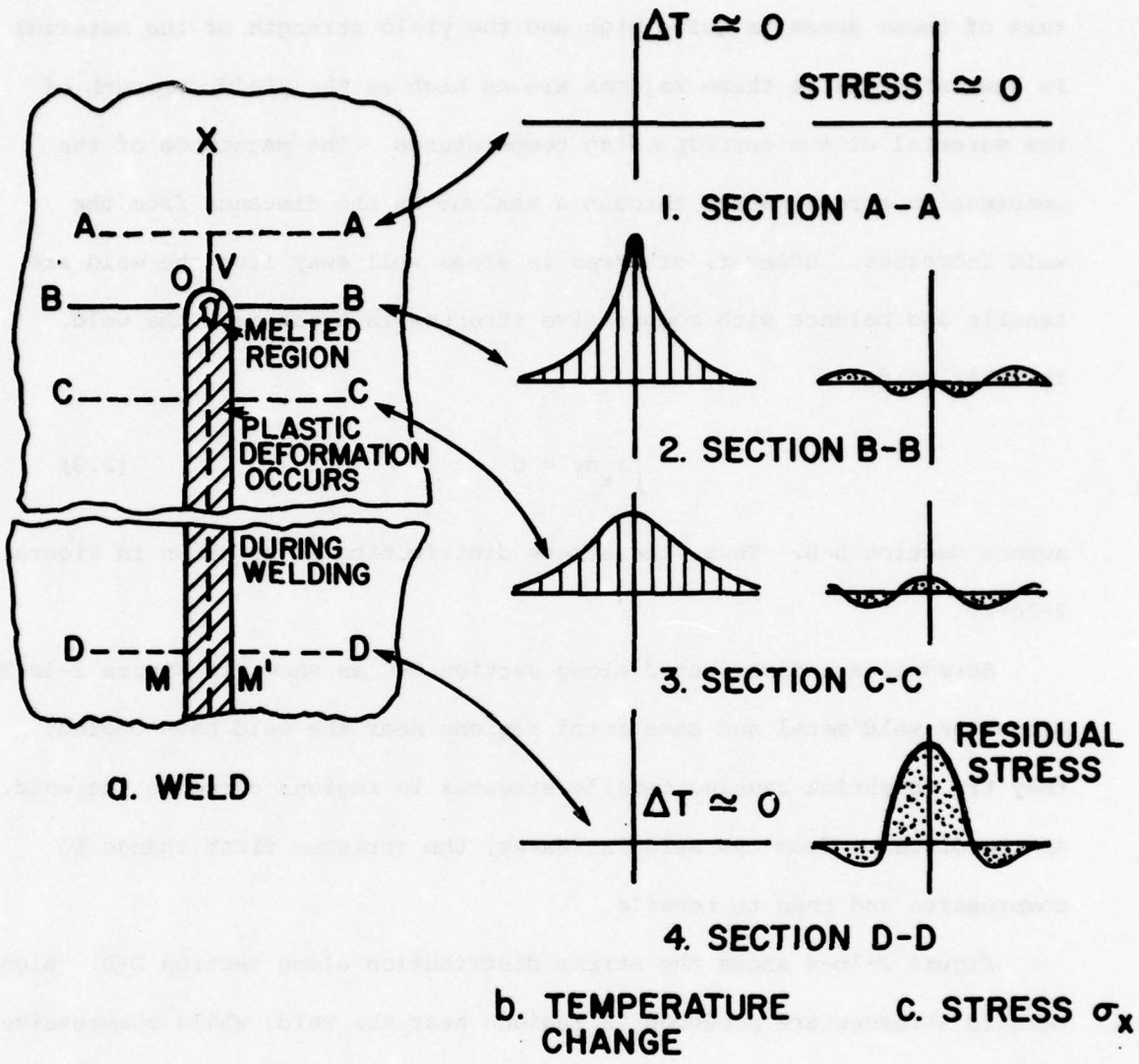

Fig. 2-1 Schematic Representation of Changes in Temperature and Stress During Welding

surrounding metal which is at a lower temperature. Since the temperature of these areas is quite high and the yield strength of the material is low, stresses in these regions are as high as the yield strength of the material at the corresponding temperatures. The magnitude of the compressive stress passes through a maximum as the distance from the weld increases. However, stresses in areas well away from the weld are tensile and balance with compressive stresses in areas near the weld. In other words

$$\int \sigma_x dy = 0 \qquad (2.3)$$

across section B-B. Thus, the stress distribution is as shown in Figure 2-1c-2.

Stresses are distributed along section C-C as shown in Figure 2-1c-3. Since the weld metal and base metal regions near the weld have cooled, they try to shrink causing tensile stresses in regions close to the weld. As the distance from the weld increases, the stresses first change to compressive and then to tensile.

Figure 2-1c-4 shows the stress distribution along section D-D. High tensile stresses are produced in regions near the weld, while compressive stresses are produced in regions away from the weld. The distribution of residual stresses that remain after welding is completed is as shown in the figure.

The cross-hatched area M-M in Figure 2-1a shows the region where plastic deformation occurs during the welding thermal cycle. The ellipse near the origin indicates the region where the metal is molten. The region outside the cross-hatched area remains elastic during the entire

thermal cycle.

AS shown in Figure 2-1, thermal stresses during welding are produced by a complex mechanisms which involves plastic deformations over a wide range of temperatures from room temperature up to the melting temperature. Because of the difficulty in analyzing plastic deformation, especially at elevated temperatures, mathematical analyses were limited for very simple cases, such as spot welding.*

At M.I.T. systematic research has been conducted since 1968 on transient thermal stresses and residual stresses, especially in connection with distortion. Computer programs were developed both for the one-dimensional and the two-dimensional cases.

The 1-D computer program** is an improvement over the one developed at Battelle [14]. Two modified versions can be found in references [10] and [15].

The current M.I.T. 2-D computer programs, as developed by Muraki [16], are based upon elasto-plastic finite-element analysis of thermal stresses and metal movement during welding. The programs are capable of computing stresses under the plane-stress and plane-strain conditions. A finite-element formulation has been derived in the general form which includes temperature dependency of material properties and the yield condition. Reference [16] describes this program.

---

*The WRC Bulletin 149 written by K. Masubuchi describes examples of past calculations.

**The 1-D program is based upon the assumption that stress changes in the welding direction are much less than those in the transverse direction, i.e. $\partial\sigma/\partial x \ll \partial\sigma/\partial y$, in Fig. 2-1. Then, from the equilibrium conditions of stresses, one can assume that: $\sigma_x = f(y)$, $\sigma_y = \tau_{xy} = 0$

2.2.3 Weld Distortion

As shown in the previous section, the nonuniform heating and cooling cycle, which occurs in the weld and the adjacent base metal, causes the existance of complex strains during welding. Their respective stresses combine and react to produce internal forces that can cause bending, rotation, and/or buckling. Collectively they are known as welding shrinkage distortion.

Three fundamental dimensional changes that occur during the welding process cause distortion in fabricated structures:

1. Transverse shrinkage perpendicular to the weld line.
2. Longitudinal shrinkage parallel to the weld line.
3. Angular distortion (rotation around the weld line).

These dimensional changes are shown in Figure 2-2 and are classified by their appearance as follows:

a. Transverse shrinkage. Shrinkage perpendicular to the weld line.

b. Angular change (or transverse distortion). A nonuniform thermal distribution in the thickness direction causes distortion (angular change) close to the weld line.

c. Rotational distortion. Angular distortion in the plane of the plate due to thermal expansion.

d. Longitudinal shrinkage. Shrinkage in the direction of the weld line.

e. Longitudinal distortion. Distortion in a plane through the weld line and perpendicular to the plate.

f. Buckling distortion. Thermal compressive stresses cause instability when the plates are thin.

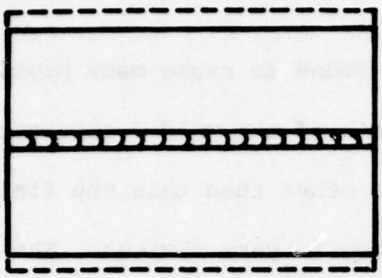

(a) TRANSVERSE SHRINKAGE

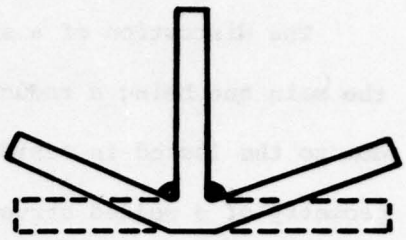

(b) ANGULAR CHANGE

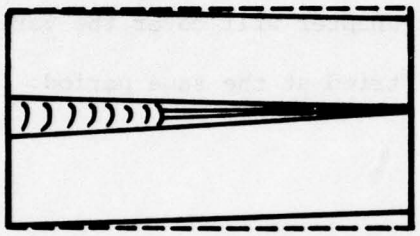

(c) ROTATIONAL DISTORTION

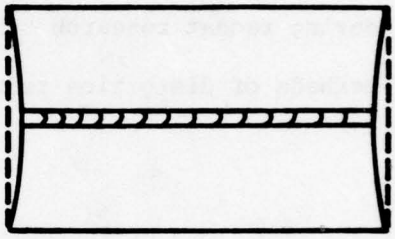

(d) LONGITUDINAL SHRINKAGE

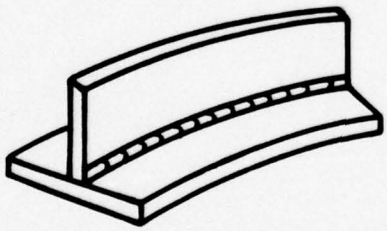

(e) LONGITUDINAL DISTORTION

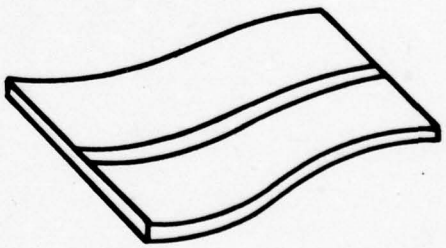

(f) BUCKLING DISTORTION

Fig. 2-2 Various Types of Weld Distortion

The distortion of a structure has been found to cause many problems, the main one being a reduction in the strength of the welded structure due to the locked-in residual stresses. But other than this the finished geometry of a welded structure with distortion is very obvious. The part of structure you end up with is not necessarily the one you require. This leads to costly repair work or total refabrication.

In the following chapters an effort will be done to summarize the state of the art of distortion evaluation as it was established at M.I.T. during recent research studies. The last chapter will cover the various methods of distortion reduction that were tried at the same period.

2.3 TRANSVERSE SHRINKAGE OF ALUMINUM BUTT WELDS

Transverse shrinkage is the shrinkage that occurs perpendicular to the weld line. Excessive shrinkage causes mismatch of joints or loss of the function of a structure. Current techniques do not allow the efficient removal of existing transverse shrinkage. Common practice, however, is to prepare structural parts to be welded in enlarged dimensions, taking into account an estimated amount of shrinkage.

Many investigators, including Capel [17], Gilde [18], Cline [19], Campus [20], Weck [21], Guyot [22], Sparangen and Ettinger [23], Malisius [24], Watanabe and Satoh [25], and Naka [26], have proposed formulas for the estimation of transverse shrinkage of butt welds, which by and large are based on empirical information. Some of these formulas are contained in Welding Research Council (WRC) Bulletins 149 and 174, written by Masubuchi [4,5].

The following sections will summarize the analytical and experimental results obtained by various investigators at M.I.T. and elsewhere.

2.3.1 Mechanism of Transverse Shrinkage in Butt Welds

The mechanisms of transverse shrinkage have been studied by several investigators including Naka [26] and Matsui [27]. Iwamura [28] also conducted analytical and experimental studies of transverse-shrinkage mechanisms in aluminum butt welds. The most important finding of these mathematical analyses was the following:

> "The major portion of transverse shrinkage of a butt weld is due to contraction of the base plate. The base plate expands during welding. When the weld metal solidifies, the expanded base metal must shrink, and this shrinkage accounts for the major part of transverse shrinkage. Shrinkage of the weld metal itself is only about 10 percent of the actual shrinkage."

Figure 3-1 is a schematic presentation that shows the changes of transverse shrinkage in a single-pass butt weld in a free joint after welding. Shortly after welding, the heat of the weld metal is transmitted into the base metal. This causes the base metal to expand, with a consequent contraction of the weld metal. During this period the points of sections A and A' do not move (Fig. 3-1b).

When the weld metal begins to resist the additional thermal deformation of the base metal, points of sections A and A' begin to move in response. This starting time of the movement of A and A' is indicated by t_s.

The various thermal deformations of both the weld and base metals are defined as follows:

δ_s: thermal expansion of the base metal at $t = t_s$.

δ: additional thermal deformation of the base metal caused in $\overline{AA'}$ at $t > t_s$.

S_W: thermal contraction of the weld metal at $t > t_s$.

The above deformations can be calculated by the following relations:

$$\delta_s = 2\int_0^{L/2} [\alpha(T) \cdot T(t_s, x) - \alpha(T_o) \cdot T_o]dx \qquad (3.1)$$

$$\delta = 2\int_0^{L/2} [\alpha(T) \cdot T(t, x) - \alpha(T) \cdot T(t_s, x)]dx \qquad (3.2)$$

$$S_W = [\alpha(T_M) \cdot T_M - \alpha(T_o) \cdot T_o] \cdot L_w \qquad (3.3)$$

where

$\alpha(T)$ = thermal expansion coefficient

$T(t, x)$ = temperature, as a function of time and position

T_M = melting temperature

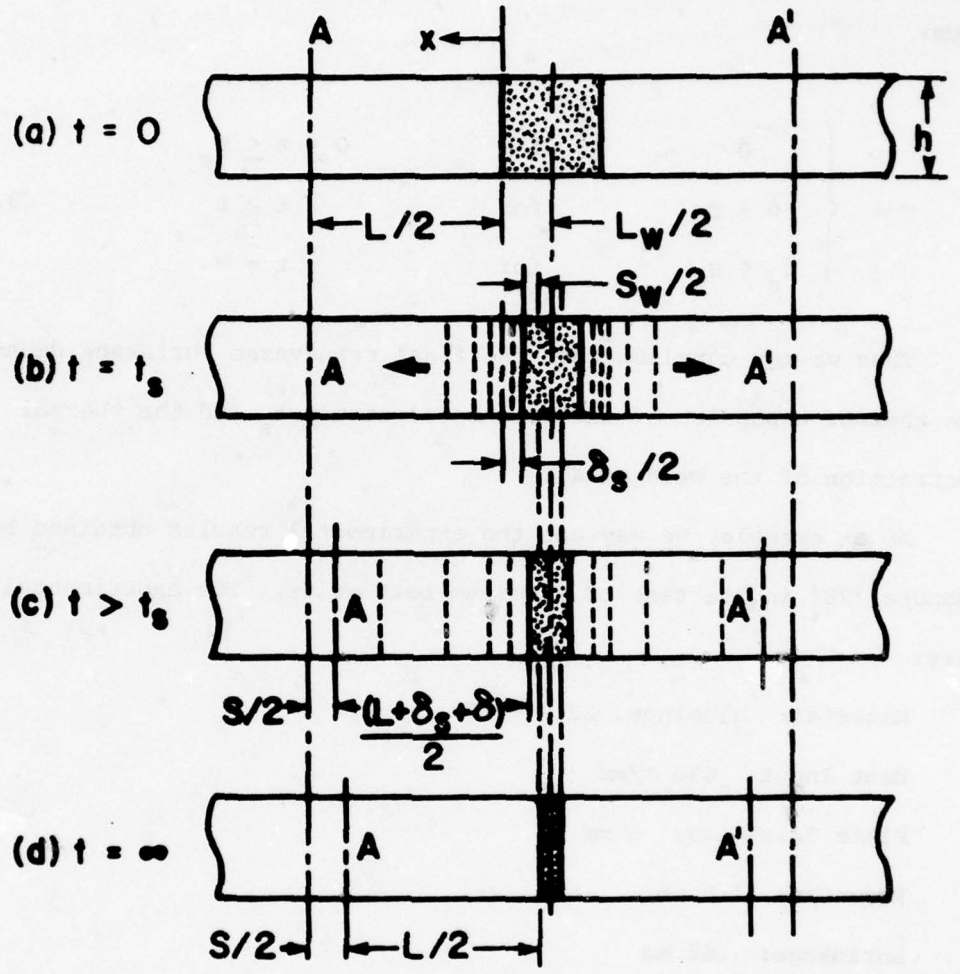

Fig. 3-1 Schematic Presentation of a Transverse Shrinkage of a Butt Weld in a Single Pass

T_o = initial and final (room) temperature.

Using these results, the transverse shrinkage can now be calculated from:

$$S = \begin{cases} 0 & \text{for} \quad 0 \leq t \leq t_s \\ -\delta + S_w & \text{for} \quad t > t_s \\ \delta_s + S_w & \text{for} \quad t = \infty \end{cases} \qquad (3.4)$$

Thus we may conclude that the final transverse shrinkage depends on the thermal expansion of the base metal at $t = t_s$ and the thermal contraction of the weld metal.

As an example, we may use the experimental results obtained by Iwamura [28] in the case of aluminum butt welds. The experimental data were:

Material: aluminum, 2219 - T87

Heat Input: 630 J/mm

Plate Thickness: 6 mm

Root Gap: 2.5 mm

Shrinkage: .66 mm

Using a constant thermal expansion coefficient, the thermal contraction of the weld metal can be estimated from equation (3.3):

$$S_w = 0.1 \times 17 \times 10^{-6} \times (1220 - 70) = .05 \text{ mm}$$

This means that S_w is less than 8% of the total shrinkage. Therefore, the thermal expansion of the base metal caused at $t = t_s$ is the most important factor in the final shrinkage of a single-pass butt weld in a

free joint.

Effect of Plate Thickness

If we use the analytical method of temperature distribution prediction for a welded plate, as discussed in Section 2.1, and make the following assumptions:

a. Constant thermal expansion coefficient,

b. thermal radiation neglected, and

c. thermal contraction of weld metal neglected,

we come up with the following formulas for the transverse shrinkage:

1. for a thin plate

$$S = \frac{Q}{c\rho h} erf(\beta_s) \tag{3.5}$$

2. for a thick plate

$$S = \frac{Q}{c\rho 2\pi\lambda t_s}[1 + 2 \sum_{n=1}^{\infty} e^{-\frac{(nh)^2}{4\lambda t_s}}] erf(\beta_s) \tag{3.6}$$

where

$\beta_s = \frac{L}{4\pi\lambda t_s}$

Q = heat input

c = specific heat

ρ = density

λ = thermal diffusivity

h = plate thickness

L = plate length

$erf(\beta_s)$ = error function

Equation (3.5) indicates that the final shrinkage decreases with increasing plate thickness.

Figure 3-2 shows the experimental results obtained by Matsui [27] on butt welds in low-carbon steel. Most of the shrinkage occurs after the weldment has cooled down to a relatively low temperature. The figure shows that in a thicker plate transverse shrinkage starts earlier, but the final value of the shrinkage is smaller. The results confirm the theoretical predictions.

Effect of Restraint

Watanabe and Satoh [25] performed a series of experiments on various degrees of restraint. They proposed an empirical formula for transverse shrinkage in restraint butt welds, as shown in Figure 3-3a. It can be seen that the final transverse shrinkage decreases as the degree of restraint increases.

Matsui [27] measured the stresses in weld metals for fixed butt welds. The weld depth for all tests was almost identical. The degree of restraint is higher as plates become thicker. Figure 3-3b shows the changes of stresses during welding and cooling. The yield stress of the material used was 40 ksi at room temperature. The stresses of two of the three tests exceeded the yield stress.

Effect of Materials

The amount of transverse shrinkage will be different for various materials because of different material properties related to equations (3.5) and (3.6). For example, aluminum alloys, in comparison with steel, have more shrinkage because of higher heat conductivity and thermal

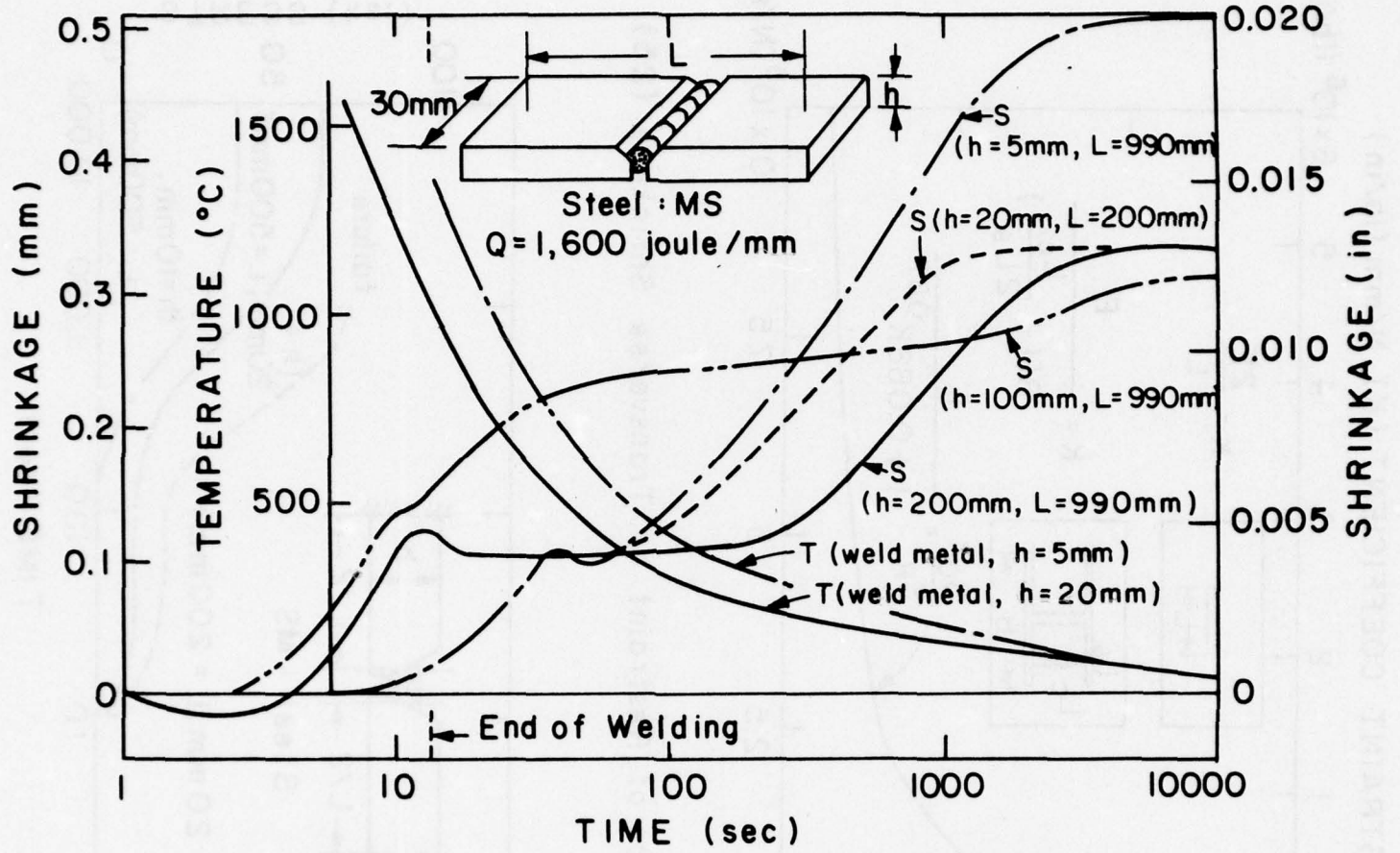

Fig.3-2 Transverse Shrinkage During Welding and Cooling for Various Plate Thicknesses (h) and Measuring Distances (L) in Free Butt Joints(27)
Note : The curves labeled T show the temperature changes, while the curves labeled S show the changes of transverse shrinkage

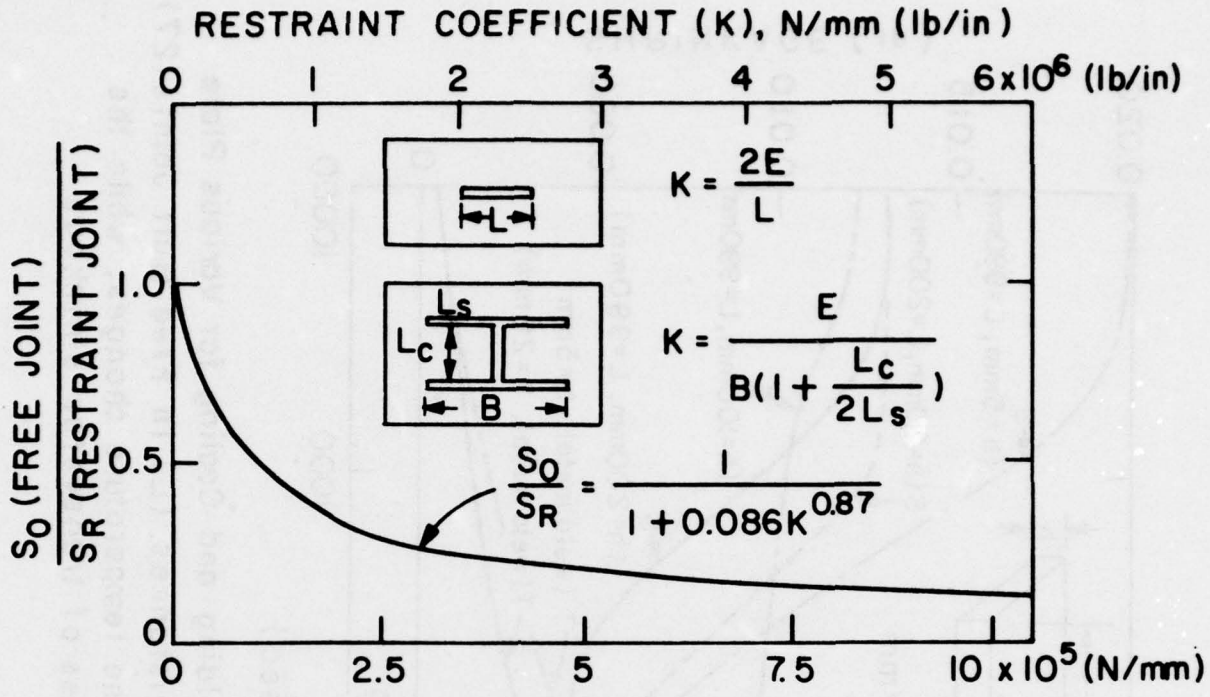

(a) Effect of Restraint on Transverse Shrinkage (25)

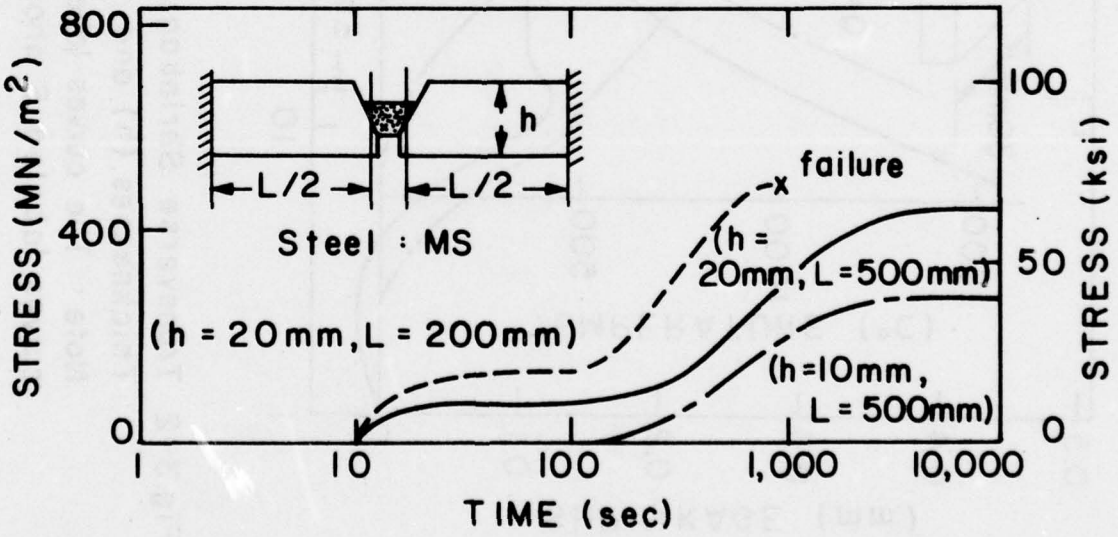

(b) Stresses in Weld Metals in a Single Pass Welding (27)

Fig. 3-3 Effects of Restraint on Transverse Shrinkage and Stress in Butt Welds

expansion coefficient.*

Phase transformation, present in ferrous materials, plays also an important role. Matsui [27] has proposed that the expansion due to phase transformation should be subtracted from the estimated shrinkage in order to predict the real shrinkage (Fig. 3-4). As one can see from the figure, the actual shrinkage in 9% nickel steel was about 70% of the extimated shrinkage by means of equation (3.6).

Effect of Multipass Welding

Kihara and Masubuchi [29] conducted empirical studies on transverse shrinkage during multipass welding of constrained butt joints in carbon steel. Figure 3-5 shows the increase of transverse shrinkage in multipass welding. It can be seen that the rate of shrinkage increase diminishes during later passes. This happens because the resistance that previous welds give against the thermal expansion of the base metal increases as the weld becomes larger.

Effect of Welding Length

The mechanism described above is based on a short weld length. The weld length in actual structures is, however, of the order of 3 to 6 meters. This makes the transverse shrinkage even more complicated, because of the influence of rotational distortion and nonuniform constraint.

*See pages 8 and 9 of WRC No. 174

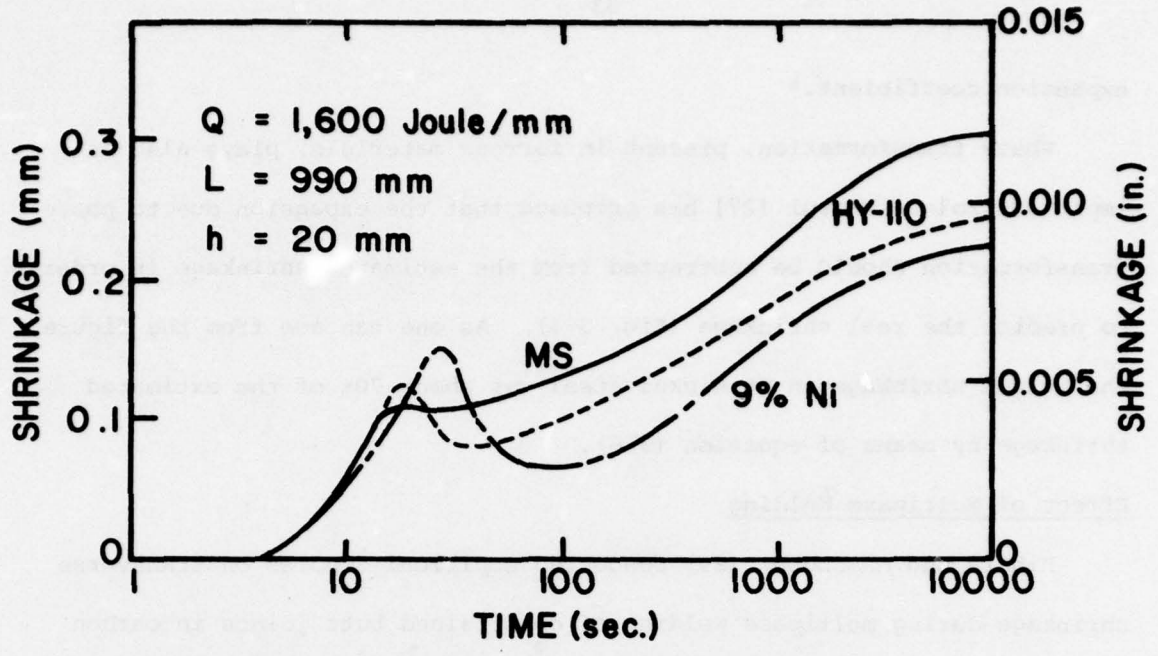

(a) TRANSVERSE SHRINKAGE DURING WELDING AND COOLING

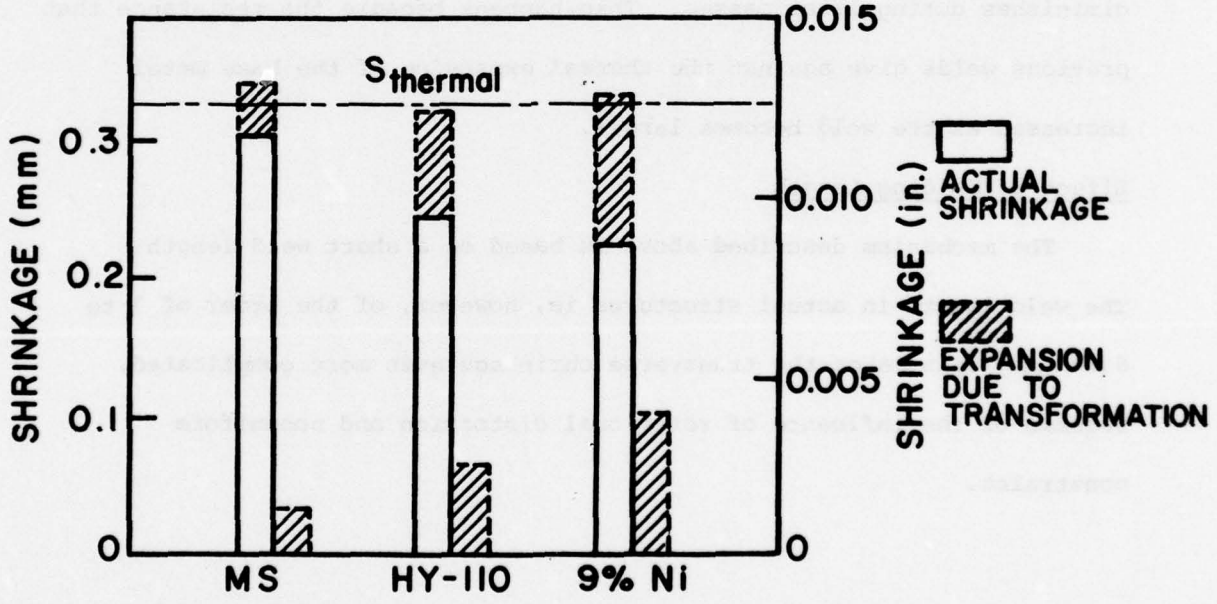

(b) FINAL TRANSVERSE SHRINKAGE

Fig. 3-4 Effects of Phase Transformation on Transverse Shrinkage

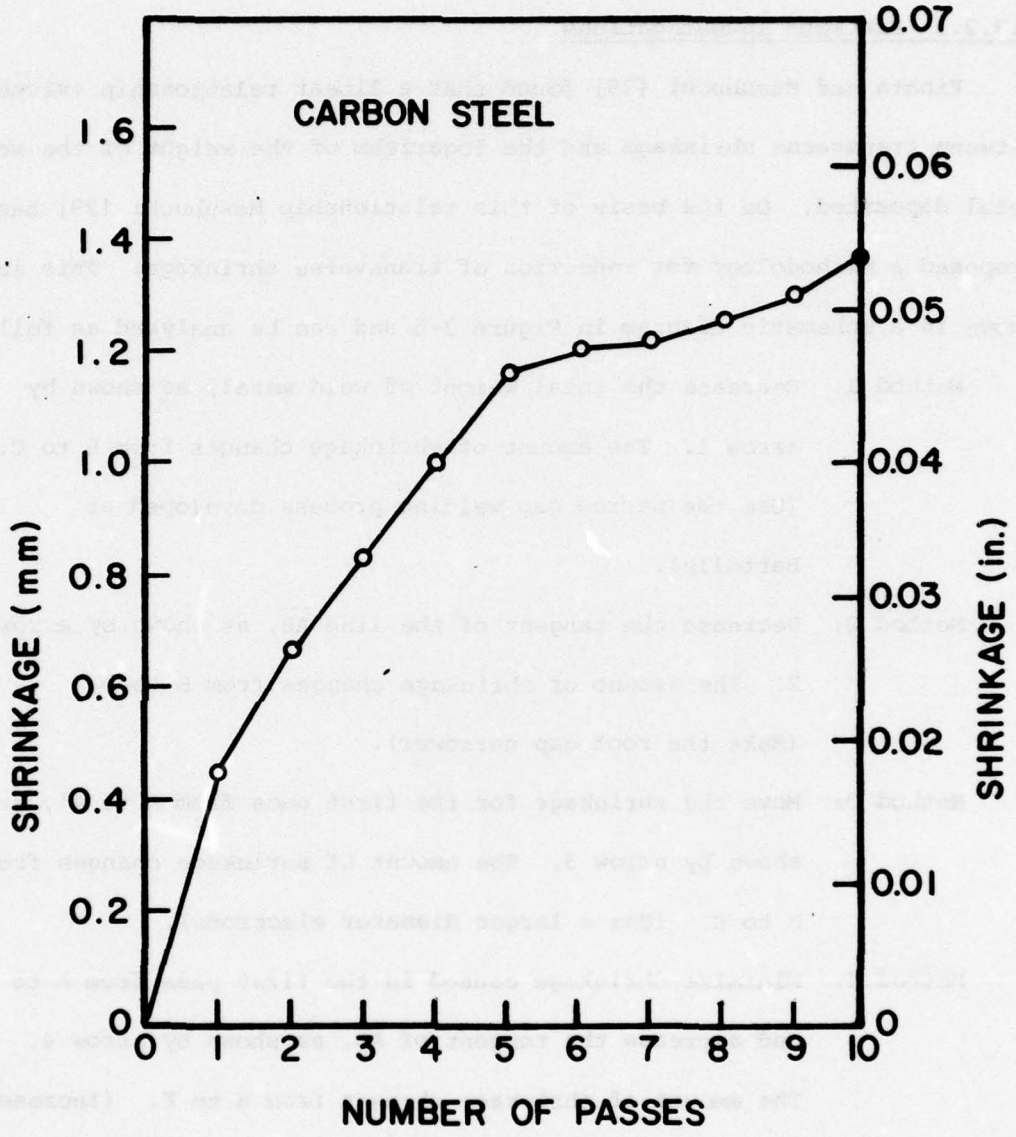

Fig. 3 - 5 Increase of Transverse Shrinkage in Multipass Welding of a Constraint Butt Joint (29)

2.3.2 Reduction of Transverse Shrinkage

2.3.2.1 Previous Investigations

Kihara and Masubuchi [29] found that a linear relationship existed between transverse shrinkage and the logarithm of the weight of the weld metal deposited. On the basis of this relationship Masubuchi [29] has proposed a methodology for reduction of transverse shrinkage. This is shown in a schematic diagram in Figure 3-6 and can be analysed as follows:

Method 1: Decrease the total weight of weld metal, as shown by arrow 1. The amount of shrinkage changes from B to C. (Use the narrow gap welding process developed at Battelle).

Method 2: Decrease the tangent of the line $\overline{AB}$, as shown by arrow 2. The amount of shrinkage changes from B to D. (Make the root gap narrower).

Method 3: Move the shrinkage for the first pass from A to A', as shown by arrow 3. The amount of shrinkage changes from B to E. (Use a larger diameter electrode).

Method 4: Minimize shrinkage caused in the first pass from A to A" and decrease the tangent of $\overline{AB}$, as shown by arrow 4. The amount of shrinkage changes from B to F. (Increase the degree of restraint).

2.3.2.2 Study Made at M.I.T.

A study was conducted by Iwamura [28] at M.I.T. which involved the effect of chilling and restraint on transverse shrinkage of butt welds in thin aluminum plates. The study included a theoretical analysis as well as a series of experiments.

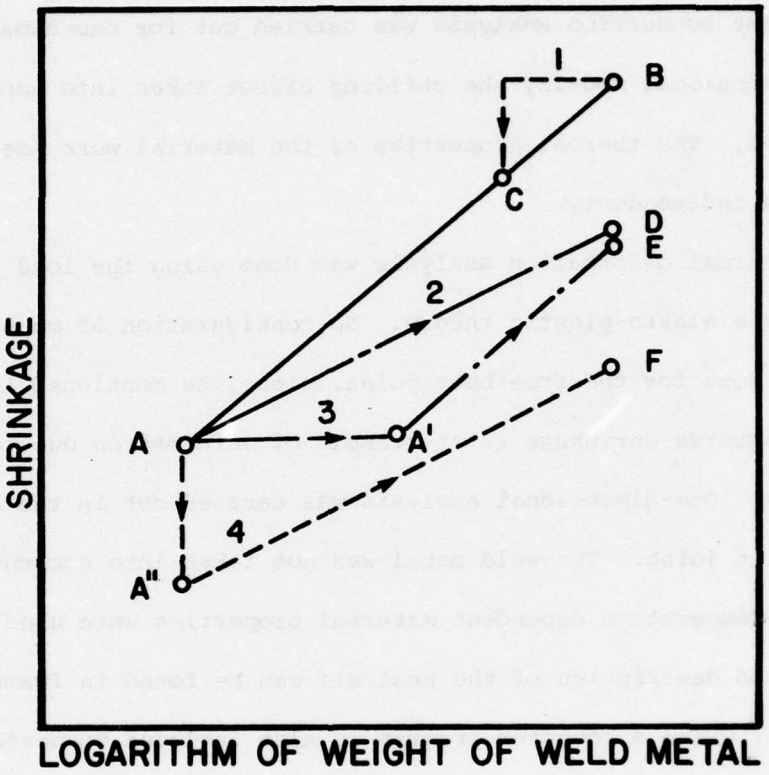

Fig. 3 – 6 Schematic Diagram Showing Four Methods of Reducing Transverse Shrinkage of Butt Welds (29)

Theoretical Analysis

The theoretical analysis included two kinds of butt joints, one free and the other H-type restraint. For both models short weld lengths were considered.

The heat conduction analysis was carried out for one-dimensional and two-dimensional models, the chilling effect taken into account in some of them. The thermal properties of the material were assumed temperature independent.

The thermal deformation analysis was done using the load increment method of the elasto-plastic theory. No consideration of mechanical strain was done for the free butt joint, since, as mentioned in Section 2.3.1, transverse shrinkage is the result of deformation due to thermal strain only. One-dimensional analysis was carried out in the case of the restraint joint. The weld metal was not taken into account in the analysis. Temperature dependent material properties were used.

Detailed description of the analysis can be found in Iwamura's thesis [28], where a computer program is also included to perform the calculations.

Experimental Analysis

A series of eight experiments was performed measuring temperature, strain and transverse shrinkage changes during welding. Material used was the 6061-T6 aluminum alloy. The plates were 6.5 mm thick. Weld length was 100 mm for all specimens, both the free butt joint and the H-type restraint ones. Four specimens two of each type, were chilled using dry-ice. There was also an effort to prevent angular change during welding. An automatic GMA welding machine was used with 200 amp.,

25 V, 6 mm /sec and heat input of 785 J/mm

A description of the test specimens is shown in Figure 3-7, where locations of strain gages and thermocouples are indicated. Figure 3-8 provides information about the constraining and chilling equipments.

Analysis of Results

The following table lists the designation of tests included in the discussion to follow:

	Joints	
Cooling	Free	Restraint
Cooled in the air	FN-1	RN-1, RN-3
Cooled with dry-ice	FC-1	RC-1

Figures 3-9 and 3-10 summarize test results on the free and the restrained joints, respectively. The temperature distribution of non-chilled specimens was modified by subtracting the room temperature. Similarly, Figures 3-11 and 3-12 show changes in temperature and shrinkage during and after welding in specimens without chilling and with chilling, respectively. Shown here are the measured values and the calculated values of temperature and transverse shrinkage.

In general, the plate expanded after the start of welding and the expansion increased until the arc passed the center. Shrinkage occurred after diminishing of the arc. The amount of expansion was relatively small in comparison with the final amount of shrinkage. The increasing rate of shrinkage decreased as time passed. When chilling was used, shrinkage occurred during welding. The final amount of shrinkage was almost the same in chilled and non-chilled specimens.

The amounts of final shrinkage of free joints were about .05 mm

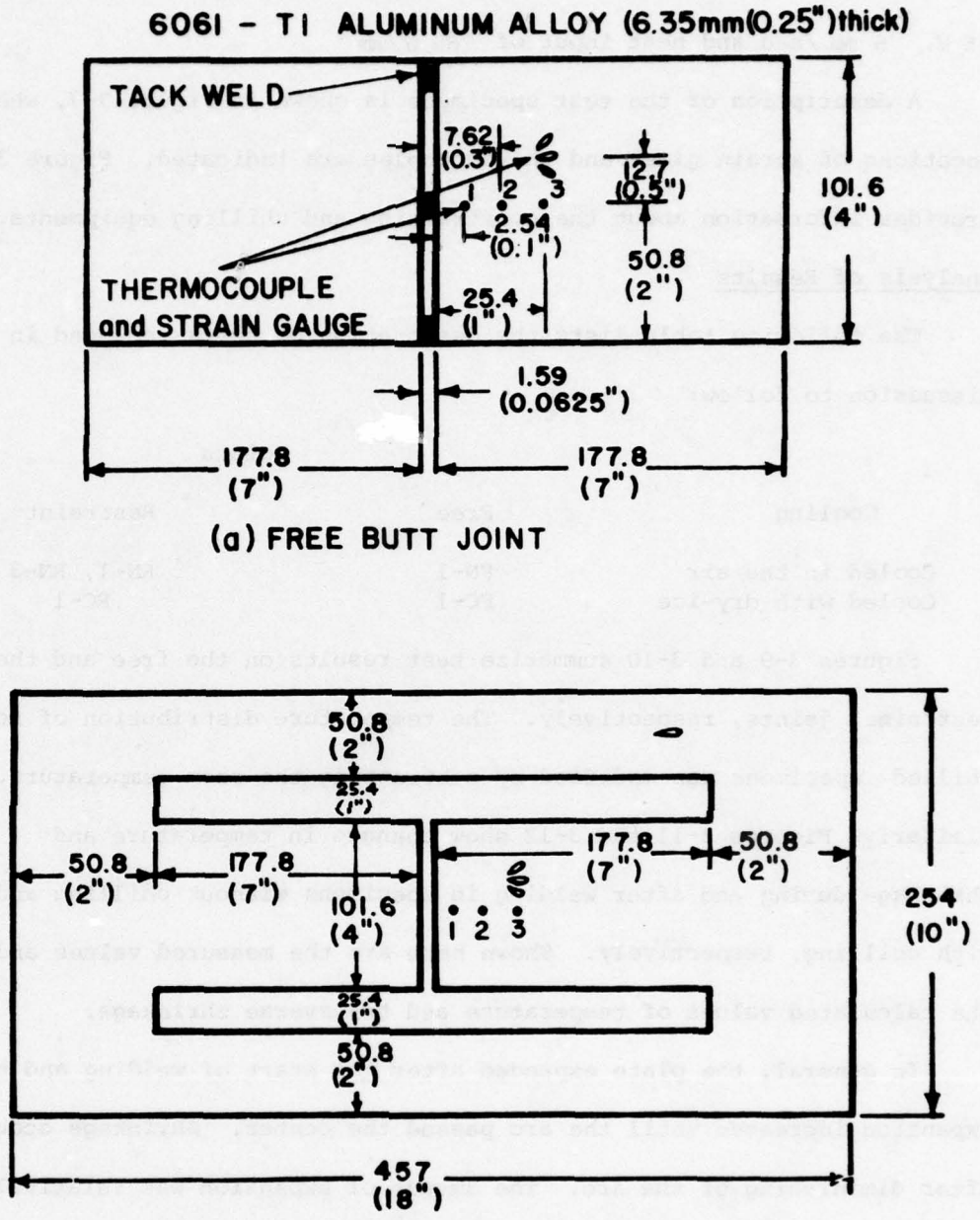

Fig. 3-7 Dimensions of Specimens and Locations of Measuring Temperature and Strain

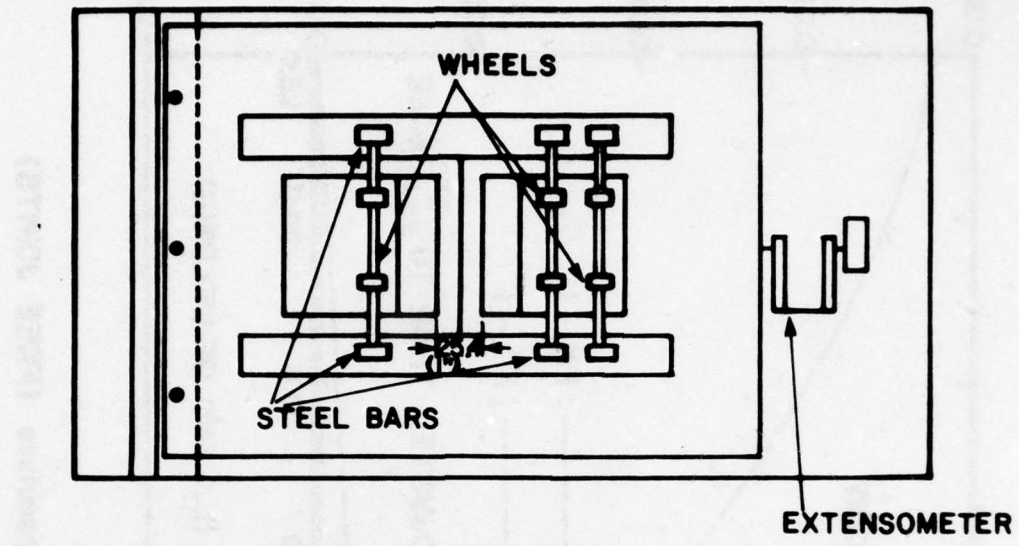

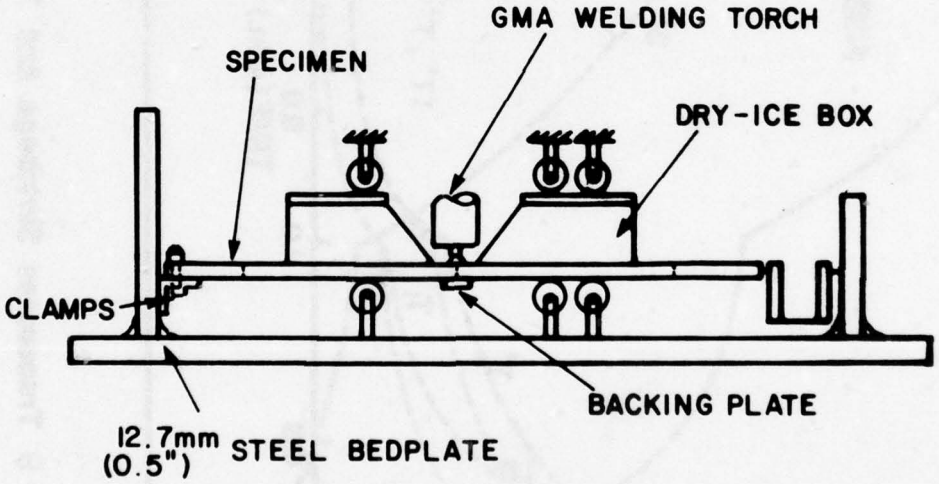

Fig. 3-8 Constraining and Chilling Equipment

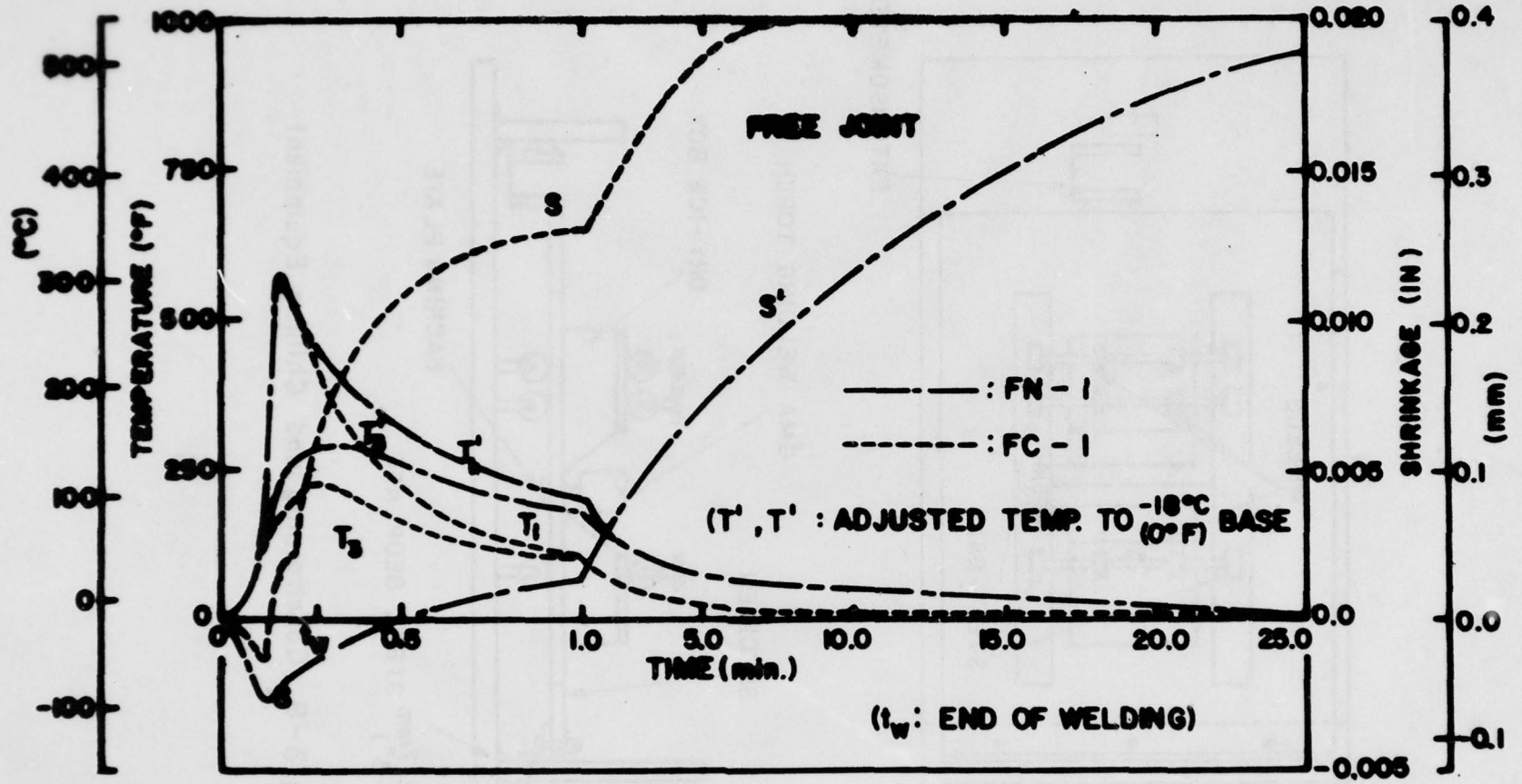

Fig. 3-9 Transverse Shrinkage And Temperature (FREE JOINTS)

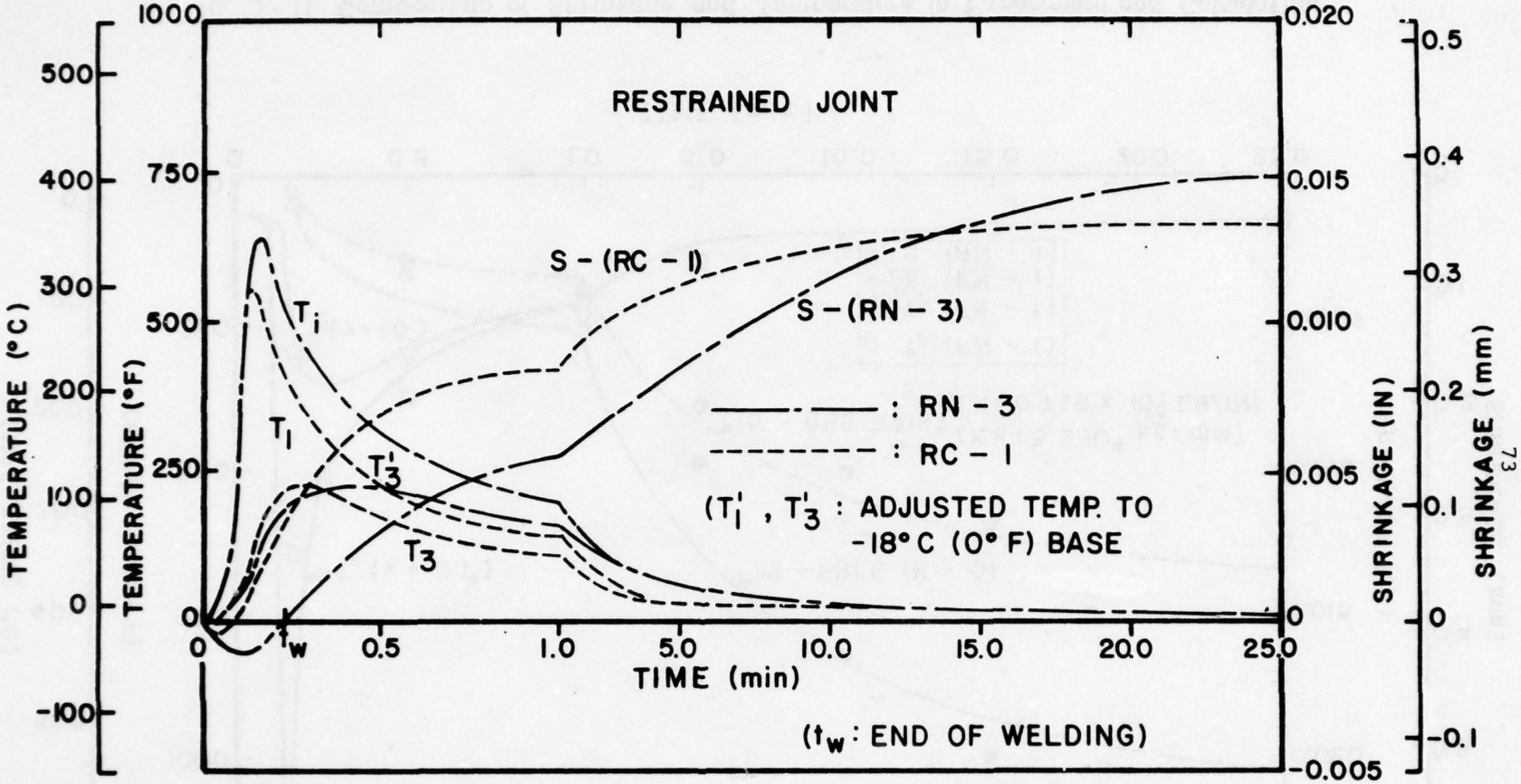

Fig. 3-10 Transverse Shrinkage and Temperature (Restrained Joint)

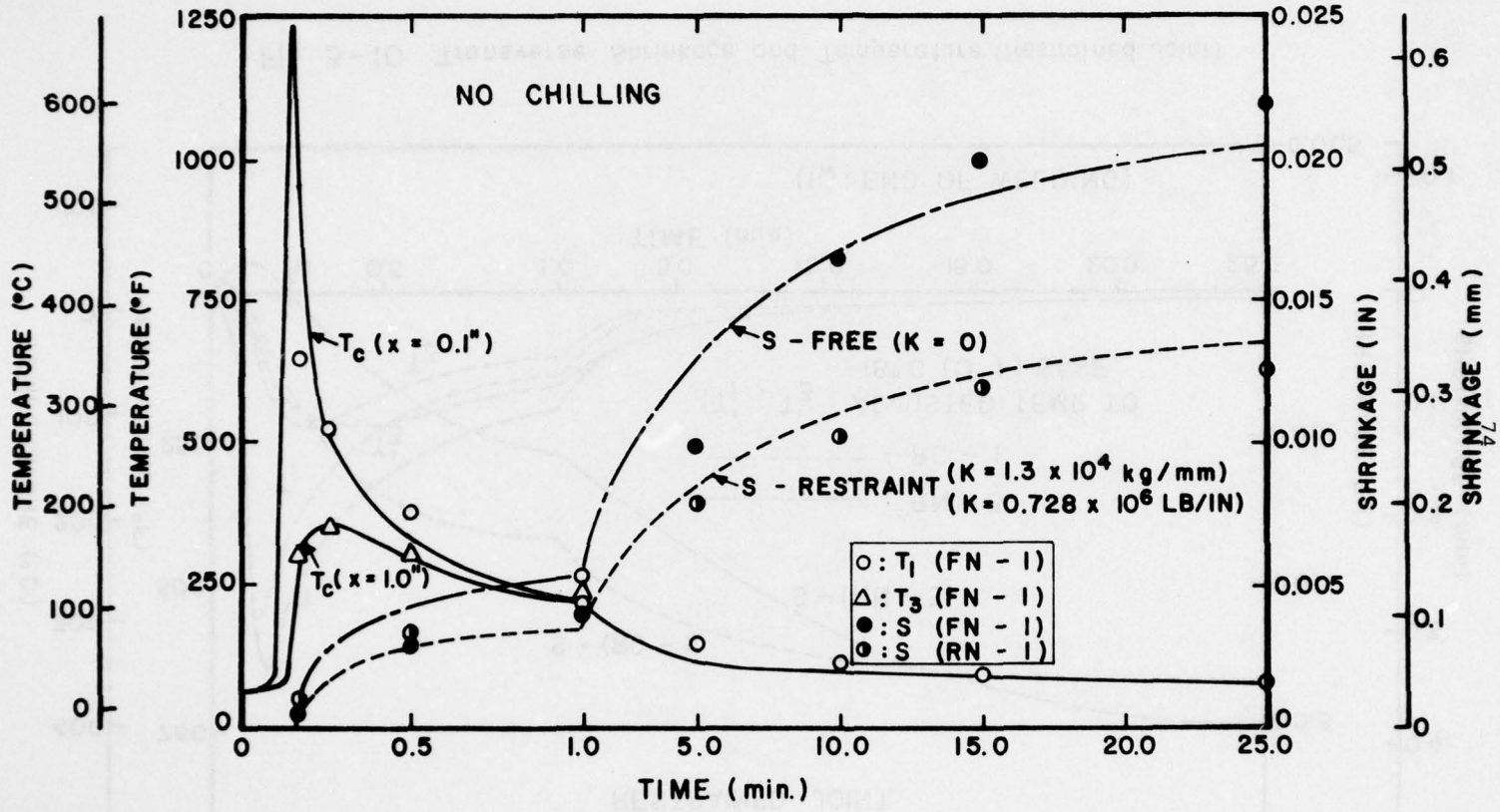

Fig. 3-11 Comparison of Shrinkage and Temperature in Experiment and Calculation

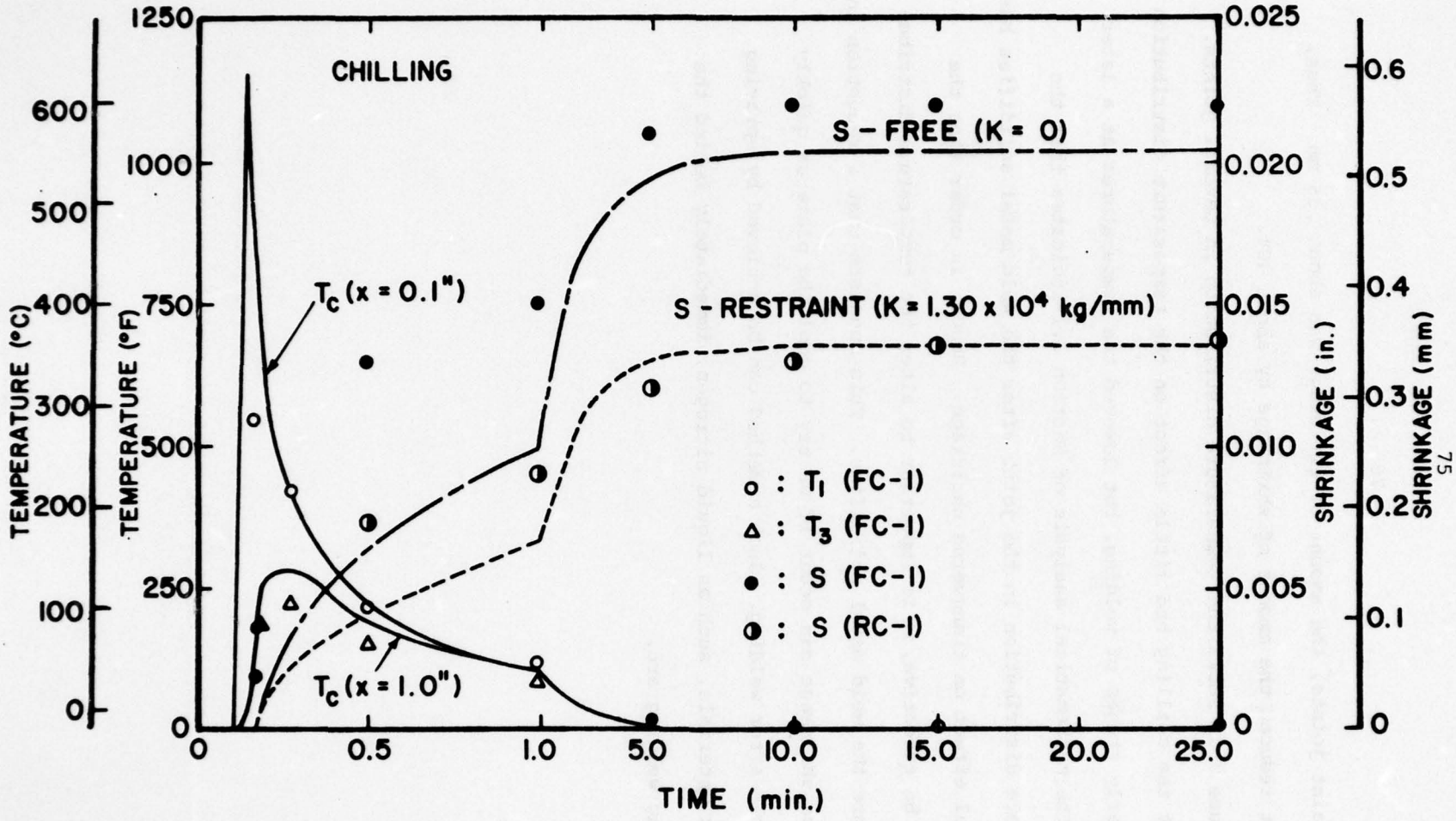

Fig. 3 - 12 Comparison of Shrinkage and Temperature in Experiment and Calculation

In restraint joints, the amount of shrinkage was about .35 mm. Thus, restraint reduced the amount of shrinkage by about 30%.

Figure 3-13 shows the temperature distribution in several joints. Note that the chilling had little effect on the temperature distribution in the early stages of welding, but lowered the temperatures at a later stage. The mathematical analysis of Section 3.1 indicates that the temperature distribution in the joint after the weld metal solidifies has a critical effect on transverse shrinkage. Hence, in order that the chilling be effective, it is important to alter the temperature distribution before the weld metal solidifies. This suggests that a reduction in transverse shrinkage can occur if we try to cool the plate as quickly as possible after welding. Such a method can be achieved by spraying cryogenic materials, such as liquid nitrogen, immediately behind the travelling welding arc.

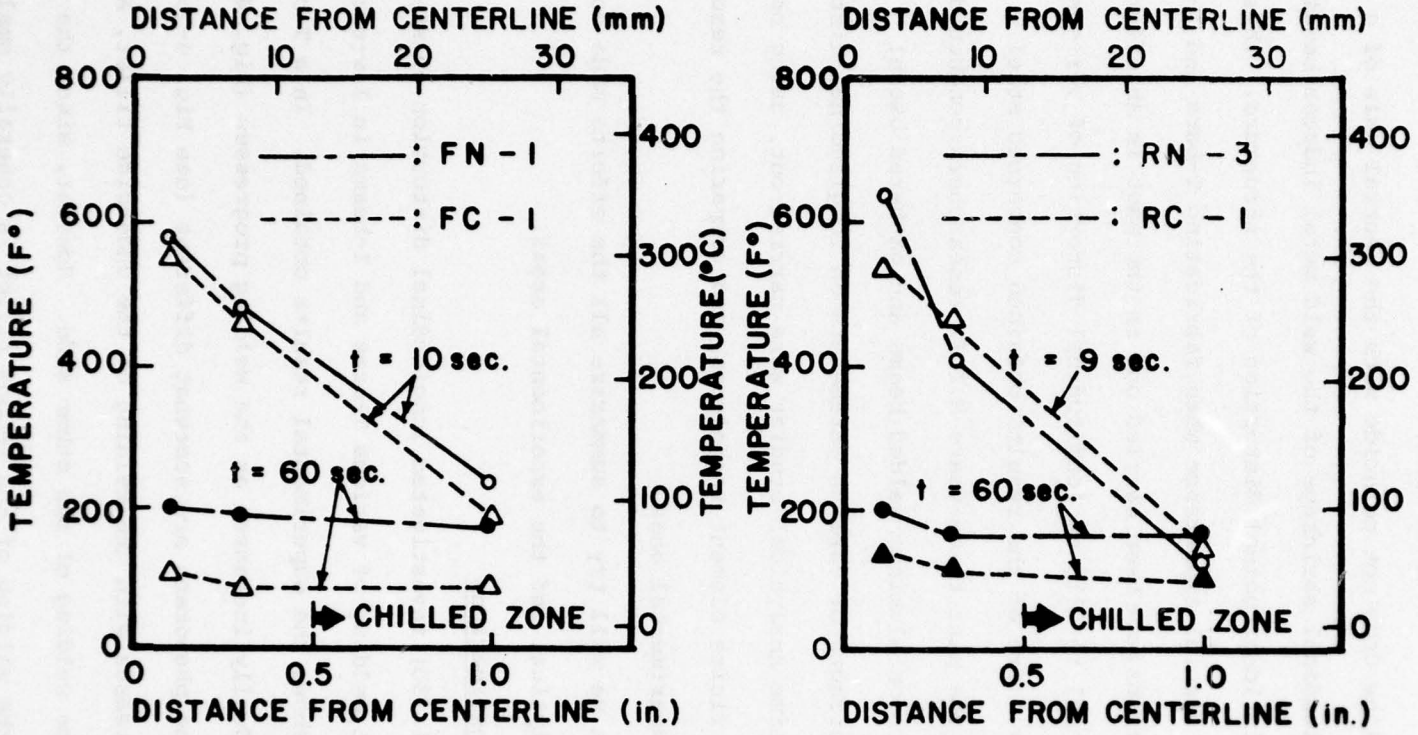

(TEMPERATURE OF FN - 1 AND RN - 3 WERE ADJUSTED TO $\frac{-18°C}{(0°F)}$ BASE)

Fig. 3-13 Temperature Distribution

2.4 LONGITUDINAL DISTORTION OF ALUMINUM BUILT-UP BEAMS

When the weld line does not coincide with the neutral axis of a weld structure, the longitudinal shrinkage of the weld metal induces bending moments, resulting in longitudinal distortion of the structure. This type of distortion is of special importance when fabricating T-bars and I-beams.

Many investigations have been carried out in the past in an effort to collect experimental results on longitudinal distortion of various structures. However, more of the results obtained concerned steel structures. During the past three years M.I.T. researchers conducted series of experiments on aluminum welded beams and gathered useful information on the effects of various parameters on longitudinal distortion. At the same time analytical studies were carried out, using both one-dimensional and finite element techniques, and comparing the results obtained with the experimental ones.

In this section we will try to summarize all the efforts made so far in both the analytical and the experimental areas.

2.4.1 Previous Investigations

Sasayama, et al. [30] investigated longitudinal distortion of steel caused in the fillet welding of various T-bars and I-beams in low-carbon steel. Figure 4-1 shows the experimental results obtained. In a T-bar the deformation gradually increases as the welding progresses (Fig. 4-1a).

In an I-beam the phenomena are somewhat different (see Fig. 4-1b); the deformation increases with the welding of the underside fillet, and it decreases with the welding of the other side. However, since the deformation due to the welding of the second fillet is generally smaller

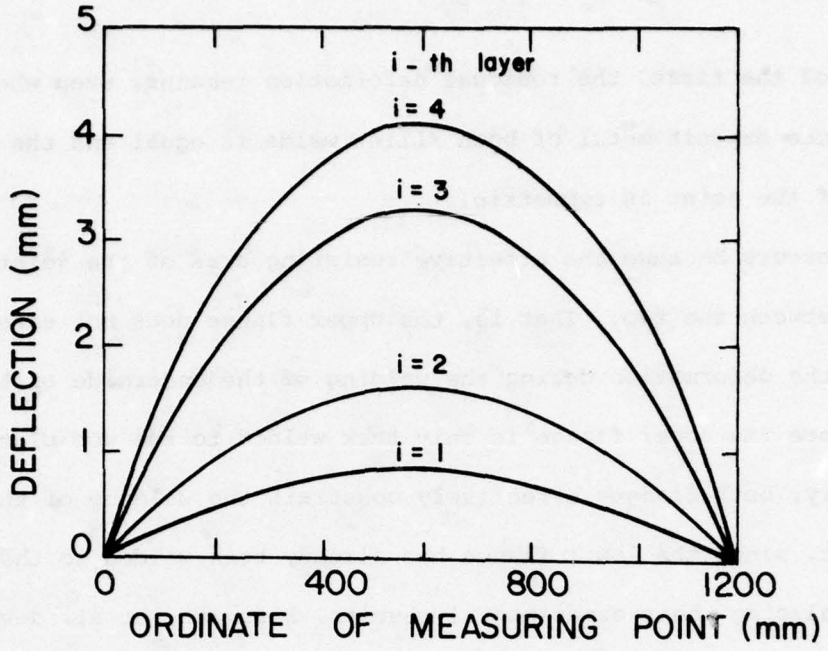

(a) 100 x 150 T-BAR

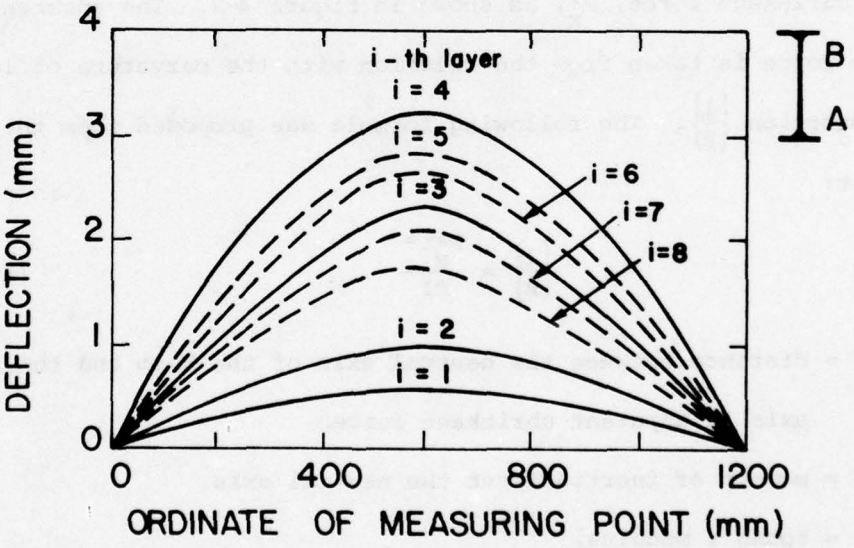

(b) I-BEAM, CONTINUOUS WELD
BOTH SIDE OF FILLET:
1st - 4th LAYER WELD A,
5th - 8th LAYER WELD B

Fig. 4-1 Longitudinal deflection of steel due to fillet welding

than that of the first, the residual deformation remains, even when the weight of the deposit metal of both fillet welds is equal and the geometry of the joint is symmetric.

This occurs because the effective resisting area of the joint differs between the two. That is, the upper flange does not effectively constrain the deformation during the welding of the underside of the fillet, since the upper flange is only tack welded to the web plate. On the contrary, both flanges effectively constrain the welding of the upper side fillet, since the lower flange has already been welded to the web.

In analyzing their experimental results, Sasayama, et al. developed a theory similar to the bending-beam theory [30]. They obtained a relation between the weight of electrode consumed per weld length and the apparent shrinkage force, P_x^*, as shown in Figure 4-2. The apparent shrinkage force is taken from the relation with the curvature of longitudinal distortion $\left(\frac{1}{R}\right)$. The following formula was proposed from the experiment:

$$\left(\frac{1}{R}\right) = \frac{P_x^* \ell^*}{EI} \tag{4.1}$$

where, ℓ^* = distance between the neutral axis of the beam and the acting axis of apparent shrinkage force

I = moment of inertia about the neutral axis.

E = Young's modulus.

For more details of the analysis one is referred to Chapter 7 of Reference 13.

Ujiie, et al. [31] of Mitsubishi Heavy Industries investigated distortion in aluminum structures and proposed a twin-GMA double-fillet

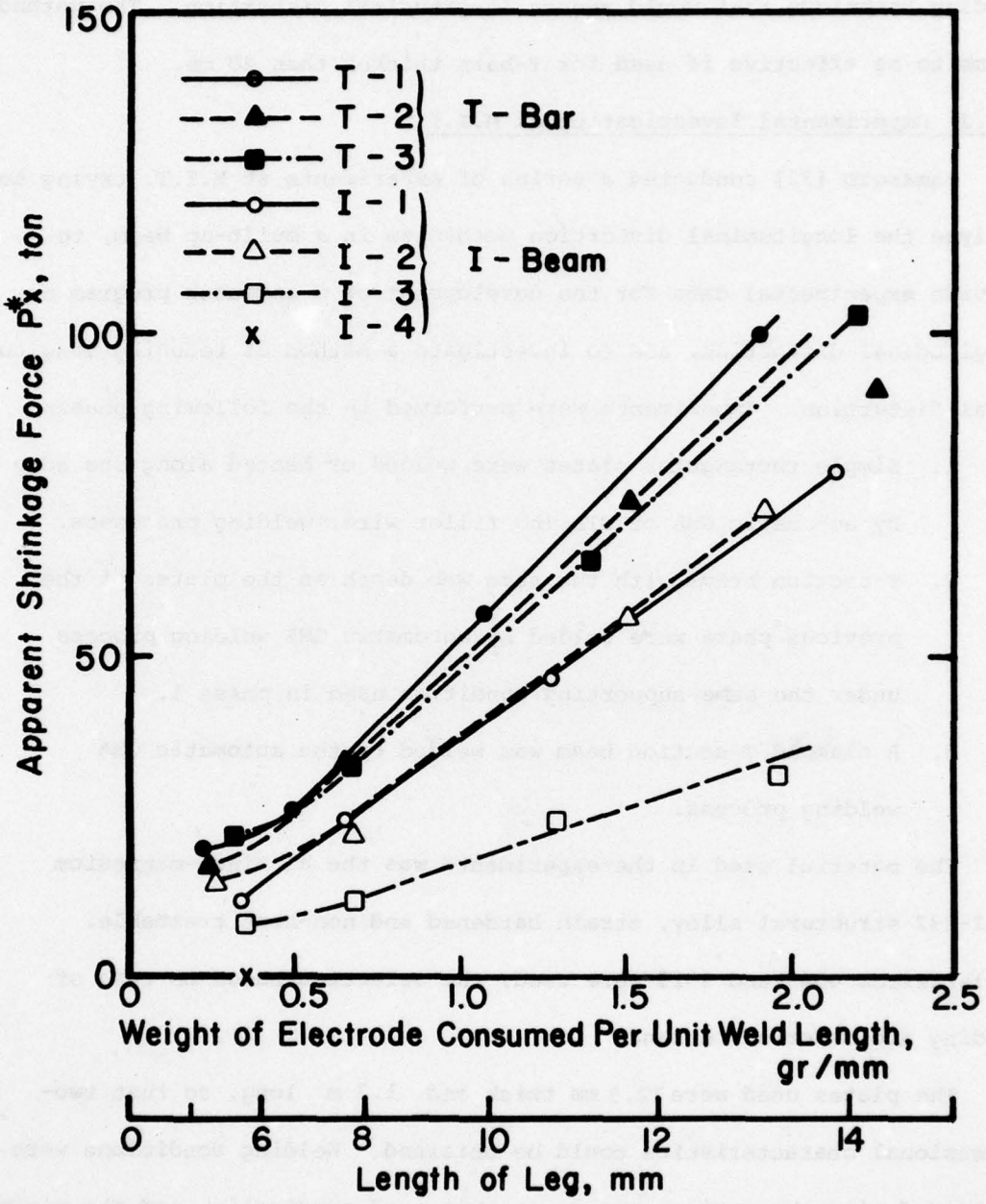

Fig. 4-2 Increase of Longitudinal Distortion During Multipass Welding (Sasayama, et al) (55)

welding technique that would reduce longitudinal distortion. The method seems to be effective if used for T-bars thicker than 20 mm.

2.4.2 Experimental Investigation at M.I.T.

Yamamoto [32] conducted a series of experiments at M.I.T. trying to analyze the longitudinal distortion mechanism in a built-up beam, to provide experimental data for the development of a computer program on longitudinal distortion, and to investigate a method of reducing longitudinal distortion. Experiments were performed in the following phases:

1. Simple rectangular plates were welded or heated along one edge by automatic GMA or GTA (no filler wire) welding processes.
2. T-section beams with the same web depth as the plates of the previous phase were welded by automatic GMA welding process under the same supporting condition used in phase 1.
3. A clamped T-section beam was welded by the automatic GMA welding process.

The material used in the experiments was the aluminum-magnesium 5052-H32 structural alloy, strain hardened and non-heat treatable. Filler wires 4043 and 2319 were used, the selection based on ease of welding and material on hand.

The plates used were 12.5 mm thick and 1.2 m long, so that two-dimensional characteristics could be obtained. Welding conditions were changed during the various passes so that good penetration and the minimum weld length for adequate joint strength could be obtained.

Figure 4-3 shows a typical test specimen. It also provides dimensions as well as strain gage and thermocouple locations. Figures 4-4 and

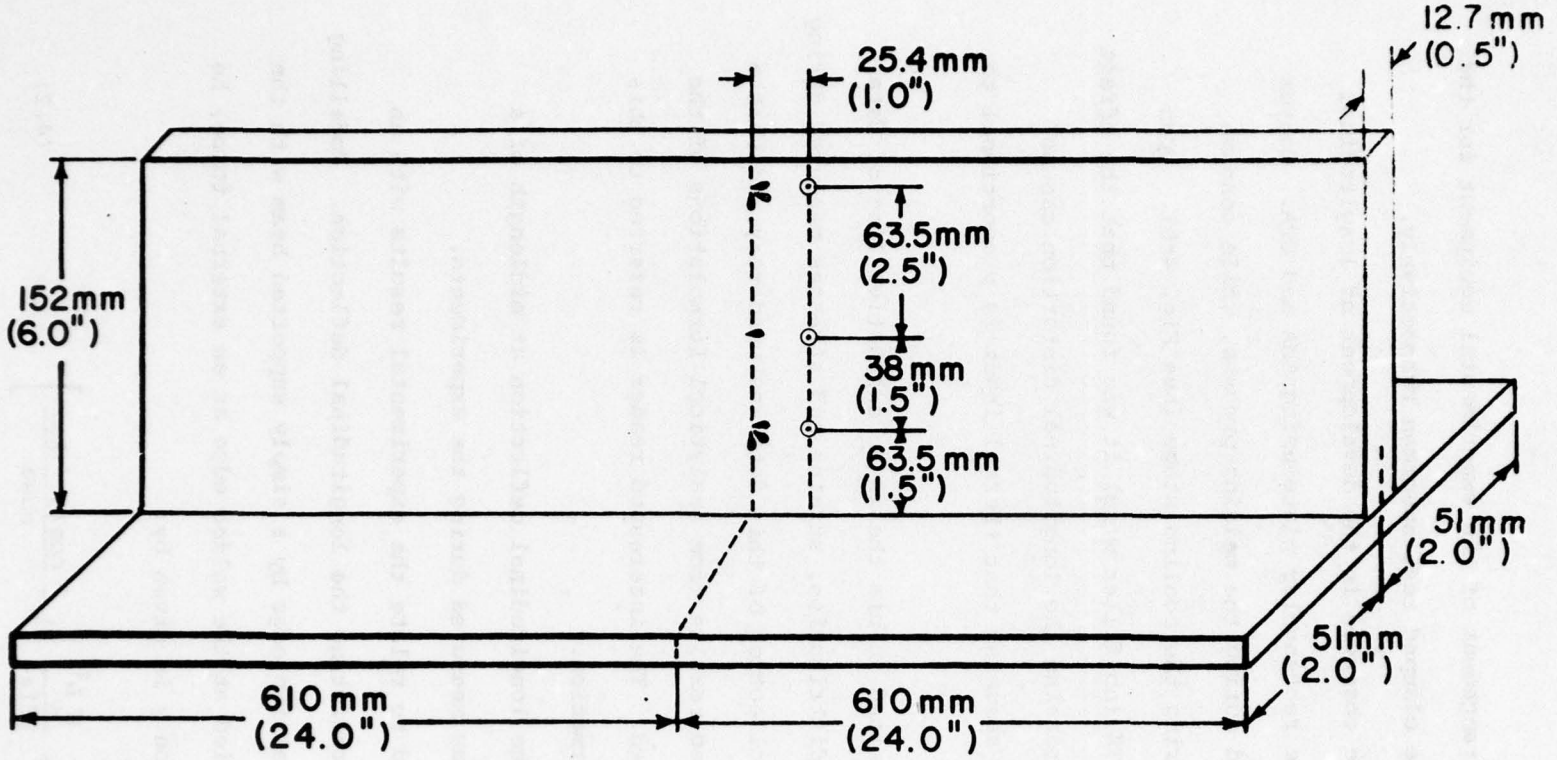

: ROSETTE STRAIN GAUGE FAER - 18RB - 12S13L

: SINGLE STRAIN GAUGE FAE - 25 - 12S13

⊙ : THERMOCOUPLE

Fig. 4 - 3 Arrangement of the Strain Gauge and Thermocouple for T- Section Beam

4-5 show the general arrangement of the experimental equipment for the simply supported and the clamped test specimen respectively.

Similar trends were observed in the development of longitudinal deflection of the simple rectangular plate using GMA and GTA. Convex deflections were observed during the welding process, while concave deflections resulted during the cooling stage (see Fig. 4-6). Upon comparison of GMA and GTA (no filler wire) it was found that the effect of deposit metal in increasing the longitudinal distortion can be estimated at about 10%, assuming that thermal input is proportional to the maximum deflection.

Yamamoto [32] contained in his thesis an exhaustive list of data concerning temperature distribution, strains and stresses measured during the experiments. The collection of this data was mandatory, so that a comparison with predicted results from analytical formulations of the problem could be obtained. The interested reader is referred to this thesis for further information.

Figure 4-7 shows the longitudinal deflection at midlength of a typical T-section beam as measured during the experiments.

Yamamoto [32] tried to relate the experimental results with an analytical method for predicting the longitudinal deflection. Modelling the simple beam welded at its edge by a simply supported beam with the shrinkage force P_x^* applied at the welded edge as an external force, he found that the deflection y is given by:

$$y = \frac{M_o L^2}{4EIu^2}\left[1 - \frac{\cos(u - kx)}{\cos u}\right] \qquad (4.2)$$

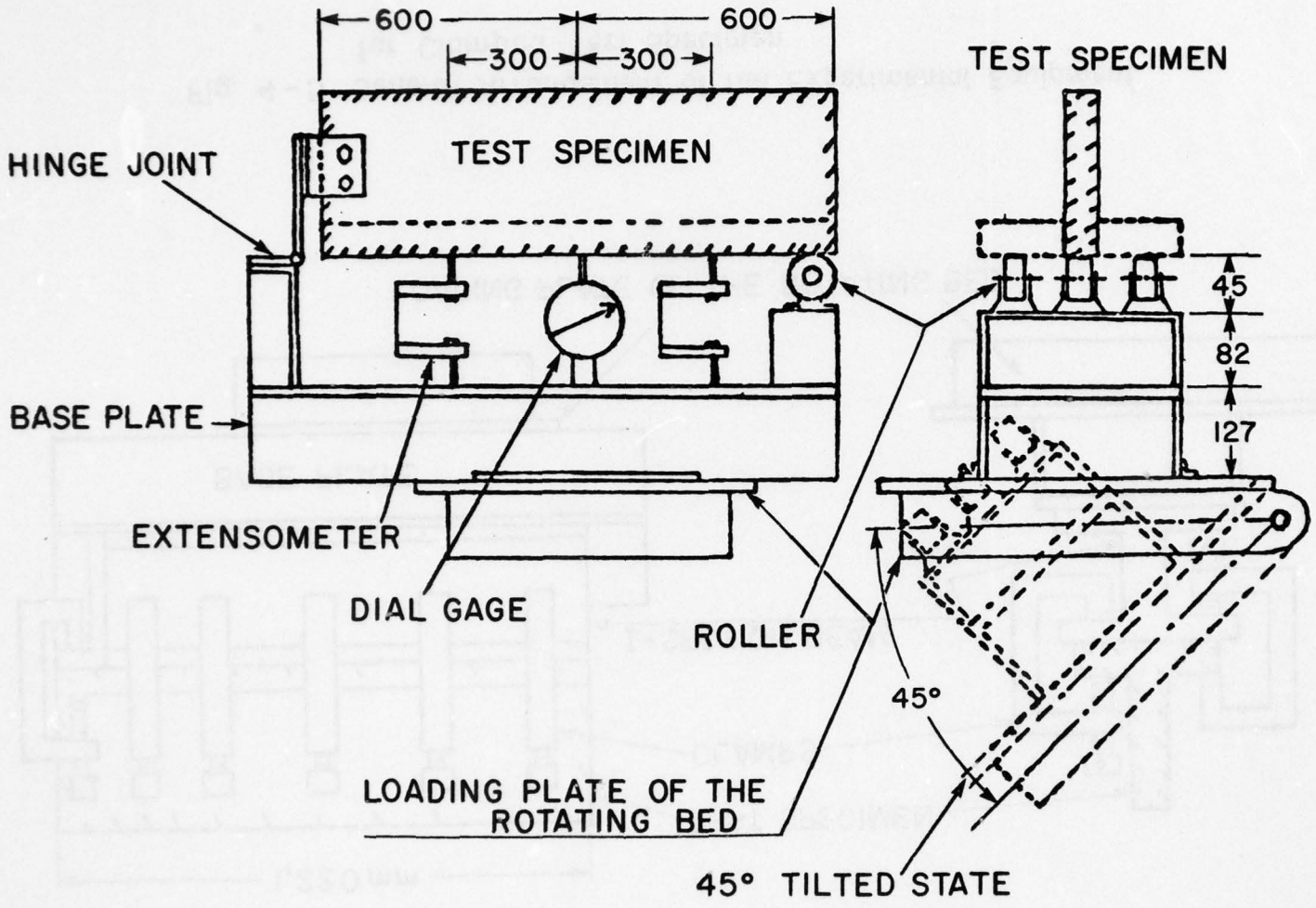

Fig. 4 - 4 General Arrangement of the Experimental Equipment for Simply Supporting Test Specimen. (dimensions in mm)

AD-A050 908 MASSACHUSETTS INST OF TECH CAMBRIDGE DEPT OF OCEAN E--ETC F/G 13/5
DEVELOPMENT OF ANALYTICAL AND EMPIRICAL SYSTEMS FOR PARAMETRIC --ETC(U)
NOV 77 V J PAPAZOGLOU, K MASUBUCHI N00014-75-C-0469

UNCLASSIFIED NL

2 OF 3
AD
A050908

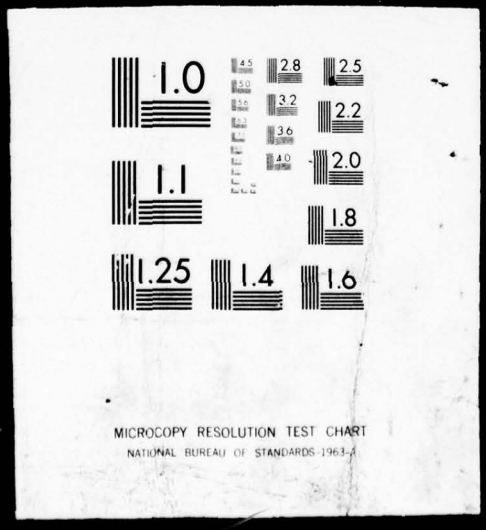

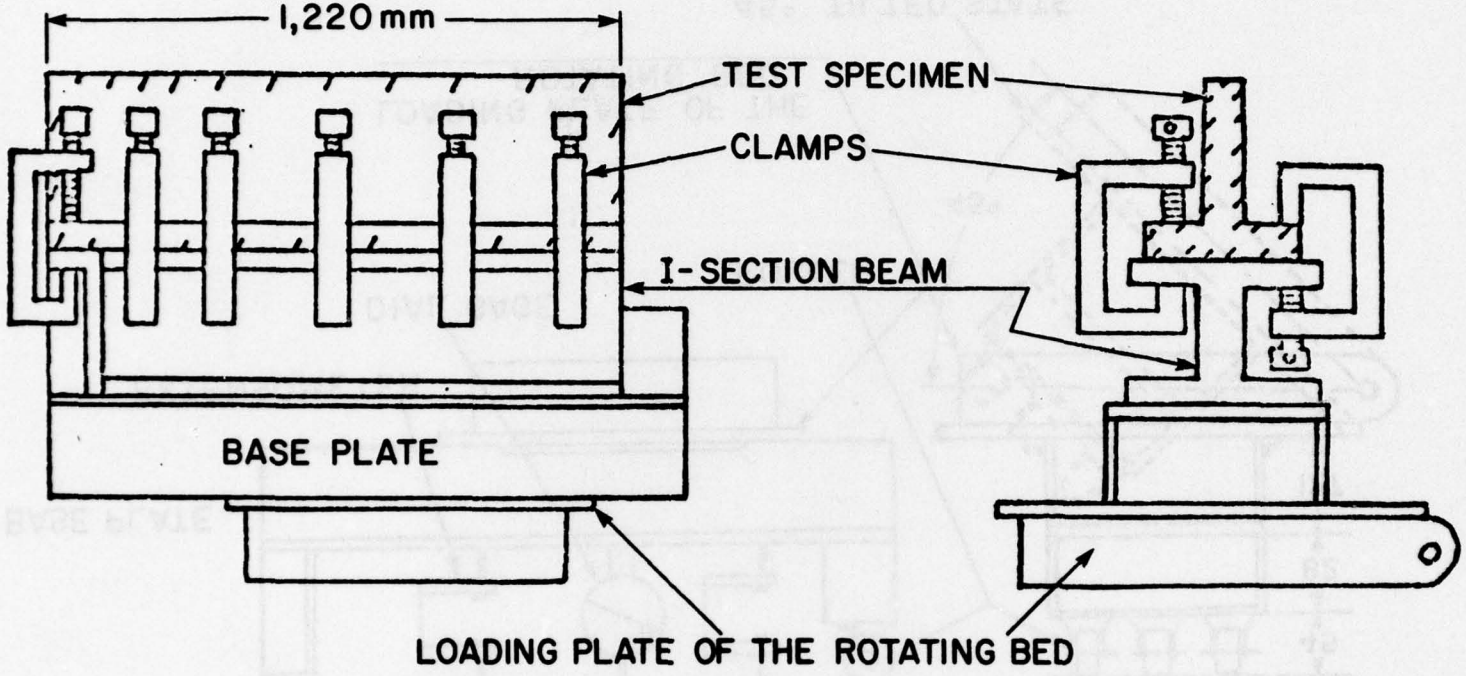

Fig. 4-5 General Arrangement of the Experimental Equipment for Clamped Test Specimen

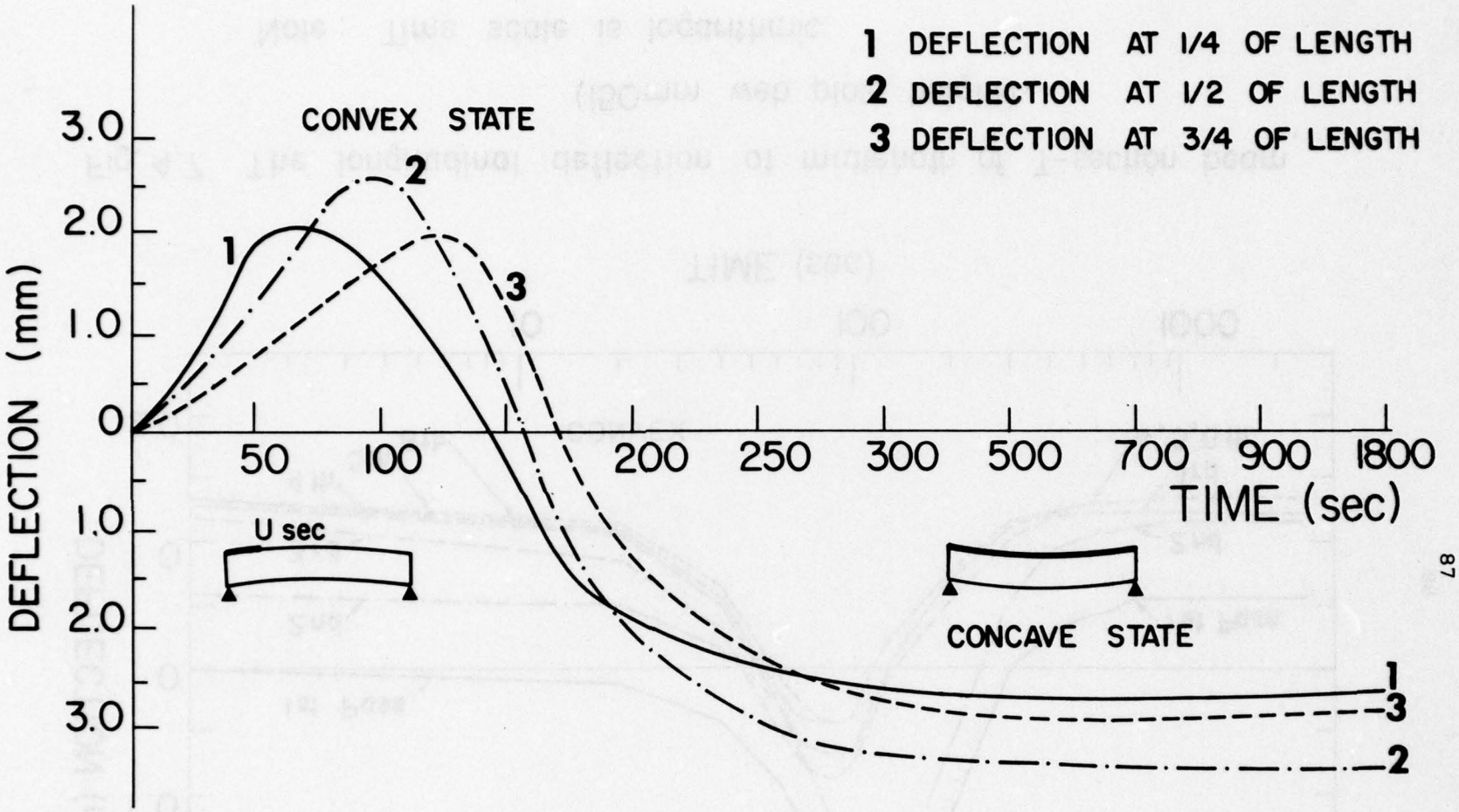

Fig. 4-6 Longitudinal deflection at different longitudinal points (mig-weld)

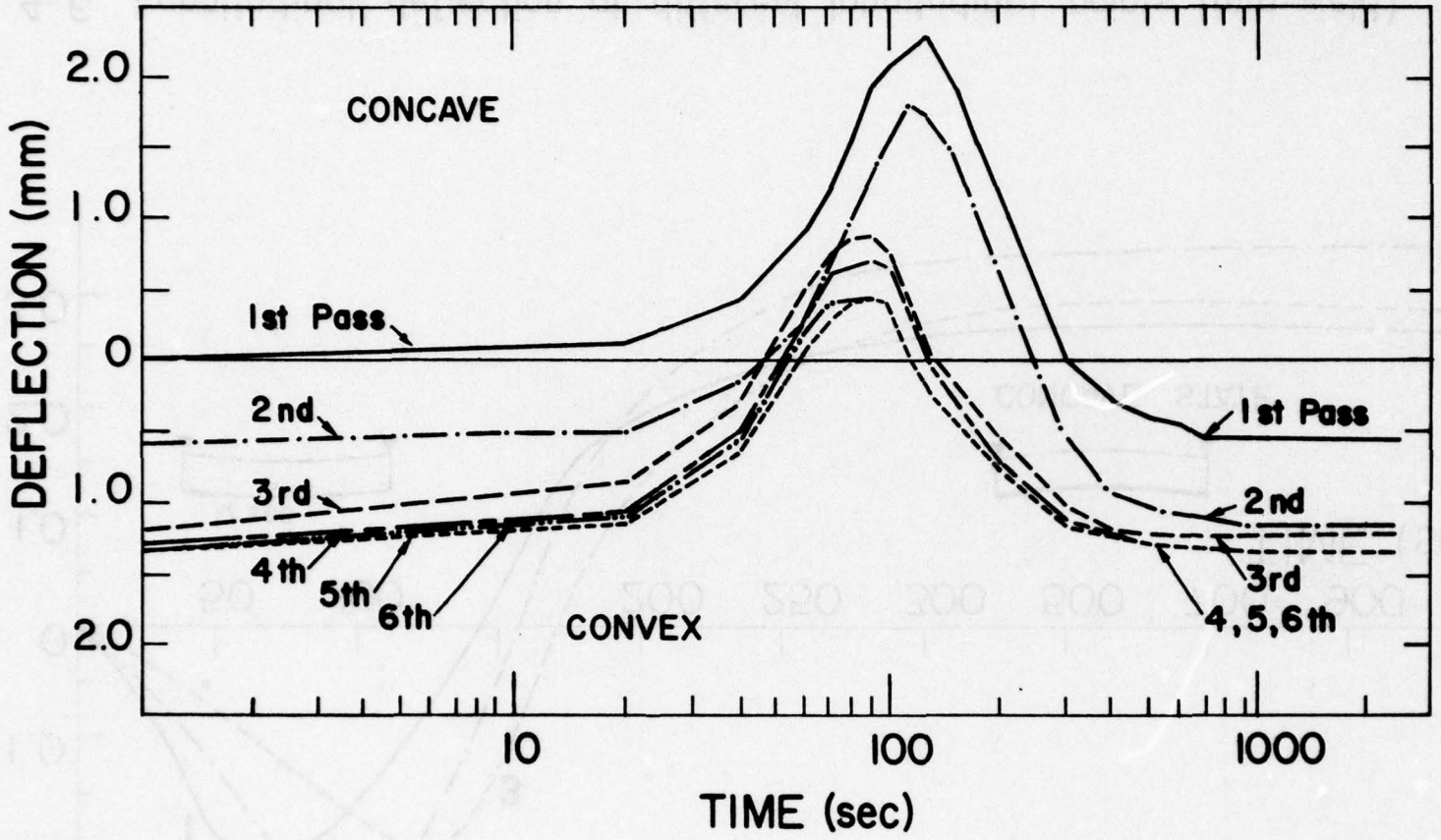

Fig. 4.7 The longitudinal deflection at midlength of T-section beam (150mm web plate height)

Note: Time scale is logarithmic

where:

$$u = \frac{kL}{2}$$

$$k = \left(\frac{P^*_x}{EI}\right) 1/2$$

$$M_o = -L_{na} \cdot P^*_x$$

L_{na} = distance between the neutral axis of the beam and the weld line

L = beam length

I = moment of inertia of beam

E = Young's modulus

P^*_x = shrinkage force

At mid length:

$$y = -\frac{M_o L^2}{8EI} \cdot \frac{2(\sec u - 1)}{u^2} \qquad (4.4)$$

Shrinkage force is calculated for both GMA and GTA welding processes using the values:

$$I = 4.2 \times 10^5 \text{ mm}^4; \quad E = 70 \times 10^3 \text{ MN/m}^2; \quad L_{na} = 75 \text{ mm}$$

S_o:

$$P^*_x = \begin{cases} + 62 \text{ kN, for GMA} \\ + 40 \text{ kN, for GTA} \end{cases}$$

(+ sign means compression)

The stresses are then calculated using

$$\sigma = \frac{M_o}{I/y} - \frac{P^*_x}{th} \qquad (4.5)$$

where

t = thickness

h = breadth

It is found:

$$\sigma = \begin{cases} 4{,}641y - 4{,}641 \text{ , for GMA} \\ 3{,}008y - 3{,}008 \text{ , for GTA} \end{cases}$$

Comparison of the stresses calculated above with the experimental ones showed good agreement everywhere, except in the region near the weld, where the discrepancy is expected due to the plastic region. Therefore, Yamamoto believes that the use of the shrinkage force obtained by the beam theory may be a useful tool in predicting longitudinal deflection.

The shrinkage force calculated above is now applied to fillet welding of a T-section beam. For a 150 mm x 100 mm T-beam, $I = 9 \times 10^6$ mm^4 and $L_{na} = 44$ mm. Substituting these values into equation (4.4) we find:

$Y_{cal} = 0.8$ mm

The corresponding experimental value was

$Y_{exp} = 0.6$ mm

Thus, deflection is overestimated by approximately 33%. Yamamoto proposed the use of a modification factor to take into account the difference between the shrinkage force P_x^* of a simple beam (edge welding) and a T-section beam (fillet welding). This modification factor was based on the observation that the heat intensity of the simple beam was 1.5 times that of the fillet welding in the T-section beam, which results in a value of 2/3 for the factor. The calculated deflection thus becomes $y_{cal} = 0.528$ mm. Comparing analytical and experimental results for other

cases, too, he finally proposed the following formula, which gives a reasonable approximation of longitudinal deflection at the mid-point of a T-section beam:

$$y = - \frac{M_o L^2}{4EI} \cdot \frac{\sec u - 1}{u^2} \qquad (4.6)$$

where

$$u = \frac{kL}{2}$$

$$k = \left(\frac{P^*_x C}{EI} \right)^{1/2}$$

$$M_o = - L_{na} \quad P^*_x$$

C = 2/3, coefficient for fillet welding of a T-section beam

P^*_x = shrinkage force calculated for an edge-welded beam.

As a result of the final stage of the experiments, it is mentioned that the clamping of the T-section beam during welding had little effect on the deflection of the beam at the completion of welding.

2.4.3 Computer Analysis

The complexity of the problem of longitudinal distortion of built-up beams makes the application of complete analytical methods almost impossible. Driven by this statement, Nishida [9] tried to apply both one-dimensional and finite element analyses to the problem.

One-Dimensional Analysis

In the one-dimensional analysis, only one-directional stresses are considered, namely those parallel to the fillet weld. Nishida assumes the quasi-stationary state, so that the Rosenthal solution for the temperature distribution can be used. A narrow strip element perpendicular

to the weld line is cut, both edges of which are assumed to remain straight (simple beam theory assumption). Then, the stress-strain relation is:

$$\varepsilon_x = \frac{1}{E}\sigma_x + \alpha T + \varepsilon_x^p \qquad (4.7)$$

where

ε_x = total strain in x-direction

σ_x = stress in x-direction

E = Young's modulus

α = thermal expansion coefficient (average)

T = temperature change from reference temperature

ε_x^p = plastic strain in x-direction

Since no external forces are present, the following equilibrium conditions hold:

$$\int_o^B \sigma_x A \, dy = 0 \qquad (4.8)$$

$$\int_o^B \sigma_x A \, y \, dy = 0 \qquad (4.9)$$

where B = plate width

By assuming $\tau_{xy} = \sigma_y = \sigma_z = 0$ the compatibility equation becomes:

$$\frac{\partial^2 \varepsilon_x}{\partial y^2} = 0 \qquad (4.10)$$

which results in:

$$\varepsilon_x = a + by \qquad (4.11)$$

Using equations (4.7) through (4.11) and an iteration procedure in cases where plastic deformation has occurred, stress σ_x, and strain ε_x can be determined.

Nishida extended the above procedure to a T-beam, treating each element separately (see Fig. 4-8) so that one-dimensional analysis can still be applied. Note that in this case an unknown reaction force R is present so that the equations become a little more complicated. A computer program is included in his thesis to carry out all the computations necessary.

Once the transient thermal strains are calculated, it is then possible to calculate the transient deflections of weld plates and built-up beams. Curvature, ρ, at a given time is equal to the quantity b in equation (4.11). Since the simple beam theory is assumed, the following relation holds:

$$\rho = \frac{d^2W(x)}{dx^2} \tag{4.12}$$

where W is the deflection in the y-direction at location x. The shape of deflection, W, can then be obtained by integrating the known ρ-curve twice along the x-direction.

The sensitivity of the results to material properties at the high temperature region was found to be great. Therefore, Nishida suggested that the precise value of high-temperature properties should be used in the above calculation.

Based on the above analysis, which as will be seen later was proven to be adequate for analyzing the problem of longitudinal distortion, Nishida conducted a parametric study to investigate the effect of various

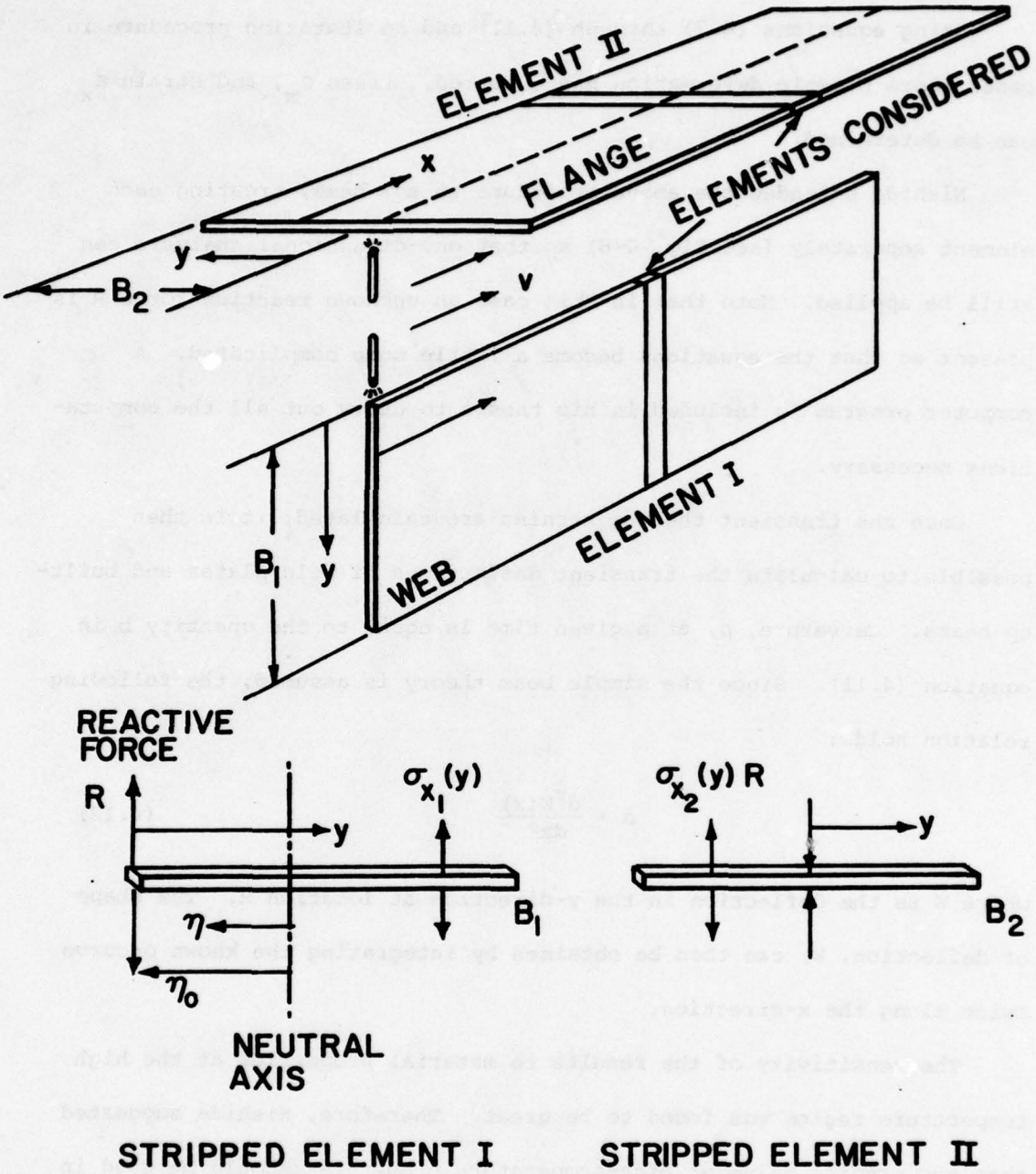

Fig. 4-8 Elements of T-shaped built-up beam

factors on values of residual deflection (deflection after welding is completed and the specimen has cooled to room temperature) at midlength. Figure 4-9 shows an example of this parametric study, in which the value of heat input was kept unchanged. It can be seen that when welding speed is increased while current, I, and voltage, V, are kept constant, the amount of distortion decreases rather drastically. On the other hand, when welding speed is increased while heat input is kept unchanged, residual distortion increases. There is also an indication that a welding speed exists where distortion becomes maximum.

Finite Element Analysis

The next step in improving the accuracy of the computation was to take into account the transverse stress σ_y, as well as the boundary at the finishing portion. Nishida tried to solve this two-dimensional problem using the incremental elasto-plastic finite element formulation, based on the flow theory of plasticity. The tangent stiffness method and the Huber-Mises-Hencky yield criterion were utilized. The phase transformation of steel and other metals was also taken into account, using the continuous cooling transformation diagram. A complete formulation of the method as well as the computer program developed (a modification of the second version of the M.I.T. 2-D F.E.M.) are included in Nishida's thesis.

Figure 4-10 shows comparison among deflection histories obtained by the F.E.M., the one-dimensional calculation and experimentally. One can see that the 2-D F.E.M. gives relatively poor results compared to the one-dimensional program. This suggests that an improvement of the F.E.M. program is mandatory. At the same time the current program is very

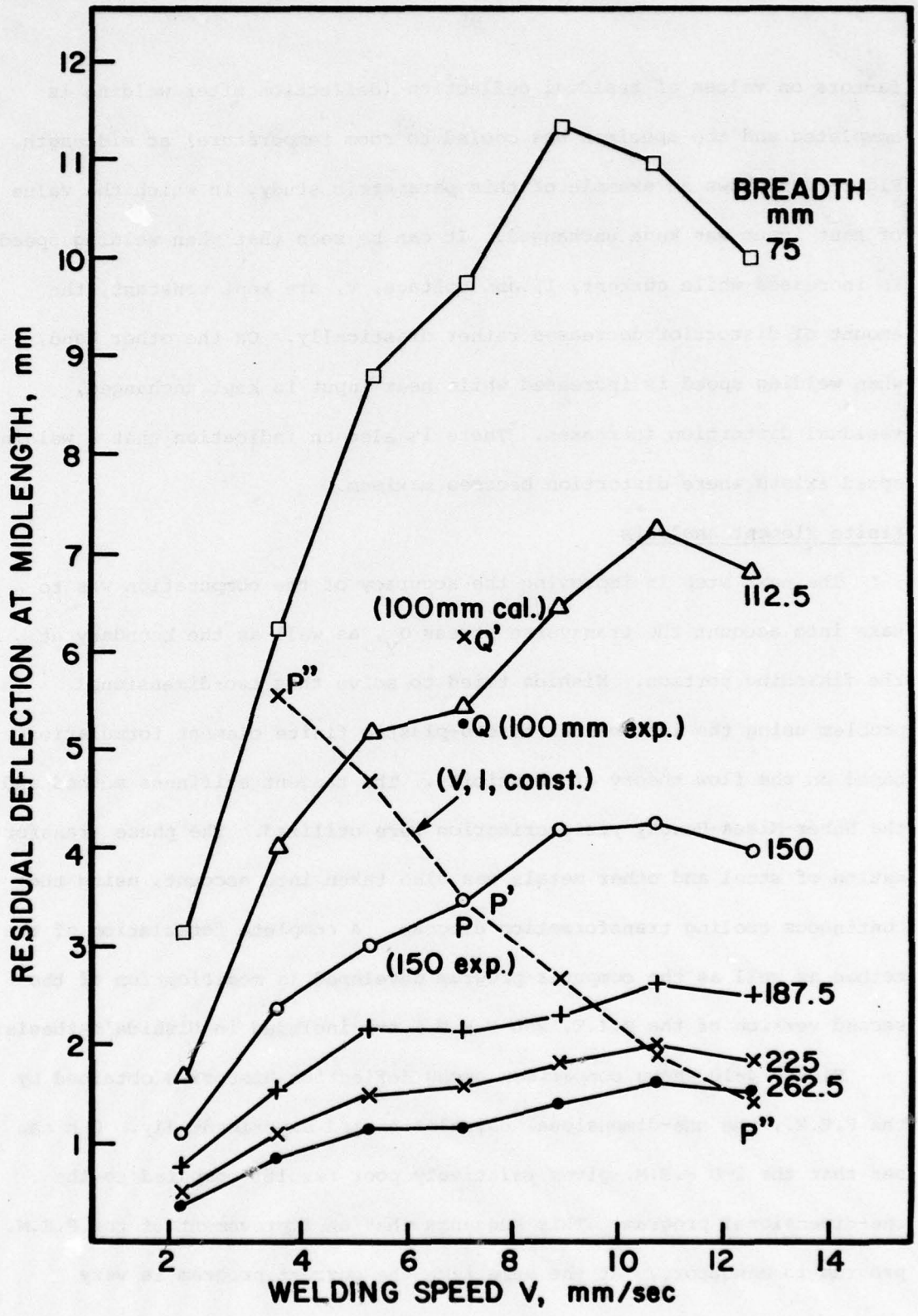

Fig. 4-9 Example of Parameter Study

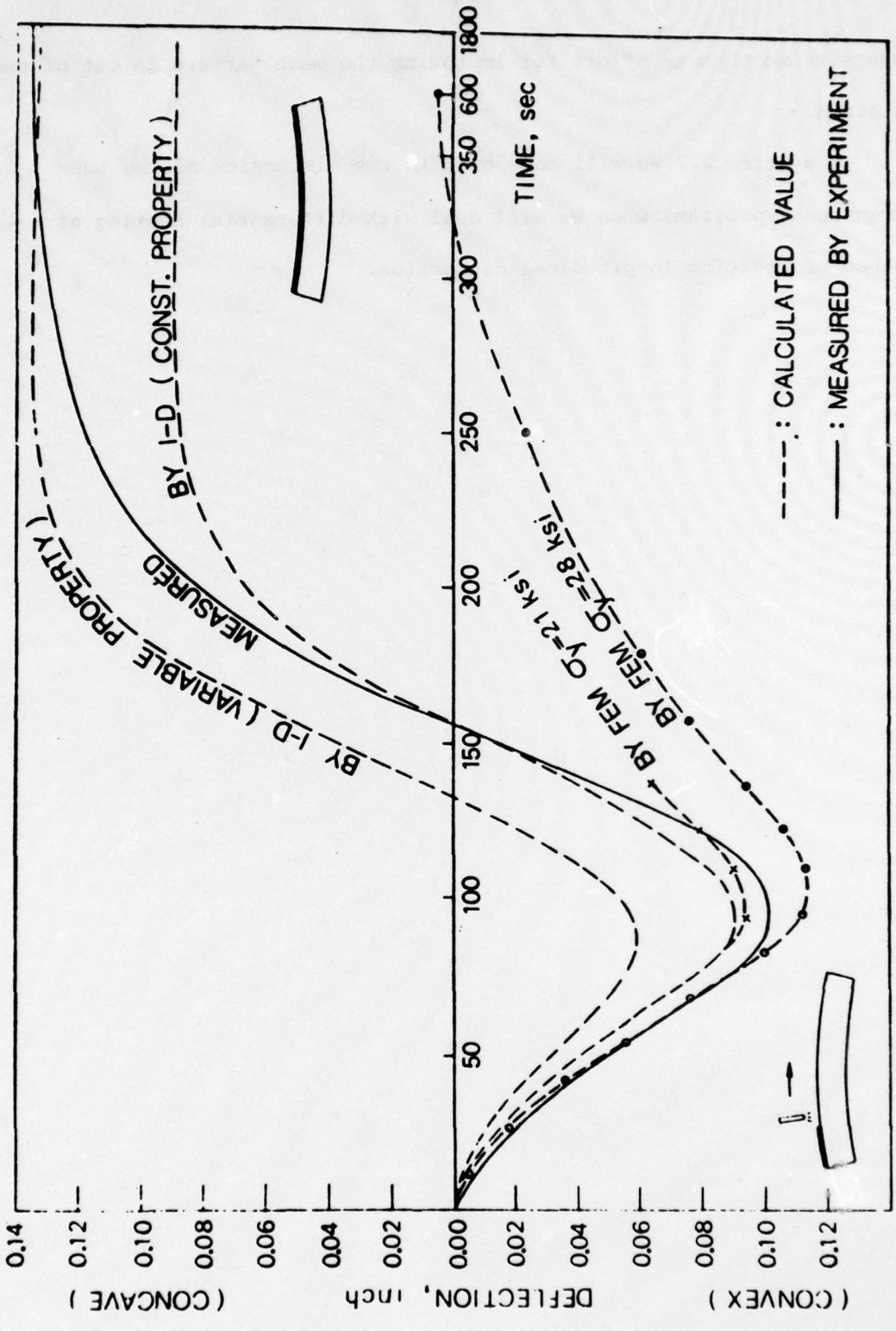

Fig. 4-10 Changes of deflection during welding

expensive so that an effort for improving the mesh pattern is out of the question.

In section 2.7 we will come back in the discussion of the one-dimensional program, when we will deal with differential heating as a method of reducing longitudinal distortion.

2.5 OUT-OF-PLANE DISTORTION IN ALUMINUM FILLET WELDS

A typical structural component of ships, aerospace and other structures is a panel structure which is composed of a flat plate and longitudinal and transverse stiffeners, fillet welded to the bottom plate as shown in Figure 5-1. The major distortion problem in the fabrication of a panel structure is that related to out-of-plane distortion caused by angular changes along the fillet welds.

Corrugation failures of bottom shell plating in some welded cargo vessels are believed to be due to the reduction of buckling strength of the plating with excessive initial distortion. This subject will be discussed in detail in Section 2.6.

When longitudinal and transverse stiffeners are fillet welded as shown in Figure 5-1, the deflection of a panel, δ, changes in both x- and y-directions. Because of the mathematical difficulties involved in the two-dimensional analysis, most studies conducted so far are one-dimensional; that is, only the change of deflection, δ, in the x-direction is taken into account. A 2-D analysis has been conducted at M.I.T., however, using the finite element method.

In this section we will try to discuss the state of the art of the mathematical analysis developed at M.I.T., as well as some of the experimental results obtained.

2.5.1 One-Dimensional Analysis

Semi-Analytical Method

Figure 5-2 shows out-of-plane distortion found in two types of simple fillet-welded structures. In both cases, the plates are narrow in

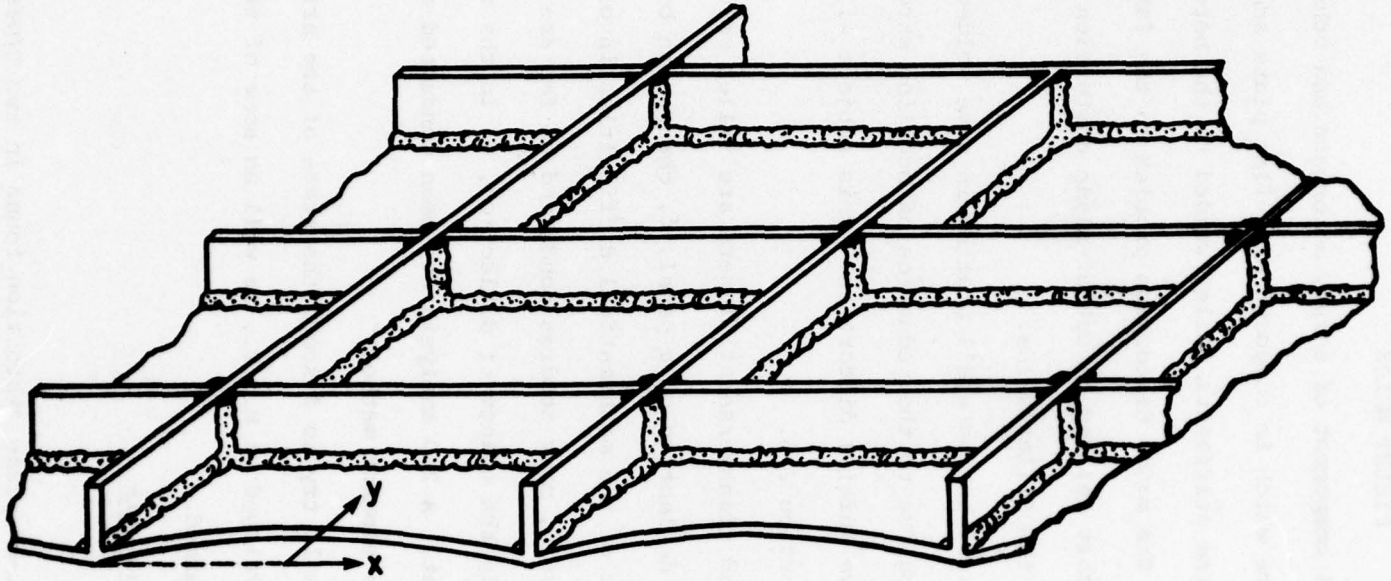

Fig. 5-1 Panel Structure with Longitudinal and Transverse Stiffeners

the y-direction and the distortion is one-dimensional.

When a fillet joint is free from external constraint, the structure simply bends at each joint and forms a polygon, as shown in Figure 5-2a. On the other hand, if the joint is constrained by some means, a different type of distortion is produced. For example, if the stiffeners are welded to a rigid beam, as shown in Figure 5-2b, the angular changes at fillet welds will cause a wavy, or arc-form, distortion of the bottom plate.

Masubuchi, et al., [33] found that the wavy distortion and resulting stresses can be analyzed as a problem of stresses in a rigid frame. In the simplest case in which the sizes of all welds are the same, the distortion of all spans are equal and the distortion, δ, can be expressed as follows:

$$\delta/\ell = [1/4 - (x/\ell - 1/2)^2] \cdot \phi \qquad (5.1)$$

where

δ = distortion at point x (Fig. 5-2b)

ϕ = angular change at a fillet weld, radians

ℓ = length of span

The maximum distortion at the panel center ($x = \ell/2$), δ_{max}, is:

$$\delta_{max} = 1/4 \cdot \phi \cdot \ell \qquad (5.2)$$

The amount of angular change, ϕ, in a restrained structure is smaller than that in a free joint, ϕ_o. The amount of ϕ also changes when the rigidity of the bottom plate, $D = Et^3/12(1 - \nu^2)$, and the length of the span, ℓ, change.

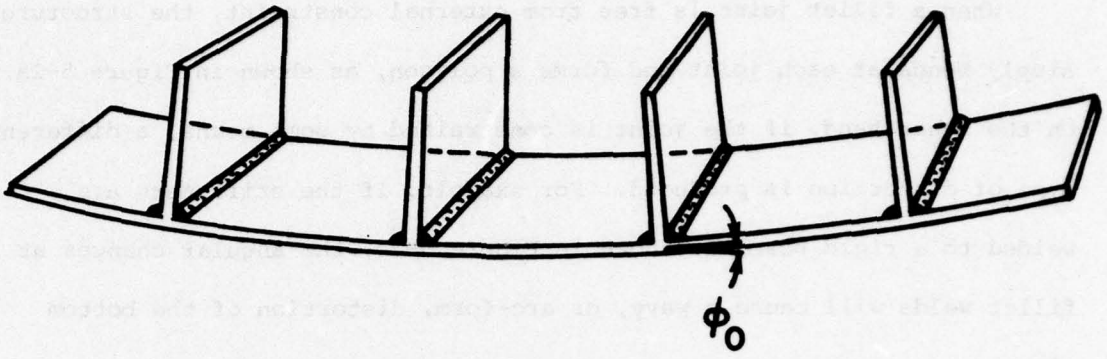

a. FREE JOINT

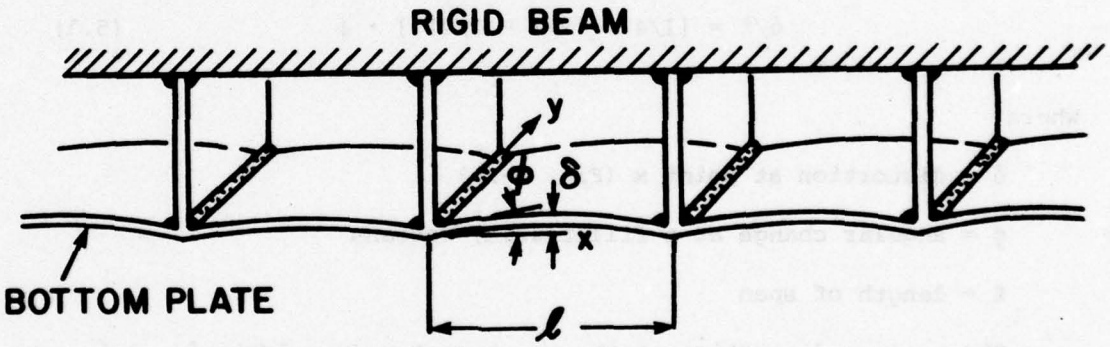

b. CONSTRAINED JOINT (FRAMED STRUCTURE)

Fig. 5 – 2 Distortion Due to Fillet Welds in Two Types of One Dimensional Models

In case of structures in low-carbon steel, Masubuchi, et al. have found that the following relationship exists:*

$$\phi = \frac{\phi_o}{1 + 2D/\ell \cdot 1/C} \qquad (5.3)$$

where C, the so-called "coefficient of rigidity for angular changes," can be determined by welding conditions and plate thickness.

A study was conducted at M.I.T. by Taniguchi [34] to determine experimentally values of ϕ_o and C for GMA welds in aluminum. The material used in the experiments was the strain hardened, aluminum magnesium structural alloy 5086-H32, largely utilized in marine and general structural applications. As for the filler metal, the recommended filler-5356 was used. Details of the experimental procedure can be found in Reference 34.

Figure 5-3 shows values of ϕ_o as a function of plate thickness, t (mm), and weight of electorde consumed per weld length, w (gr/cm). One should notice the fact that the angular change is maximum when plate thickness is around 7 mm. When the plate is thinner than 7 mm, the amount of angular change is reduced with the plate thickness. This is because the plate is heated more evenly in the thickness direction, thus reducing the bending moment. When the plate is thicker than 7 mm, the amount of angular change is reduced as the plate thickness increases because of the increase in the rigidity of the plate.

---

*The derivation of Equation (5.3) is given in Section 2.5.2; see Equations (5.6) through (5.10).

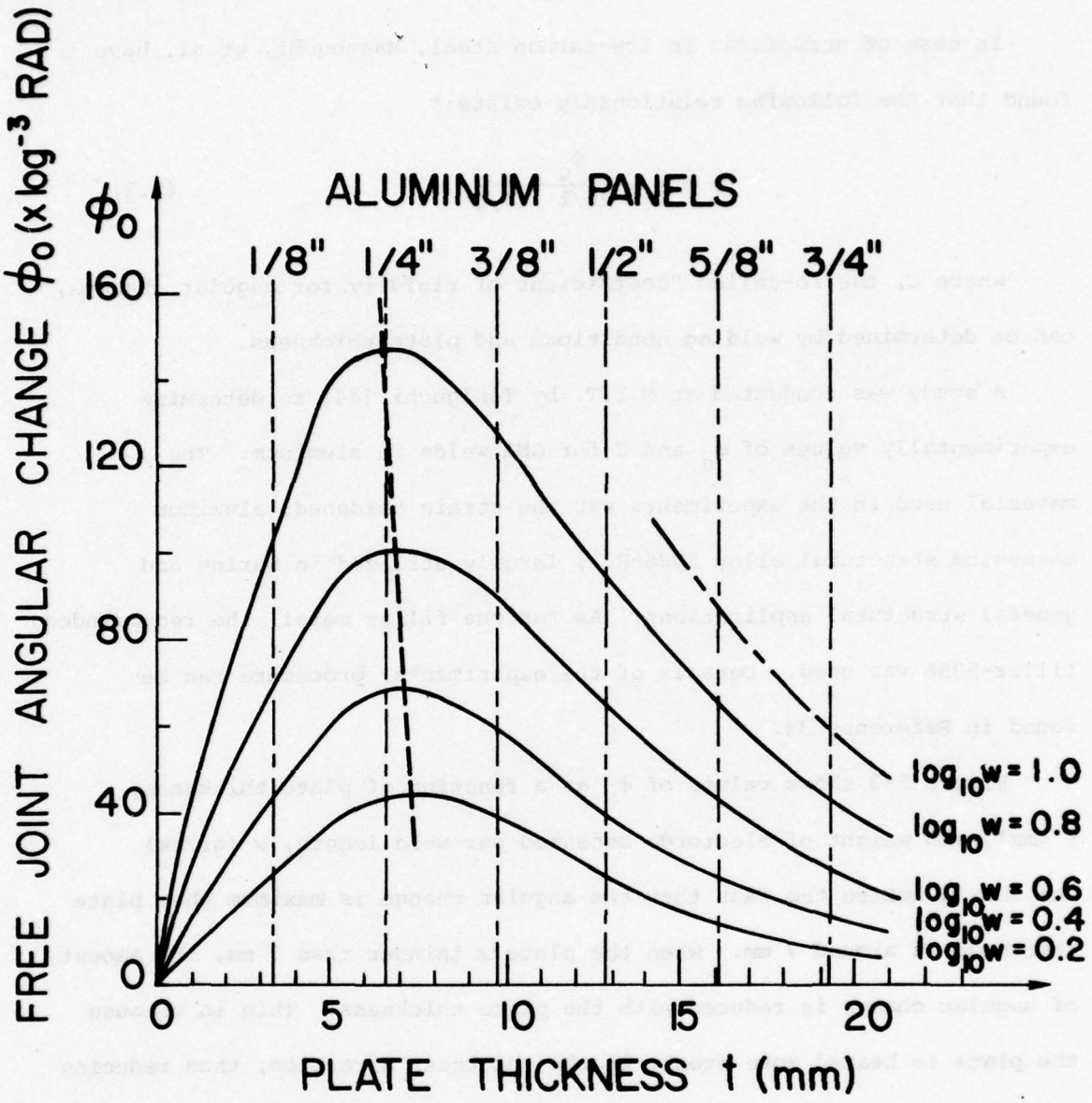

Fig. 5-3 Variation of free joint angular change, ϕ_0, as a function of plate thickness, t, and weight of electrode consumed per weld length, w. (Aluminum).

The wavy distortion shape, which is found in the constraint-joint case (see Figure 5-2b), is a consequence of the development of highly concentrated residual stresses near the weld zone and of the reaction stresses which result from the constraint. These reaction stresses were observed to be uniformly distributed over the whole region of the welded joint. It can, therefore, be assumed that the induced bending moments at the weld joints are constant. Under this assumption and using simple beam theory Taniguchi [34] arrived at the following relation:

$$\phi_{max} = \frac{M_o}{2EI} \tag{5.4}$$

where

ϕ_{max} = maximum value of ϕ (at $x = 0$)

M_o = induced bending moment

E = Young's modulus

I = moment of inertia of cross section

Good correlation was found between experimental values of ϕ_{max} and values obtained by the above analysis.

Figure 5-4 shows experimental values of the coefficient of rigidity C as a function of plate thickness, t, and weight of electrodes consumed per weld length, w (for 5086-H32 aluminum alloy). Carrying out a regression analysis, Taniguchi proposed the following equation:

$$C = 6.35t^{(2.67 - 0.065w)} \tag{5.5}$$

which is valid for the following cases:

$$1.58 \leq W \leq 6.30 \quad (w \text{ in g/cm})$$

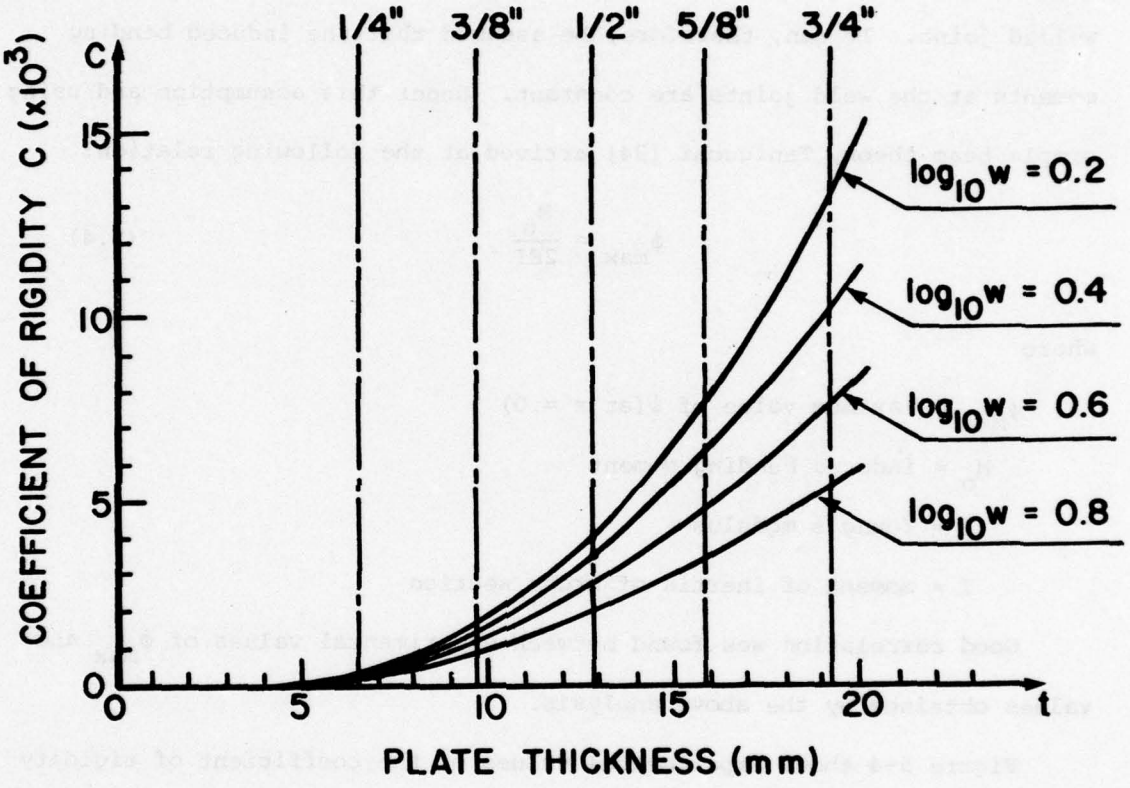

Fig. 5 – 4 Values of the Coefficient "C" Plotted Against Plate Thickness and Constant Values of $\log_{10} w$

$6 \text{ mm} \leq t \leq 19 \text{ mm}$ (t in mm)

Analytical Method

An effort was undertaken by Taniguchi [34] to approach the problem using a purely analytical method. The analysis included the determination of the temperature distribution through the plate thickness and accounted for the shrinkage of the fillet weld.

Table 5.1 summarizes and compares the experimental and analytical results obtained in the analysis. Results for mild steel from previous investigations were also included. The results show that the experimental values are quite above the theoretical ones, especially in the lower thickness range. It is believed that the disagreement is due to the many simplifications introduced in the analysis.

It is felt, however, that if a more comprehensive and accurate analysis is conducted taking into account such factors as the cooling rate, the temperature dependence of material properties, the stiffness of the structure, the number of welding passes, the welding sequence, etc., a better agreement with the experiments will be achieved.

2.5.2 Two-Dimensional Analysis

A two-dimensional analysis was conducted at M.I.T. by Shin [35] using the finite element method. A summary of this analysis will be included here.

Equation (5.3), developed by Masubuchi [33] for the one-dimensional case, was induced by using the minimum energy principle. As was stated in Section 2.5.1, the amount of angular change ϕ in a constrained structure is smaller than that in a free joint, ϕ_o. This indicates that

Table 5.1 Values of ϕ_o for Aluminum and Steel Obtained From theoretical Calculation and From Experiments

t (mm)	ϕ_o ($\times 10^{-3}$ rad)							
	5086-H32-Aluminum				Mild Steel			
	Due to plate heating	Due to fillet shrinkage	Total ϕ_o Calc.	Exp.	Due to plate heating	Due to fillet shrinkage	Total ϕ_o Calc.	Exp.
6.350	0.02	8.20	8.22	42.0	5.50	8.90	14.40	38.0
9.525	0.55	6.90	7.45	39.0	9.15	7.10	16.25	56.0
12.700	1.75	5.70	7.45	26.0	11.25	5.40	16.65	36.0
15.875	2.50	4.70	7.20	14.0	11.10	4.30	15.40	26.0
19.050	2.05	3.80	5.85	9.0	8.45	3.40	11.85	19.0

$D_{f\ Al}$ = 7.52 mm corresponding to $\log_w$ = 0.200

D_f steel = 6.10 mm corresponding to $\log_w$ = 0.650

Fillet sizes obtained from the recommended welding conditions for aluminum and steel.

a certain amount of energy is necessary to decrease the angular change from ϕ_o to ϕ. If the necessary energy is represented by U_w, one may write:

$$U_w = \int_0^{\phi_o - \phi} \frac{dU_w}{d(\phi_o - \phi)} d(\phi_o - \phi) \tag{5.6}$$

On the other hand, the strain energy stored in the constrained plate per unit width, U_p, can be expressed, using the elastic beam theory, as:

$$U_p = \frac{D}{\ell} \phi^2 \tag{5.7}$$

Since U_p increases and U_w decreases as the constrained angle increases, the condition for equilibrium of this system requires that the total energy $U_t = U_w + U_p$ should be minimum. Furthermore, for the simplification of the problem, the ratio of incremental welding energy change to angular change is assumed to be linear as follows:

$$\frac{dU_w}{d(\phi_o - \phi)} = C(\phi_o - \phi) \tag{5.8}$$

From equations (5.6) and (5.8), welding energy per unit width can be expressed as:

$$U_w = \frac{C}{2}(\phi_o - \phi)^2 \tag{5.9}$$

Accordingly, the condition of equilibrium is as follows:

$$\frac{\partial U_t}{\partial \phi} = - C(\phi_o - \phi) + \frac{2D}{\ell} \phi = 0 \tag{5.10}$$

From the above, equation (5.3) is obtained.

Extending the same principle to the distortion of a rectangular plate

with fillet welds along the four edges, we can express the deflection $\delta(x, y)$ at any point as:

$$\delta(x, y) = c_1 + c_2 x + c_3 y + \ldots \tag{5.11}$$

The strain energy stored in the rectangular plate, with length a and width b, is then given by:

$$U_p = \frac{D}{2}\int_0^a \int_0^b \left[\left(\frac{\partial^2\delta}{\partial x^2} + \frac{\partial^2\delta}{\partial y^2}^{\ 2}\right) - 2(1-\nu)\left(\frac{\partial^2\delta}{\partial x^2}\cdot\frac{\partial^2\delta}{\partial y^2} - \frac{\partial^2\delta}{\partial x\partial y}\right)^2\right] dxdy \tag{5.12}$$

The welding energy stored in the fillet welds along the four edges is:

$$U_w = \int_0^a \frac{C_y}{2}(\phi_o - \phi_y)^2 dx + \int_0^b \frac{C_x}{2}(\phi_o - \phi_x)^2 dy \tag{5.13}$$

where, C_y and C_x are C-values of the welds parallel to the y- and x-axis respectively, and ϕ_y and ϕ_x are angular changes at welds parallel to the y- and x- axis respectively.

For equilibrium, the variation of the total energy should be zero:

$$\delta U_T = \delta U_p + \delta U_w = 0 \tag{5.14}$$

The finite element method was used to conduct the numerical analysis. Figure 5-5 shows how the rectangular plate was divided.

In an effort to verify the validity of this analysis, comparison was made of analytically determined panel distortions and experimental data obtained by Duffy [36]. Although absolute agreement of analytical and experimental results was not accomplished, the shapes of distortion

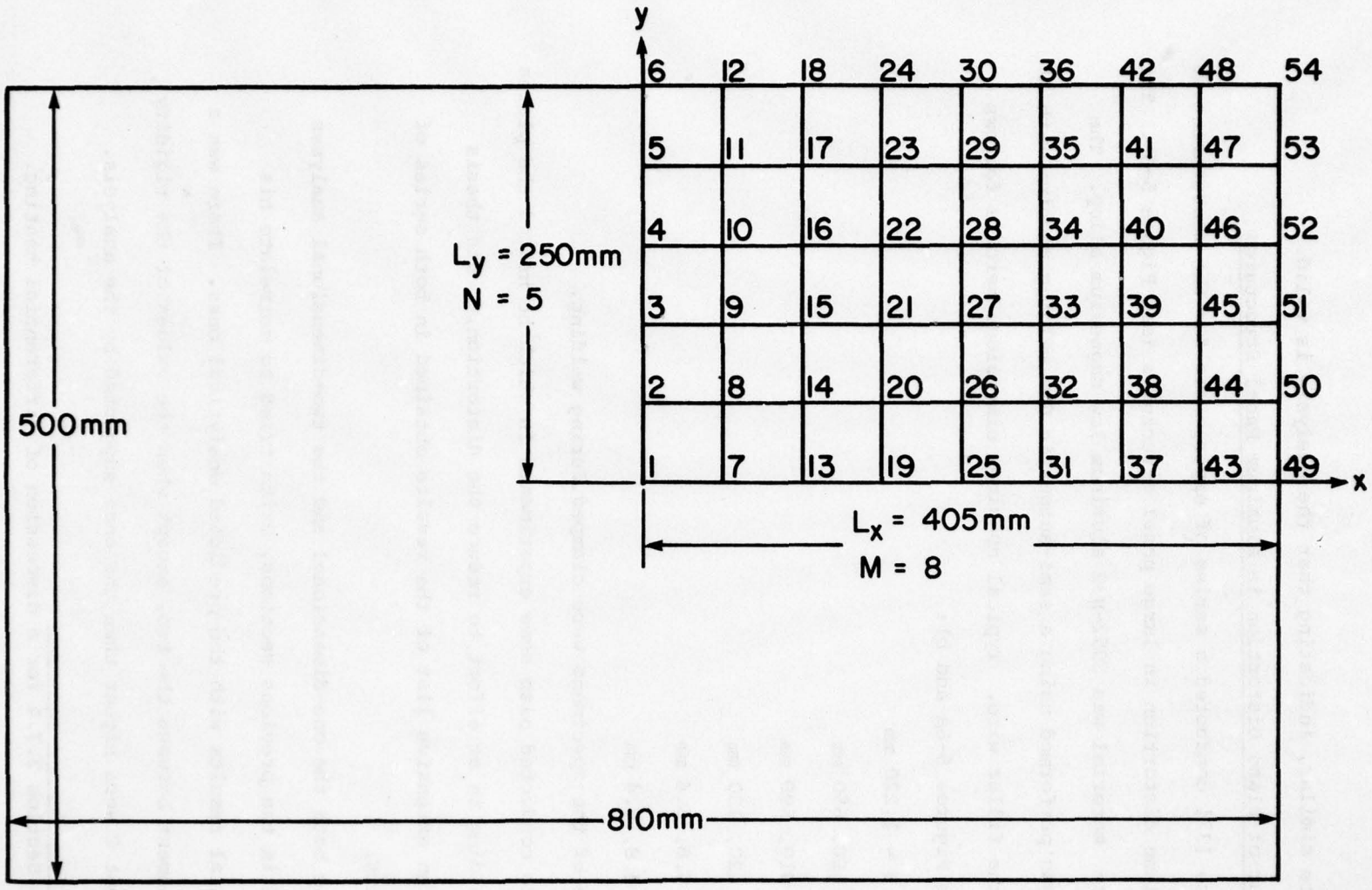

Fig. 5-5 Dimensions and Element Meshes of One-quarter of the Plate for Computer Input

were quite similar, indicating that the analysis is valid.

2.5.3 Out-of-Plane Distortion in Aluminum Panel Structures

Brito [37] conducted a series of experiments for the measurement of out-of-plane distortion in large panel structures (see Figure 5-6). The base plate material was 5052-H32 aluminum low magnesium alloy. The welding was performed using a semi-automatic GMA welding machine with Al 4043 as the filler wire. Typical specimen dimensions were as follows (refer to Figures 5-6a and b):

A = B = 1,220 mm

a = 600, 650 mm

b = 410, 590 mm

T = 120, 130 mm

h = 4.8, 6.4 mm

H = 4.8, 6.4 mm

Some of the specimens were clamped during welding.

Brito conducted also some experiments in which he heated the plates before welding in an effort to reduce the distortion.* His thesis contains an extensive list of the results obtained in both series of experiments.

Using both the one-dimensional and the two-dimensional analyses described in the previous sections, Brito tried to correlate his experimental results with the predicted analytical ones. There was a poor agreement between the two, except when the values of the rigidity coefficient C were higher than the ones suggested by the analysis.

*See Section 2.7.4 for a discussion of differential heating.

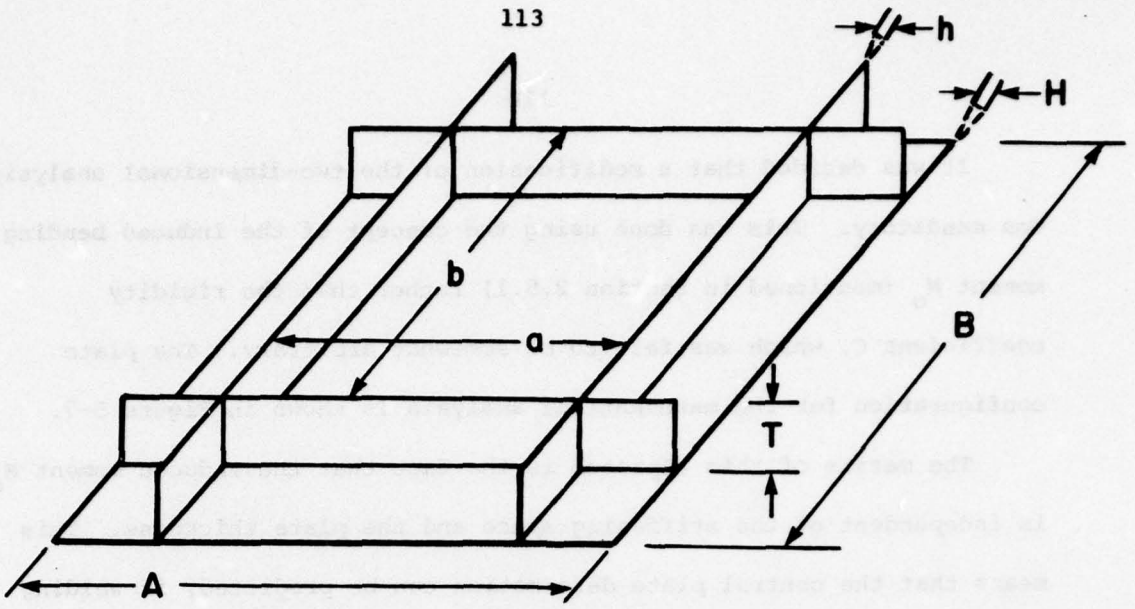

Fig. 5-6a

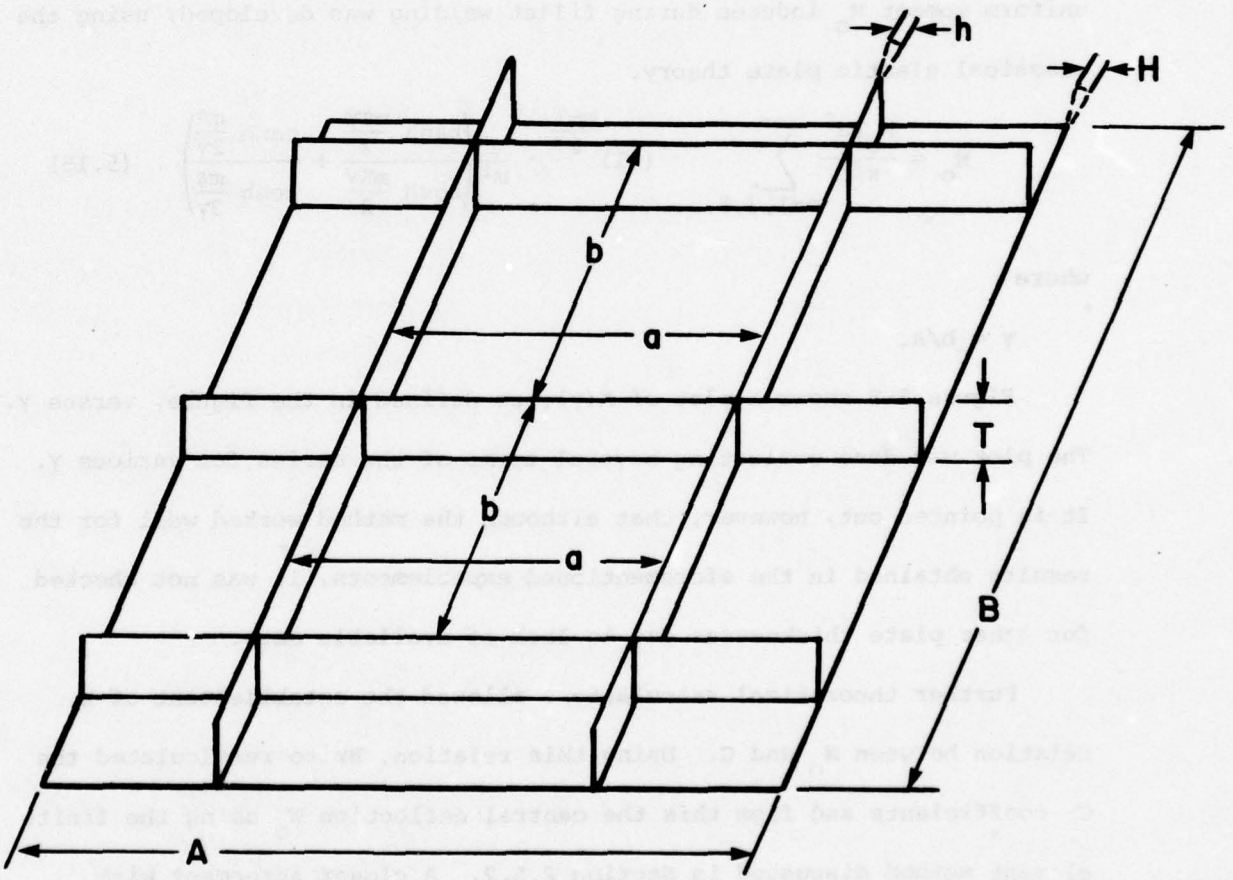

Fig. 5-6b

Fig. 5-6 Experimental Plate Dimensions and Configuration

It was decided that a modification of the two-dimensional analysis was mandatory. This was done using the concept of the induced bending moment M_o (mentioned in section 2.5.1) rather than the rigidity coefficient C, which was felt to be somewhat arbitrary. The plate configuration for the mathematical analysis is shown in Figure 5-7.

The merits of this approach is the fact that the induced moment M_o is independent of the stiffening space and the plate thickness. This means that the central plate deformation can be predicted, if welding parameters are known.

As equation relating the central deflection W_o and the equivalent uniform moment M_o induced during fillet welding was developed, using the classical elastic plate theory:

$$W_o = \frac{M_o \gamma a^2}{\pi^2 D} \sum_{m=1,3,5,\ldots} (-1)^{\frac{m-1}{2}} \cdot \frac{1}{m^2} \left(\frac{\tanh \frac{m\pi\gamma}{2}}{\cosh \frac{m\pi\gamma}{2}} + \frac{\tanh \frac{m\pi}{2\gamma}}{\cosh \frac{m\pi}{2\gamma}} \right) \qquad (5.15)$$

where

$\gamma = b/a$.

Figure 5-8 shows a plot of $K(\gamma)$, as defined in the figure, versus γ. The plot was done evaluating several terms of the series for various γ. It is pointed out, however, that although the method worked well for the results obtained in the aforementioned experiements, it was not checked for other plate thicknesses due to lack of available data.

Further theoretical calculations allowed the establishment of a relation between M_o and C. Using this relation, Brito recalculated the C- coefficients and from this the central deflection W_o using the finite element method discussed in Section 2.5.2. A closer agreement with experimental results was found, as shown in Figure 5-9.

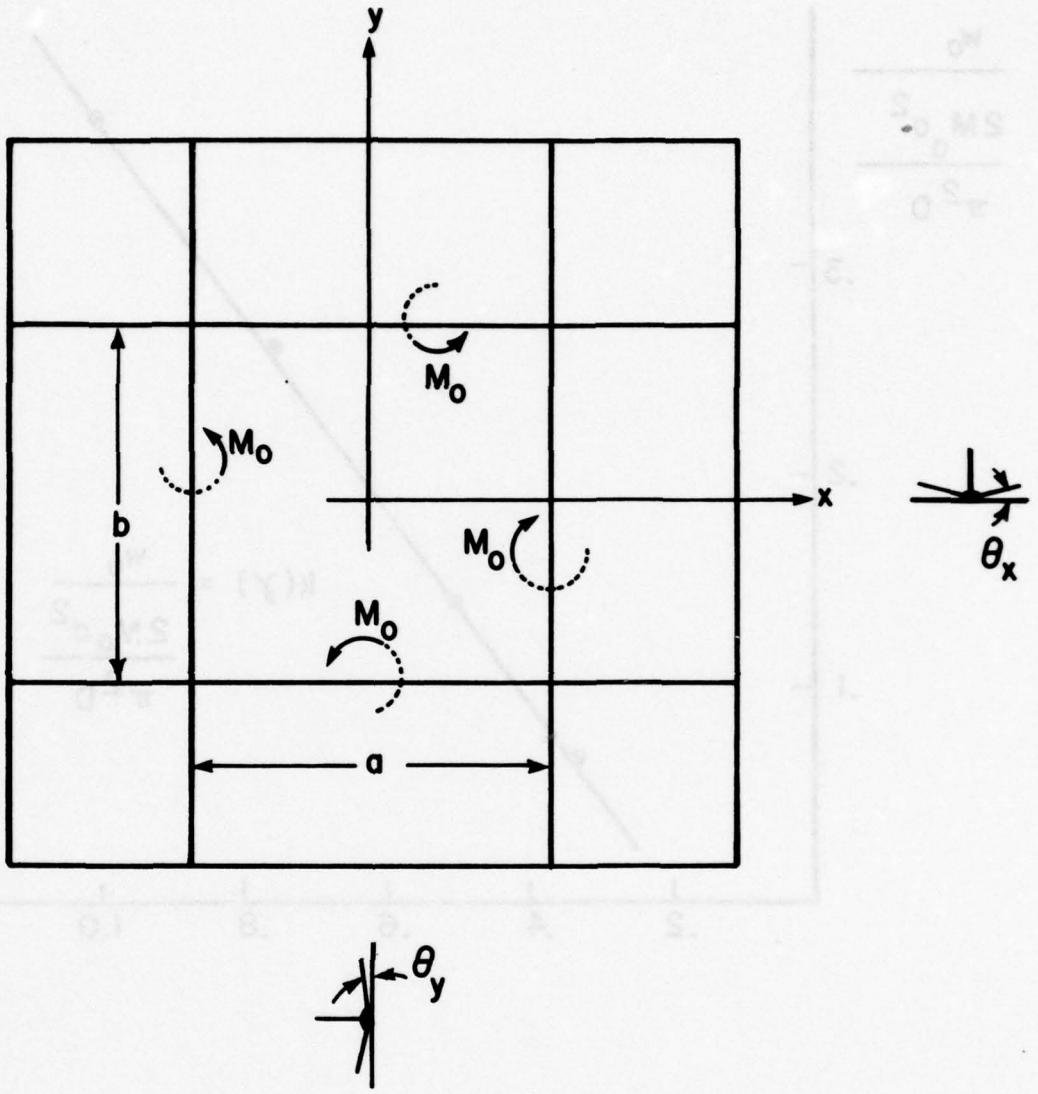

Fig. 5-7 Plate Configuration

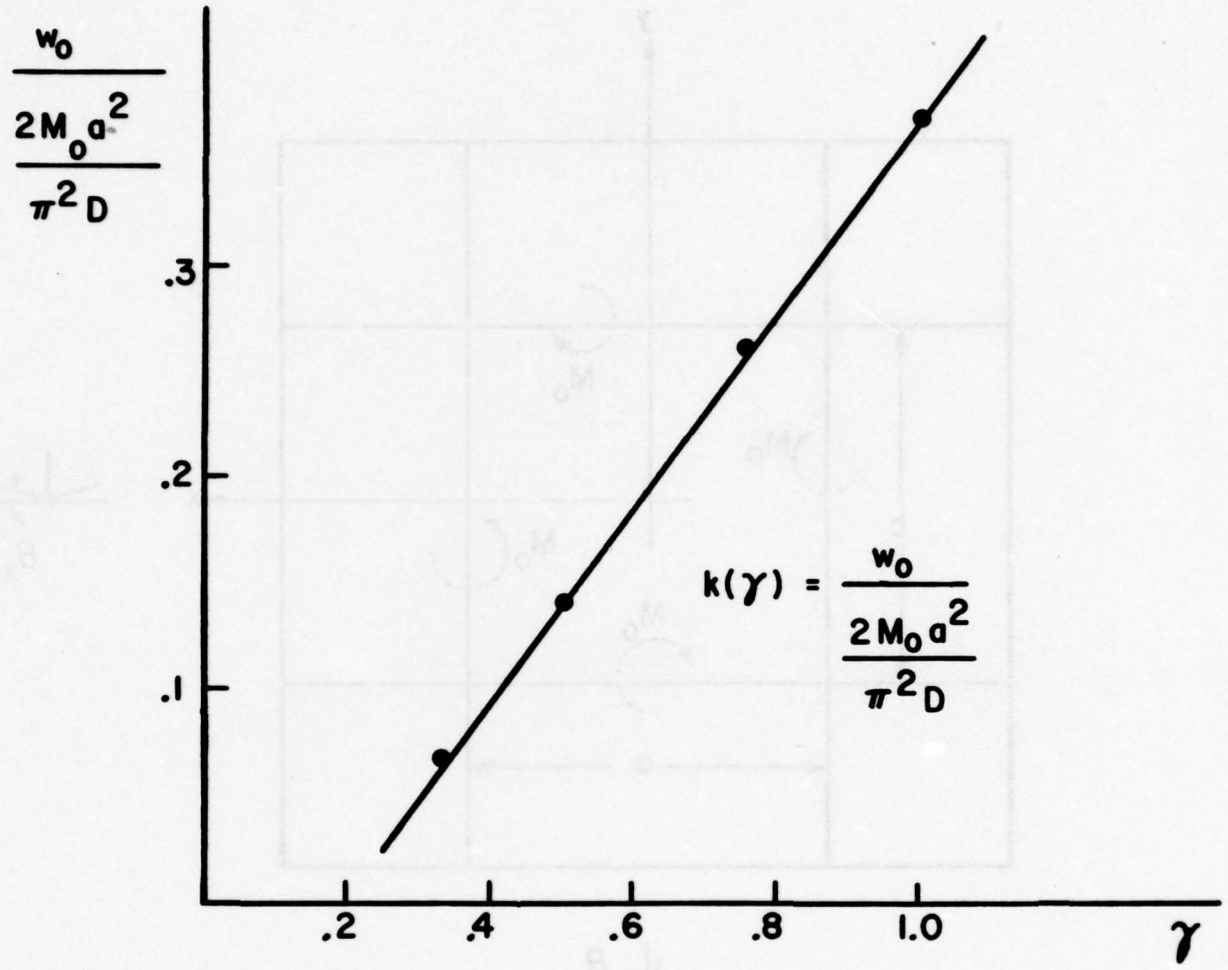

Fig. 5 – 8 Calculation of k (γ)

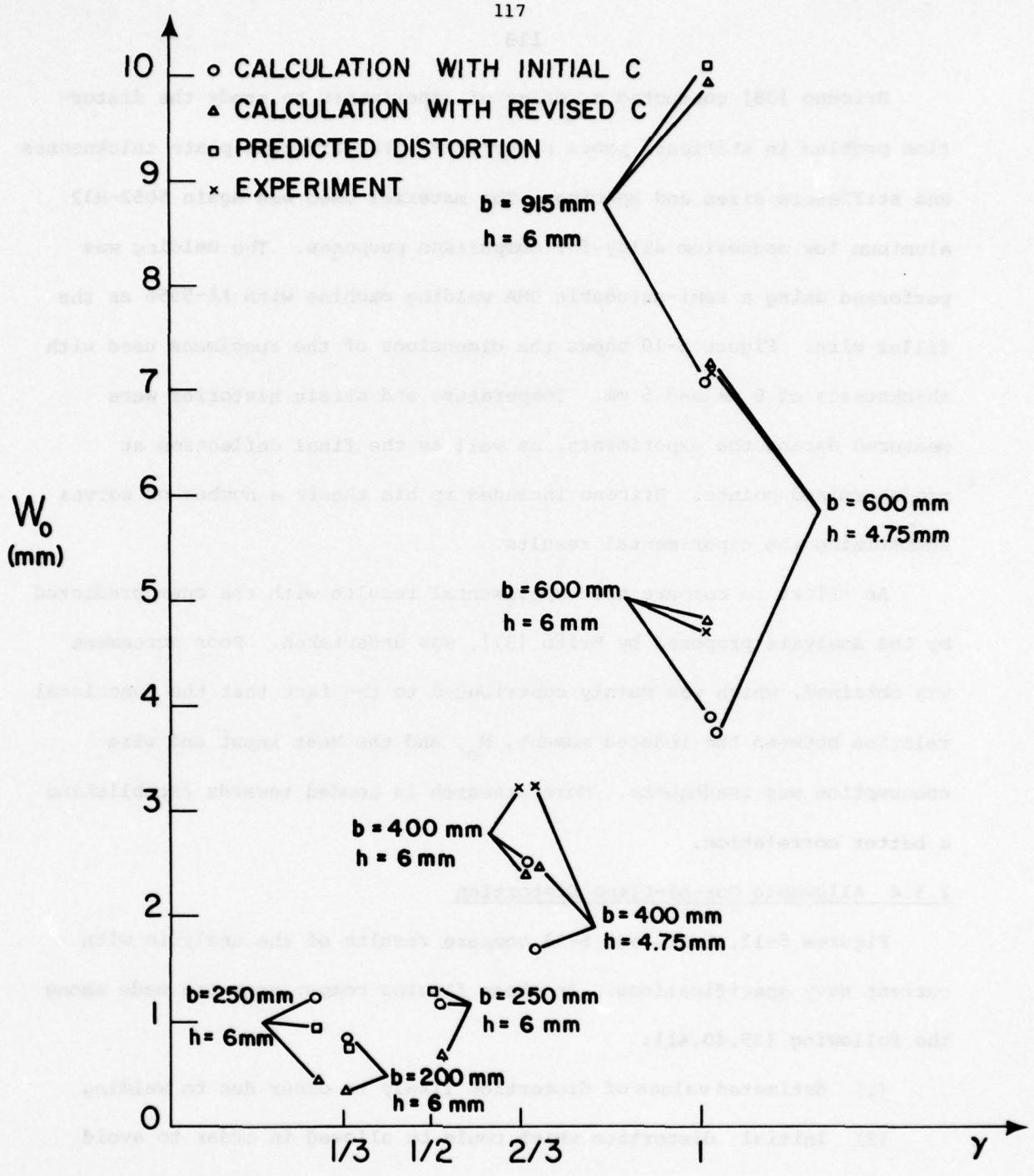

Fig. 5-9 Comparison between calculated, predicted and experimental central plate deflection

Briceno [38] conducted a series of experiments to study the distortion problem in stiffened panel structures with different plate thicknesses and stiffeners sizes and spacing. The material used was again 5052-H32 aluminum low magnesium alloy for comparison purposes. The welding was performed using a semi-automatic GMA welding machine with Aℓ-5356 as the filler wire. Figure 5-10 shows the dimensions of the specimens used with thicknesses of 6 mm and 5 mm. Temperature and strain histories were measured during the experiments, as well as the final deflection at predetermined points. Briceno included in his thesis a number of curves summarizing the experimental results.

An effort to compare the experimental results with the ones predicted by the analysis proposed by Brito [37], was undertaken. Poor agreement was obtained, which was mainly contributed to the fact that the functional relation between the induced moment, M_o, and the heat input and wire consumption was inadequate. More research is needed towards establishing a better correlation.

2.5.4 Allowable Out-of-Plane Distortion

Figures 5-11, 5-12, and 5-13 compare results of the analysis with current Navy specifications. In these figures comparisons are made among the following [39,40,41]:

(1) Estimated values of distortion likely to occur due to welding

(2) Initial distortion which could be allowed in order to avoid buckling of the panel under certain service conditions

(3) Distortion allowed in NAVSHIPS specifications

Figure 5-11 shows the results for steel structures with a fixed span length of 800 mm using various thicknesses. Figures 5-12 and 5-13 show

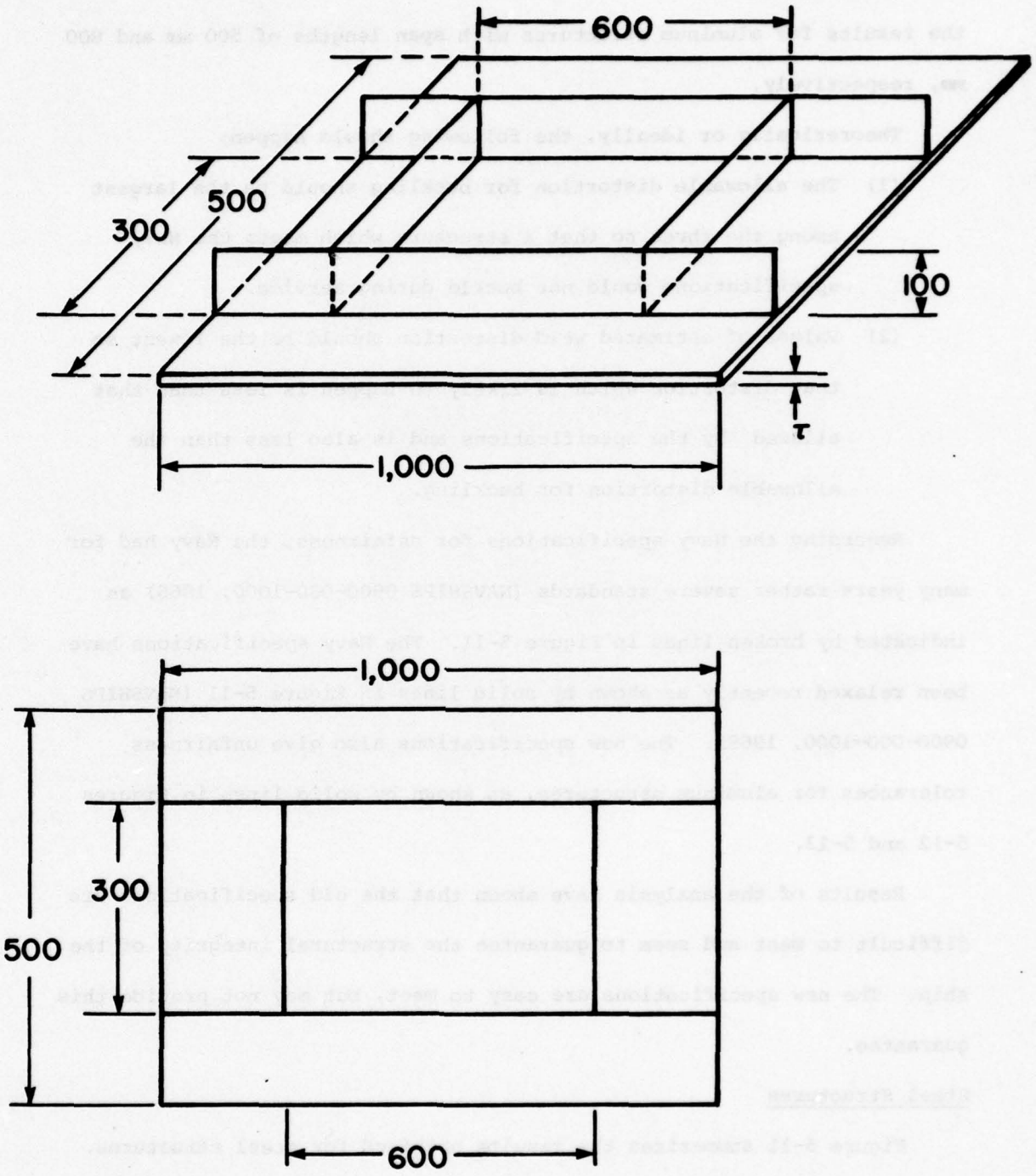

Fig. 5 – 10 Dimensions of the Standard Specimen For the Experiments

the results for aluminum structures with span lengths of 500 mm and 800 mm, respectively.

Theoretically or ideally, the following should happen:

(1) The allowable distortion for buckling should be the largest among the three so that a structure which meets the Navy specifications would not buckle during service.

(2) Values of estimated weld distortion should be the lowest so that distortion which is likely to happen is less than that allowed by the specifications and is also less than the allowable distortion for buckling.

Regarding the Navy specifications for unfairness, the Navy had for many years rather severe standards (NAVSHIPS 0900-000-1000, 1966) as indicated by broken lines in Figure 5-11. The Navy specifications have been relaxed recently as shown by solid lines in Figure 5-11 (NAVSHIPS 0900-000-1000, 1969). The new specifications also give unfairness tolerances for aluminum structures, as shown by solid lines in Figures 5-12 and 5-13.

Results of the analysis have shown that the old specifications are difficult to meet and seem to guarantee the structural integrity of the ship. The new specifications are easy to meet, but may not provide this guarantee.

Steel Structures

Figure 5-11 summarizes the results obtained for steel structures. Values of weld distortion estimated by Masubuchi (based on experiments made in Japan) and by Okerblom (based on experiments in Russia) are definitely lower than the solid lines but slightly higher than the broken

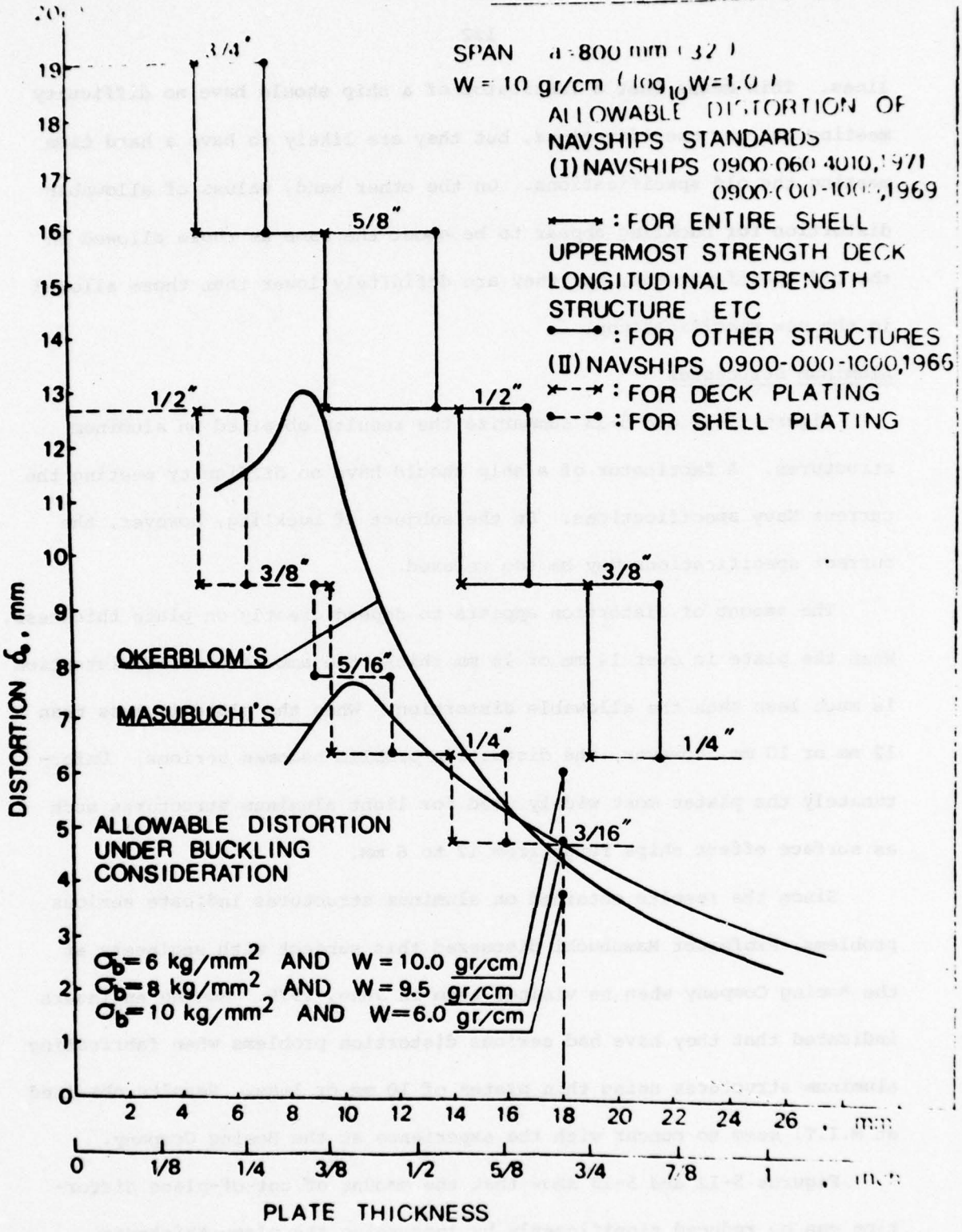

Fig. 5-11 Comparison between (i) possible distortion estimated from formulas by Masubuchi and Okerblom, (ii) allowable distortion by Navy specifications, and (iii) allowable distortion under buckling consideration

lines. This means that a fabricator of a ship should have no difficulty meeting the new specifications, but they are likely to have a hard time meeting the old specifications. On the other hand, values of allowable distortion for buckling appear to be about the same as those allowed in the old specifications, but they are definitely lower than those allowed in the new specifications.

Aluminum Structures

Figures 5-12 and 5-13 summarize the results obtained on aluminum structures. A fabricator of a ship should have no difficulty meeting the current Navy specifications. On the subject of buckling, however, the current specifications may be too relaxed.

The amount of distortion appears to depend greatly on plate thickness. When the plate is over 14 mm or 16 mm thick, the amount of weld distortion is much less than the allowable distortion. When the plate is less than 12 mm or 10 mm, however, the distortion problem becomes serious. Unfortunately the plates most widely used for light aluminum structures such as surface effect ships range from 12 to 6 mm.

Since the results obtained on aluminum structures indicate serious problems, Professor Masubuchi discussed this subject with engineers at the Boeing Company when he visited them in June, 1975. Boeing engineers indicated that they have had serious distortion problems when fabricating aluminum structures using thin plates of 10 mm or less. Results obtained at M.I.T. seem to concur with the experience at the Boeing Company.

Figures 5-12 and 5-13 show that the amount of out-of-plane distortion can be reduced significantly by increasing the plate thickness, for example from 10 to 12 mm. But this significantly increases the weight

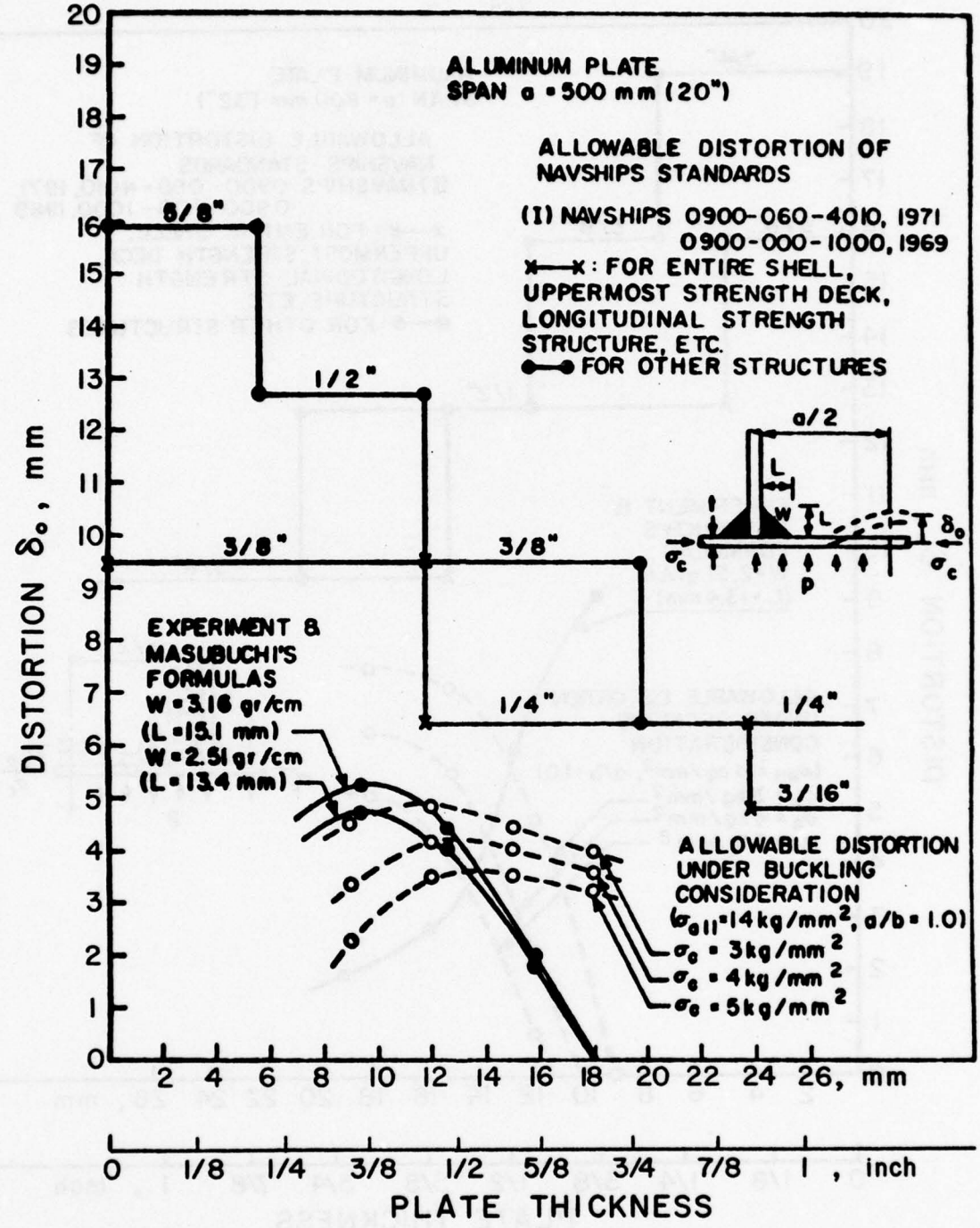

Fig. 5-12 Comparison Among (1) Possible Distortion Estimated from Formulas by Masubuchi, (2) Allowable Distortion by Navy Specification and (3) Allowable Distortion Under Buckling Consideration for Aluminum Plate of 500 mm span

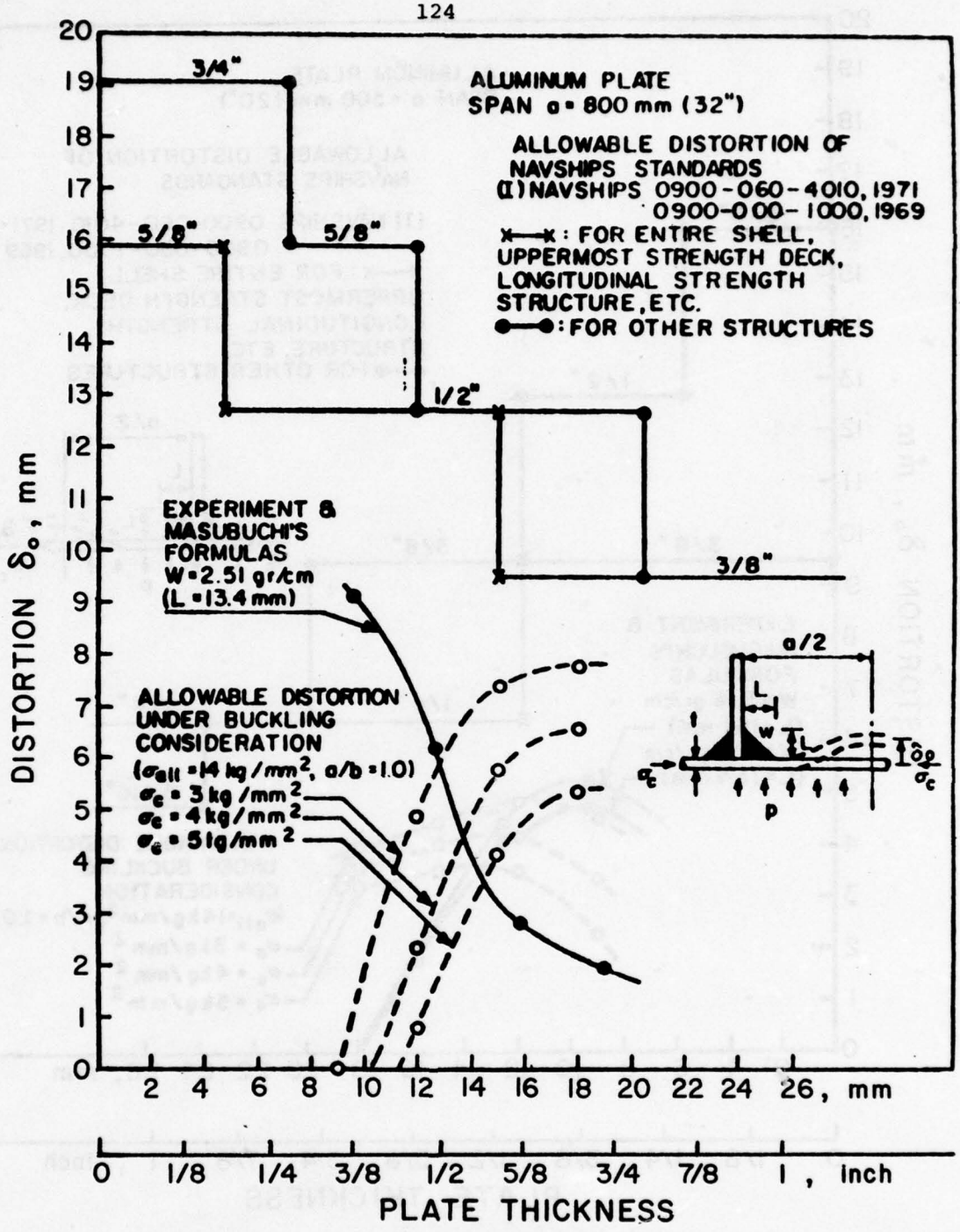

Fig. 5-13 Comparison Among (1) Possible Distortion Estimated from Formulas by Masubuchi, (2) Allowable Distortion by Navy Specification and (3) Allowable Distortion Under Buckling Consideration for Aluminum Plate of 800 mm span

of the structure. One way to solve the problem is to reduce the length of span, for example, from 800 mm to 500 mm. Figures 5-12 and 5-13 show that in fabricating structures with plates 10 mm thick, for example, weld distortion can be reduced and the amount of allowable distortion increased by reducing the span from 800 mm to 500 mm.

The results indicate that distortion analysis is important in structural design. An optimum design must take into account structural integrity, welding fabrication, structural weight as well as fabrication cost.

2.6 BUCKLING DISTORTION OF THIN ALUMINUM PLATES

When thin plates are welded, residual compressive stresses occur in areas away from the weld and cause buckling. Buckling distortion occurs when the specimen length exceeds the critical length for a given thickness in a given specimen size. In studying weld distortion in thin plated structures, it is important to first determine whether the distortion is being produced by buckling or by bending. Buckling distortion differs from bending distortion in that:

1. There are more than one stable deformed shapes.
2. The amount of deformation in buckling distortion is much greater.

Basic information about buckling distortion and its effect on the service performance of structures can be found in references 4, 5, and 13, written by Masubuchi. In this section, the analytical and experimental investigations carried out recently at M.I.T. will be summarized.

2.6.1 Analytical Investigation

Pattee [42] carried out an analytical study of buckling distortion, in an effort to determine the critical load of a plate under various boundary conditions. For simplicity he assumed that longitudinal residual stresses (parallel to the weld line) exist only. Furthermore, he assumed the presence of a uniform tension zone of width 2δ and magnitude T_{tx} and a uniform compression zone of magnitude T_{cx}. If the plate width is b, the equilibrium condition can be written as:

$$T_{tx} \cdot (2\delta) = T_{cx} \cdot (b - 2\delta) \qquad (6.1)$$

where the compressive stresses are taken as positive.

Assuming linear elasticity, the governing differential equation can then be written as:

$$\frac{\partial^4 w}{\partial x^4} + 2\frac{\partial^4 w}{\partial x^2 \partial y^2} + \frac{\partial^4 w}{\partial y^4} + \frac{1}{D}(N_x + \eta_x)\frac{\partial^2 w}{\partial x^2} = 0 \qquad (6.2)$$

where

w = deflection [mm]

D = flexural rigidity of the plate = $\frac{Eh^3}{12(1 - \nu^2)}$

E = Young's modulus [N/m]

ν = Poisson's ratio

h = plate thickness [mm]

N_x = mid-plane load [N/m]

η_x = residual stress distribution [N/m]

Equation (6.2) can be solved either by assuming a solution of the form

$$w = f(y) \cdot \sin \frac{m\pi x}{a} \qquad (6.3)$$

where

a = plate length [mm]

m = number of half-lengths in x-direction

or by using the so-called "energy method."

Pattee solved the equation for the four boundary conditions shown in Table 6.1 in the case of a butt weld. Due to the complexity of the calculations, however, the solutions could not be found in closed form.

Papazoglou [45] tried to solve the equation in closed form. Using the method developed by Yoshiki, et al. [44] he transformed the partial

Table 6.1 Boundary Conditions and Their Analogs

BOUNDARY CONDITIONS	ANALOGS
1. 4 edges simply-supported	1. Butt-welded plates which are large in both directions
2. Loaded edges simply-supported opposite edges free and free	2a. Long, narrow unrestrained plates 2b. The unclamped test plate
3. Loaded edges simply-supported opposite edges clamped and free	3a. The "outboard" section of a stiffened panel 3b. The partially unclamped test plate
4. Loaded edges simply-supported opposite edges clamped and clamped	4a. Plate clamped during welding 4b. Sections of stiffened plates between stiffeners

differential equation into the following integral equation.

$$w(x, y) = -\int_0^a \int_0^b [(N_x + \eta_x) \frac{\partial^2 w}{\partial \xi^2}] \cdot G(x, y; \xi, \eta) d\xi d\eta \qquad (6.4)$$

where

$G(x, y; \xi, \eta)$ = appropriate Green's function to satisfy the boundary conditions.

The integral equation was solved for the cases of butt welds and edge welds for both simply supported and clamped boundary conditions. To illustrate the procedure the case of simply supported butt weld will be solved.

To satisfy the simply supported boundary conditions the following assumptions are made:

$$G(x, y; \xi, \eta) = \sum_{m=1}^{\infty} \sum_{n=1}^{\infty} \frac{\phi_{mn}(x,y) \cdot \phi_{mn}(\zeta,\eta)}{\lambda^2_{mn}} \qquad (6.5a)$$

$$w(x, y) = \sum_{m=1}^{\infty} \sum_{n=1}^{\infty} a_{mn} \phi_{mn}(x,y) \qquad (6.5b)$$

$$w(\xi, \eta) = \sum_{r=1}^{\infty} \sum_{s=1}^{\infty} a_{rs} \phi_{rs}(\xi,\eta) \qquad (6.5c)$$

where

$$\phi_{mn}(x, y) = \frac{2}{\sqrt{ab}} \sin \frac{m\pi x}{a} \sin \frac{n\pi y}{b} \qquad (6.6a)$$

$$\lambda^2_{mn} = D\left[\left(\frac{m\pi}{a}\right)^2 + \left(\frac{n\pi}{b}\right)^2\right]^2 \qquad (6.6b)$$

Substituting the above relations into equation (6.4) one gets:

$$\lambda^2_{mn} a_{mn} = \sum_{r=1}^{\infty} \sum_{s=1}^{\infty} a_{rs} \left(\frac{r\pi}{a}\right)^2 (A_{rsmn} + L_{rsmn}) \qquad (6.7)$$

where

$$A_{rsmn} = \int_0^a \int_0^b N_x(\xi, \eta)\ \phi_{rs}(\xi, \eta)\ \phi_{mn}(\xi, \eta) d\xi d\eta \qquad (6.8a)$$

$$L_{rsmn} = \int_0^a \int_0^b \eta_x(\xi, \eta)\ \phi_{rs}(\xi, \eta)\ \phi_{mn}(\xi, \eta) d\xi d\eta \qquad (6.8b)$$

Solving equation (6.7) one finally gets:

$$\sigma_{cr} = \frac{E\pi^2}{12(1 - \nu^2)} \left(\frac{h}{b}\right)^2 \left(m\frac{b}{a} + \frac{1}{m}\frac{a}{b}\right)^2 + \sigma_c \cdot \left[\sin \frac{2\pi\delta}{b} \Big/ \frac{2\pi\delta}{b}\right] \qquad (6.9)$$

where

σ_c = magnitude of compressive residual stresses [N/m^2]

$\sigma_{cr} = N_{x,cr}/h$ [N/m^2]

Tables 6.2 and 6.3 show the results of the analysis for the cases on simply supported and built-in loading edges respectively. Note that the results are very similar to the ones obtained by investigators at Kawasaki Heavy Industries [43].

Figures 6-1 through 6-4 show plots of non-dimensionalized critical stress, σ_{cr}/σ_y (σ_y = yield stress of material used), as a function of b/h and δ/b for the case of square plates (a = b) and m = 1.

It can be seen from the figures that in the cases of welding on the plate center, there is an increase of the critical load as the tensile zone increases, irregardless of the boundary conditions. In the cases of edge welding the opposite thing happens; the critical stress decreases as the tensile zone width increases and it even becomes negative. This indicates the fact that the plate will buckle even in the absence of external compressive loading or even if tensile external loading is

Table 6.2 Buckling of Simply Supported Rectangular Plate Under Uniaxial Compressive Stresses

(a) The center of plate y = b/2 is welded

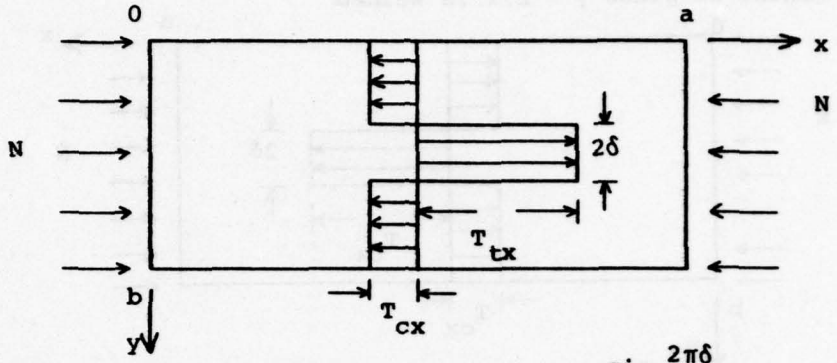

$$\sigma_{cr} = \frac{E\pi^2}{12(1-\nu^2)} \left(\frac{h}{b}\right)^2 \left(m\frac{b}{a} + \frac{1}{m}\frac{a}{b}\right)^2 + \sigma_c \cdot \frac{\sin\frac{2\pi\delta}{b}}{\frac{2\pi\delta}{b}}$$

(b) Both sides y = 0 and y = b are welded

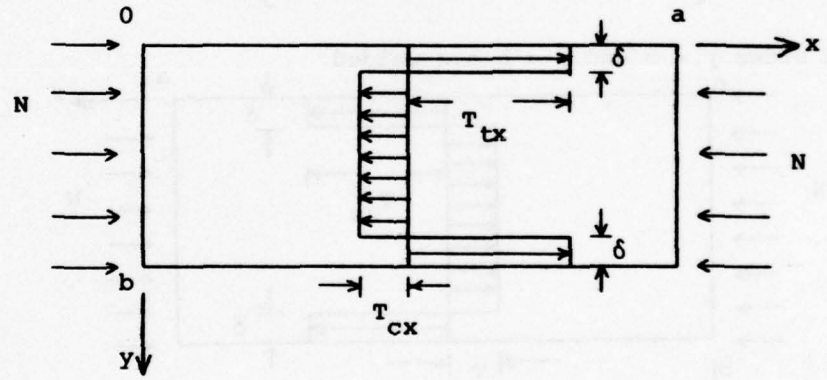

$$\sigma_{cr} = \frac{E\pi^2}{12(1-\nu^2)} \left(\frac{h}{b}\right)^2 \left(m\frac{b}{a} + \frac{1}{m}\frac{a}{b}\right)^2 - \sigma_c \cdot \frac{\sin\frac{\pi(b-2\delta)}{b}}{\frac{2\pi\delta}{b}}$$

Table 6.3 Buckling of Clamped Rectangular Plate Under Uniaxial Compressive Stresses

(a) The center of plate y = b/2 is welded

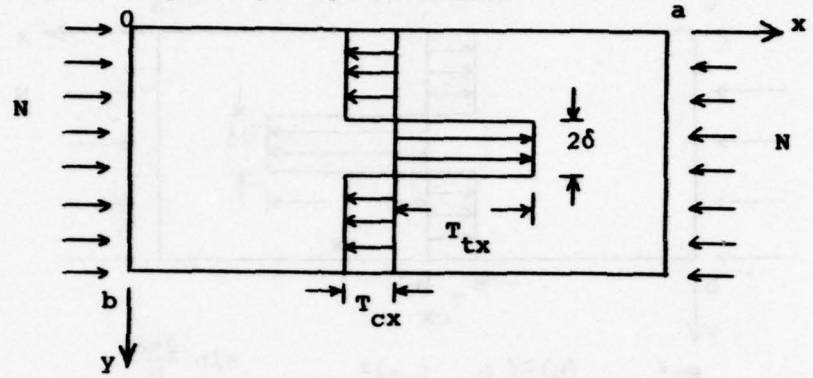

$$\sigma_{cr} = \frac{E\pi^2}{144(1-\nu^2)} \cdot \left(\frac{h}{b}\right)^2 \cdot \left[48\, m^2 \left(\frac{b}{a}\right)^2 + 48\, \frac{1}{m^2} \left(\frac{a}{b}\right)^2 + 32\right]$$

$$+ \sigma_c \cdot \left[\frac{2b}{3\pi\delta} \cdot \sin\frac{2\pi\delta}{b} + \frac{b}{12\pi\delta} \cdot \sin\frac{4\pi\delta}{b}\right]$$

(b) Both sides y = 0 and y = b are welded

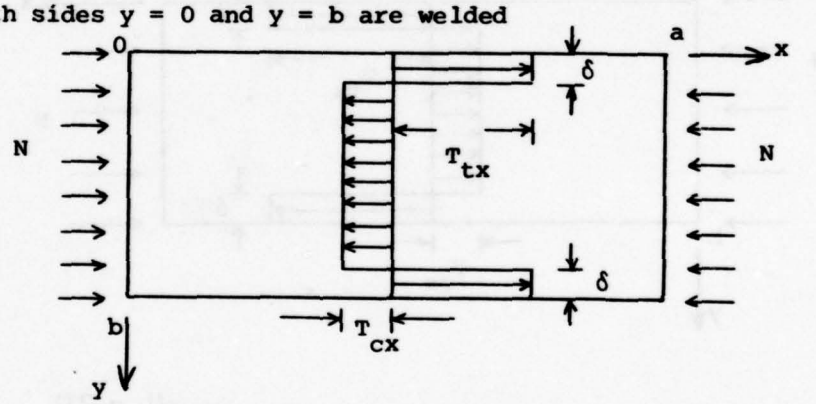

$$\sigma_{cr} = \frac{E\pi^2}{144(1-\nu^2)} \cdot \left(\frac{h}{b}\right)^2 \cdot \left[48\, m^2 \left(\frac{b}{a}\right)^2 + 48\, \frac{1}{m^2} \left(\frac{a}{b}\right)^2 + 32\right]$$

$$- \sigma_c \cdot \left[\frac{2b}{3\pi\delta} \cdot \sin\frac{2\pi\delta}{b} - \frac{b}{12\pi\delta} \cdot \sin\frac{4\pi\delta}{b}\right]$$

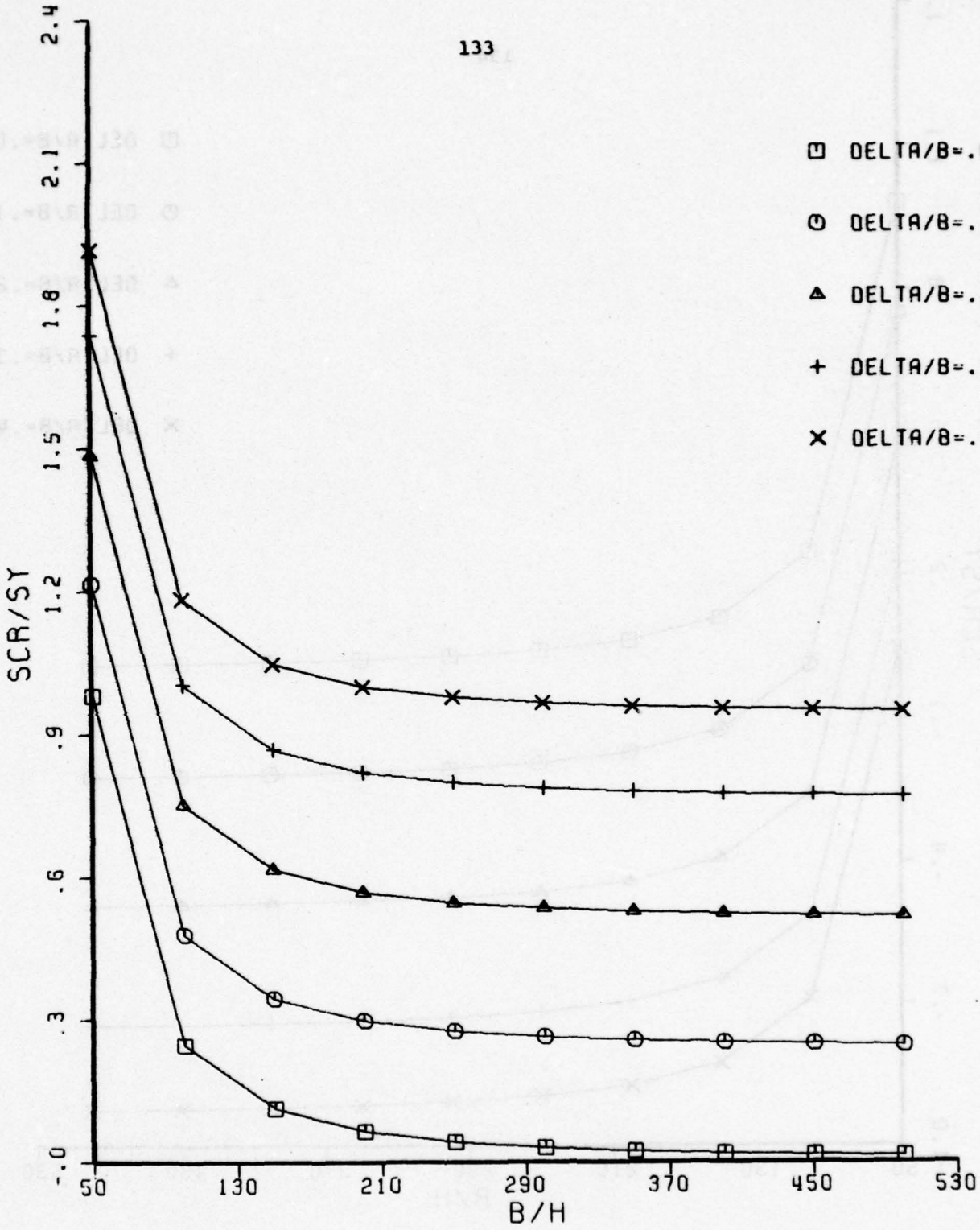

Fig. 6-1 Critical Stress for a Simply Supported Square Plate with Bead-on-Plate Weld

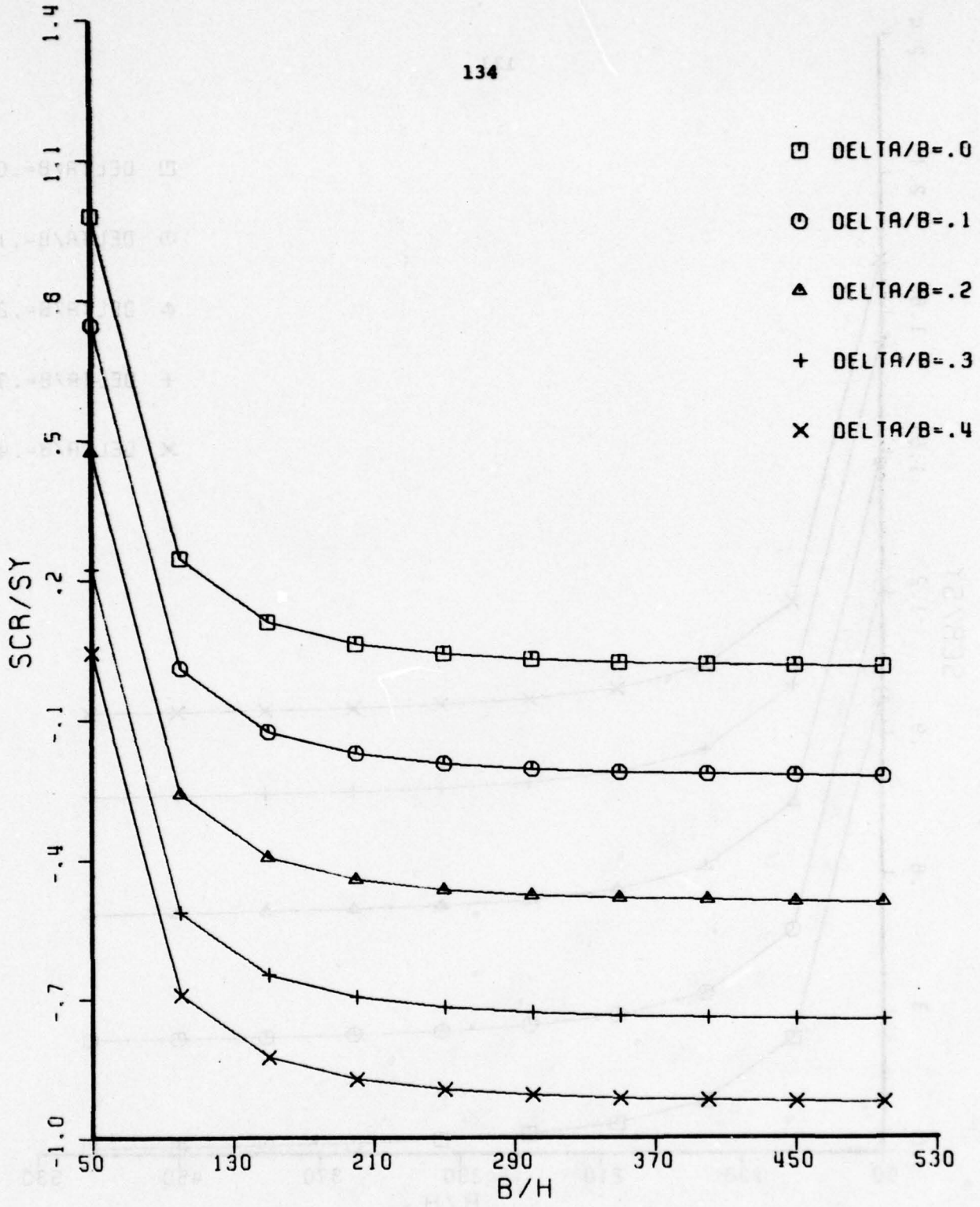

Fig. 6-2 Critical Stress for a Simply Supported Square Plate with two Edge Welds

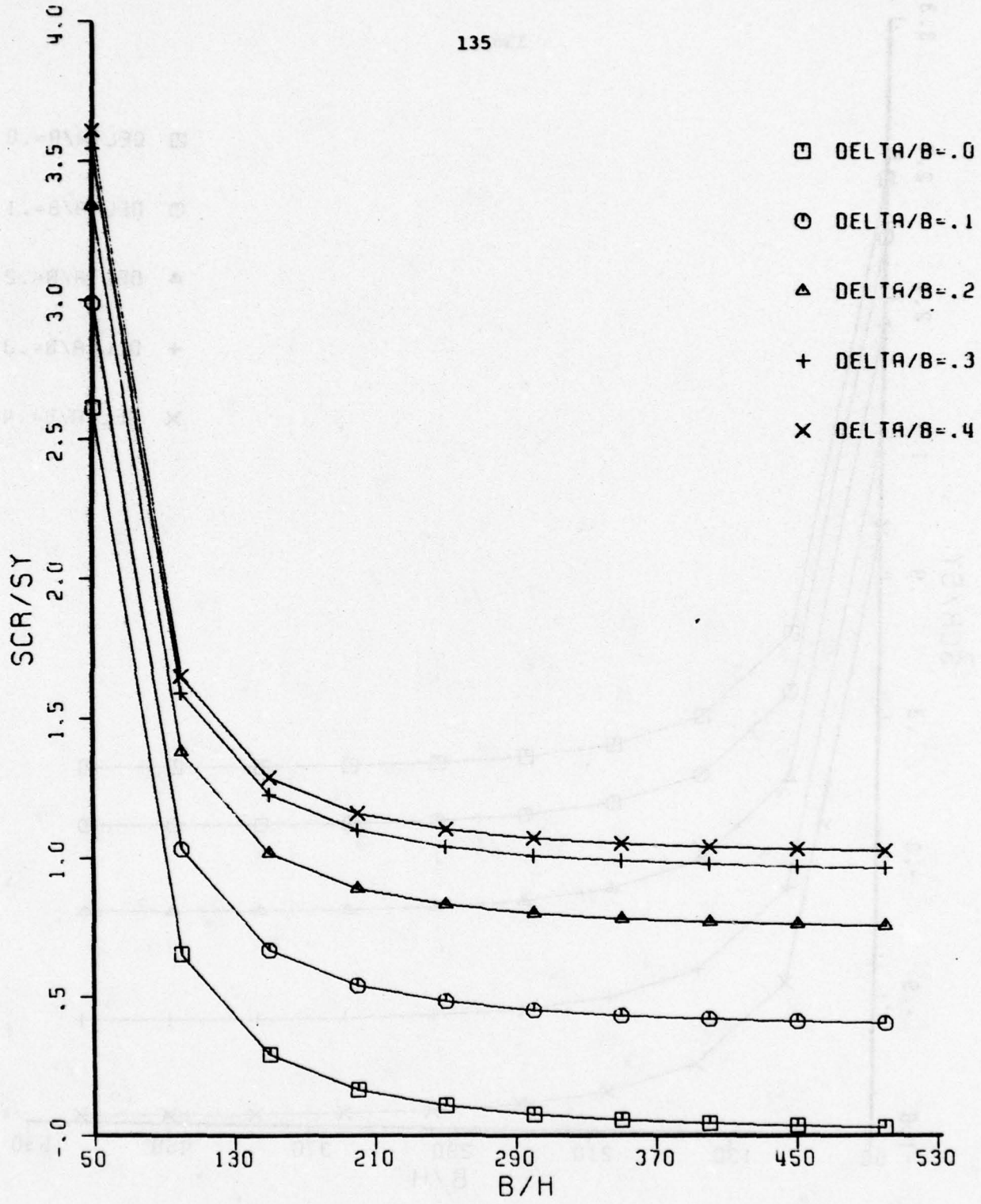

Fig. 6-3 Critical Stress for a Clamped Square Plate with Bead-on-Plate Weld

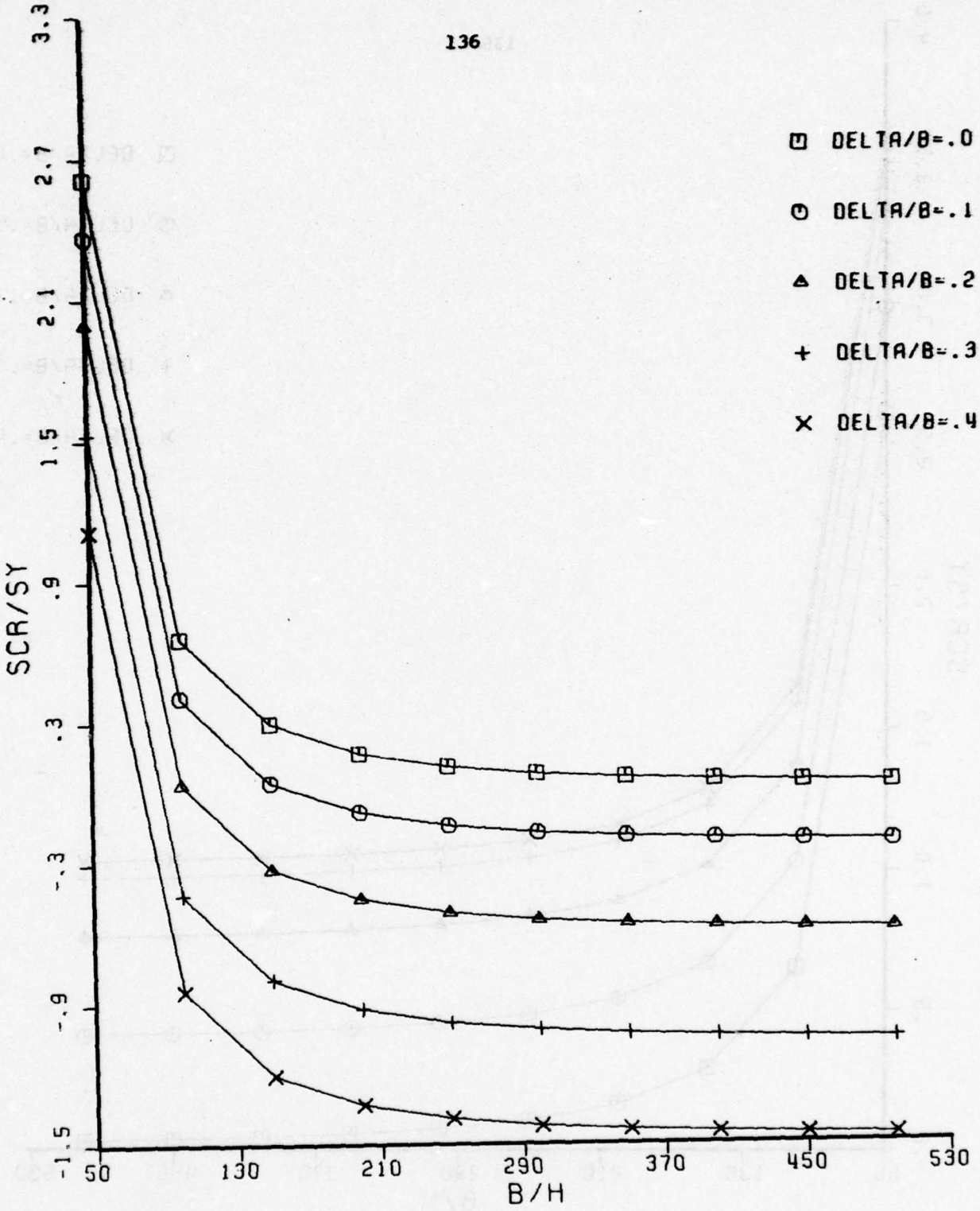

Fig. 6-4 Critical Stress for a Clamped Square Plate with two Edge Welds

applied.

This observation suggest that buckling distortion may be prevented if tensile external stresses higher than the critical ones are applied during welding on the plate. The technique should be tested experimentally. It is worth noting, however, that stretching and heating methods are successfully used by Kawasaki Heavy Industries [43] for reducing out-of-plane distortion.

One should be very careful when utilizing the above analytical results. It is well established that, for a given plate, critical dimensions exist which will prevent buckling. A problem in buckling, however, has five variables, namely plate material, length, width, thickness, and critical stress. Hence, it is necessary to specify four of these in order to find the fifth, or three in order to find a ratio between the other two (e.g. aspect ratio).

A normal design sequence will define material choice and plate dimensions first. Then a critical stress will be found. If one wishes to know another variable's value, one must predict the welding stress. This becomes an iterative procedure best suited to preliminary design.

The main reason for caution is a misinterpretation of what critical dimensions will allow. One might suppose that any smaller length or width and any greater thickness is always good. This is not entirely true.

The critical load, for uniform compression, can be calculated by the general formula

$$(N_x)_{cr} = k\frac{\pi^2 D}{b^2} \qquad (6.10)$$

where k is a function of a/b and the boundary conditions. As the width decreases, the critical stress rises. Hence, one can make b so small relative to the length that the plate behaves like a beam; and it is well known that beams are not so stiff as plates.

If the length is decreased, the critical load will also rise, but not greatly. Also, increasing the plate thickness is always safe, but not necessarily economical.

Plastic Buckling

Papazoglou [45] further expanded the study of compressive strength of welded plates to cover plastic buckling. As a first step he generalized the analysis developed by Fujita and Yoshida [47] and which was based on Stowell's deformation theory of plasticity [46]. Only the cases of simply supported rectangular plates were investigated with welds made along the center and along the two edges. For each of these two cases three subcases were considered:

1. The whole plate is in the plastic region
2. Only the portion of the plate where compressive residual stresses exist is in the plastic region
3. The whole plate is in the elastic region (in which case the results obtained by the linear elasticity analysis were recovered).

The assumptions regarding the residual stress distribution which were made in the elasticity analysis were also made here. Linear strain hardening was assumed. Closed form analytical solutions were found and the interested reader is referred to Papazoglou's thesis [45].

The results obtained were cheched versus available experimental

data and generally good correlation was observed. Papazoglou thinks that this is strange because the deformation theory of plasticity is approximate and cannot be justified mathematically. On the other hand, results obtained by other investigations using the incremental theory of plasticity on ordinary plates (unwelded) appear to be in considerable disagreement with experimental data. This may be due to the high sensitivity the more accurate incremental approach has on initial distortion and the difficulty in obtaining perfectly flat plates in the experiments.

Despite this drawback, Papazoglou decided to carry an analysis using the incremental theory of plasticity as developed by Handelman and Prager [48]. Results of this highly complicated mathematical analysis can be found in Reference 45.

2.6.2 Experimental Investigation

Pattee [42] conducted a series of experiments to determine the buckling behaviour (during and after welding) of variously dimensioned aluminum plates with a number of different boundary conditions. Material used was the 5052-H32 aluminum alloy. 18 specimens were tested with thickness of 1.5, 3, and 4.5 mm. All specimens were 1,800 mm long, with widths 300, 600 and 1,200 mm. Two specimens were tested for each combination of the above parameters. Thermocouples and strain-gages were located on each of them in order to measure temperature and strain distributions. An automatic GTA system was chosen for the welding, using 5456 alloy filler wire. Since welding of thin plates can cause many problems (local buckling, "burn-through," etc.), the back-up plates and the test specimens were preheated and continuous heating was applied in front of

the arc. The welding quality was mixed (good and bad), but generally speaking acceptable.

During the experiments four types of data were collected: temperature, strain, stress and photographic. Figures 6-5 through 6-8 show typical curves for strain, stress and temperature versus time respectively (all curves are for the same specimen). Note that only the longitudinal strain ε_x was measured and hence the longitudinal stress σ_x could only be calculated.

The temperature curves looked much as expected. The traces from the thermocouples nearest the weld-line show very steep slopes as the arc approaches. Those further from the weld are not as steep or high. The temperature approaches room temperature asymptotically during cool-down.

The stress and strain curves had four distinct regions, as can be seen from Figures 6-5 and 6-6. In region 1 the welding has started but few effects are noted in the center of the plate. In region 2 the arc is approaching and there are large strains in the plate. The arc has passed in region 3. The metal is cooling and residual stresses are forming. Finally, in region 4 the plates are unclamped.

Local buckling was a major problem while welding the 1.5 mm plate. Whenever the plate became too hot, the surface would rear up and cause numerous problems. Arc instability would result. Without the presence of the back-up plate, burn-through would occur. The wave length of this buckling was about 150 mm. The occurrance of this local buckling was not predicted by the analysis discussed in the previous paragraph, since the measured welding stresses were much smaller than the analytically predicted critical ones. It is felt that the reason for this is that the

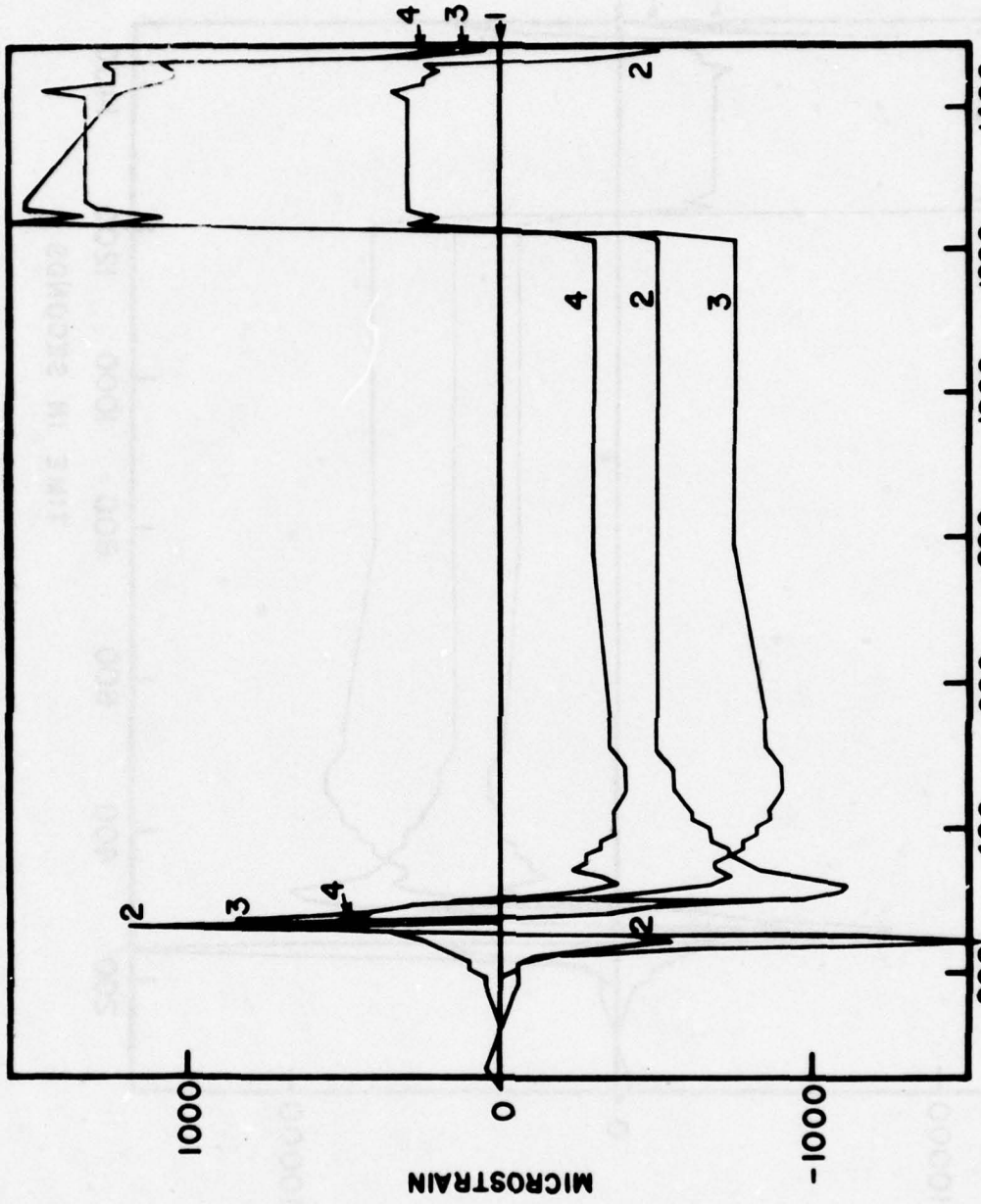

Fig. 6-5 Test I-B Strain

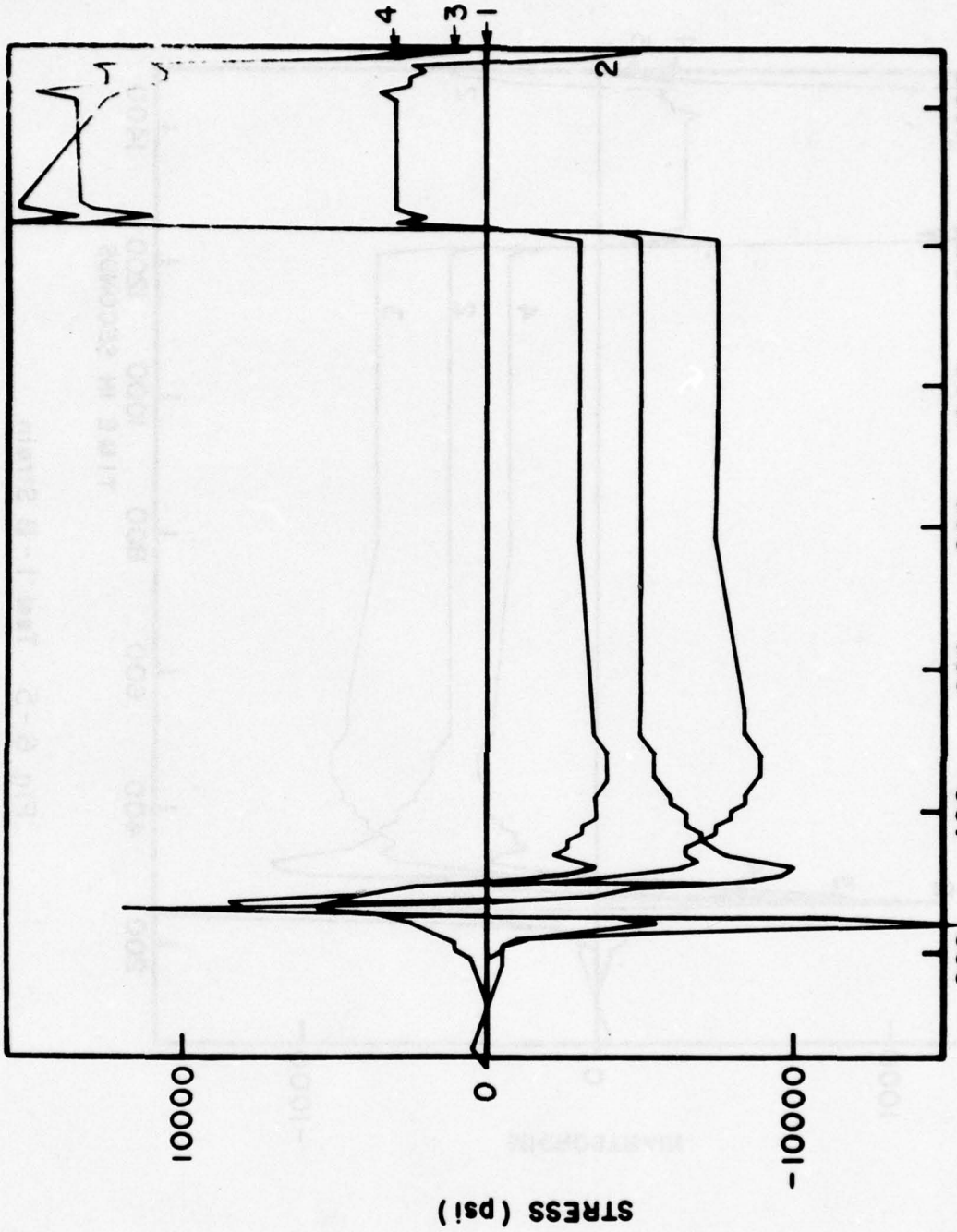

Fig. 6-6 Test I-B Stress

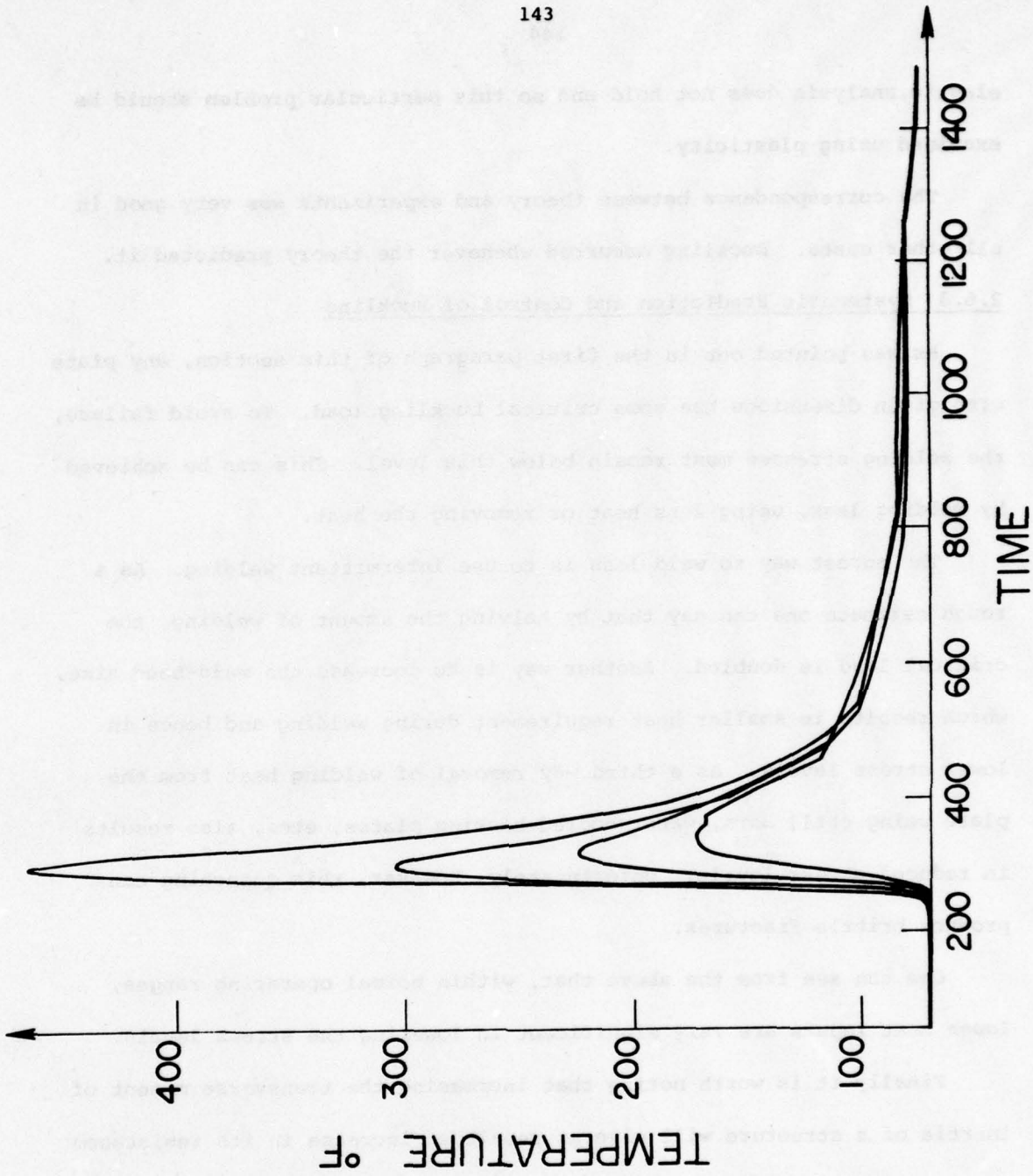

Fig. 6-7 Temperature vs. time

elastic analysis does not hold and so this particular problem should be examined using plasticity.

The correspondence between theory and experiments was very good in all other cases. Buckling occurred whenever the theory predicted it.

2.6.3 Systematic Prediction and Control of Buckling

As was pointed out in the first paragraph of this section, any plate with given dimensions has some critical buckling load. To avoid failure, the welding stresses must remain below this level. This can be achieved by welding less, using less heat or removing the heat.

The surest way to weld less is to use intermittent welding. As a rough estimate one can say that by halving the amount of welding, the critical load is doubled. Another way is to decrease the weld-bead size, which results in smaller heat requirement during welding and hence in lower stress levels. As a third way removal of welding heat from the plate using chill bars, water-cooled backing plates, etc., also results in reduced stress levels. Unfortunately, however, this quenching can produce brittle fractures.

One can see from the above that, within normal operating ranges, lower heat inputs are very significant in lowering the stress levels.

Finally it is worth noting that increasing the transverse moment of inertia of a structure will give as result an increase in its resistance of buckling. This can be achieved by a plate thickening or by a decrease in stiffener plating. Both ways, however, are not always the reliable alternative, since both require more welding and more material which result in an increase in weight and cost.

Driven by these observations and based on the analytical and

experimental investigations conducted so far, Pattee proposed a systematic approach to the buckling problem. A flow chart of this "system" is shown in Figure 6-8. Its components can be described as follows:

(1) Derivations that described the buckling due to welding of thin plates with commonly encountered boundary conditions (as described in section 6.1).

(2) Flexible computer program which calculate either critical load or critical dimensions.

(3) A welding simulation program to predict residual stresses (as M.I.T.'s 1-D or 2-D computer programs discussed in Section 2.2).

(4) Calculation which determine the effect of any corrective measures (as those described in the beginning of this paragraph).

An example showing how this system works can be found in reference 42.

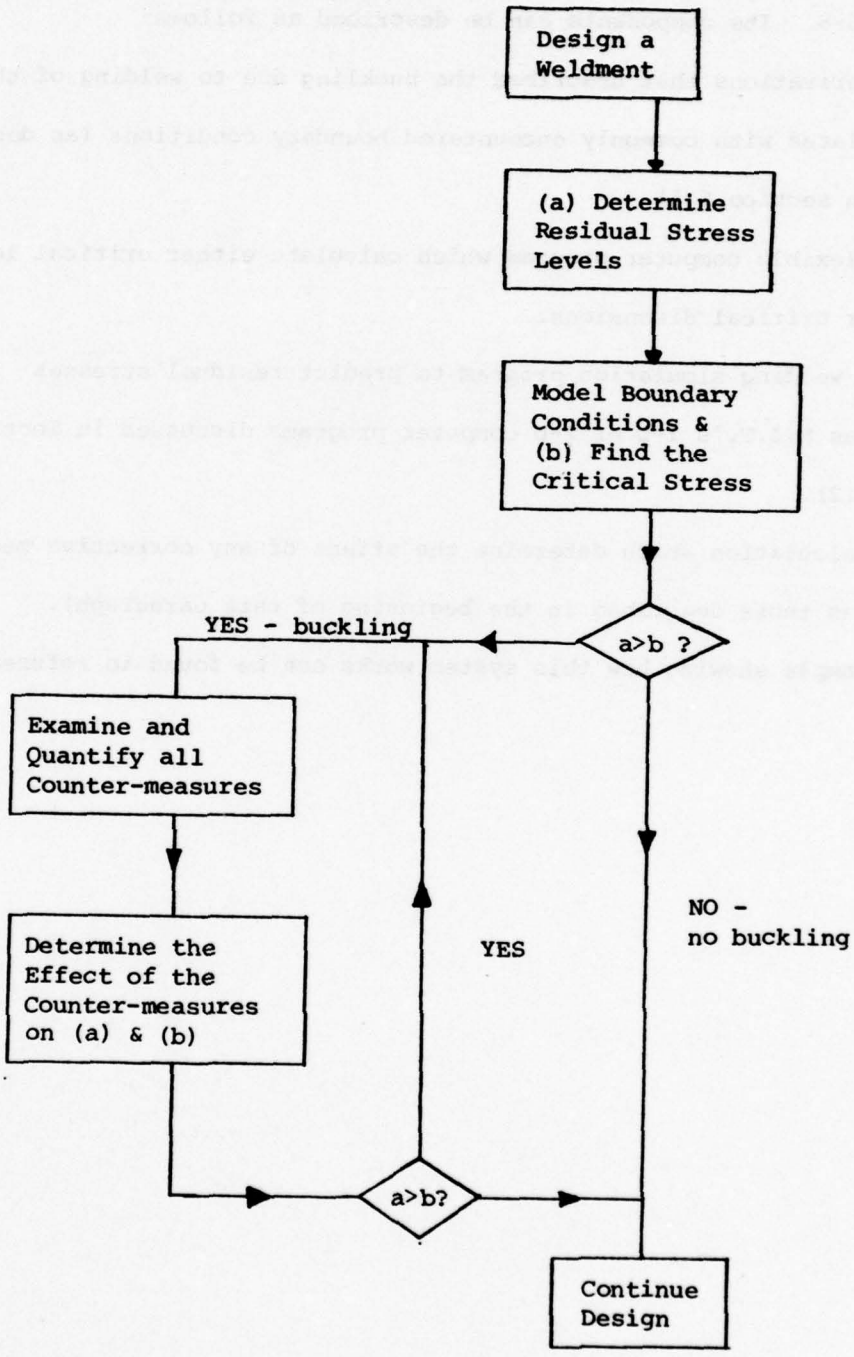

Fig. 6-8 Flow Chart for the "SYSTEM"

2.7 METHODS OF DISTORTION REDUCTION IN ALUMINUM WELDMENTS

The reliability of a welded structure is often decreased by the presence of residual stresses and distortion. First of all, excessive shrinkage and distortion can cause joint mismatch which reduces the joint strength. High tensile residual stresses in regions near the weld may accelerate growth of a crack under cyclic loading. Compressive residual stresses in the base plate region may reduce the buckling strength of a structural member subjected to compressive loading. This effect is especially big when the member has, in addition to residual stresses, out-of-plane distortion.

All the previous sections dealt with the efforts undertaken at M.I.T. towards an understanding of the mechanisms of the various kinds of distortion as well as with the investigations carried out for the analytical prediction of those distortions. This last section will try to analyze the methods experimented at M.I.T. for distortion reduction in aluminum weldments.

2.7.1 Commonly Used Methods for Distortion Reduction

Methods presently used to reduce weld distortion include proper selection of the weldment dimensions, welding process, welding sequence, forced cooling, stress-relief annealing, peening, flame straightening, vibratory stress-relief, electromagnetic hammer and external constraints. Each of these methods is briefly discussed below [49].

Weldment Dimension

The length and width of a plate determine the magnitudes of its residual stresses. As length or width is increased, the residual

stress will increase to a point and then remain constant.

The effect of thickness on angular distortion of a free joint, as shown in Figure 5-5 and explained in section 2.5.1, is also an indication of the importance of the plate dimensions.

Welding Process

Since residual stress is an indirect function of welding heat input, if one uses processes that have high heat inputs, one can expect greater residual distortions, not to mention reduced ultimate strengths. The Marshall Space Flight Center investigators found that reduced heat input and narrow weld-metal areas gave higher weld strengths and smaller distortion [50].

Electron-beam welding (EBW) gives many hopes from that aspect. Dr. Terai, in some recent lectures he gave at M.I.T., mentioned that they succeeded welding a 300 mm thick 5083 Aluminum Alloy section with one pass and without distortion for engineering purposes [51].

Welding Sequence

Kihara [52] observed that, as far as residual stresses are concerned, the effect of welding sequence has only a minor influence on longitudinal stresses. On the other hand, transverse residual stresses were largely affected by the welding sequence.

Many investigators have also observed that differences in welding sequence cause significant difference in transverse distortion. Block welding sequences were generally found to cause less shrinkage than the multi-layer sequence approach. Symmetrical welding sequences were also found to generate less non-uniformity than multi-pass methods.

Forced Cooling

It was previously mentioned that residual distortion is a function of heat input. Since maximum arrival temperature and time it is achieved are significant in measuring effective weld heat input, one can sepculate that by controlling these two, one can, in effect, control residual distortion.

This can be achieved in one way by the absorption of heat from the base plate by forced cooling with cryogenic liquids such as CO_2 or liquid nitrogen. A follow-up auxiliary heating was found to be very effective.

Stress-Relief Annealing

Just as cold work induced stresses are relieved by annealing, residual stresses due to welding can be relieved in the same manner. By proper annealing, the microscopic grain number, size and growth rate are controlled to reduce induced stresses. In the same manner as cryogenic cooling, proper tempering of a weld's thermal cycle can be used to reduce distortion.

Flame Straightening

The use of this method for reducing distortion is universally accomplished by an oxyacetylene flame for essentially the application of heat to a localized area of metal to cause dimensional changes.

In practice, three types of flame straightening techniques are used, often in combination with water quenching:

(1) Line heating parallel to the weld line

(2) Line heating on the back side of the weld line

(3) Spot heating

As a general observation it can be said that high temperature flame straightening has detrimental effects on the material properties of the base metal.

Vibratory Stress Relief

During cooling the plate is forced to vibrate at its resonant frequency for a time length depending on the weight of the work-piece. During this time, the low frequency vibrations induce a realingment of the lattice structure, reducing the residual stress level.

Electromagnetic Hammer

This technique relies on a magnetic field induced in the base plate to increase the plate's kinetic energy during metal forming. A rapid and predictable acceleration of the deformation is allowed, which results in distortion reduction.

External Constraints

A common practice in the fabrication of welded structures is the use of external constraints for distortion reduction. By the selection of appropriate strong-backs, jigs, clamps and rollers, investigators have found that induced distortions can be reduced.

2.7.2 Elastic-Plastic Prestraining

The angular distortion of a fillet weld can be reduced if an initial angular distortion is provided in the negative direction. There are basically two ways of doing this [13]: plastic prebending and elastic prestraining.

In elastic prestraining, a structure is restrained in a fixture with predetermined negative distortion. The method is particularly suited

for controlling distortion of a panel with a number of stiffeners fillet welded to the panel. It is believed that elastic prestraining is in practice the most reliable technique for controlling angular distortion.

Although the method was extensively used in the past for steel structures, not enough information was readily available for aluminum structures.

Henry [49] studied how effectively elastic prestraining could reduce the angular distortion of weldments in 5456 aluminum alloy. Using a uniform plate span and length, and relying on the GMA welding process, he investigated how angular distortion is affected by the degree of prestraining, the plate thickness, and the number of passes.

Figure 7-1 shows schematically the prestraining method used in the experiments. Note that the clamps hold only the bottom plate tips to the table and do not force them to be tangent. The round bar is placed under the plate along the longitudinal centerline (weld line) to induce a reverse curvature counteracting the out-of-plane distortion caused by the welding.

All test specimens were 600 mm by 600 mm. Thicknesses of 6, 9, and 12 mm were used because they appear to have the greatest susceptibility to welding distortion. The degree of prestraining (i.e. liner height) was calculated using a surface strain model and relied on the experimental strain-measurement data obtained from 5052-H32 aluminum alloy plates of the same thicknesses but of a different size (450 mm span, 300 mm length). By assuming a linear approximation of liner height versus plate length, Figure 7-2 was developed. This was done in the hope that these numbers would give the liner diameter for minimum angular distortion.

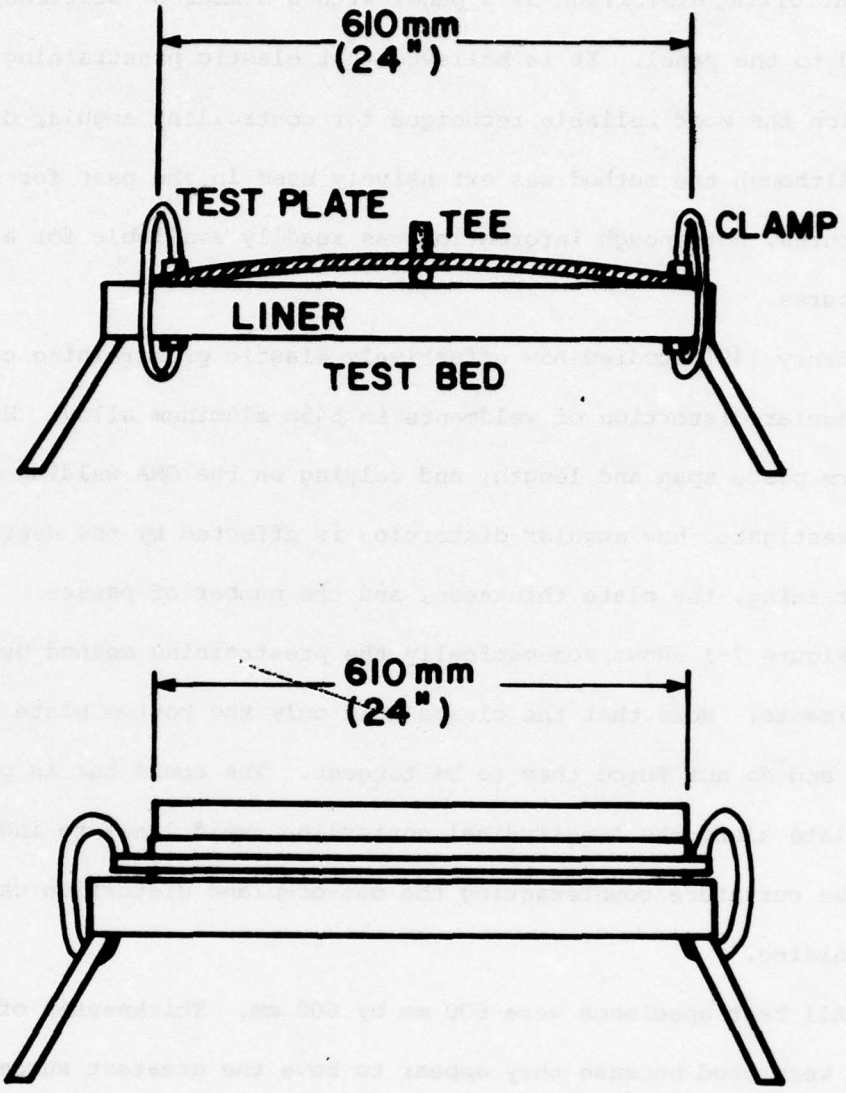

Fig. 7-1 Schematic Pictorial of Test Setup

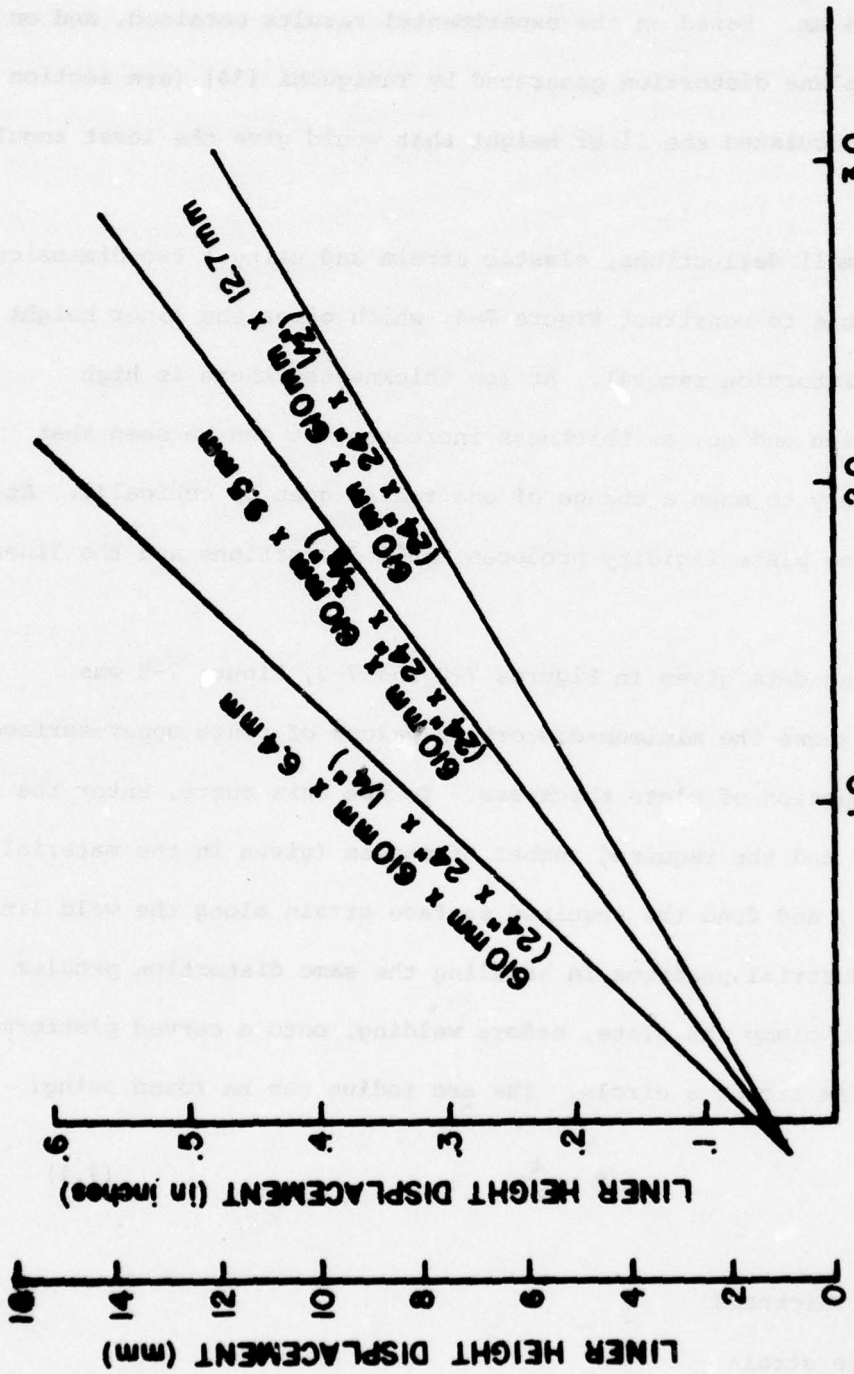

Fig. 7-2 Centerline Max. Strain (ϵ_y) Versus Liner Size For Several Plate Thicknesses From a Linear Extension Done From Data With 5052 - H32 Al. Alloy

Figure 7-3 plots the liner height versus the plate thickness for a tee height of 75 mm. Based on the experimental results obtained, and on data of out-of-plane distortion generated by Taniguchi [34] (see section 2.5.1), Henry calculated the liner height that would give the least angular distortion.

Assuming small deflections, elastic strain and using a two-dimensional model, he was able to construct Figure 7-4, which gives the liner height necessary for distortion removal. At low thicknesses there is high angular distortion and so, as thickness increases, it can be seen that the load necessary to make a change of one radian goes up cubically. At large thicknesses plate rigidity produces small distortions and the liner size decreases.

By combining data given in Figures 7-2 and 7-3, Figure 7-5 was developed. It shows the minimum-distortion values of plate upper-surface strains as a function of plate thickness. To use this curve, enter the plate thickness and the required number of passes (given in the material specifications), and find the required surface strain along the weld line.

Common industrial practice in handling the same distortion problem with steel is to clamp the plate, before welding, onto a curved platform in the form of an arc of a circle. The arc radius can be found using:

$$R = \frac{t}{2\varepsilon} \qquad (7.1)$$

where

t = plate thickness

ε = surface strain

From this formula and Figure 7-5, Henry calculated Figure 7-6 which

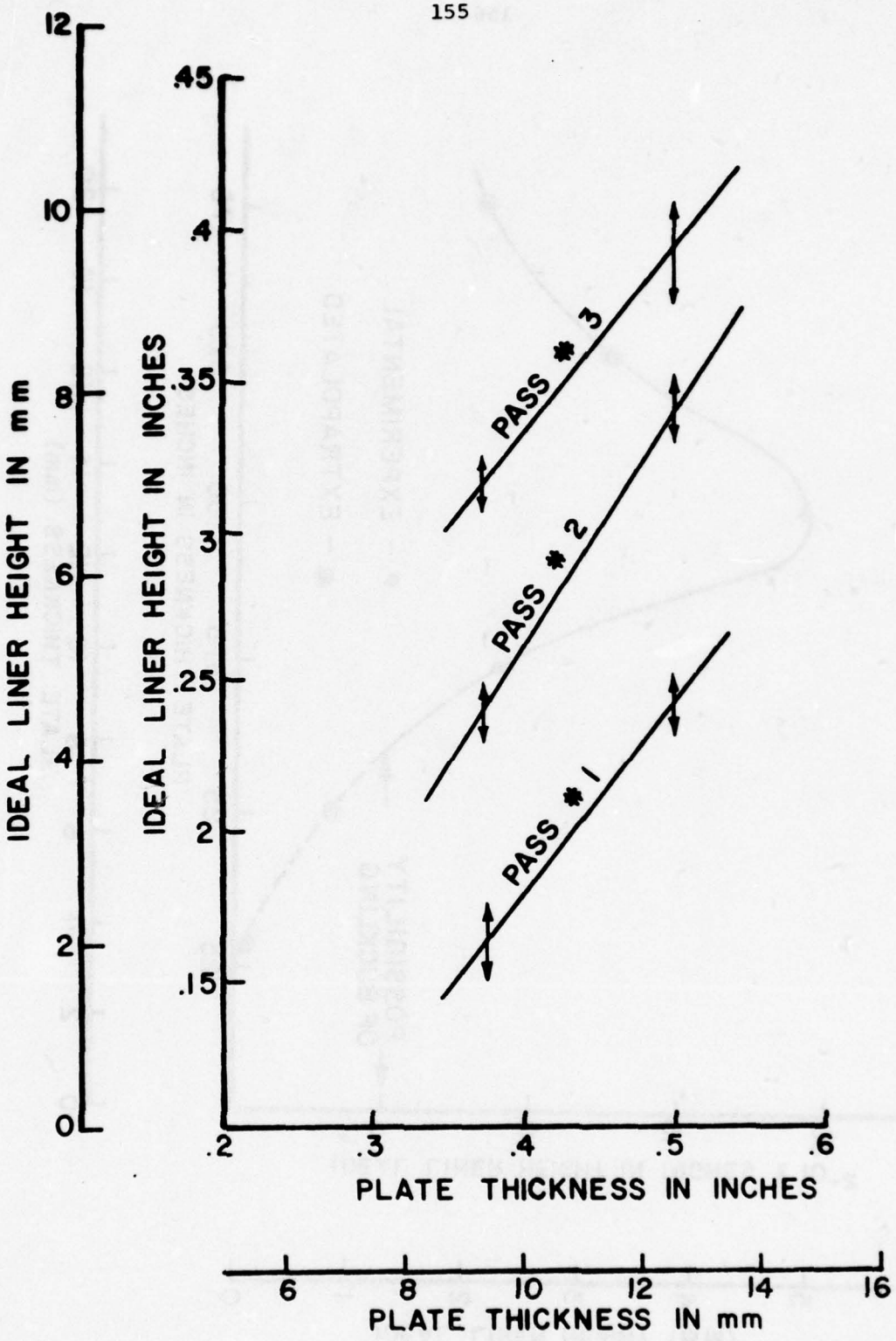

Fig. 7-3 Curves of Ideal Liner Height Versus Plate Thickness for a Tee Height of 150 mm (6"), 5456 Al. Alloy, Plate Size 610 mm x 610 mm (24" x 24")

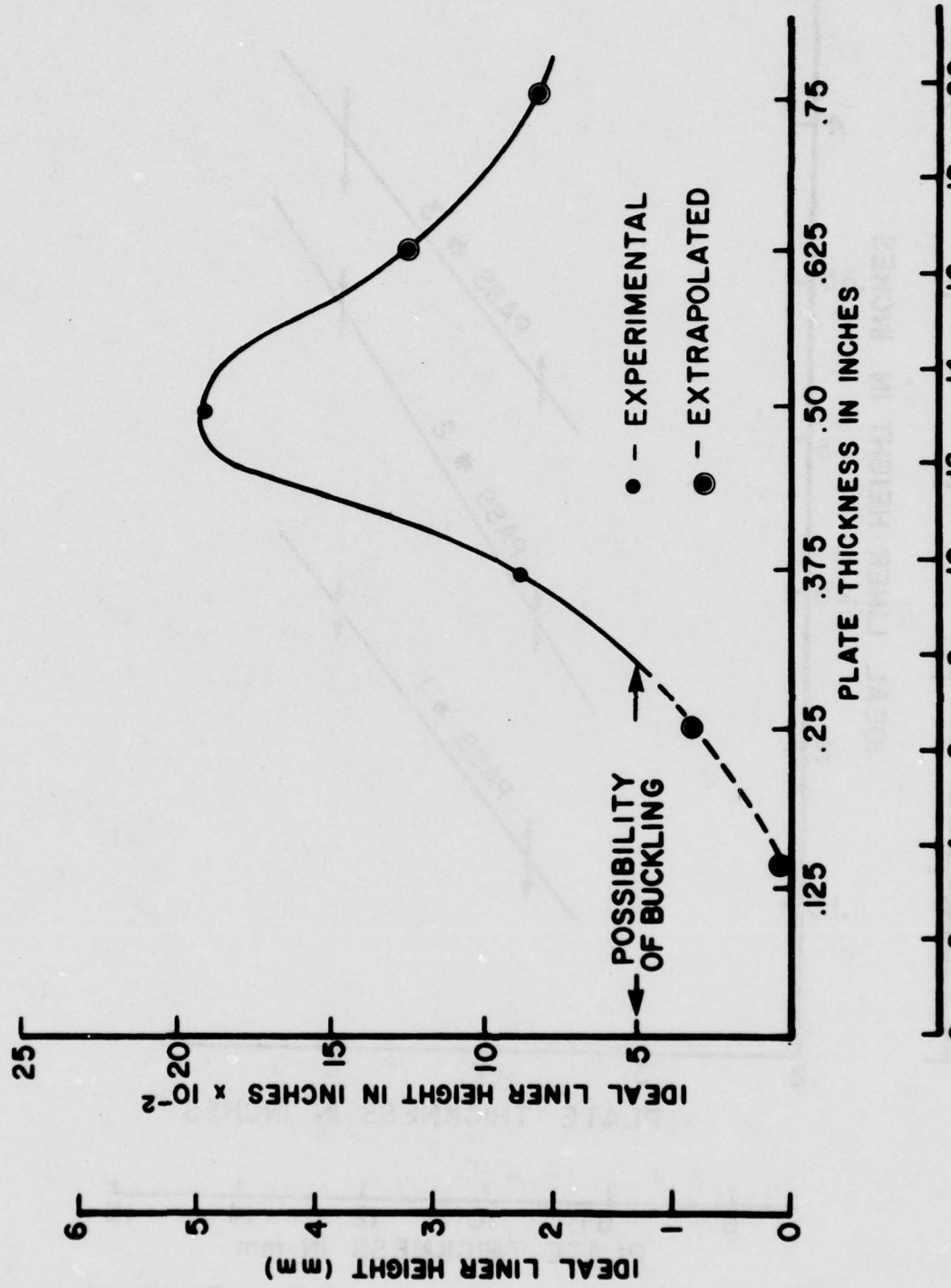

Fig. 7-4 Ideal Liner Height Versus Plate Thickness

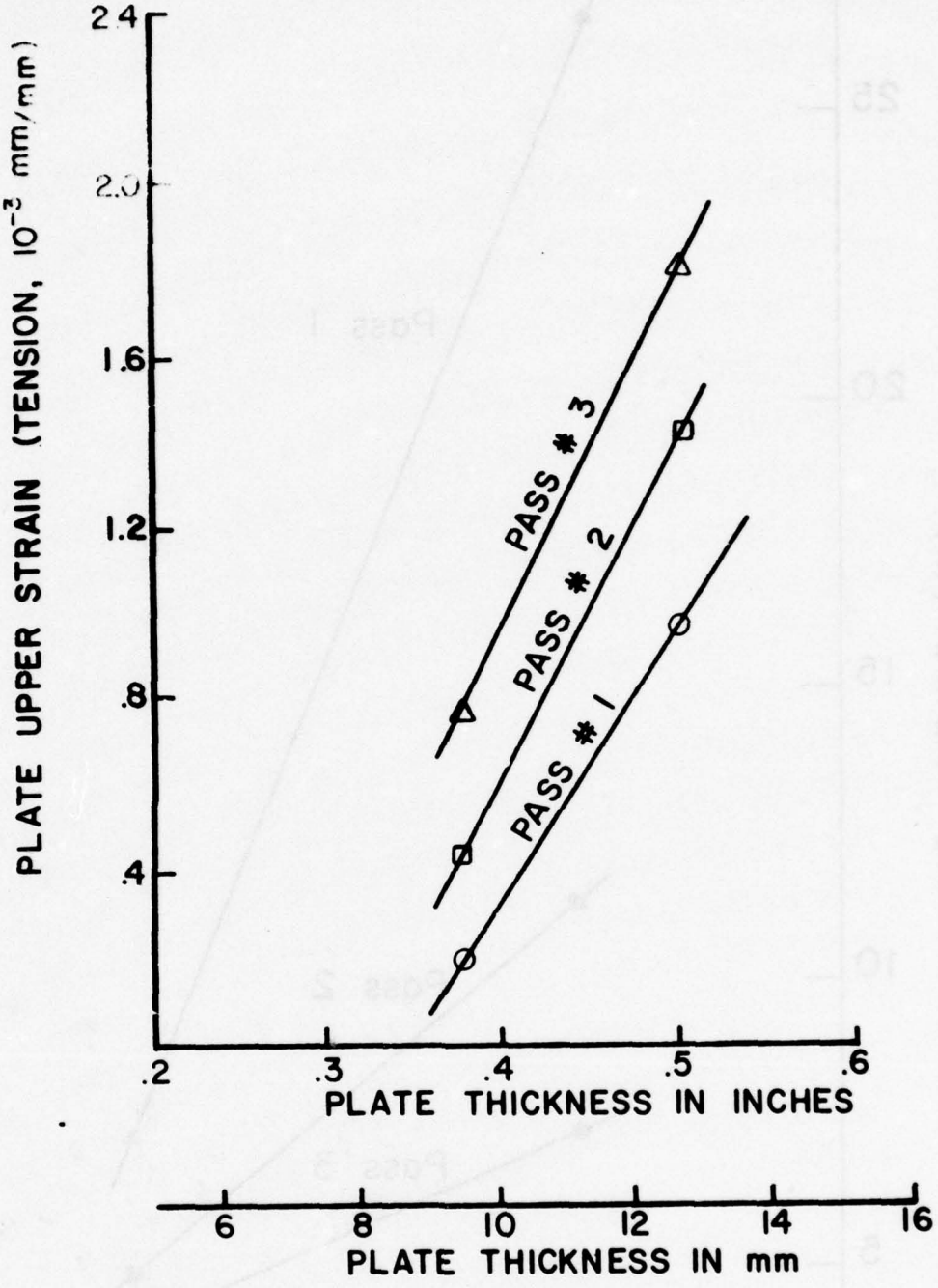

Fig. 7-5 Max. Upper Strain (Tension) Versus Plate Thickness for 75 mm 3" Tees With 1, 2 and 3 Passes

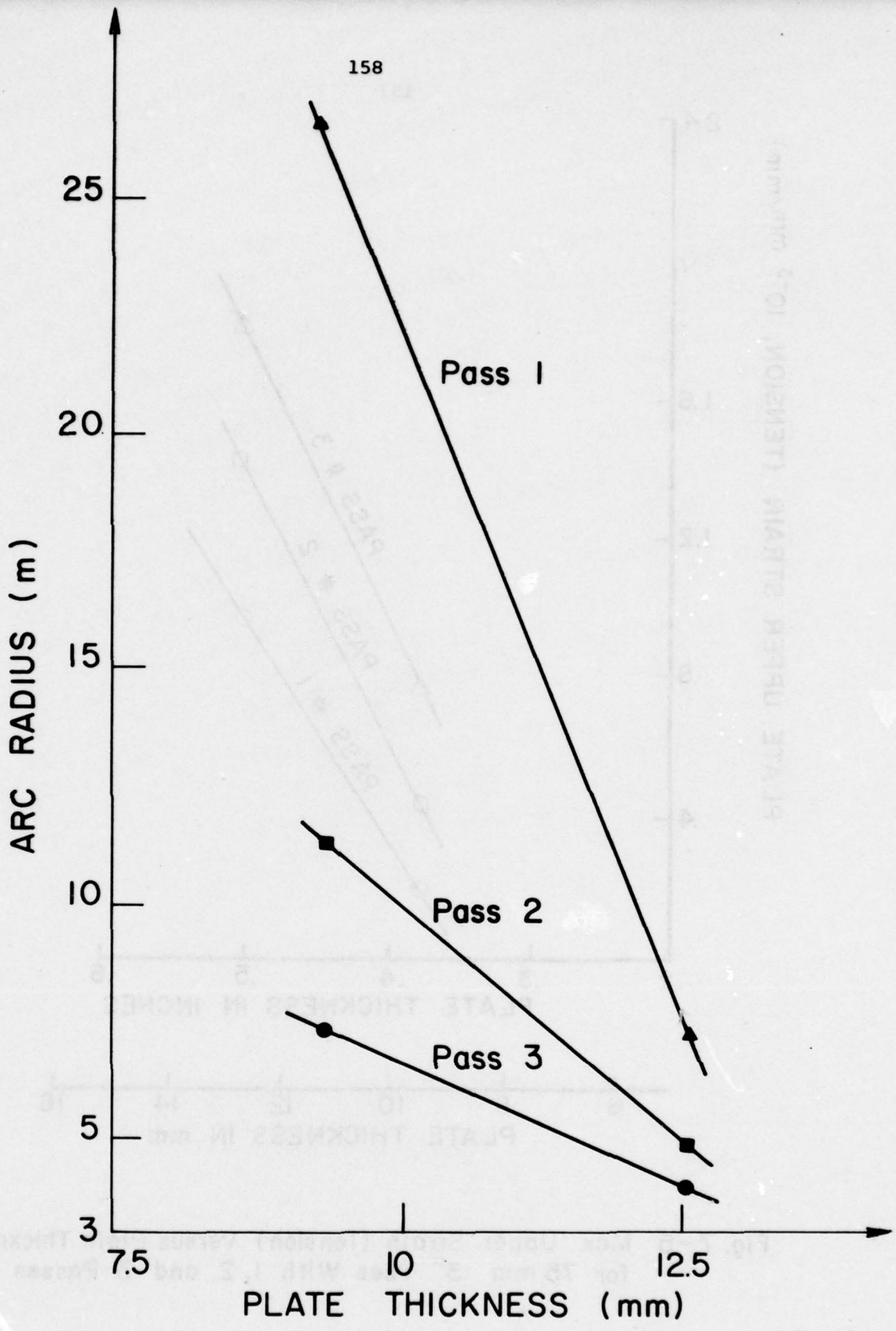

Fig. 7-6 Arc radius versus plate thickness for 7.5mm tees with 1, 2, and 3 passes

gives the required arc versus plate thickness.

A drawback of Henry's experimental investigation was the failure to get reliable results from the 6 mm plates. Distortions, in both the angular and longitudinal directions, coupled with plate buckling to produce complex curvatures.

Beauchamp [53] continued and extended the work done by Henry in an effort to study elastic prestraining as a means of reducing angular distortion in plate thicknesses less than 6 mm. He thought that the failure to get experimental results was due to the clamping method used (pictured in Figure 7-1). Instead of calmping the plate at its four corners, Beauchamp used a steel channel section to distribute the clamping force along the plate's edge. In this case the plate can be modeled as being made up of a finite number of simple beams with a uniform strain pattern.

Using the forementioned method he conducted experiments on 5052-432 aluminum alloy plates. The geometry of the models was chosen to represent a typical stiffened panel which can be found in a vessel. The model, thus, has two stiffened panels joined by a butt weld. Figures 7-7 and 7-8 show the two model configurations used for the sitffened panels. Locations of strain gages and thermocouples are also shown on the figures. After the welding of the stiffeners, the models were joined by a butt weld to result in the configuration shown in Figure 7-9. The dimensions of the models are also shown in Figures 7-7 and 7-8. Investigations were carried out for plate thickness of 6, 4.5 and 3 mm. GMA welding was used with 5556 aluminum alloy as the filler wire.

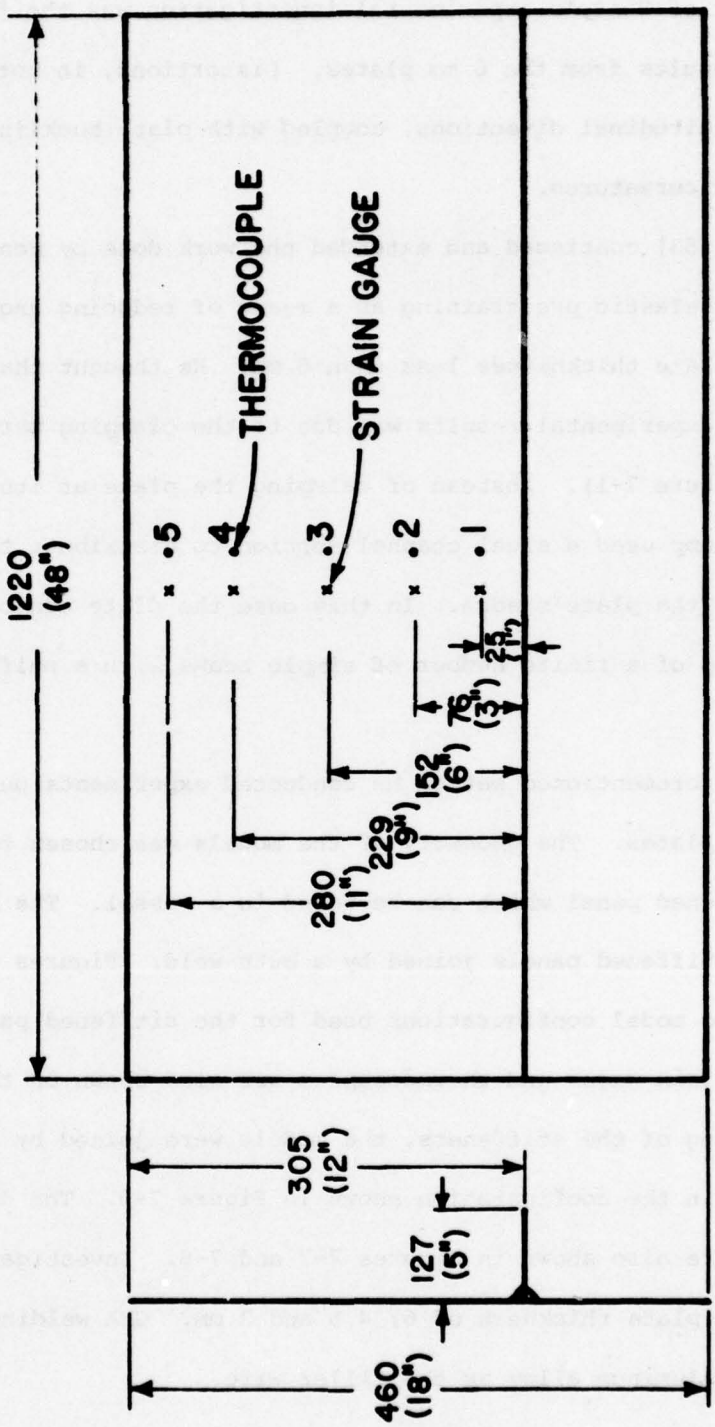

Fig. 7-7 Dimensions of Model A

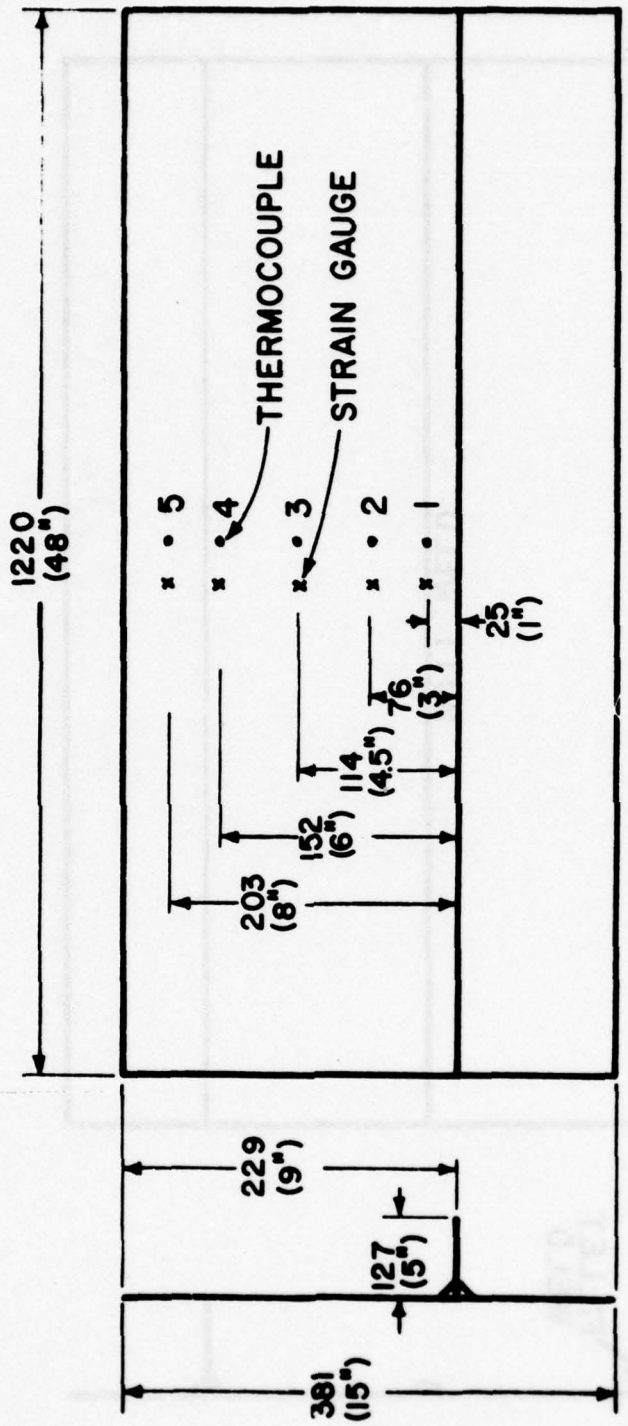

Fig. 7-8 Dimensions of Model B

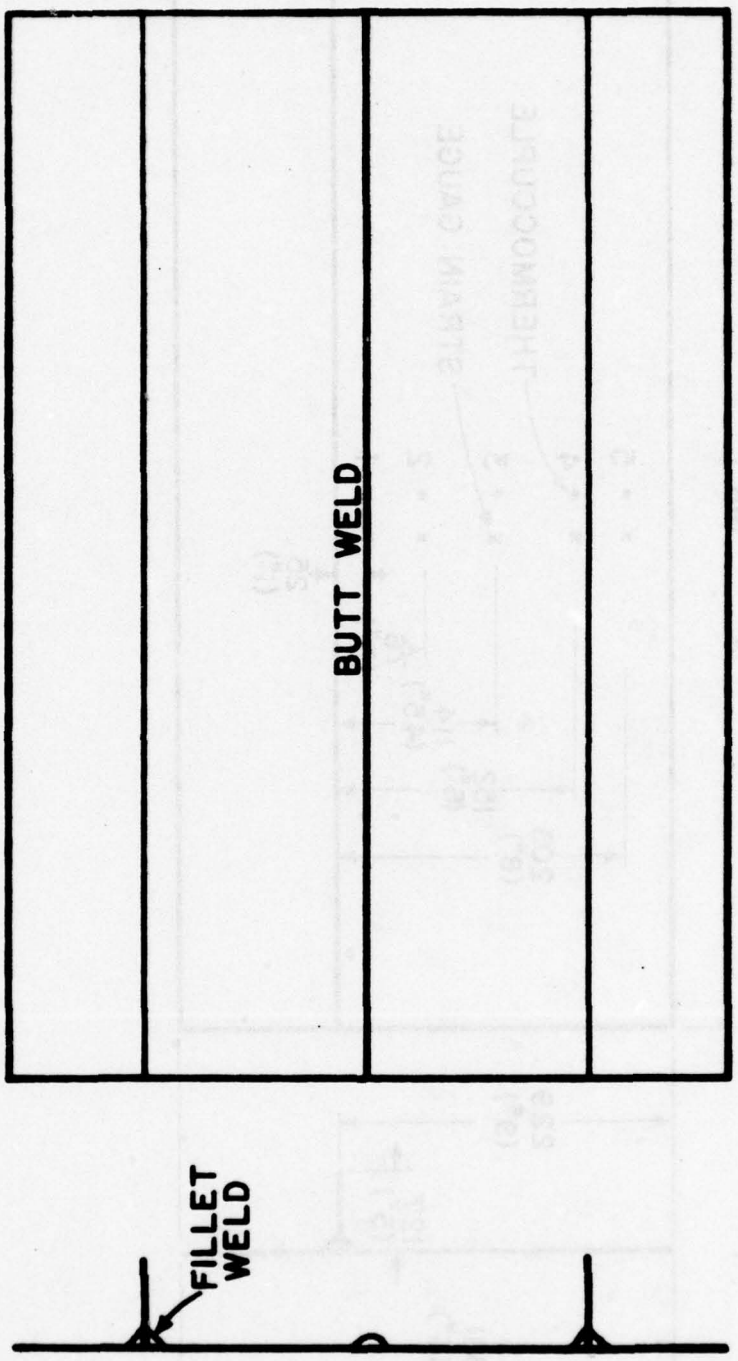

Fig. 7-9 Completed Panel Configuration

All fillet weldings were carried out using elastic prestraining. After the commencement of each fillet weld and the cooling of it to room temperature, the plates were unclamped and residual stresses were measured. Only transverse strains and stresses were measured.

Beauchamp modeled the specimens as simply supported beams experiencing a force concentrated at a point not at its midlength. Using simple beam theory, he came up with the following relation:

$$\varepsilon_y = \frac{3 \cdot d \cdot t \cdot x}{2a\ b} \qquad (7.2)$$

where

ε_y = transverse strain

d = deflection under web (due to elastic prestraining)

t = plate thickness

a = 300 or 225 mm (refer to Figs. 7-7 and 7-8)

b = 150 mm

x = 0 at plate edge

= 300 or 225 mm at web

Comparing the analytically predicted results from equation (7.2) with the measured ones after the plates were prestrained and clamped, an error of approximately 25% was found. Beauchamp thinks that this was due to the fact that the measurement of deflection was not accurate enough.

Temperature was also measured during the welding operation and until everything was cooled down to room temperature. Good agreement was found between the measured values and the predicted ones, using the two-dimensional computer program mentioned in Section 2.2.

Finally, strains were also measured and converted to stresses using a data-reduction computer program. Figure 7-10 shows a typical stress versus time curve (for model B, shown in Fig. 7-8 and gage 1). The two fillet welds are labelled 1 and 2 and the butt weld is labelled 3. Due to the fact that the technique of elastic prestraining was used to reduce distortion, an amount of strain was introduced into the plate before welding was started. This value of stress is indicated by the curve's intercept with the vertical axis at time zero. The vertical line for the last value of time indicates the amount of stress released when the clamps were removed.

The development of stress in the models is presented in Figures 7-11 through 7-16. The graphs show the effect of the clamping on the residual stress levels. There are six segments in each graph; the first three are for the fillet weld on one side of the web and the last three for the second fillet weld.

When the plate is free there is no stress. After clamping is completed, stress has been introduced into the plate. The amount of stress present is a function of the clamping force used and the deflection. The six graphs display this characteristic very well. The stress in the plate then undergoes a transition on the completion of welding. In every model except one the stress decreased. Model B-1 (6 mm thickness, Fig. 7-8) experienced an increase in stress. After the weld had cooled down, the clamps were removed and a new value of stress was recorded. This value is the amount of stress present in the plate due to the welding. If on the release of the clamps a zero reading for stress had arisen, this would mean that no residual stress was generated by welding.

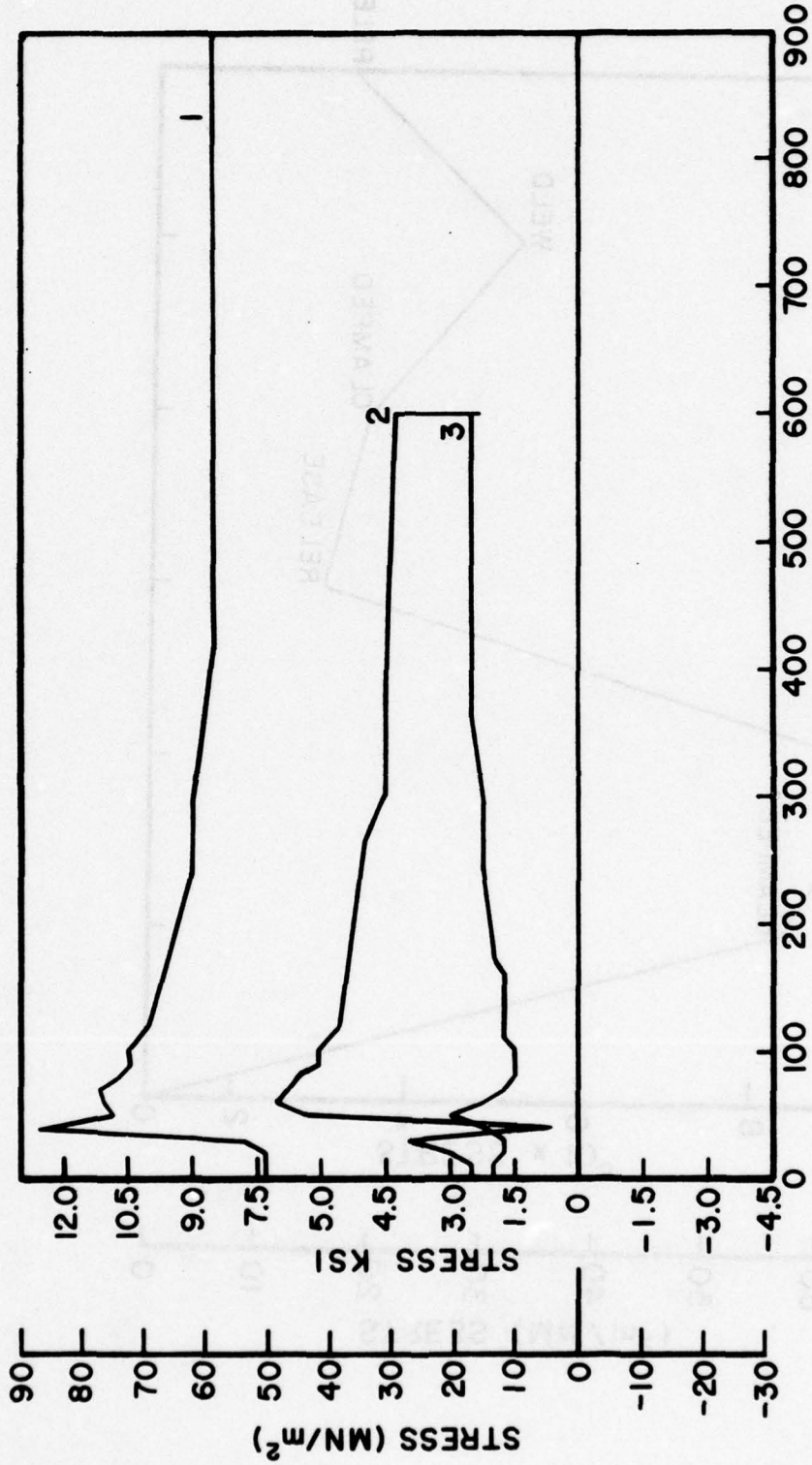

Fig. 7-10 Stress Model B-1, Gauge 1

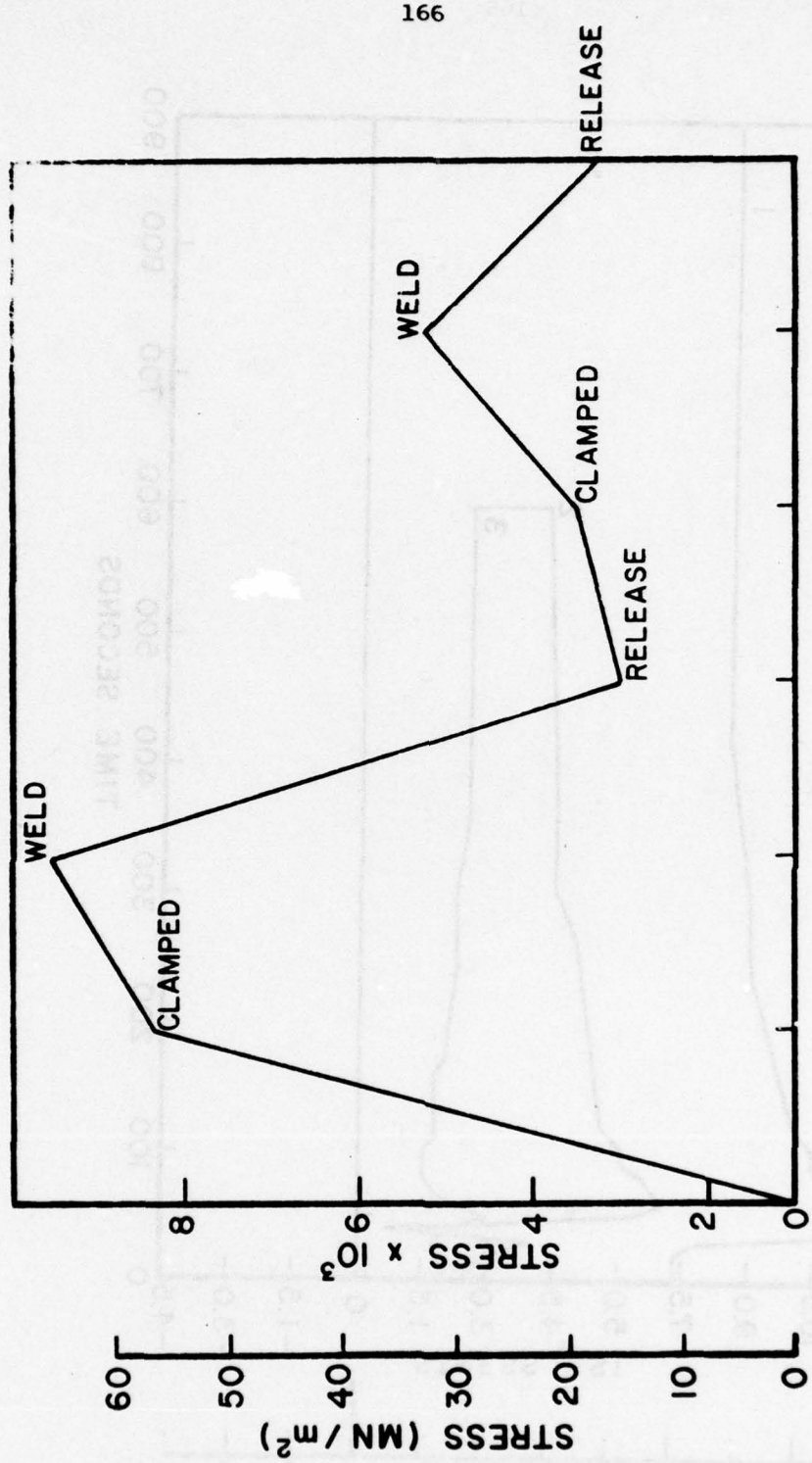

Fig. 7-11 Development of Stress Model B-1

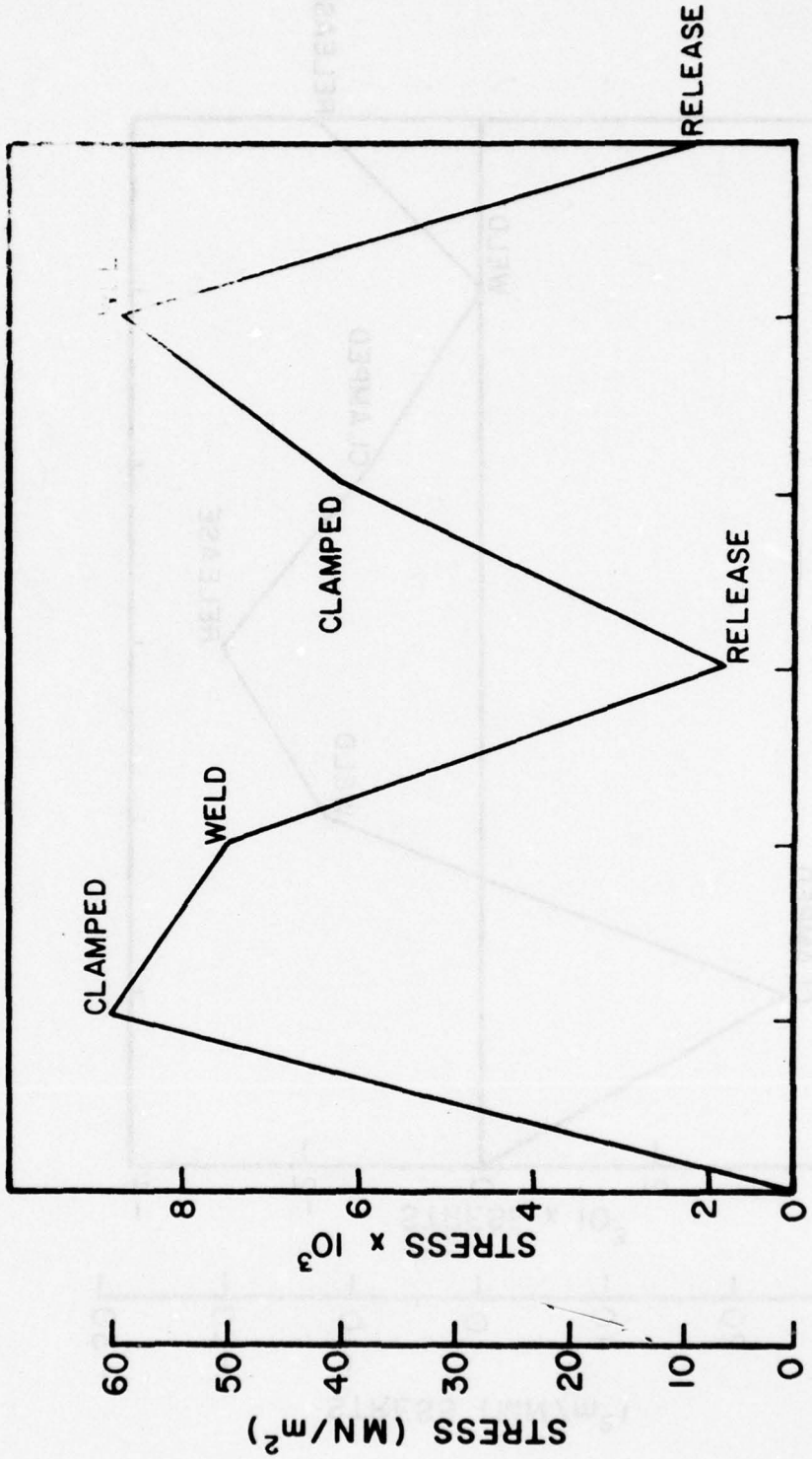

Fig. 7-12 Development of Stress Model B-2

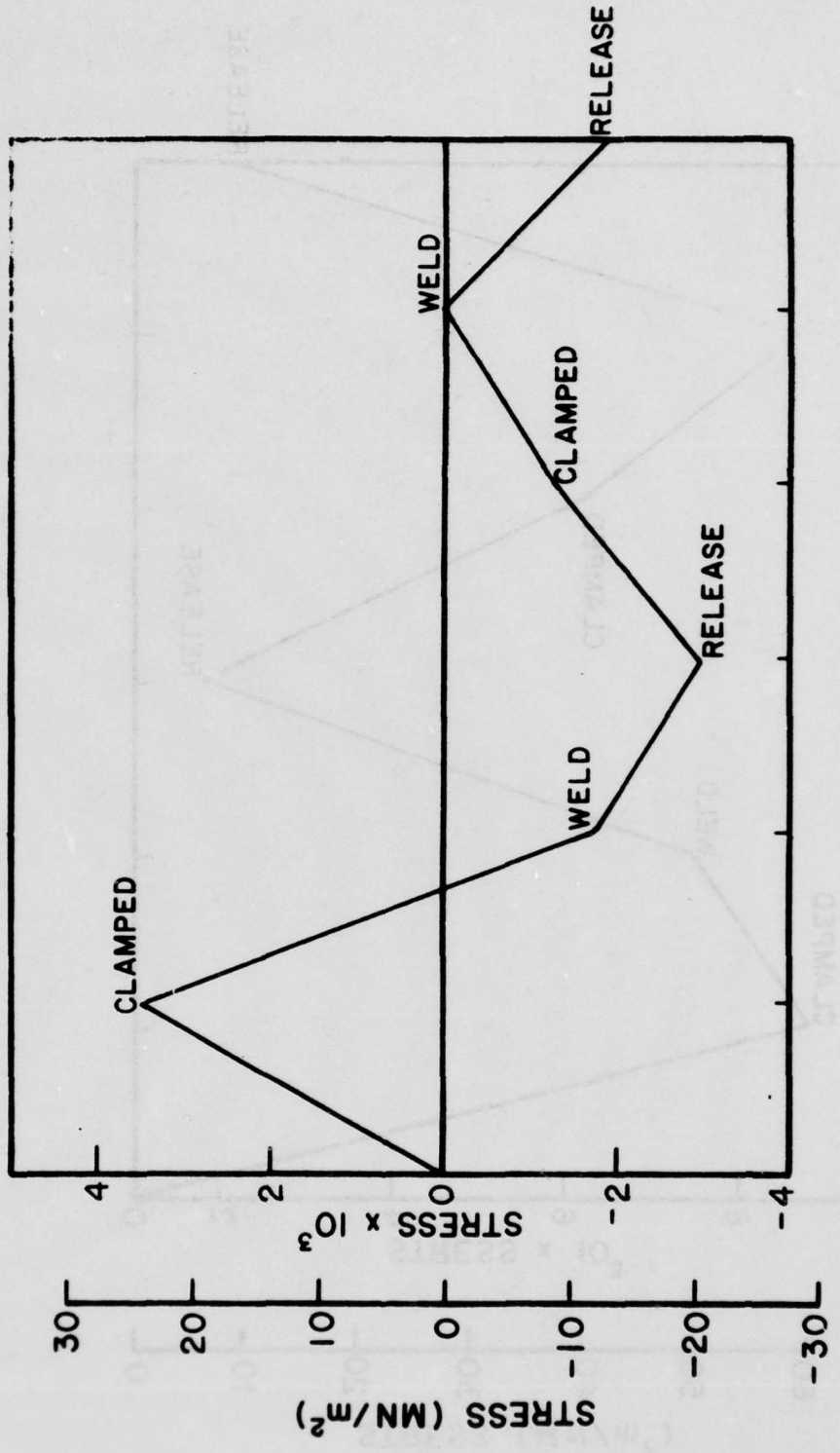

Fig. 7-13 Development of Stress Model B-3

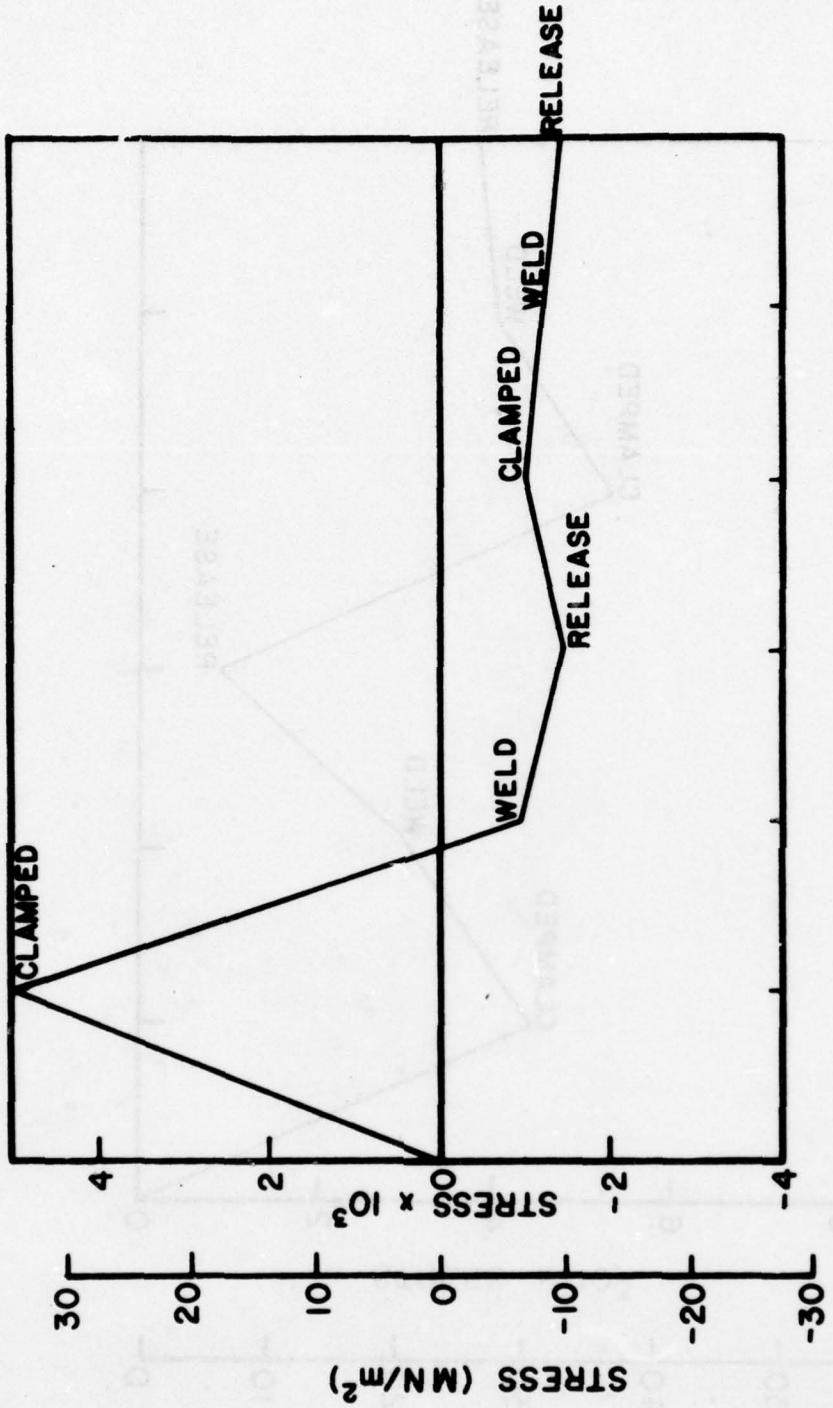

Fig. 7-14 Development of Stress Model B-4

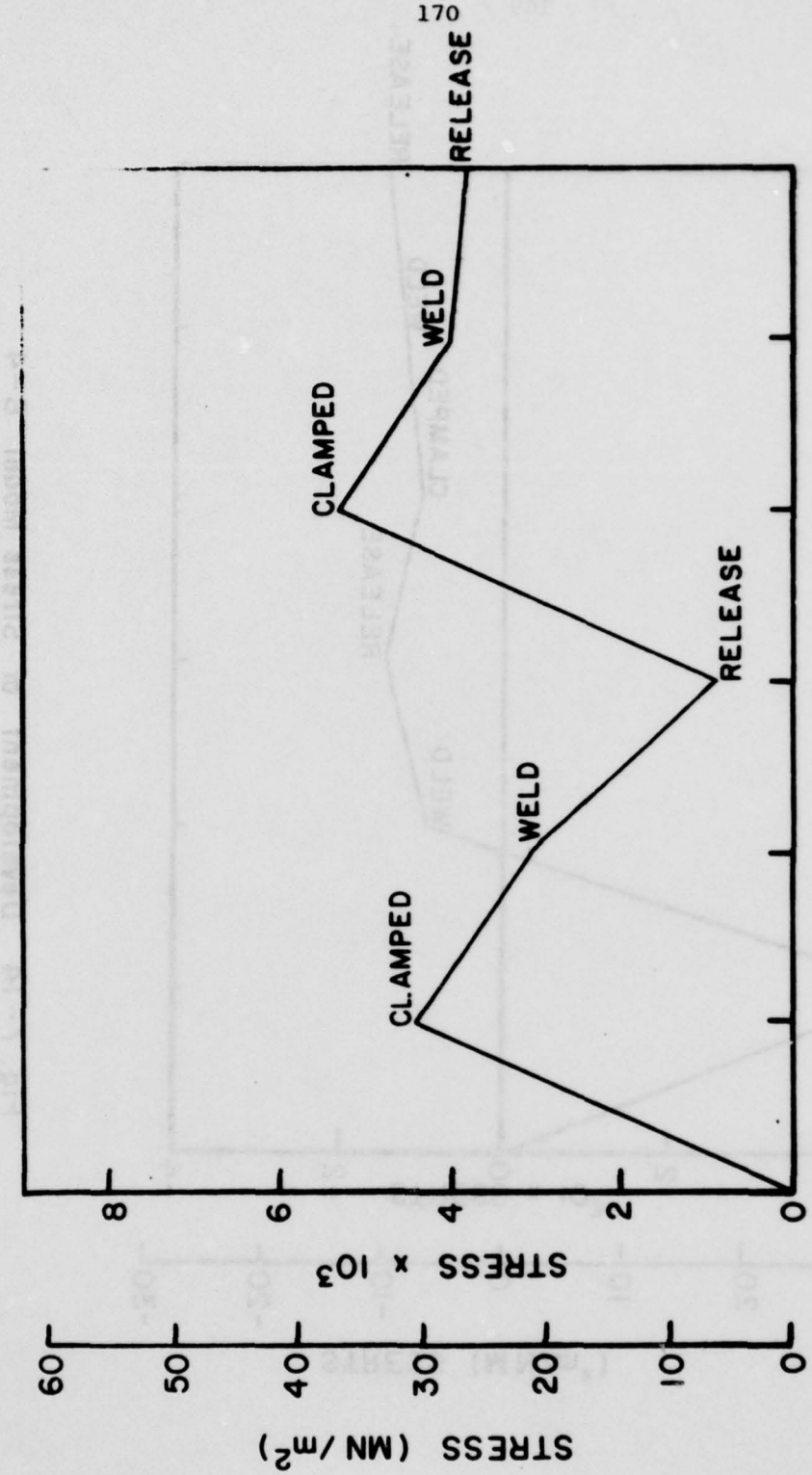

Fig. 7-15 Development of Stress Model B-5

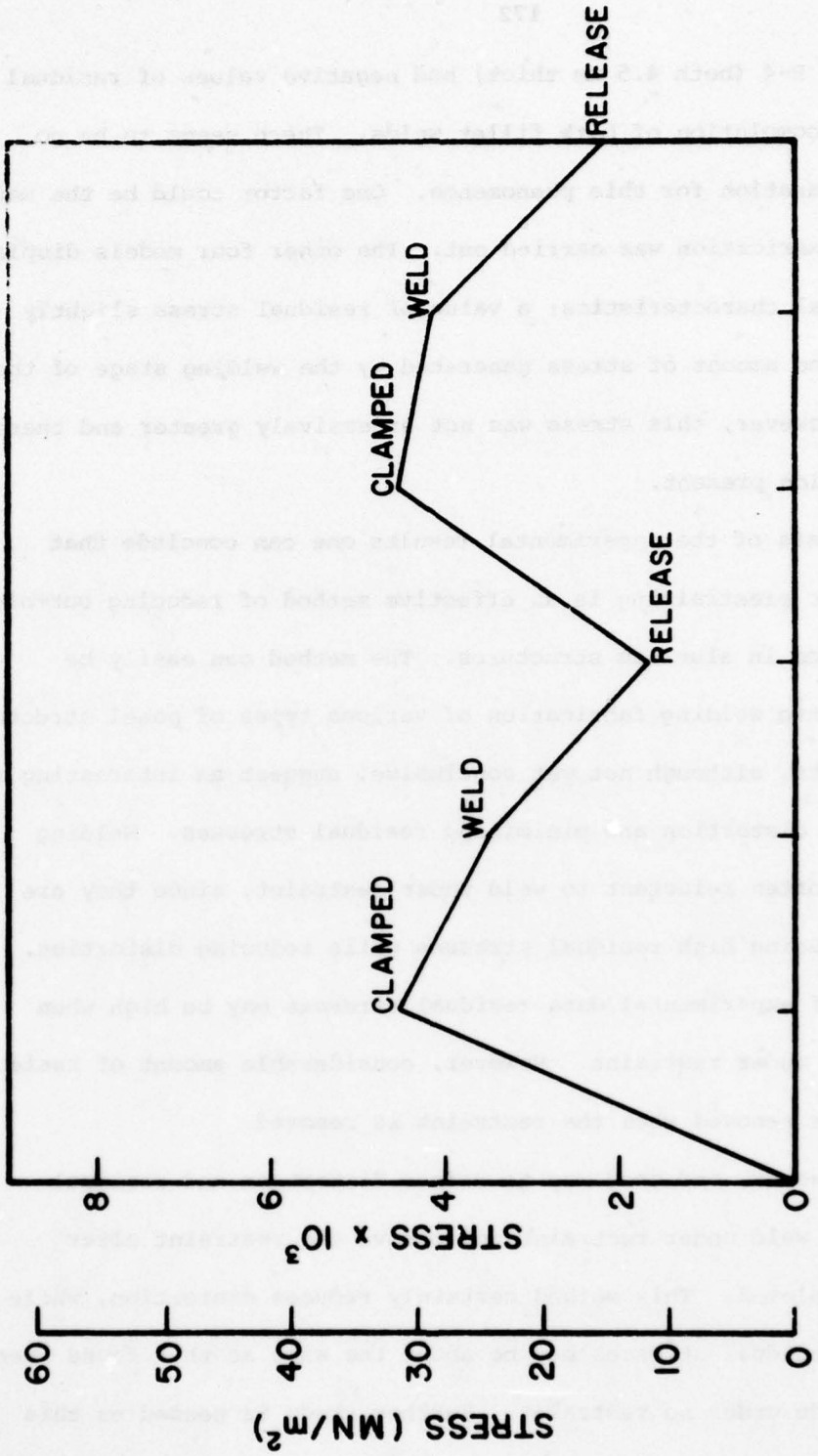

Fig. 7-16 Development of Stress Model B-6

Models B-3 and B-4 (both 4.5 mm thick) had negative values of residual stress on the completion of both fillet welds. There seems to be no clear cut explanation for this phenomenon. One factor could be the manner in which the fabrication was carried out. The other four models displayed the same general characteristics; a value of residual stress slightly greater than the amount of stress generated by the welding stage of the experiment. However, this stress was not excessively greater and there was no distortion present.

On the basis of the experimental results one can conclude that elastic-plastic prestraining is an effective method of reducing out-of-plane distortion in aluminum structures. The method can easily be incorporated into welding fabrication of various types of panel structures.

The results, although not yet conclusive, suggest an interesting idea about reducing distortion and minimizing residual stresses. Welding engineers are often reluctant to weld under restraint, since they are afraid of producing high residual stresses while reducing distortion. On the basis of experimental data residual stresses may be high when welds are made under restraint. However, considerable amount of residual stresses may be removed when the restraint is removed.

In other words, one good way to reduce distortion and residual stresses is to weld under restraint and remove the restraint after welding is completed. This method certainly reduces distortion, while the level of residual stresses may be about the same as that found when the weld is made under no restraint. Further study is needed on this subject.

2.7.3 Clamping Method

The clamping method is widely used in industry, but it is not helpful in reducing residual distortion in every situation (sometimes only transient distortion is prevented). However, it is still useful in the prevention of transient distortions from the point of view of controlling such welding conditions as root gap and arc-torch distance.

As discussed in Section 2.4.2, Yamamoto's [32] experiments have shown that the clamping method is not effective in reducing the final deflection of T-shaped built up beams. Test specimen and clamping method used are shown in Figures 4-3 and 4-5 of Section 2.4.2.

Nishida [9] conducted an analytical study on the clamping method using the one-dimensional computer program discussed in Section 2.4.3. He simulated the clamping condition as follows:

During the welding only x-direction movement is allowed and the plastic strain built in the beam is kept. After the welding, this plastic strain is determined and a recalculation is made to make the force balance. At this time the beam is allowed to bend. Using the assumption $\frac{d^2w}{dx^2} = b$ (refer to equation 4.11) and simple support boundary conditions at both ends, the final deflection at the center becomes:

$$\text{deflection} = \frac{1}{8} lb^2 \qquad (7.3)$$

where,

w = transverse deflection of beam

l = length of beam

The result of this calculation is shown in Figure 7-17. This

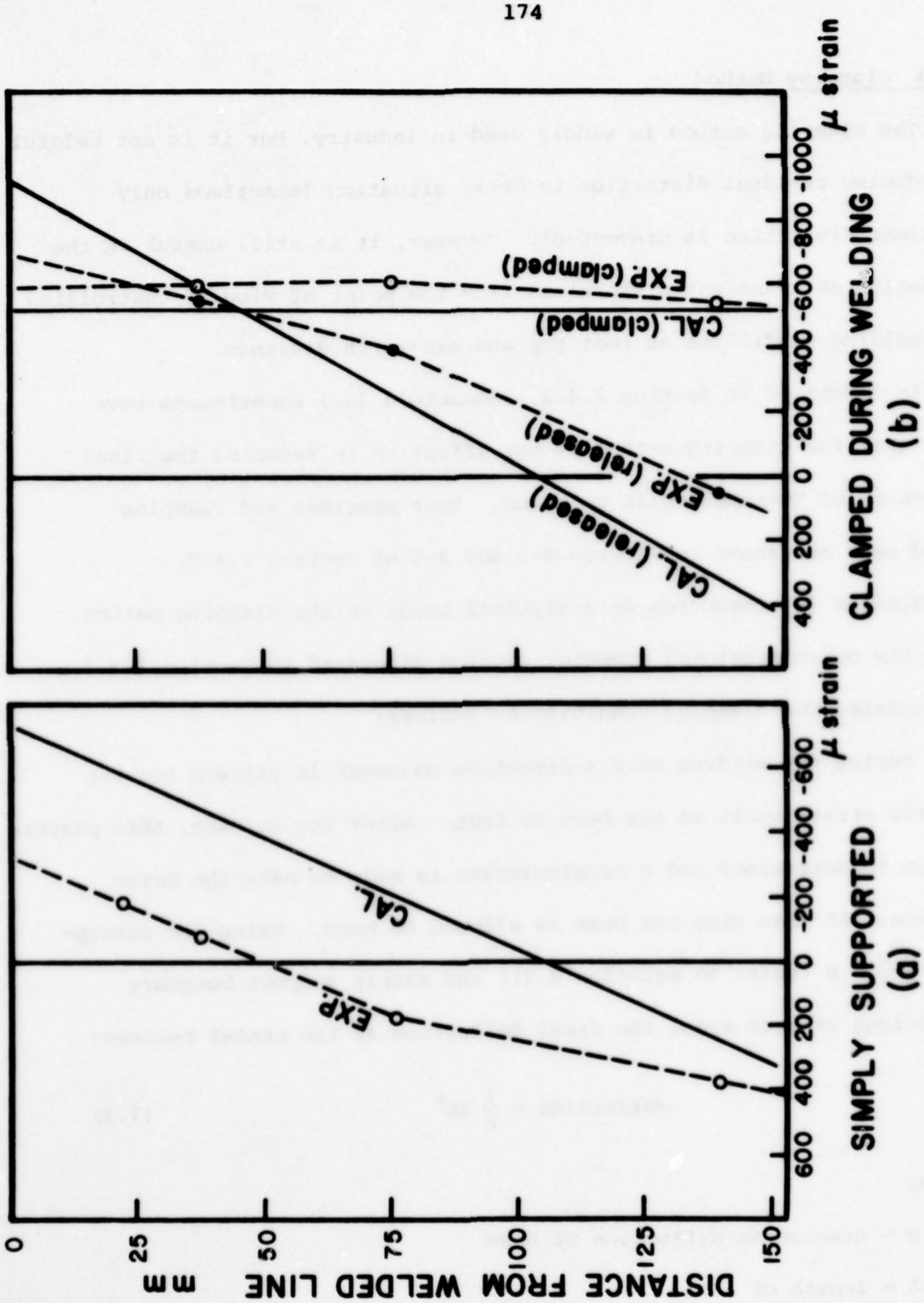

Fig. 7 - 17 Residual Strain of Clamped Method

result indicates the same tendency of the final deflection to increase if clamping is used, as did the experimental data.

If predicted strains are reasonably close to measured strain - and they are - then this method of calculating distortion can be used in other experiments involving clamping. Before attempting any trial-and-error sequence, it would be useful to run this program to predict the effectiveness of the clamping method in a particular problem or situation.

2.7.4 Differential Heating

The term "differential heating," as coined by Masubuchi, refers to a powerful technique for distortion reduction. One of the two components to be joined is heated to some predetermined temperature. The parts are then joined and allowed to cool. The preheated part cools and contracts more than the part initially at room temperature. The thermal stress that is generated can offset residual bending stresses that would be generated if both parts had been at the same temperature when joined. This results in a distortion reduction.

In this section we will summarize the experimental and analytical investigations carried out at M.I.T.

Experimental Investigation

Serotta [54] conducted a series of experiments to investigate the effect of differential heating on the reduction of longitudinal distortion of T-shaped built-up beams. As a material he chose the 5052-H32 aluminum alloy, a strain-hardened and non-heat-treatable alloy, to permit ready comparison with results obtained by Yamamoto [32]. Dimensions and general arrangement of the experimental equipment were

also the same as the ones used by Yamamoto and are shown in Figures 4-3 and 4-4 of Section 2.4.2 respectively.

The aluminum plates, both the web and the flange were 12 mm thick. The experimental procedure used was the following. The base plate was positioned on the support under the welding head. The web was then heated to the desired temperature using electric resistance heaters. The dial indicator was zeroed, allingment was verified and the heated web was placed in position and manually tack-welded at the end opposite to that end from which welding was to begin. Upon commencement of welding, a read-out of the dial indicator at predetermined intervals was made, until no change was being recorded. The second pass (i.e. the pass on the opposite side of the web) was made with the specimen at room temperature. It was felt that a temperature gradient of sufficient magnitude to be effective could not be maintained once the two components had been joined. Furthermore, the additional restraint provided by the first pass would reduce the tendency of the specimen to bend.

Figures 7-18 and 7-19 present deflection versus time after commencement of welding, for various preheating temperatures. Figure 7-20 is a graph of final deflection versus preheating temperature.

If one assumes that the deflection resulting from welding a T-shaped member is approximately linear with length, the temperature difference which eliminates distortion for one length should eliminate distortion for all lengths. This can be easily verified by experiments on specimens of other lengths.

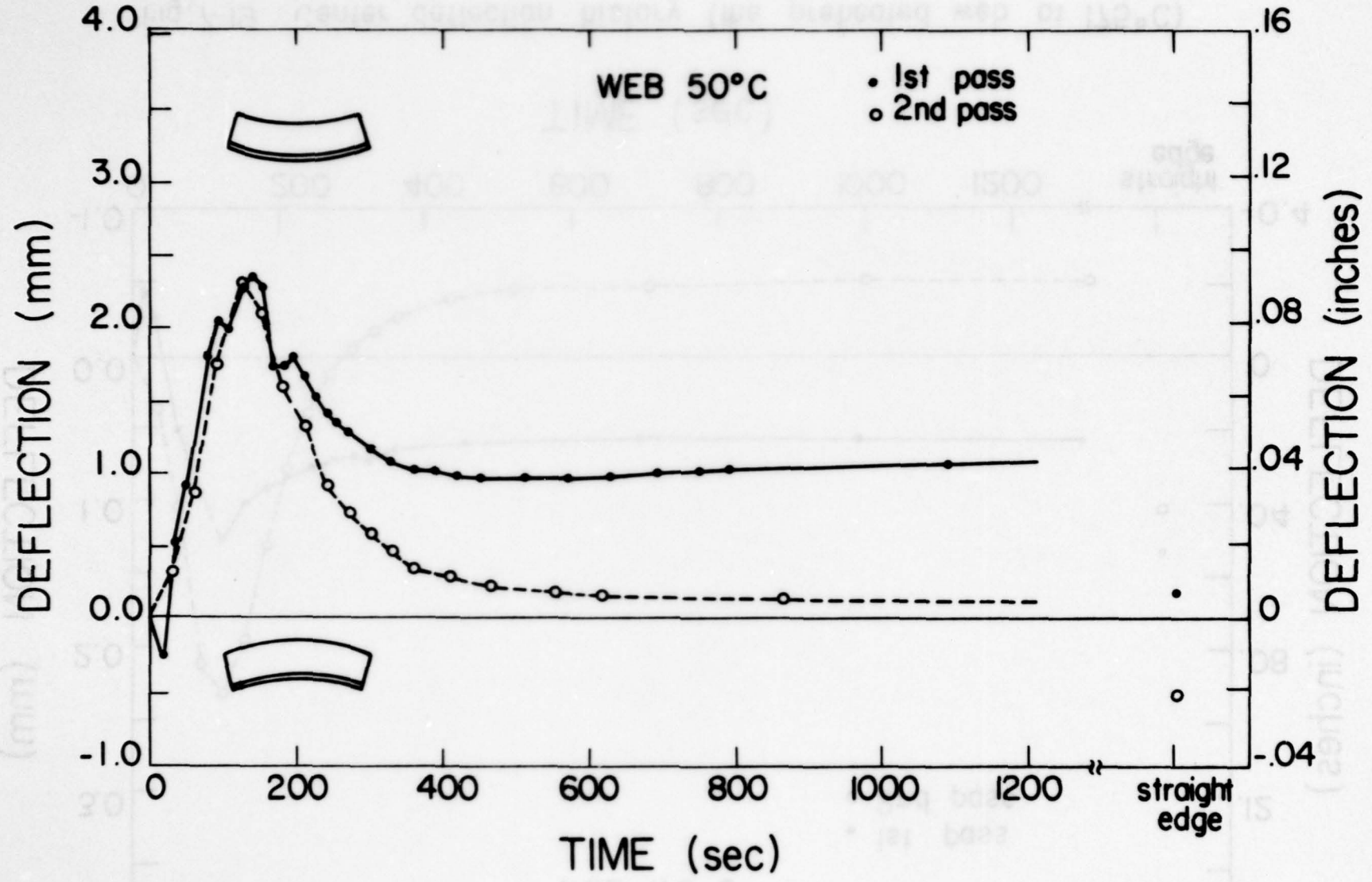

Fig. 7-18 Center deflection history (the preheated web at 50° C)

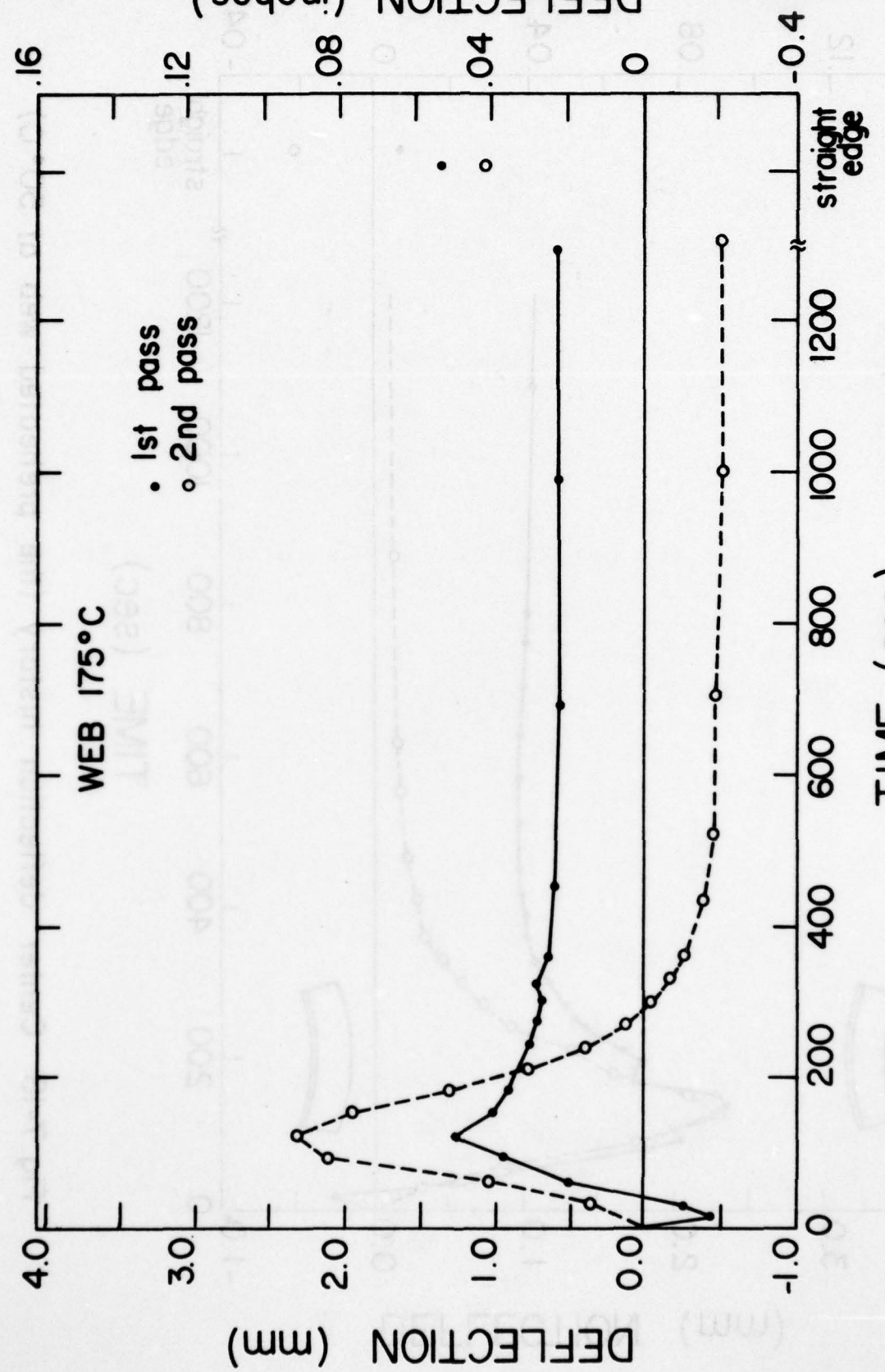

Fig. 7-19 Center deflection history (the preheated web at 175°C)

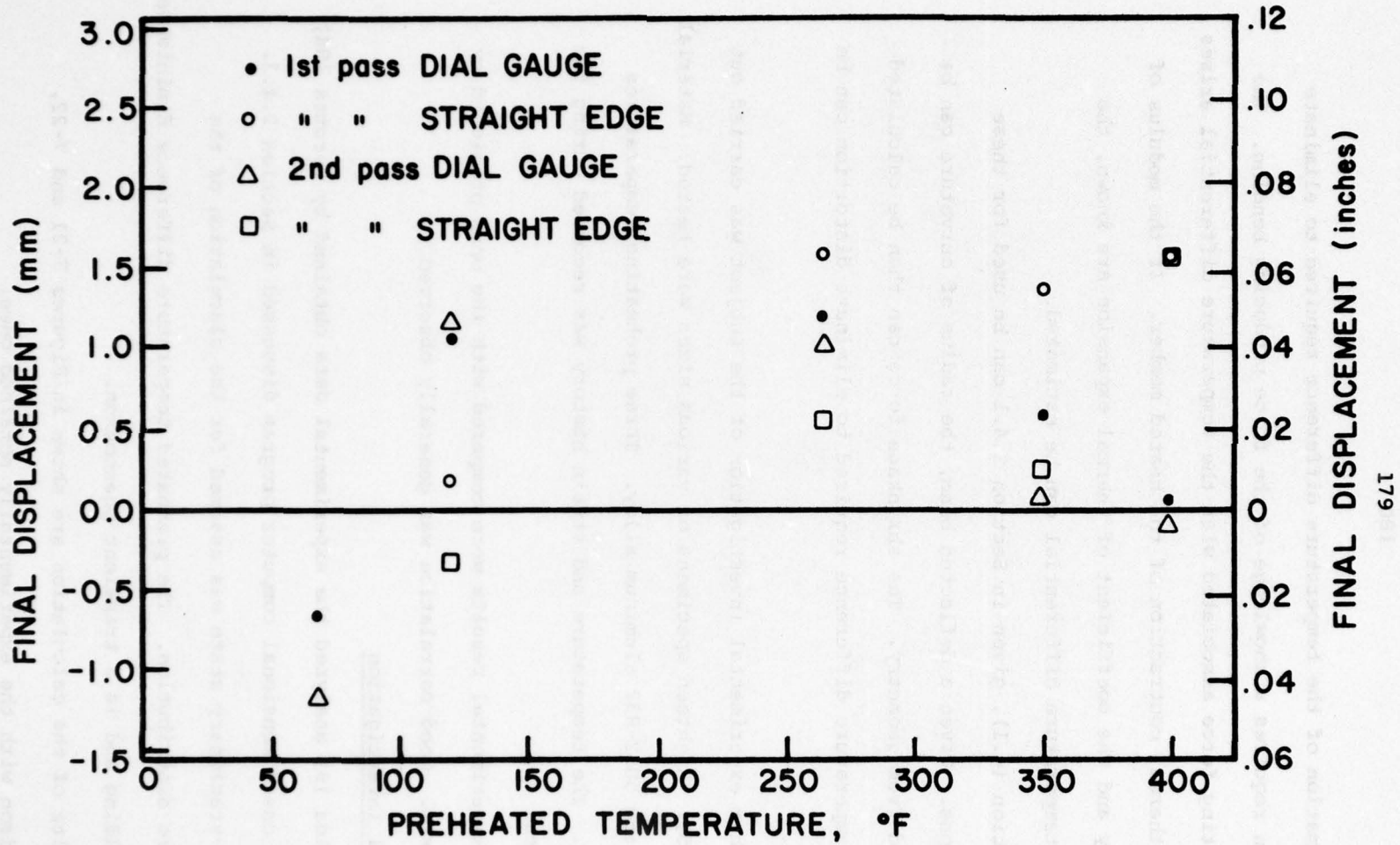

Fig. 7 – 20 Final Center Deflection vs. Preheating Temperature of the Web

Estimation of the temperature difference required to eliminate distortion requires a knowledge of the force producing bending. The counteracting force associated with the temperature differential arises from the thermal contraction of the heated member. If the modulus of elasticity and the coefficient of thermal expansion are known, the required temperature differential can be estimated.

Equation (4.1), given in Section 2.4.1 can be used for these calculations. Given a deflected beam, the radius of curvature can be determined from geometry. The shrinkage force can then be calculated and the temperature difference required to eliminate distortion can be estimated.

Further experimental investigation of the subject was carried out by Lin [55]. Eighteen specimens of various sizes were tested. Material used was the 5052-H32 aluminum alloy. Three preheating temperatures were used. The temperature and strain history was recorded during the experiments.

The experimental results were compared with the ones predicted by the analysis. Good correlation was generally observed.

Analytical Investigation

Nishida [9] analyzed the experimental data obtained by Serotta [54] using the one-dimensional computer program disucssed in Section 2.4.3. The quasi-stationary state was assumed for the claculation of the temperature distribution. The preheated temperature difference diminishes during welding and is a transient phenomenon.

Results of the calculation are shown in Figures 7-21 and 7-22, in comparison with the experimentally obtained ones.

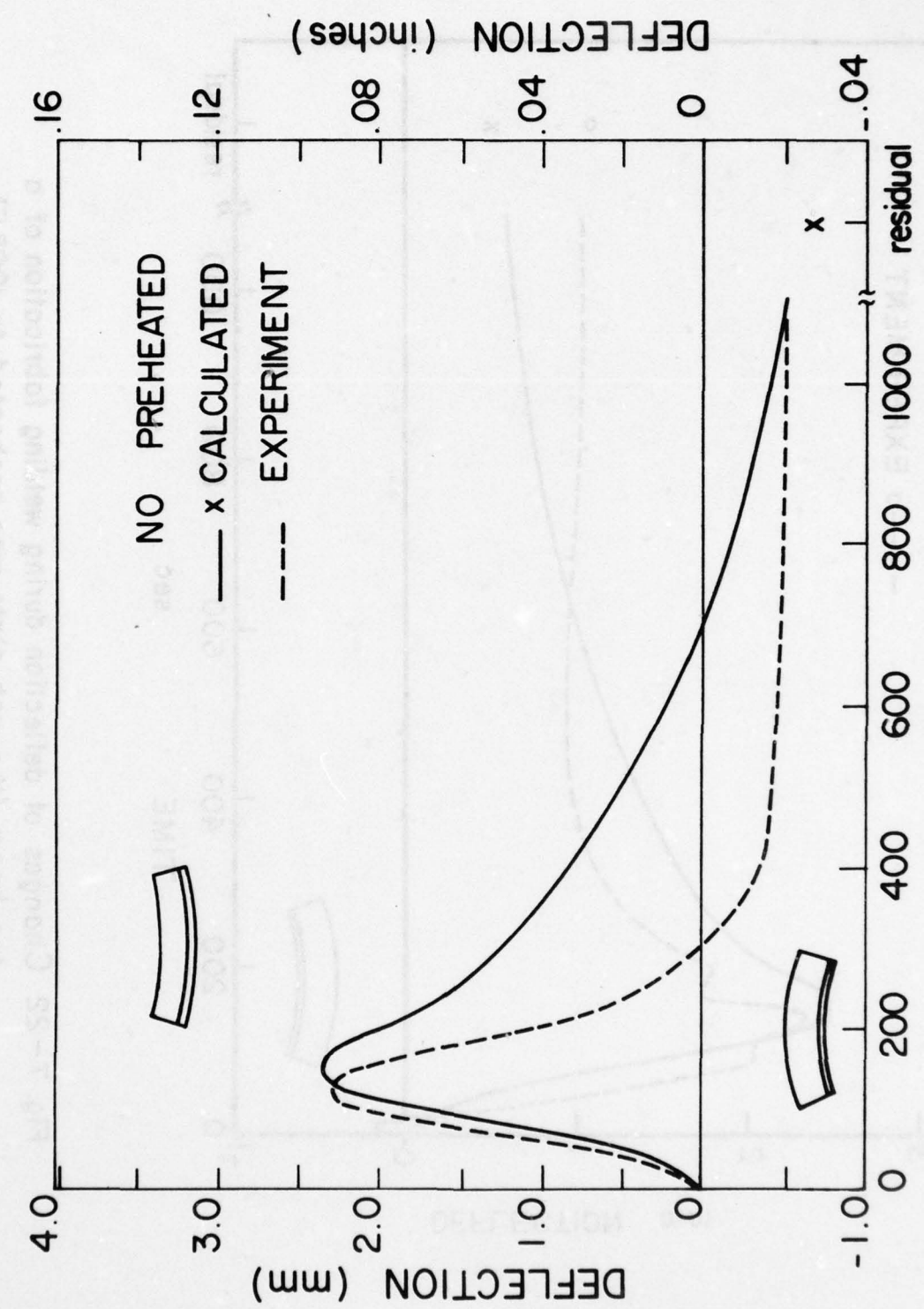

Fig. 7-21 Calculated center deflection history (no preheat)

AD-A050 908 MASSACHUSETTS INST OF TECH CAMBRIDGE DEPT OF OCEAN E--ETC F/6 13/5
DEVELOPMENT OF ANALYTICAL AND EMPIRICAL SYSTEMS FOR PARAMETRIC --ETC(U)
NOV 77 V J PAPAZOGLOU, K MASUBUCHI N00014-75-C-0469

UNCLASSIFIED NL

3 OF 3
AD
A050908

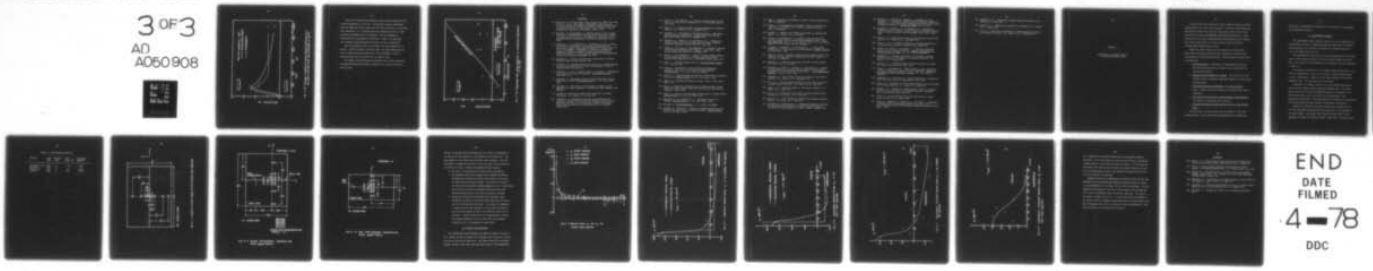

END
DATE
FILMED
4-78
DDC

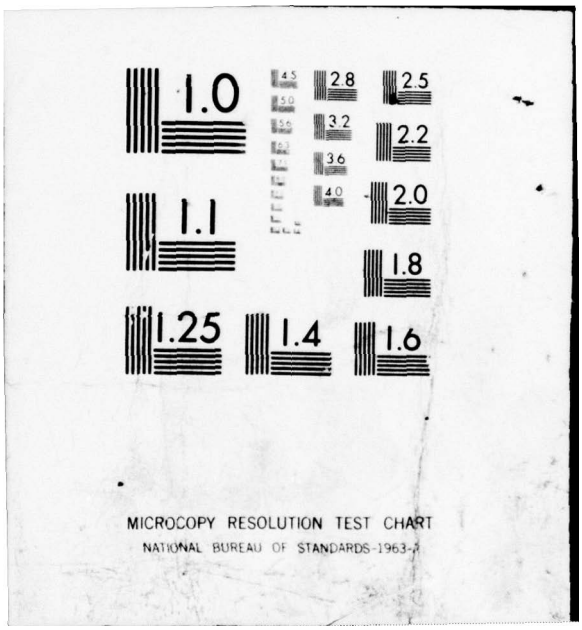
1.0
1.1
1.25
1.4
1.6
1.8
2.0
2.2
2.5
2.8
3.2
3.6
4.0
4.5
5.0
5.6
MICROCOPY RESOLUTION TEST CHART
NATIONAL BUREAU OF STANDARDS-1963-A

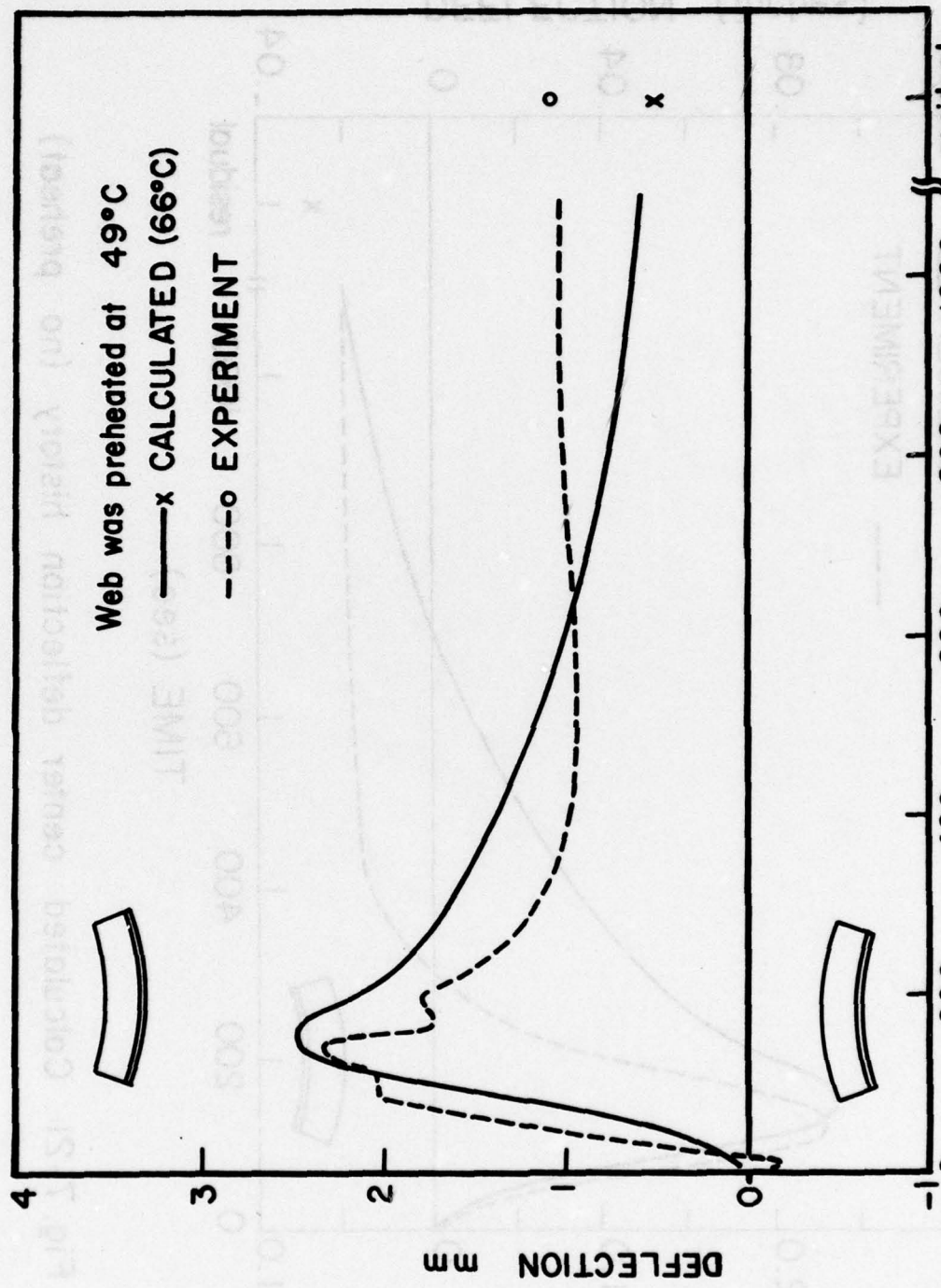

Fig. 7-22 Changes of deflection during welding fabrication of a tee-beam (the web plate was preheated to 120°F)

Figure 7-23 shows how the deflection after welding changes with the preheated temperature of the web. Discrepancies between experimental data and analytical results appear when the web is heated to a relatively high temperature. It is believed that the experimental data for high preheating temperatures are not accurate, since the temperature differential will be reduced by conduction. Figure 7-23 shows that zero deflection can be achieved by heating the web to around 50°C.

When the welding is done in two passes, the best technique is to produce a slightly positive distortion after the first welding pass by using a higher preheating temperature, 75°C for example, so that distortion after the second pass will be close to zero.

The computer program developed by Nishida can be used to determine the optimum welding and preheating conditions for joining T-beams of various sizes.

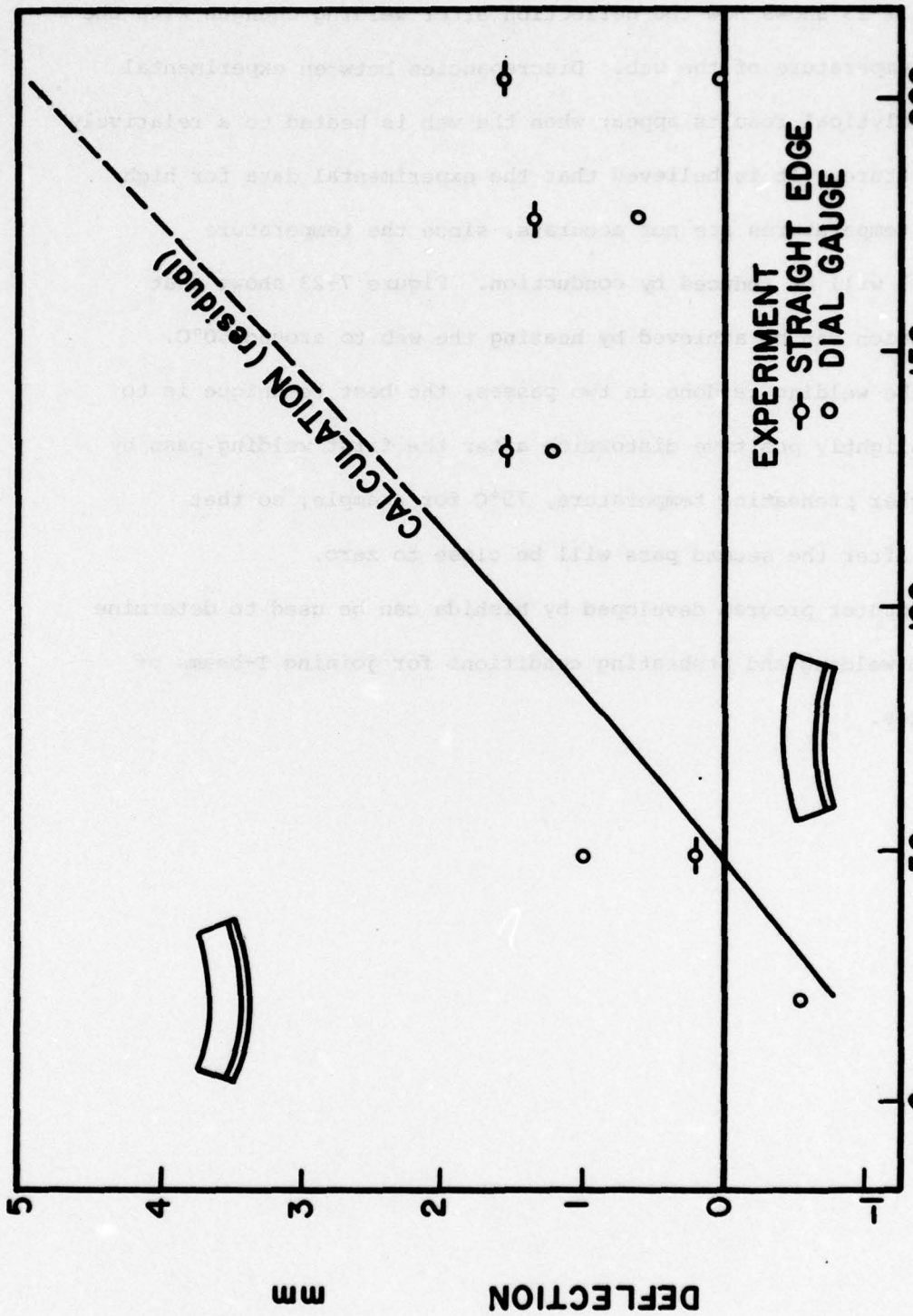

Fig. 7-23 Calculated final center deflection vs. preheating temperature of the web

REFERENCES

[1] Masubuchi, K., Progress Report under Contract No. N00014-75-C-0469, NR 031-773 (M.I.T. OSP #82558) "Development of Analytical and Practical Systems for Parametric Studies of Design and Fabrication of Welded Structures," to the Office of Naval Research from the Massachusetts Institute of Technology, June 7, 1976.

[2] Kitamura, K., and Masubuchi, K., Special Report on "Out-of-Plane Distortion of Welded Panel Structures" under Contract No. N00014-75-C-0469, NR 031-773 (M.I.T. OSP #82558) to the Office of Naval Research from the Massachusetts Institute of Technology, July 3, 1975.

[3] Papazoglou, V., and Masubuchi, K., "Integration of M.I.T. Studies on Prediction and Control of Distortion in Welded Aluminum Structures," prepared under Contract #N00014-75-C-0469, NR 031-773 (M.I.T. OSP #82558), "Development of Analytical and Empirical Systems for Parametric Studies on Design and Fabrication of Welded Structures," to Office of Naval Research from Massachusetts Institute of Technology, September 20, 1976.

[4] Masubuchi, K., "Control of Distortion and Shrinkage in Welding," Welding Research Council Bulletin 149.

[5] Masubuchi, K., "Residual Stresses and Distortion in Welded Aluminum Structures and Their Effects on Service Performance," Welding Research Council Bulletin 174.

[6] Rosenthal, D., et al., "Thermal Study of Arc Welding -- Experimental Verification of Theoretical Formulas," The Welding Journal, 17, April 1938, 2-8.

[7] Rosenthal, D., "Mathematical Theory of Heat Distribution During Welding and Cutting," The Welding Journal, 20 (5), 220-s-234-s, 1941.

[8] Rosenthal, D., "The Theory of Moving Sources of Heat and Its Application to Metal Treatments," Transactions ASME, November 1946, 849-866.

[9] Nishida, M., "Analytical Prediction of Distortion in Welded Structures," M.S. Thesis, M.I.T., May 1976.

[10] Papazoglou, V., "Computer Programs for the One-Dimensional Analysis of Thermal Stresses and Metal Movement During Welding," Manual #2, Section IV of "The Analysis on Welded Structures - Some Design and Fabrication Considerations" by K. Masubuchi, January 1977.

[11] Muraki, T., and Masubuchi, K., "Computer Programs Useful for the Analysis of Heat Flow in Weldments," M.I.T. OSP #81499, #22016, June, 1974.

[12] Tsai, C. L., "Parametric Study on Cooling Phenomena in Underwater Welding," Ph.D. Thesis, M.I.T., September 1977.

[13] Masubuchi, K., "The Analysis of Welded Structures - Some Design and Fabrication Considerations," prepared under ONR contract #N00014-75-C-0469, NR 031-773, November 1977.

[14] Masubuchi, K., Simmons, F. B., and Monroe, R. E., "Analysis of Thermal Stresses and Metal Movement During Welding," Redstone Scientific Information Center, RSIC-820, July 1968.

[15] Andrews, J. B., Arita, M., and Masubuchi, K., "Analysis of Thermal Stress and Metal Movement During Welding," Final Report under Contract NAS8-24365 from M.I.T., December 1970.

[16] Muraki, T., and Masubuchi, K., "Manual of Finite Element Program for Two-Dimensional Analysis of Thermal Stresses and Metal Movement During Welding," M.I.T., OSP #81499, #22016, April 1975.

[17] Capel, L., "Aluminum Welding Practice," British Welding Journal, 8 (5), 245-248, 1961.

[18] Gilde, W., "Contribution to the Calculation of Transverse Shrinkage," (Beitrag zur Berechnung der Quershrumpfung), Schweisstechnik, 7 (1), 10-11, 1957 (in German).

[19] Cline, C. L., "Weld Shrinkage and Control of Distortion in Aluminum Butt Welds," Welding Journal, 44 (11), 523-s-528-s, 1965.

[20] Campus, F., "Transverse Shrinkage of Welds," ibid., 26 (8), 485-s-488-s, 1947.

[21] Weck, R., "Transverse Contractions and Residual Stresses in Butt-Welded Mild Steel Plates," Report No. R4, Admiralty Ship Welding Committee, January 1947.

[22] Guyot, F., "A Note on the Shrinkage and Distortion of Welded Joints," Welding Journal, 26 (9), 519-s-529-s, 1947.

[23] Sparangen, W., and Ettinger, W. G., "Shrinkage Distortion in Welding," Welding Journal, 23 (11), 545-s-559-s, 1944.

[24] Malisius, R., Electroschweissen, 7, 1-7, 1936, (in German).

[25] Watanabe, M., and Satoh, K., "Effect of Welding Conditions on the Shrinkage and Distortion in Welded Structures," Welding Journal, 40 (8), 377-s-384-s, 1961.

[26] Naka, T., "Shrinkage and Cracking in Welds," Komine Publishing Co., 1950 (in Japanese).

[27] Matsui, S., "Investigation of Shrinkage, Restraint Stresses and Cracking in Arc Welding," Ph.D. Thesis at Osaka University, 1964 (in Japanese).

[28] Iwamura, Y., "Reduction of Transverse Shrinkage in Aluminum Butt Welds," M.S. Thesis, M.I.T., May 1974.

[29] Kihara, H., and Masubuchi, K., "Studies on the Shrinkage and Residual Welding Stress of Constrained Fundamental Joint," Intl. Soc. Naval Arch., Jap. Pt. 1, 95, 181-195, 1954; Pt. 2, 96, 99-108, 1955; Pt. 3, 97, 95-104, 1955 (in Japanese).

[30] Sasayama, T., Masubuchi, K., and Moriguchi, S., "Longitudinal Deformation of a Long Beam Due to Fillet Welding," Welding Journal, 34, 581-s-582-s, 1955.

[31] Ujiie, A., et al., "Automatic Welding of 5083 Aluminum Alloy," The Committee of Light Metals for Shipbuilding Industry, Report 14, 1970-1972 (in Japanese).

[32] Yamamoto, G., "Study of Longitudinal Distortion of Welded Beam," M.S. Thesis, M.I.T., May 1975.

[33] Masubuchi, K., Ogura, Y., Ishihara, Y., and Hoshino, J., "Studies on the Mechanism of the Origin and the Method of Reducing the Deformation of Shell Plating in Welded Ships," Intl. Shipbuilding Progress, 3 (19), 123-133, 1956.

[34] Taniguchi, C., "Out-of-Plane Distortion Caused by Fillet Welds in Aluminum," M.S. Thesis, M.I.T., September 1972.

[35] Shin, D. B., "Finite Element Analysis of Out-of-Plane Distortion of Welded Panel Structures," O.E. Thesis, M.I.T., May 1972.

[36] Duffy, D. K., "Distortion Removal in Structural Weldments," M.S. Thesis, M.I.T., May 1970.

[37] Brito, V. M., "Reduction of Distortion in Welded Aluminum Frame Structures," O.E. Thesis, M.I.T., May 1976.

[38] Briceno, G. E., "The Distortion of Welded Thin Aluminum Stiffened Panels," O.E. Thesis, M.I.T., May 1977.

[39] Goncalves, E., and Taniguchi, C., "Comparative Analysis of Methods for Predicting Weld Distortion in Panel Structures," Escola Politecnica da Universidade de Sao Paulo, Brazil, December 1974.

[40] Masubuchi, K., Nishida, M., Yamamoto, G., Kitamura, K., and Taniguchi, C., "Analysis of Thermal Stresses and Metal Movement of Weldments: A Basic Study Toward Computer-Aided Analysis and Control of Welded Structures," Transactions SNAME, Vol. 83, 1975.

[41] Masubuchi, K., Kitamura, K., and Taniguchi, C., "Buckling as a Limiting Criteria to Control Initial Distortion of Welded Structure Panels," Escola Politecnica da Universidade de Sao Paulo, Brazil, 1975.

[42] Pattee, F. M., "Buckling Distortion of Thin Aluminum Plates During Welding," M.S. Thesis, M.I.T., September 1975.

[43] Terai, K., et al., "Study on Prevention of Welding Deformation in Thin-Skin Plate Structures," Kawasaki Heavy Industries.

[44] Yoshiki, M., Fujita, Y., and Kawai, T., "Influence of Residual Stresses on the Buckling of Plates," Journal of the Society of Naval Architects of Japan, Vol. 107, 1960 (in Japanese).

[45] Papazoglou, V., "Analysis and Control of Distortion in Welded Aluminum Structures with Emphasis on Buckling Distortion," M.S. Thesis, M.I.T., January 1978.

[46] Stowell, E. Z., "A Unified Theory of Plastic Buckling of Columns and Plates," NACA Report No. 898, 1948.

[47] Fujita, Y., and Yoshida, K., "Plastic Design in Steel Structures - Influence of Residual Stresses on Plate Instability," Journal of the Society of Naval Architects of Japan, Vol. 115, 1964 (in Japanese).

[48] Handelman, G. H. and Prager, W., "Plastic Buckling of a Rectanbular Plate Under Edge Thrusts," NACA Report No. 946, 1949.

[49] Henry, R. W., "Reduction of Out-of-Plane Distortion in Fillet Welded High Strength Aluminum," M.S. Thesis, M.I.T. May 1974.

[50] Masubuchi, K., "Integration of NASA Sponsored Studies on Aluminum Welding," under contract No. NAS8-24364 to George C. Marshall Space Flight Center, NASA, June 1972.

[51] Terai, K., "Recent Progress on Electron Beam Welding in Japan," Lecture given at M.I.T., March 1976.

[52] Kihara, H., Watanabe, M., Masubuchi, K., and Satoh, K., "Researches on Welding Stress and Shrinkage Distortion in Japan," Vol. 4, 60th Anniversary Series of the Society of Naval Architects of Japan, Tokyo, 1959.

[53] Beauchamp, D. G., "Distortion in Welded Aluminum Structures," M.S. Thesis, M.I.T., May 1976.

[54] Serotta, M. D., "Reduction of Distortion in Weldments," O.E. Thesis, M.I.T., August 1975.

[55] Lin, C. H., "Reduction of Distortion in Welded Aluminum Structures by Differential Heating," M.S. Thesis, M.I.T., February 1977.

APPENDIX A

Investigation of Residual Stresses in Laser Butt-Welded Joints

In recent years there has been an effort towards a deeper and better understanding of the laser welding process. The initial inspections from experimental studies have shown that high quality laser welds could be formed with excellent metallographic and mechanical properties. Tests carried out on CO_2 laser welded specimens from materials used in fabrication of naval ships (HY 130, HY 180, Ti-6Al-4V alloy and 5456 Al) indicated these perspectives [A1, A2].

Further CO_2 laser welding process's features, as those listed below, make this process technically and economically attractive for the aerospace and shipbuilding industry. These features could be listed as follows [A3]:

1. Narrow Deep Welds. Experiments on representative materials have shown deep penetration, similar to that achieved by the electron-beam welding
2. Workpiece is not Enclosed in a Vacuum. This gives to CO_2 laser welding process an inherrent advantage compared to electron beam welding process.
3. Characteristically Long Telescope - To - Work Distances. Hence, a better view of the workpiece is achieved with obvious advantages.
4. One Laser Can Carry Out Two or More Operations Simultaneously. This feature is achieved by beam splitting.
5. One Laser Can Service Several Work Stations on a Time Sharing Basis.

From the above, one may conclude that the benefits of CO_2 laser welding process, if well established and parametrically investigated,

should help in expanding the application of the process to the aerospace and shipbuilding industry.

A.1 Experimental Procedure

The experimental study, primarily carried out at the laboratories of Massachusetts Institute of Technology under the supervision of Professor Koichi Masubuchi, was intended to determine the residual stresses in laser butt welded joints [A4, A5].

The experiments were carried out on four specimens made of low-carbon steel, Ti-6Al-4V alloy, Inconel 718 and Ultra High Strength Steel AISI 4130. The composition and properties of the materials used are summarized in Table A.1.

The welds were carried out at Avco Everett Research Laboratory, Inc., Everett, Massachusetts, because of the lack of a laser welding machine at M.I.T. laboratories. Table A.2 lists, where available, the welding parameters used. All welds were done in one pass.

Measurement of residual stresses in the butt-welded specimens was done using the complete stress-relaxation technique [A6]. The strain gages used were of the type BLH #FAET-18D-S6 with a resistance of 120 Ohm and gage factor 1.98, furnishing strain measurements in two perpendicular directions. They were bonded on the surface of the specimens with cement Eastman #910 and covered for protection with Barrier C.

Figures A-1 through A-3 show the titanium alloy, Inconel 718 and AISI 4130 specimens correspondingly with indication of the locations of the strain gages. Strain gages were installed on both faces of the specimens to account for bending stresses. Note that in the case of the

Table A.1 Properties of Materials Used

Low Carbon Steel		
Composition:	C:	0.21 max
	Mn:	0.80 - 1.10
	P:	0.05 max
	S:	0.05 max
Tensile strength:	400 MN/m^2	min
Yield Strength:	220 MN/m^2	
Elongation:	28%	
6Al-4V Titanium Alloy		
Composition:	Al:	5.50 - 6.75
	V:	3.50 - 4.50
	Fe:	0.30 max
	C:	0.10 max
	N:	0.07 max
	H:	0.015 max
	O:	0.20 max
	Other:	0.40 max
Tensile strength:	900 MN/m^2	
Yield strength:	830 MN/m^2	
Elongation:	8%	
Inconel 718		
Composition:	Fe:	18.5
	Cr:	19.0
	Ni:	52.5
	Mo:	3.05
	Cb:	5.13
	Ti:	0.90
	Al:	0.50
	Mn:	0.18
	C:	0.04
	S:	0.008
Tensile strength:	1,410 MN/m^2	
Yield strength:	1,180 MN/m^2	
Elongation:	20%	
AISI 4130		
Composition:	Cr:	0.95
	C:	0.3
	Mn:	0.5
	Si:	0.3
	Mo:	0.2
Tensile strength:	-	
Yield strength:	1,170 MN/m^2	
Elongation	-	

Table A.2 Laser Welding Conditions

Material	Weld Type	Thickness (mm)	Laser Power (kW)	Weld Speed (mm/min)
Low Carbon Steel	Butt	6	8.4	2,540
Ti-6Al-4V	Butt	6	-	-
Inconel 718	Butt	6	8.0	2,540
AISI 4130	Butt	6	8.5	2,540

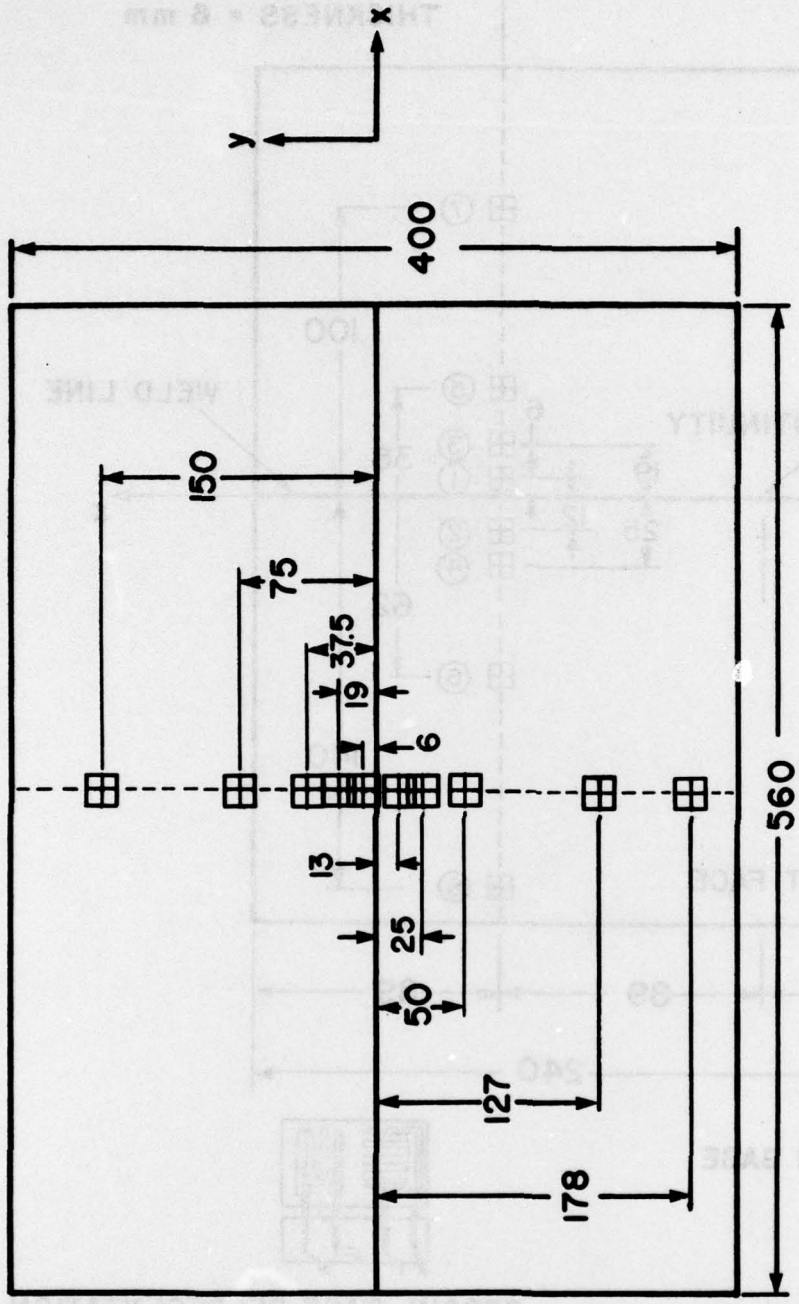

Fig. A-1 Location of Strain Gages on the Titanium Alloy Specimen

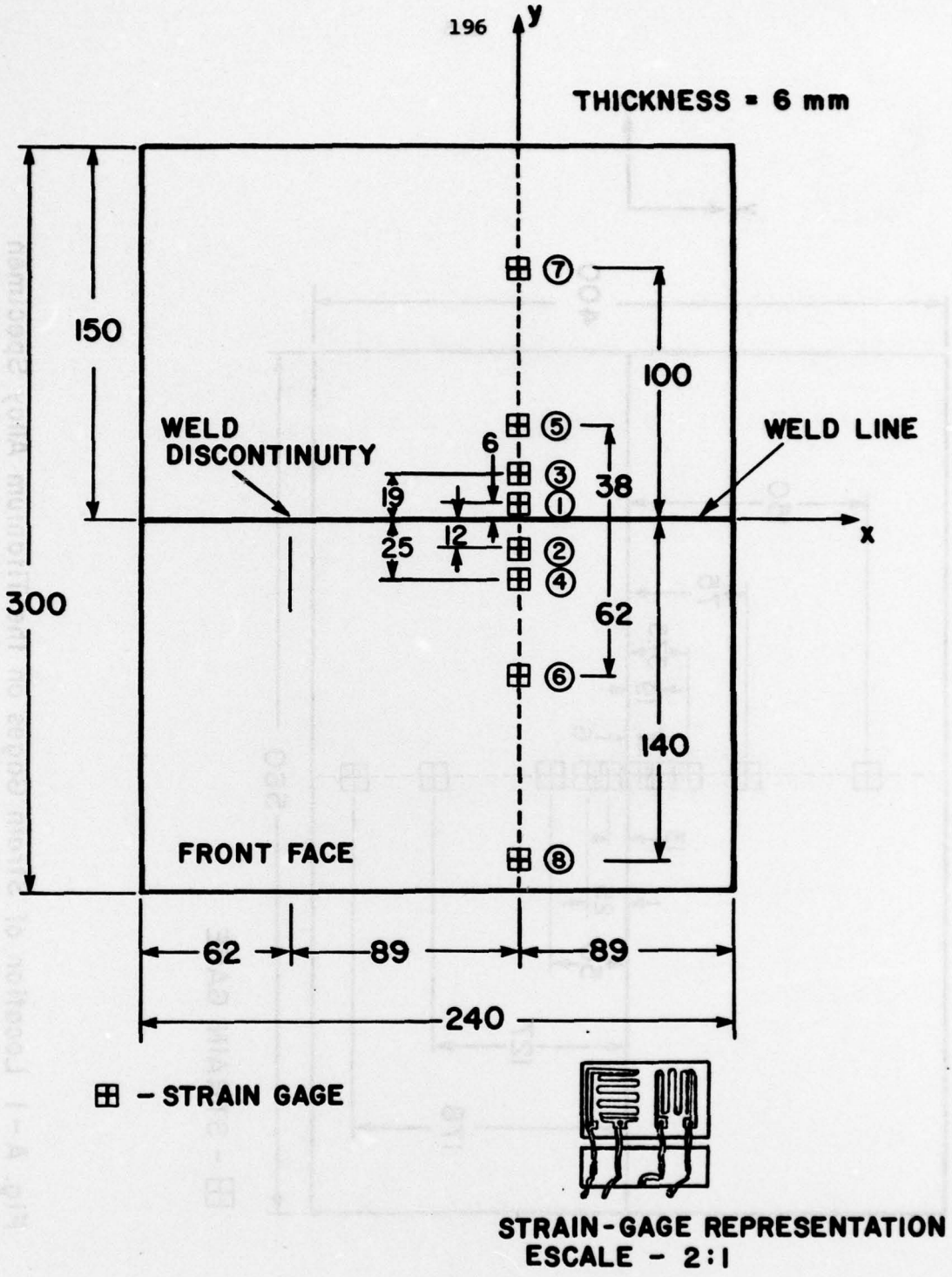

Fig. A-2 Inconel 718 Specimen – Dimension and Strain-gages Position

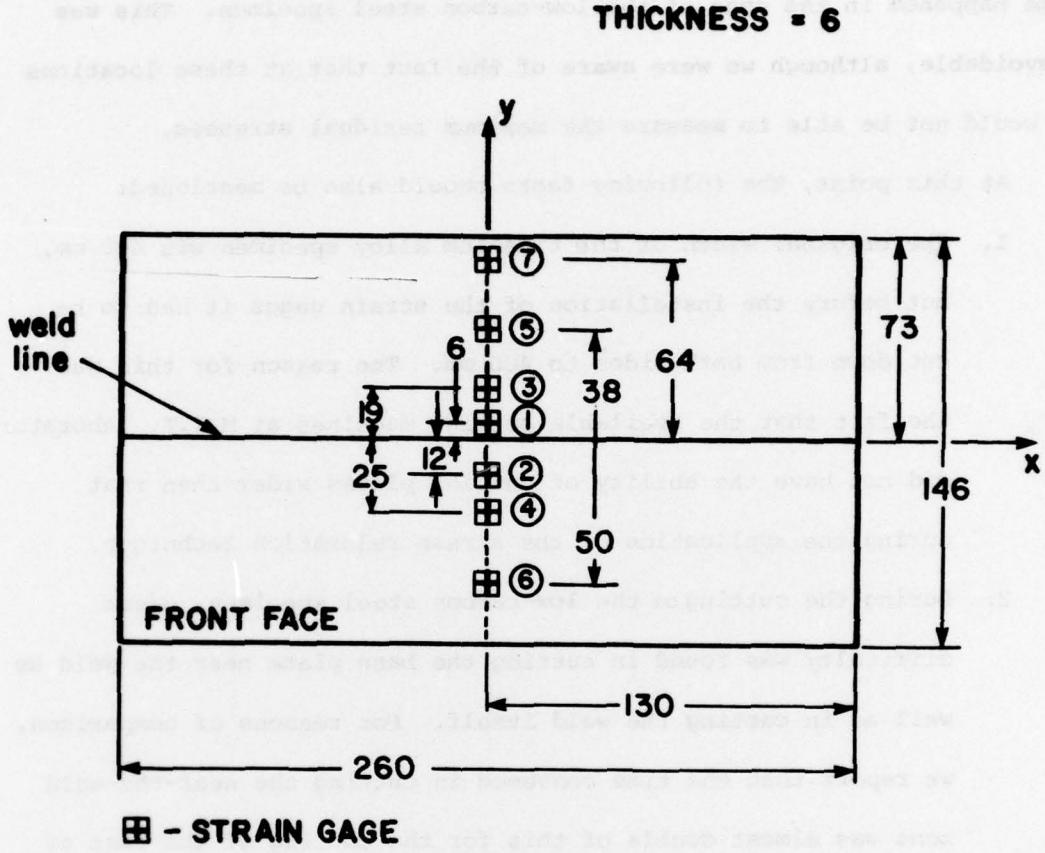

Fig. A - 3 AISI 4130 Specimen - Dimension and Strain - gages Position

Inconel 718 specimen the strain gages were not located at midlength of the weld due to the presence of a discontinuity (see Figure A-2). The same happened in the case of the low-carbon steel specimen. This was unavoidable, although we were aware of the fact that at these locations we would not be able to measure the maximum residual stresses.

At this point, the following facts should also be mentioned:

1. The original width of the titanium alloy specimen was 480 mm, but before the installation of the strain gages it had to be cut down from both sides to 400 mm. The reason for this was the fact that the available cutting machines at M.I.T. laboratories did not have the ability of cutting plates wider than that during the application of the stress relaxation technique.
2. During the cutting of the low-carbon steel specimen, great difficulty was found in cutting the base plate near the weld as well as in cutting the weld itself. For reasons of comparison, we report that the time consumed in cutting the near-the-weld zone was almost double of this for the cutting of the rest of the plate. Similar difficulty was not encountered in cutting the titanium specimen, due to the fact that it was equally difficult to cut it throughout its whole width.

A.2 Results and Conclusions

The experimental results obtained are shown in Figures A-4 through A-8. Results for the low-carbon steel specimen were strange and inconclusive and so they are not shown here. The results show that the maximum residual stress is much lower than the yield stress at room temperature,

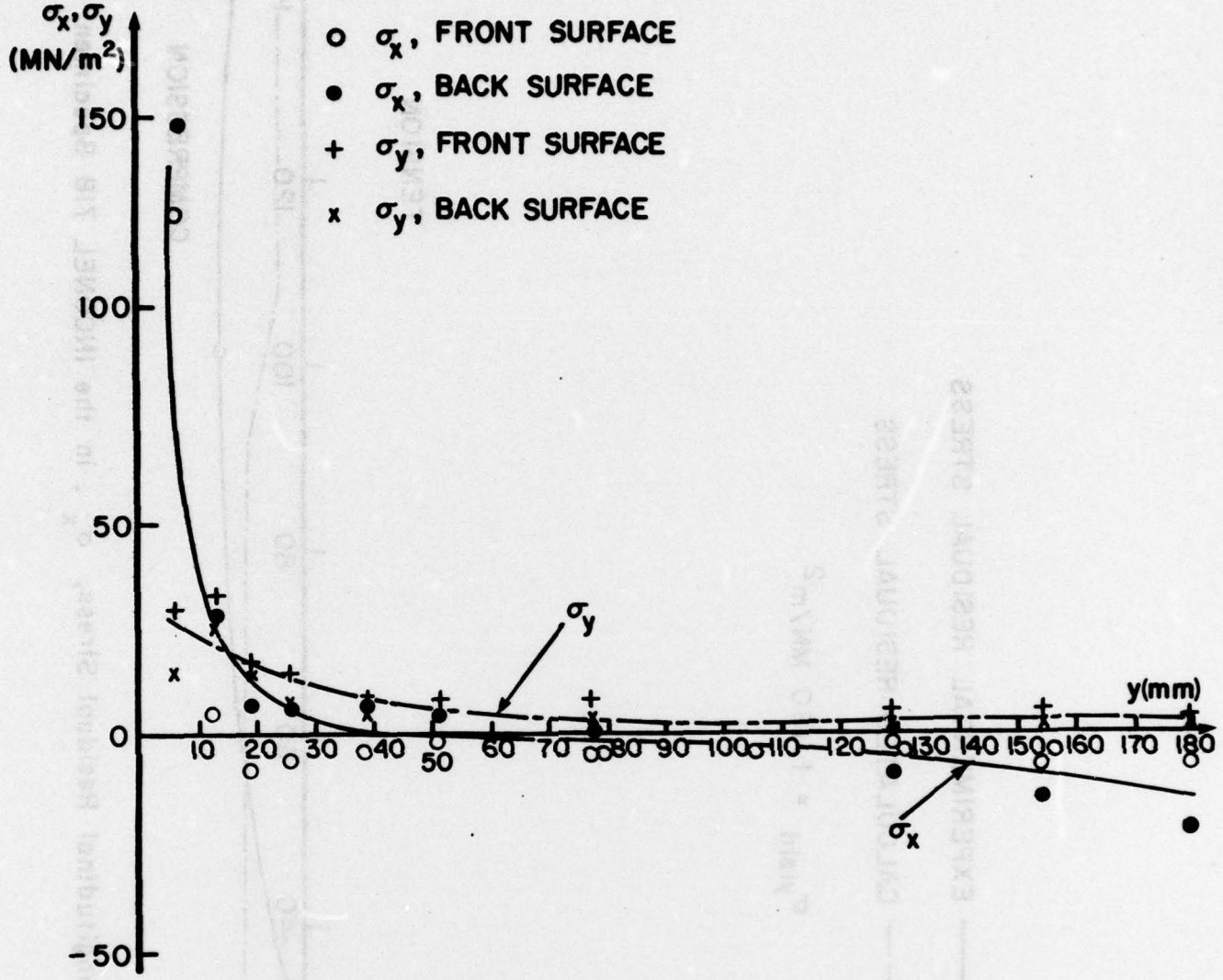

Fig. A-4 Residual Stress σ_x and σ_y the Titanium Alloy Specimen

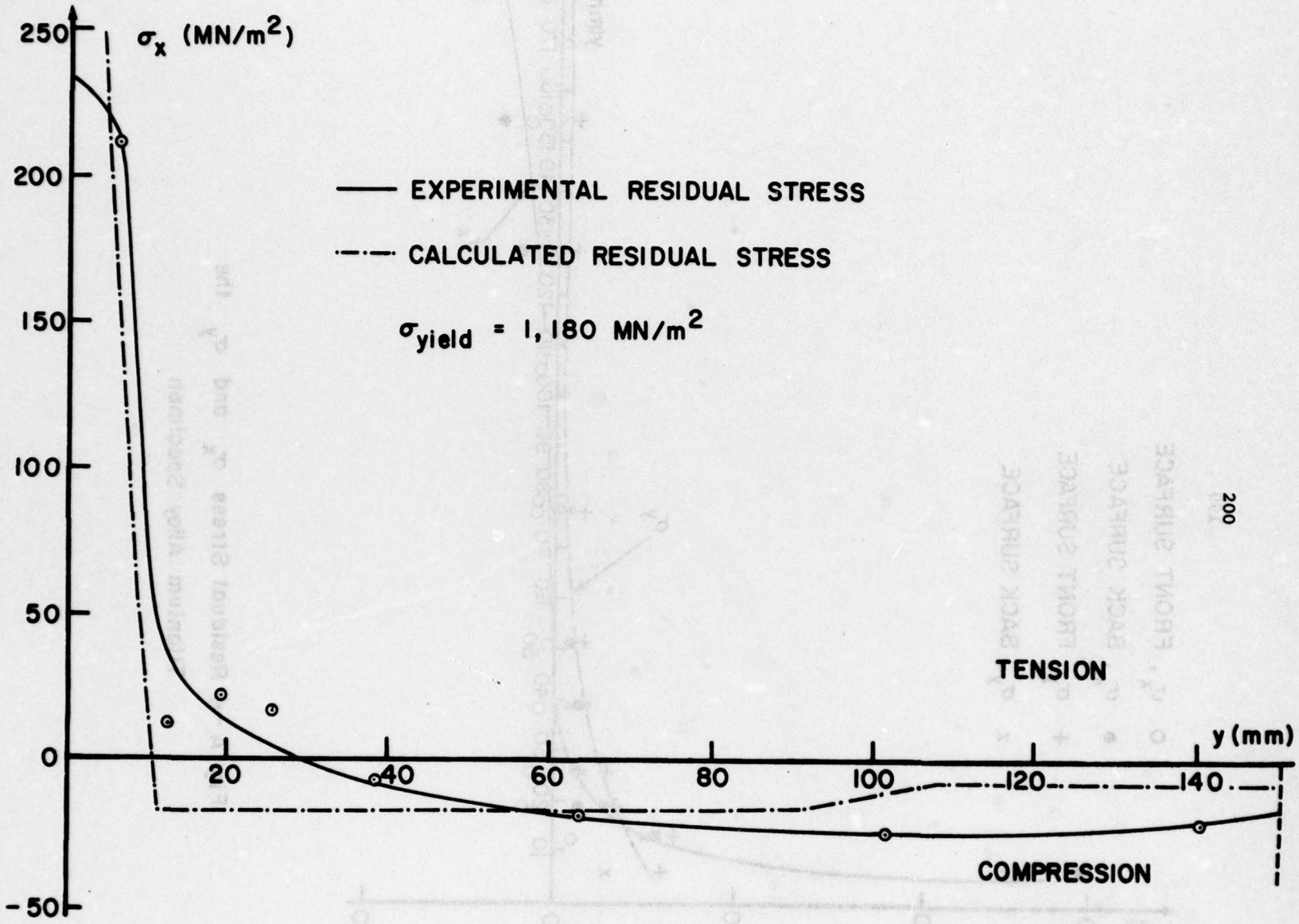

Fig. A-5 Longitudinal Residual Stress, σ_x, in the INCONEL 718 Specimen

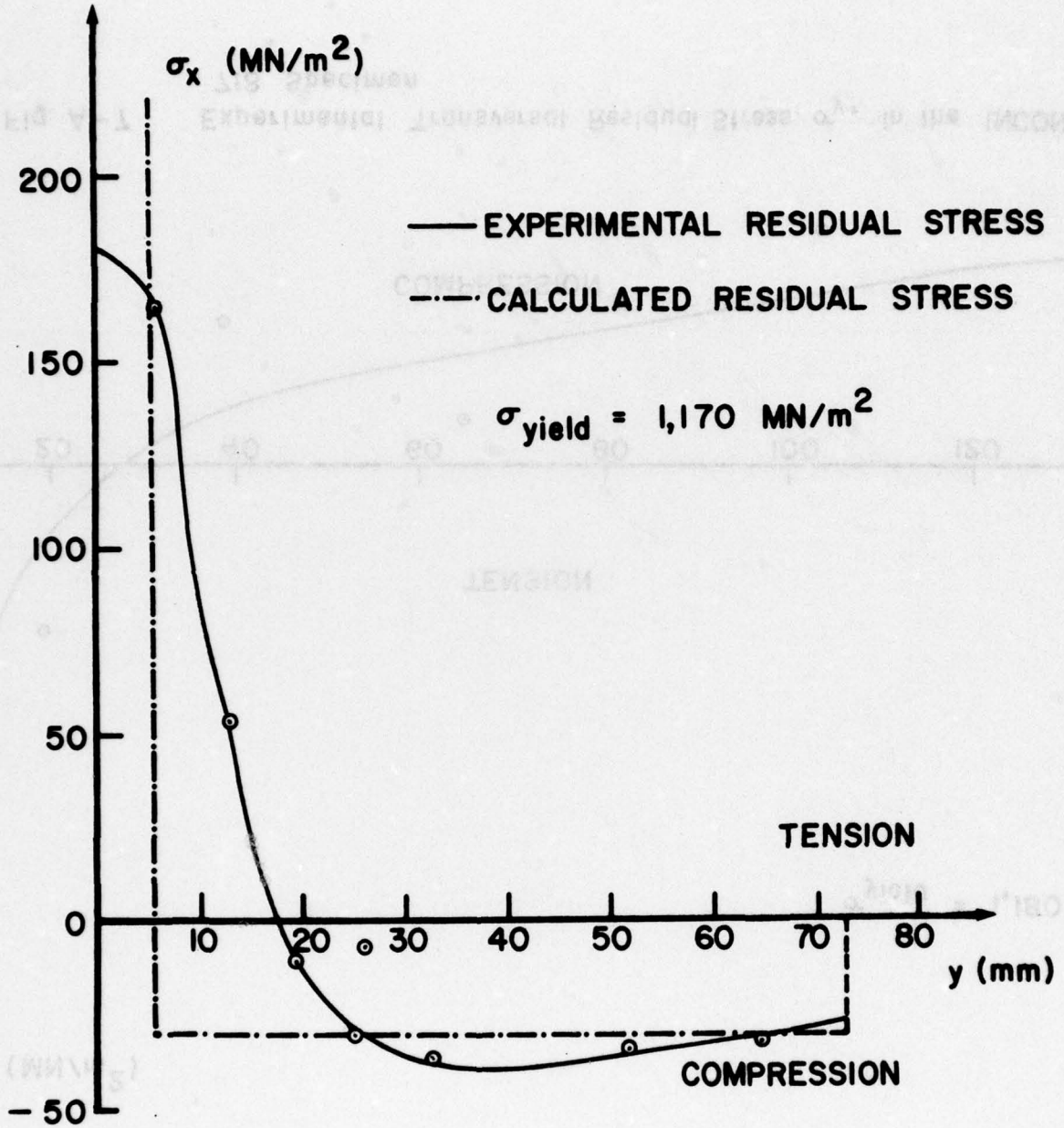

Fig. A-6 Longitudinal Residual Stress, σ_x, in the AISI 4130 Specimen

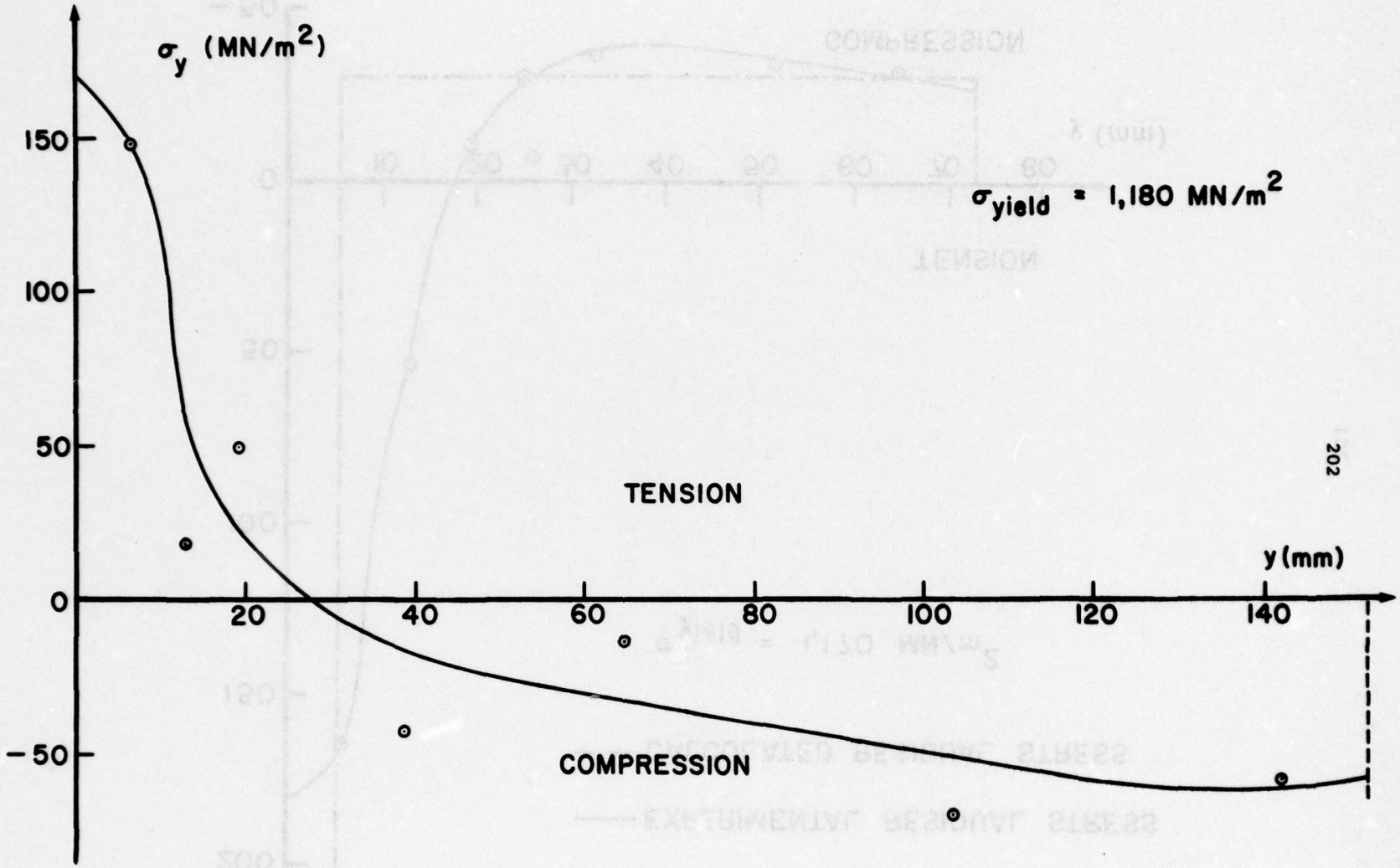

Fig. A-7 Experimental Transversal Residual Stress, σ_y, in the INCONEL 718 Specimen

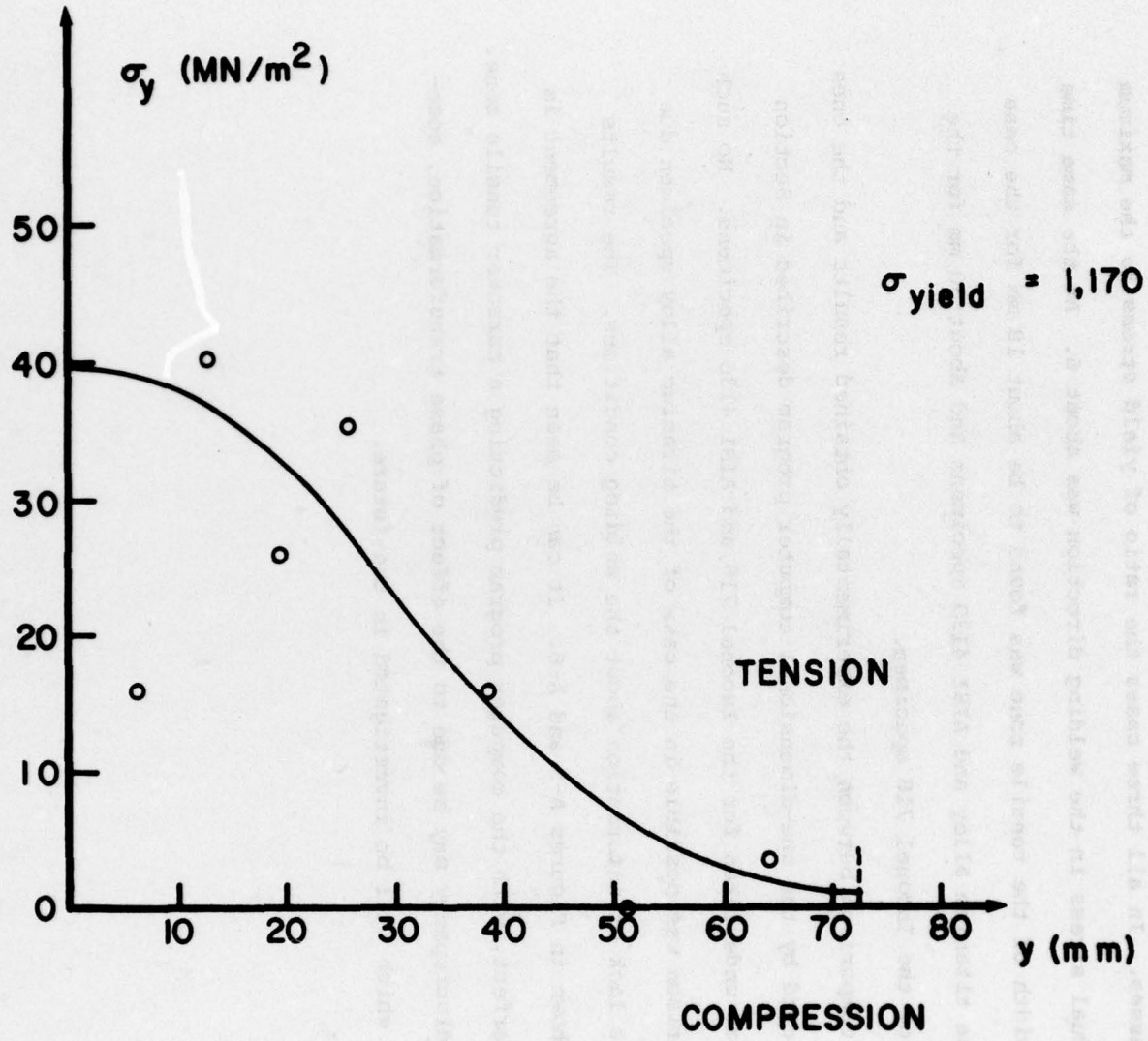

Fig. A-8 Experimental Transversal Residual Stress, σ_y, in the AISI 4130 Specimen

as is commonly the case when welding with the conventional welding processes. In all three cases the ratio of yield stress to the maximum residual stress in the welding direction was about 6. At the same time the width of the tensile zone was found to be about 18 mm for the case of the titanium alloy and AISI 4130 specimens and about 30 mm for the case of the Inconel 718 specimen.

Comparison between the experimentally obtained results and the ones predicted by the one-dimensional computer program described in Section 2.2 was undertaken for the Inconel 718 and AISI 4130 specimens. No such comparison was possible in the case of the titanium alloy specimen due to the lack of information about the welding conditions. The results are shown in Figures A-5 and A-6. It can be seen that the agreement is not perfect, with the computer program predicting a narrower tensile zone. This discrepancy may be due to the effect of phase transformation, something which will be investigated in the future.

REFERENCES

[A1] Banas, C. M., "Laser Welding of Navy Ship Construction Materials," United Aircraft Research Labs, East Hartford, Conn., August 1973.

[A2] Locke, E., "Laser Welding Techniques for Fabrication of Naval Vessels," Avco Everett Research Lab., Inc., Everett, Mass., July 1973.

[A3] Seaman, F. D., "Establishment of a Continuous Wire Laser Welding Process," Sciaky Bros., Inc., Chicago, Ill. 9th Interim Engineering Progress Report. January 1976.

[A4] Papazoglou, V., "Investigation of Residual Stresses in Laser Welding," Term paper for Course 13.39, M.I.T., May 1976.

[A5] Gonçalves, E., "Residual Stress Analysis in Laser Butt Welded Joints," Special project in Ocean Engineering, M.I.T., Summer 1977.

[A6] Masubuchi, K., "Textbook for Course 13.17J, Welding Engineering," M.I.T.


78